

JOURNAL OF

# CHROMATOGRAPHY

INCLUDING ELECTROPHORESIS AND OTHER SEPARATION METHODS

**EDITORS**

U.A.Th. Brinkman (Amsterdam)  
 R.W. Giese (Boston, MA)  
 J.K. Haken (Kensington, N.S.W.)  
 K. Macek (Prague)  
 L.R. Snyder (Orinda, CA)

EDITORS, SYMPOSIUM VOLUMES,  
 E. Heftmann (Orinda, CA), Z. Deyl (Prague)

**EDITORIAL BOARD**

D.W. Armstrong (Rolla, MO)  
 W.A. Aue (Halifax)  
 P. Boček (Brno)  
 A.A. Boulton (Saskatoon)  
 P.W. Carr (Minneapolis, MN)  
 N.H.C. Cooke (San Ramon, CA)  
 V.A. Davankov (Moscow)  
 Z. Deyl (Prague)  
 S. Dilli (Kensington, N.S.W.)  
 H. Engelhardt (Saarbrücken)  
 F. Erni (Basle)  
 M.B. Evans (Hatfield)  
 J.L. Glajch (N. Billerica, MA)  
 G.A. Guiochon (Knoxville, TN)  
 P.R. Haddad (Hobart, Tasmania)  
 I.M. Hais (Hradec Kralove)  
 W.S. Hancock (San Francisco, CA)  
 S. Hjertén (Uppsala)  
 S. Honda (Higashi-Osaka)  
 Cs. Horváth (New Haven, CT)  
 J.F.K. Huber (Vienna)  
 K.-P. Hupe (Waldbronn)  
 T.W. Hutchens (Houston, TX)  
 J. Janák (Brno)  
 P. Jandera (Pardubice)  
 B.L. Karger (Boston, MA)  
 J.J. Kirkland (Newport, DE)  
 E. sz. Kováts (Lausanne)  
 A.J.P. Martin (Cambridge)  
 L.W. McLaughlin (Chestnut Hill, MA)  
 E.D. Morgan (Keele)  
 J.D. Pearson (Kalamazoo, MI)  
 H. Poppe (Amsterdam)  
 F.E. Regnier (West Lafayette, IN)  
 P.G. Righetti (Milan)  
 P. Schoenmakers (Eindhoven)  
 R. Schwarzenbach (Dübendorf)  
 R.E. Shoup (West Lafayette, IN)  
 R.P. Singhel (Wichita, KS)  
 A.M. Sioffi (Marseille)  
 D.J. Strýdom (Boston, MA)  
 N. Tanaka (Kyoto)  
 S. Terabe (Hyogo)  
 K.K. Unger (Mainz)  
 R. Verpoorte (Leiden)  
 Gy. Vigh (College Station, TX)  
 J.T. Watson (East Lansing, MI)  
 B.D. Westerlund (Uppsala)

**EDITORS, BIBLIOGRAPHY SECTION**

Z. Deyl (Prague), J. Janák (Brno), V. Schwartz (Prague)

ELSEVIER

# JOURNAL OF CHROMATOGRAPHY

INCLUDING ELECTROPHORESIS AND OTHER SEPARATION METHODS

**Scope.** The *Journal of Chromatography* publishes papers on all aspects of **chromatography, electrophoresis** and related methods. Contributions consist mainly of research papers dealing with chromatographic theory, instrumental developments and their applications. The section *Biomedical Applications*, which is under separate editorship, deals with the following aspects: developments in and applications of chromatographic and electrophoretic techniques related to clinical diagnosis or alterations during medical treatment; screening and profiling of body fluids or tissues related to the analysis of active substances and to metabolic disorders; drug level monitoring and pharmacokinetic studies; clinical toxicology; forensic medicine; veterinary medicine; occupational medicine; results from basic medical research with direct consequences in clinical practice. In *Symposium volumes*, which are under separate editorship, proceedings of symposia on chromatography, electrophoresis and related methods are published.

**Submission of Papers.** The preferred medium of submission is on disk with accompanying manuscript (see *Electronic manuscripts* in the Instructions to Authors, which can be obtained from the publisher, Elsevier Science Publishers B.V., P.O. Box 330, 1000 AH Amsterdam, Netherlands). Manuscripts (in English; four copies are required) should be submitted to: Editorial Office of *Journal of Chromatography*, P.O. Box 681, 1000 AR Amsterdam, Netherlands, Telefax (+31-20) 5862 304, or to: The Editor of *Journal of Chromatography, Biomedical Applications*, P.O. Box 681, 1000 AR Amsterdam, Netherlands. Review articles are invited or proposed in writing to the Editors who welcome suggestions for subjects. An outline of the proposed review should first be forwarded to the Editors for preliminary discussion prior to preparation. Submission of an article is understood to imply that the article is original and unpublished and is not being considered for publication elsewhere. For copyright regulations, see below.

**Publication.** The *Journal of Chromatography* (incl. *Biomedical Applications*) has 40 volumes in 1993. The subscription prices for 1993 are:

*J. Chromatogr.* (incl. *Cum. Indexes, Vols. 601-650*) + *Biomed. Appl.* (Vols. 612-651):

Dfl. 8520.00 plus Dfl. 1320.00 (p.p.h.) (total ca. US\$ 5466.75)

*J. Chromatogr.* (incl. *Cum. Indexes, Vols. 601-650*) only (Vols. 623-651):

Dfl. 7047.00 plus Dfl. 957.00 (p.p.h.) (total ca. US\$ 4446.75)

*Biomed. Appl.* only (Vols. 612-622):

Dfl. 2783.00 plus Dfl. 363.00 (p.p.h.) (total ca. US\$ 1747.75).

**Subscription Orders.** The Dutch guilder price is definitive. The US\$ price is subject to exchange-rate fluctuations and is given as a guide. Subscriptions are accepted on a prepaid basis only, unless different terms have been previously agreed upon. Subscriptions orders can be entered only by calendar year (Jan.-Dec.) and should be sent to Elsevier Science Publishers, Journal Department, P.O. Box 211, 1000 AE Amsterdam, Netherlands, Tel. (+31-20) 5803 642, Telefax (+31-20) 5803 598, or to your usual subscription agent. Postage and handling charges include surface delivery except to the following countries where air delivery via SAL (Surface Air Lift) mail is ensured: Argentina, Australia, Brazil, Canada, China, Hong Kong, India, Israel, Japan\*, Malaysia, Mexico, New Zealand, Pakistan, Singapore, South Africa, South Korea, Taiwan, Thailand, USA. \*For Japan air delivery (SAL) requires 25% additional charge of the normal postage and handling charge. For all other countries airmail rates are available upon request. Claims for missing issues must be made within six months of our publication (mailing) date, otherwise such claims cannot be honoured free of charge. Back volumes of the *Journal of Chromatography* (Vols. 1-611) are available at Dfl. 230.00 (plus postage). Customers in the USA and Canada wishing information on this and other Elsevier journals, please contact Journal Information Center, Elsevier Science Publishing Co. Inc., 655 Avenue of the Americas, New York, NY 10010, USA, Tel. (+1-212) 633 3750, Telefax (+1-212) 633 3764.

**Abstracts/Contents Lists** published in Analytical Abstracts, Biochemical Abstracts, Biological Abstracts, Chemical Abstracts, Chemical Titles, Chromatography Abstracts, Current Awareness in Biological Sciences (CABS), Current Contents/Life Sciences, Current Contents/Physical, Chemical & Earth Sciences, Deep-Sea Research/Part B: Oceanographic Literature Review, Excerpta Medica, Index Medicus, Mass Spectrometry Bulletin, PASCAL-CNRS, Referativnyi Zhurnal, Research Alert and Science Citation Index.

**US Mailing Notice.** *Journal of Chromatography* (ISSN 0021-9673) is published weekly (total 52 issues) by Elsevier Science Publishers (Sara Burgerhartstraat 25, P.O. Box 211, 1000 AE Amsterdam, Netherlands). Annual subscription price in the USA US\$ 4446.75 (subject to change), including air speed delivery. Second class postage paid at Jamaica, NY 11431. **USA POSTMASTERS:** Send address changes to *Journal of Chromatography*, Publications Expediting, Inc., 200 Meacham Avenue, Elmont, NY 11003. Airfreight and mailing in the USA by Publications Expediting.

**See inside back cover** for Publication Schedule, Information for Authors and information on Advertisements.

© 1993 ELSEVIER SCIENCE PUBLISHERS B.V. All rights reserved.

0021-9673/93/\$06.00

No part of this publication may be reproduced, stored in a retrieval system or transmitted in any form or by any means, electronic, mechanical, photocopying, recording or otherwise, without the prior written permission of the publisher, Elsevier Science Publishers B.V., Copyright and Permissions Department, P.O. Box 521, 1000 AM Amsterdam, Netherlands.

Upon acceptance of an article by the journal, the author(s) will be asked to transfer copyright of the article to the publisher. The transfer will ensure the widest possible dissemination of information.

**Special regulations for readers in the USA.** This journal has been registered with the Copyright Clearance Center, Inc. Consent is given for copying of articles for personal or internal use, or for the personal use of specific clients. This consent is given on the condition that the copier pays through the Center the per-copy fee stated in the code on the first page of each article for copying beyond that permitted by Sections 107 or 108 of the US Copyright Law. The appropriate fee should be forwarded with a copy of the first page of the article to the Copyright Clearance Center, Inc., 27 Congress Street, Salem, MA 01970, USA. If no code appears in an article, the author has not given broad consent to copy and permission to copy must be obtained directly from the author. All articles published prior to 1980 may be copied for a per-copy fee of US\$ 2.25, also payable through the Center. This consent does not extend to other kinds of copying, such as for general distribution, resale, advertising and promotion purposes, or for creating new collective works. Special written permission must be obtained from the publisher for such copying.

No responsibility is assumed by the Publisher for any injury and/or damage to persons or property as a matter of products liability, negligence or otherwise, or from any use or operation of any methods, products, instructions or ideas contained in the materials herein. Because of rapid advances in the medical sciences, the Publisher recommends that independent verification of diagnoses and drug dosages should be made.

Although all advertising material is expected to conform to ethical (medical) standards, inclusion in this publication does not constitute a guarantee or endorsement of the quality or value of such product or of the claims made of it by its manufacturer.

This issue is printed on acid-free paper.

Printed in the Netherlands

## CONTENTS

(Abstracts/Contents Lists published in Analytical Abstracts, Biochemical Abstracts, Biological Abstracts, Chemical Abstracts, Chemical Titles, Chromatography Abstracts, Current Awareness in Biological Sciences (CABS), Current Contents/Life Sciences, Current Contents/Physical, Chemical & Earth Sciences, Deep-Sea Research/Part B: Oceanographic Literature Review, Excerpta Medica, Index Medicus, Mass Spectrometry Bulletin, PASCAL-CNRS, Referativnyi Zhurnal, Research Alert and Science Citation Index)

## REGULAR PAPERS

*Column Liquid Chromatography*

- Assessment of peak homogeneity in liquid chromatography using multivariate chemometric techniques  
by H.R. Keller, P. Kiechle and F. Erni (Basle, Switzerland), D.L. Massart (Brussels, Belgium) and J.L. Excoffier (Walnut Creek, CA, USA) (Received January 19th, 1993). . . . . 1
- Chiral stationary phase design. Use of intercalative effects to enhance enantioselectivity  
by W.H. Pirkle and P.G. Murray (Urbana, IL, USA) (Received January 19th, 1993) . . . . . 11
- Use of homologous series of analytes as mechanistic probes to investigate the origins of enantioselectivity on two chiral stationary phases  
by W.H. Pirkle, P.G. Murray and J.A. Burke (Urbana, IL, USA) (Received January 19th, 1993) . . . . . 21
- High-performance chiral displacement chromatographic separations in the normal-phase mode. I. Retention and adsorption studies of potential displacers developed for the Pirkle-type naphthylalanine silica stationary phase  
by P.L. Camacho-Torralba and Gy. Vigh (College Station, TX, USA) and D.H. Thompson (Beaverton, OR, USA) (Received February 23rd, 1993) . . . . . 31
- Liquid chromatographic chiral separations of the N-6-(endo-2-norbornyl)-9-methyladenine enantiomers  
by D.T. Witte (Groningen, Netherlands), M. Ahnoff and K.-E. Karlsson (Möln dal, Sweden) and J.-P. Franke and R.A. de Zeeuw (Groningen, Netherlands) (Received March 2nd, 1993) . . . . . 39
- Shape-selective separation of polycyclic aromatic hydrocarbons by reversed-phase liquid chromatography on tetraphenylporphyrin-based stationary phases  
by C.E. Kibbey and M.E. Meyerhoff (Ann Arbor, MI, USA) (Received March 9th, 1993) . . . . . 49
- Solid-phase extraction of phenols using membranes loaded with modified polymeric resins  
by L. Schmidt, J.J. Sun and J.S. Fritz (Ames, IA, USA) and D.F. Hagen, C.G. Markell and E.E. Wisted (St. Paul, MN, USA) (Received March 5th, 1993). . . . . 57
- Analytical gel filtration of dextran for study of the glomerular barrier function  
by L. Hagel (Uppsala, Sweden) and A. Hartmann and K. Lund (Oslo, Norway) (Received December 23rd, 1992) 63
- Analysis and purification of monomethoxy-polyethylene glycol by vesicle and gel permeation chromatography  
by B. Selisko, C. Delgado and D. Fisher (London, UK) and R. Ehwald (Berlin, Germany) (Received March 18th, 1993) . . . . . 71
- Phytoecdysteroid analysis by high-performance liquid chromatography-thermospray mass spectrometry  
by M.-P. Marco, F.J. Sánchez-Baeza, F. Camps and J. Coll (Barcelona, Spain) (Received March 3rd, 1993). . . . 81
- Trace determination of weathered atrazine and terbuthylazine and their degradation products in soil by high-performance liquid chromatography-diode-array detection  
by R. Schewes, F.X. Mairl and G. Fischbeck (Freising-Weihenstephan, Germany) and J. Lepschy von Gleissenthal and A. Süß (Freising, Germany) (Received March 10th, 1993) . . . . . 89
- Isolation and determination of AAL phytotoxins from corn cultures of the fungus *Alternaria alternata* f. sp. *lycopersici*  
by G.S. Shephard, P.G. Thiel, W.F.O. Marasas and E.W. Sydenham (Tygerberg, South Africa) and R. Vleggaar (Pretoria, South Africa) (Received February 10th, 1993). . . . . 95
- Chromatographic behaviour of some platinum(II) complexes on octadecylsilica dynamically modified with a mixture of a cationic and an anionic amphiphilic modifier  
by M. Macka and J. Borák (Brno, Czech Republic) (Received January 18th, 1993) . . . . . 101

(Continued overleaf)

ห้องสมุดกรมวิทยาศาสตร์บริการ

๒๑ ก.ค. ๒๕๓๖



Contents (continued)

Gas Chromatography

- Systematic analysis of naturally occurring linear and branched polyamines by gas chromatography and gas chromatography-mass spectrometry  
by M. Niitsu and K. Samejima (Saitama, Japan), S. Matsuzaki (Tochigi, Japan) and K. Hamana (Gunma, Japan)  
(Received February 22nd, 1993) . . . . . 115

Supercritical Fluid Chromatography

- Quantitative analysis of polyethoxylated octylphenol by capillary supercritical fluid chromatography  
by Z. Wang and M. Fingas (Ottawa, Canada) (Received March 8th, 1993) . . . . . 125
- Specific effects of modifiers in subcritical fluid chromatography of carotenoid pigments  
by E. Lesellier (Orsay, France), A.M. Krstulović (Meudon-la-Forêt, France) and A. Tchapla (Orsay, France)  
(Received February 12th, 1993) . . . . . 137

Electrophoresis

- Inter-company cross-validation exercise on capillary electrophoresis. I. Chiral analysis of clenbuterol  
by K.D. Altria (Ware, UK), R.C. Harden (Windlesham, UK), M. Hart (Dagenham, UK), J. Hevizi (Welwyn Garden City, UK), P.A. Hailey (Sandwich, UK), J.V. Makwana (Nottingham, UK) and M.J. Portsmouth (Loughborough, UK) (Received March 16th, 1993) . . . . . 147
- Automated isotachopheretic analyte focusing for capillary zone electrophoresis in a single capillary using hydrodynamic back-pressure programming  
by N.J. Reinhoud, U.R. Tjaden and J. van der Greef (Leiden, Netherlands) (Received January 25th, 1993) . . . . . 155
- Optimizing dynamic range for the analysis of small ions by capillary zone electrophoresis  
by G.W. Tindall, D.R. Wilder and R.L. Perry (Kingsport, TN, USA) (Received February 23rd, 1993) . . . . . 163

SHORT COMMUNICATIONS

Column Liquid Chromatography

- Determination of proline by reversed-phase high-performance liquid chromatography with automated pre-column *o*-phthalaldehyde derivatization  
by G. Wu (College Station, TX, USA) (Received March 12th, 1993) . . . . . 168
- New labelling agent, 2-[2-(isocyanate)ethyl]-3-methyl-1,4-naphthoquinone, for high-performance liquid chromatography of hydroxysteroids with electrochemical detection  
by M. Nakajima, H. Wakabayashi, S. Yamato and K. Shimada (Niigata, Japan) (Received March 31st, 1993) . . . . . 176
- Analytical studies of *dl*-stylopine in *Chelidonium majus* L. using high-performance liquid chromatography  
by J.-P. Rey, J. Levesque and J.-L. Pousset (Poitiers, France) (Received April 6th, 1993) . . . . . 180
- Reversed-phase high-performance liquid chromatographic determination of sulphide in an aqueous matrix using 2-iodo-1-methylpyridinium chloride as a precolumn ultraviolet derivatization reagent  
by E. Bald and S. Sypniewski (Łódź, Poland) (Received March 5th, 1993) . . . . . 184

Gas Chromatography

- Capability of a carbon support to improve the gas chromatographic performance of a liquid crystal phase in a packed column for some volatile oil constituents  
by T.J. Betts (Perth, Australia) (Received April 2nd, 1993) . . . . . 189
- Unusual deuterium isotope effect on the retention of formamides in gas-liquid chromatography  
by J. Mráz (Prague, Czech Republic), P. Jheeta and A. Gescher (Birmingham, UK) and M.D. Threadgill (Bath, UK)  
(Received March 26th, 1993) . . . . . 194
- Quantitative determination of dehydroabietic acid methyl ester in disproportionated rosin  
by M.J. Brites, A. Guerreiro, B. Gigante and M.J. Marcelo-Curto (Queluz, Portugal) (Received April 5th, 1993) 199

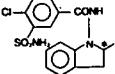
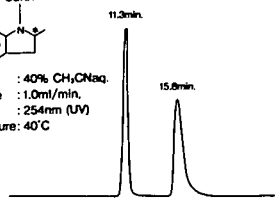
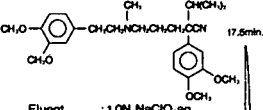
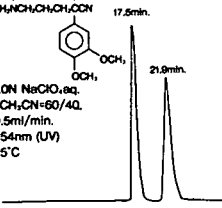
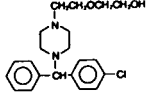
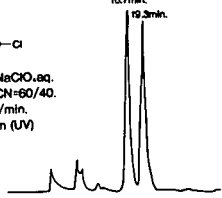
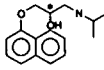
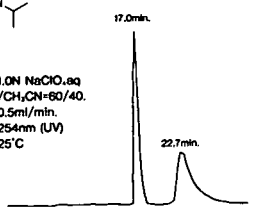
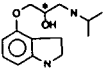
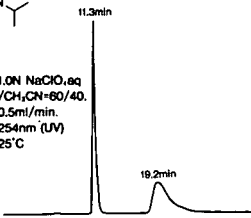
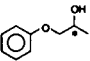
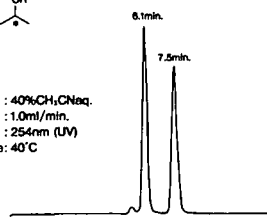
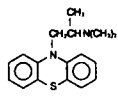
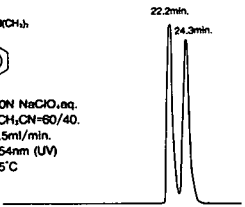
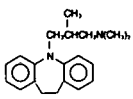
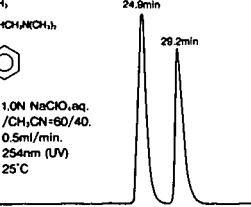
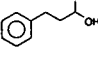
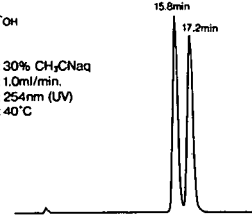
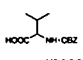
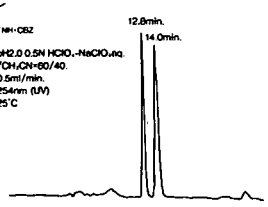
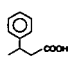
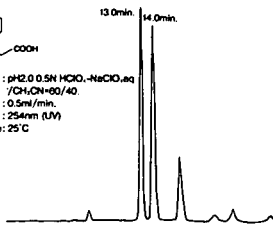
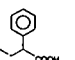
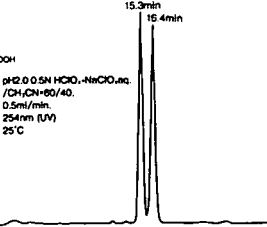
BOOK REVIEW

- A practical guide to HPLC detection (edited by D. Parriott), reviewed by E.S. Yeung (Ames, IA, USA) . . . . . 203



# Reversed Phase CHIRAL HPLC Column

## NEW CHIRALCEL® OD-R

<p><b>Indapamide</b></p>  <p>Eluent : 40% CH<sub>3</sub>CN/aq. Flow Rate : 1.0ml/min. Detection : 254nm (UV) Temperature: 40°C</p> 	<p><b>Verapamil</b></p>  <p>Eluent : 1.0N NaClO<sub>4</sub>aq. /CH<sub>3</sub>CN=60/40. Flow Rate : 0.5ml/min. Detection : 254nm (UV) Temperature: 25°C</p> 	<p><b>Hydroxyzine</b></p>  <p>Eluent : 1.0N NaClO<sub>4</sub>aq. /CH<sub>3</sub>CN=60/40. Flow Rate : 0.5ml/min. Detection : 254nm (UV) Temperature: 25°C</p> 
<p><b>Propranolol</b></p>  <p>Eluent : 1.0N NaClO<sub>4</sub>aq. /CH<sub>3</sub>CN=60/40. Flow Rate : 0.5ml/min. Detection : 254nm (UV) Temperature: 25°C</p> 	<p><b>Pindolol</b></p>  <p>Eluent : 1.0N NaClO<sub>4</sub>aq. /CH<sub>3</sub>CN=60/40. Flow Rate : 0.5ml/min. Detection : 254nm (UV) Temperature: 25°C</p> 	<p><b>1-Phenoxy-2-Propanol</b></p>  <p>Eluent : 40%CH<sub>3</sub>CN/aq. Flow Rate : 1.0ml/min. Detection : 254nm (UV) Temperature: 40°C</p> 
<p><b>Alimemazine</b></p>  <p>Eluent : 1.0N NaClO<sub>4</sub>aq. /CH<sub>3</sub>CN=60/40. Flow Rate : 0.5ml/min. Detection : 254nm (UV) Temperature: 25°C</p> 	<p><b>Trimepramine</b></p>  <p>Eluent : 1.0N NaClO<sub>4</sub>aq. /CH<sub>3</sub>CN=60/40. Flow Rate : 0.5ml/min. Detection : 254nm (UV) Temperature: 25°C</p> 	<p><b>4-Pheny-2-butanol</b></p>  <p>Eluent : 30% CH<sub>3</sub>CN/aq. Flow Rate : 1.0ml/min. Detection : 254nm (UV) Temperature: 40°C</p> 
<p><b>CBZ-Val.</b></p>  <p>Eluent : pH2.0 0.5N HClO<sub>4</sub>-NaClO<sub>4</sub>aq. /CH<sub>3</sub>CN=60/40. Flow Rate : 0.5ml/min. Detection : 254nm (UV) Temperature: 25°C</p> 	<p><b>3-Phenylbutyric acid</b></p>  <p>Eluent : pH2.0 0.5N HClO<sub>4</sub>-NaClO<sub>4</sub>aq. /CH<sub>3</sub>CN=60/40. Flow Rate : 0.5ml/min. Detection : 254nm (UV) Temperature: 25°C</p> 	<p><b>2-Phenylbutyric acid</b></p>  <p>Eluent : pH2.0 0.5N HClO<sub>4</sub>-NaClO<sub>4</sub>aq. /CH<sub>3</sub>CN=60/40. Flow Rate : 0.5ml/min. Detection : 254nm (UV) Temperature: 25°C</p> 

For more information about CHIRALCEL OD-R column, please give us a call.



**DAICEL CHEMICAL INDUSTRIES, LTD.**

CHIRAL CHEMICALS DIVISION 8-1, Kasumigaseki 3-chome, Chiyoda-ku, Tokyo 100, JAPAN  
Phone: +81-3-3507-3151 Facsimile: +81-3-3507-3193

**AMERICA**  
CHIRAL TECHNOLOGIES, INC.  
730 SPRINGDALE DRIVE  
DRAWER I EXTON, PA 19341  
Phone: 215-594-2100  
Facsimile: 215-594-2325

**EUROPE**  
DAICEL (EUROPA) GmbH  
Ost Street 22  
4000 Düsseldorf 1, Germany  
Phone: +49-211-369848  
Facsimile: +49-211-364429

**ASIA/OCEANIA**  
DAICEL CHEMICAL (ASIA) PTE. LTD.  
65 Chulia Street #40-07  
OCBC Centre, Singapore 0104.  
Phone: +65-5332511  
Facsimile: +65-5326454

# Capillary Electrophoresis

## Principles, Practice and Applications

by S.F.Y. LI, National University of Singapore, Singapore

NOW ALSO  
IN PAPERBACK

Journal of Chromatography Library Volume 52

Capillary Electrophoresis (CE) has had a very significant impact on the field of analytical chemistry in recent years as the technique is capable of very high resolution separations, requiring only small amounts of samples and reagents. Furthermore, it can be readily adapted to automatic sample handling and real time data processing. Many new methodologies based on CE have been reported. Rapid, reproducible separations of extremely small amounts of chemicals and biochemicals, including peptides, proteins, nucleotides, DNA, enantiomers, carbohydrates, vitamins, inorganic ions, pharmaceuticals and environmental pollutants have been demonstrated. A wide range of applications have been developed in greatly diverse fields, such as chemical, biotechnological, environmental and pharmaceutical analysis.

This book covers all aspects of CE, from the principles and technical aspects to the most important applications. It is intended to meet the growing need for a thorough and balanced treatment of CE. The book will serve as a comprehensive reference work and can also be used as a textbook for advanced undergraduate and graduate courses. Both the experienced analyst and the newcomer will find the text useful.

### Contents:

**1. Introduction.** Historical Background. Overview of High Performance CE. Principles of Separations. Comparison with Other Separation Techniques.  
**2. Sample Injection Methods.** Introduction. Electrokinetic

Injection. Hydrodynamic Injection. Electric Sample Splitter. Split Flow Syringe Injection System. Rotary Type Injector. Freeze Plug Injection. Sampling Device with Feeder. Microinjectors. Optical Gating. **3. Detection Techniques.** Introduction. UV-Visible Absorbance Detectors. Photodiode Array Detectors. Fluorescence Detectors. Laser-based Thermo-optical and Refractive Index Detectors. Indirect Detection. Conductivity Detection. Electrochemical Detection. Mass Spectrometric Detection. **4. Column Technology.** Uncoated Capillary Columns. Coated Columns. Gel-filled Columns. Packed Columns. Combining Packed and Open-Tubular Column. **5. Electrophoretic Media.** Electrophoretic Buffer Systems. Micellar Electrokinetic Capillary Chromatography. Inclusion Pseudophases. Metal-complexing Pseudophases. Other Types of Electrophoretic Media. **6. Special Systems and Methods.** Buffer Programming. Fraction Collection. Hyphenated Techniques. Field Effect Electroosmosis. Systematic Optimization of Separation. **7. Applications of CE.** Biomolecules. Pharmaceutical and Clinical Analysis. Inorganic Ions. Hydrocarbons. Foods and Drinks. Environmental Pollutants. Carbohydrates. Toxins. Polymers and Particles. Natural Products.

Fuel. Metal Chelates. Industrial Waste Water. Explosives. Miscellaneous Applications. **8. Recent Advances and Prospect for Growth.** Recent Reviews in CE. Advances in Injection Techniques. Novel Detection Techniques. Advances in Column Technology. Progress on Electrolyte Systems. New Systems and Methods. Additional Applications Based on CE. Future Trends.

### References. Index.

1992 608 pages Hardbound  
US\$ 225.75 / Dfl. 395.00

ISBN 0-444-89433-0

1993 608 pages Paperback  
Price: US\$ 114.25 / Dfl. 200.00

ISBN 0-444-81590-2

*"Everything seems to be there, any detection system you have ever dreamed of, any capillary coating, enough electrolyte systems to saturate your wits, and more..."*

*"...by far the most thorough and comprehensive book in the field yet to appear."*

P.G. Righetti, Milan

### ORDER INFORMATION

For USA and Canada

ELSEVIER SCIENCE

PUBLISHERS

Judy Weislogel,

P.O. Box 945

Madison Square Station,

New York, NY 10160-0757

Fax: (212) 633 3880

In all other countries

ELSEVIER SCIENCE

PUBLISHERS

P.O. Box 211,

1000 AE Amsterdam

The Netherlands

Fax: (+31-20) 5803 705

US\$ prices are valid only for the USA & Canada and are subject to exchange rate fluctuations; in all other countries the Dutch guilder price (Dfl.) is definitive. Customers in the European Community should add the appropriate VAT rate applicable in their country to the price(s). Books are sent postfree if prepaid.



ELSEVIER  
SCIENCE PUBLISHERS

JOURNAL OF CHROMATOGRAPHY

VOL. 641 (1993)





# JOURNAL of CHROMATOGRAPHY

INCLUDING ELECTROPHORESIS AND OTHER SEPARATION METHODS

## EDITORS

U.A.Th. BRINKMAN (Amsterdam), R.W. GIESE (Boston, MA), J.K. HAKEN (Kensington, N.S.W.), K. MACEK (Prague),  
L.R. SNYDER (Orinda, CA)

## EDITORS, SYMPOSIUM VOLUMES

E. HEFTMANN (Orinda, CA), Z. DEYL (Prague)

## EDITORIAL BOARD

D.W. Armstrong (Rolla, MO), W.A. Aue (Halifax), P. Boček (Brno), A.A. Boulton (Saskatoon), P.W. Carr (Minneapolis, MN), N.H.C. Cooke (San Ramon, CA), V.A. Davankov (Moscow), Z. Deyl (Prague), S. Dilli (Kensington, N.S.W.), H. Engelhardt (Saarbrücken), F. Erni (Basle), M.B. Evans (Hatfield), J.L. Glajch (N. Billerica, MA), G.A. Guiochon (Knoxville, TN), P.R. Haddad (Hobart, Tasmania), I.M. Hais (Hradec Králové), W.S. Hancock (San Francisco, CA), S. Hjertén (Uppsala), S. Honda (Higashi-Osaka), Cs. Horváth (New Haven, CT), J.F.K. Huber (Vienna), K.-P. Hupe (Waldbronn), T.W. Hutchens (Houston, TX), J. Janák (Brno), P. Jandera (Pardubice), B.L. Karger (Boston, MA), J.J. Kirkland (Newport, DE), E. sz. Kováts (Lausanne), A.J.P. Martin (Cambridge), L.W. McLaughlin (Chestnut Hill, MA), E.D. Morgan (Keele), J.D. Pearson (Kalamazoo, MI), H. Poppe (Amsterdam), F.E. Regnier (West Lafayette, IN), P.G. Righetti (Milan), P. Schoenmakers (Eindhoven), R. Schwarzenbach (Dübendorf), R.E. Shoup (West Lafayette, IN), R.P. Singhal (Wichita, KS), A.M. Siouffi (Marseille), D.J. Strydom (Boston, MA), N. Tanaka (Kyoto), S. Terabe (Hyogo), K.K. Unger (Mainz), R. Verpoorte (Leiden), Gy. Vigh (College Station, TX), J.T. Watson (East Lansing, MI), B.D. Westerlund (Uppsala)

## EDITORS, BIBLIOGRAPHY SECTION

Z. Deyl (Prague), J. Janák (Brno), V. Schwarz (Prague)



ELSEVIER  
AMSTERDAM — LONDON — NEW YORK — TOKYO

*J. Chromatogr.*, Vol. 641 (1993)

ห้องสมุดกรมวิทยาศาสตร์บริการ

© 1993 ELSEVIER SCIENCE PUBLISHERS B.V. All rights reserved.

0021-9673/93/\$06.00

No part of this publication may be reproduced, stored in a retrieval system or transmitted in any form or by any means, electronic, mechanical, photocopying, recording or otherwise, without the prior written permission of the publisher, Elsevier Science Publishers B.V., Copyright and Permissions Department, P.O. Box 521, 1000 AM Amsterdam, Netherlands.

Upon acceptance of an article by the journal, the author(s) will be asked to transfer copyright of the article to the publisher. The transfer will ensure the widest possible dissemination of information.

Submission of an article for publication entails the authors' irrevocable and exclusive authorization of the publisher to collect any sums or considerations for copying or reproduction payable by third parties (as mentioned in article 17 paragraph 2 of the Dutch Copyright Act of 1912 and the Royal Decree of June 20, 1974 (S. 351) pursuant to article 16 b of the Dutch Copyright Act of 1912) and/or to act in or out of Court in connection therewith.

**Special regulations for readers in the USA.** This journal has been registered with the Copyright Clearance Center, Inc. Consent is given for copying of articles for personal or internal use, or for the personal use of specific clients. This consent is given on the condition that the copier pays through the Center the per-copy fee stated in the code on the first page of each article for copying beyond that permitted by Sections 107 or 108 of the US Copyright Law. The appropriate fee should be forwarded with a copy of the first page of the article to the Copyright Clearance Center, Inc., 27 Congress Street, Salem, MA 01970, USA. If no code appears in an article, the author has not given broad consent to copy and permission to copy must be obtained directly from the author. All articles published prior to 1980 may be copied for a per-copy fee of US\$ 2.25, also payable through the Center. This consent does not extend to other kinds of copying, such as for general distribution, resale, advertising and promotion purposes, or for creating new collective works. Special written permission must be obtained from the publisher for such copying.

No responsibility is assumed by the Publisher for any injury and/or damage to persons or property as a matter of products liability, negligence or otherwise, or from any use or operation of any methods, products, instructions or ideas contained in the materials herein. Because of rapid advances in the medical sciences, the Publisher recommends that independent verification of diagnoses and drug dosages should be made.

Although all advertising material is expected to conform to ethical (medical) standards, inclusion in this publication does not constitute a guarantee or endorsement of the quality or value of such product or of the claims made of it by its manufacturer.

This issue is printed on acid-free paper.

Printed in the Netherlands



CHROM. 25 026

# Assessment of peak homogeneity in liquid chromatography using multivariate chemometric techniques

H.R. Keller\*, P. Kiechle and F. Erni

*Sandoz Pharma AG, Analytical Research and Development, CH-4002 Basle (Switzerland)*

D.L. Massart

*Pharmaceutical Institute, Vrije Universiteit Brussel, Laarbeeklaan 103, B-1090 Brussels (Belgium)*

J.L. Excoffier

*Varian Chromatography Systems, 2700 Mitchell Drive, Walnut Creek, CA 94598 (USA)*

(First received November 6th, 1992; revised manuscript received January 19th, 1993)

---

## ABSTRACT

The performance of three new chemometric techniques was evaluated systematically for assessment of peak homogeneity in liquid chromatography with photodiode-array detection. Multi-component analysis, window evolving factor analysis and the HELP method performed equally well in this study. Without making any assumption about peak shape or spectra, these methods were able to detect less than 1% of a spectrally similar impurity under a chromatographic peak, even if the chromatographic separation was low. The limitations of these techniques are also discussed.

---

## INTRODUCTION

One of the most general and demanding problems in liquid chromatography (LC) is the assessment of peak homogeneity. After the synthesis of a drug, for instance, one has to ensure the absence of side products, isomers and degradation products. In practice, less than 1% of such impurities needs to be detected. As these impurities are often chemically related to the substance of interest, their chromatographic behaviour and spectra are often very similar. As a consequence, assurance of peak homogeneity is far from being trivial.

Single-wavelength UV detectors usually cannot solve such serious problems in LC, and a spectroscopic instrument is used instead. Most frequently, a photodiode-array detector (DAD) is coupled to the chromatographic system. Such a coupled instrument measures a complete UV spectrum at each chromatographic data point. Alternatively, one may say that many chromatograms are measured, each at a different wavelength. One common way of representation is a data table (matrix), where the rows correspond to the consecutively recorded spectra and the columns represent the chromatograms measured at different wavelengths. The amount of data obtained from a single experiment is very large and the problem is to extract the relevant information.

---

\* Corresponding author. Present address: Ciba-Geigy Ltd., Central Analytics, CH-4002 Basle, Switzerland.

Owing to its simplicity, the ratiogram method is probably the most popular technique for the assessment of peak homogeneity in LC–DAD [1,2]. This method works on the signals from two different wavelengths and can only be applied successfully if the spectra of all analytes are known in advance, which is generally not the case. Further, ratiograms are difficult to interpret. Visual inspection of spectra and chromatograms, spectral suppression using two discrete wavelengths and derivative chromatography have also been proposed for the assessment of peak homogeneity [3–6]. These methods have in common that they work on a very small part of the LC–DAD data only. As a consequence, they cannot solve the general problem, where a small amount of an unknown impurity with a similar spectrum has to be detected, even if chromatographic separation is low. Castledine *et al.* [7,8] have recently introduced very promising correlation-based algorithms. Using reference samples of known purity, they were able to detect as little as 1% of an impurity under a chromatographic peak, no matter how low the chromatographic separation was.

For cases where pure reference samples are not *a priori* available, multivariate methods have been developed that can be applied successfully for the assessment of peak homogeneity in LC–DAD.

## THEORY

The main idea of all the three multivariate techniques compared in this study is to monitor the shape of the spectra as a function of analysis time. If the shape of the spectra remains constant within the noise, the chromatographic peak is considered to be homogeneous.

### Multi-component analysis (MCA)

Multi-component analysis (MCA) is a least-squares deconvolution technique that has been known for many years [9,10]. Provided that the number of analytes and their spectra are known, MCA can be used to determine the concentration of the individual species from the spectrum of the mixture. Excoffier *et al.* [11] proposed MCA for rapid quantitative analysis in

LC–DAD. They also introduced a modification of MCA for the assessment of peak homogeneity that works as follows.

First, an average spectrum is calculated for the peak of interest. Every measured spectrum is then compared with that reference spectrum using a root-mean-square (RMS) value:

$$\text{RMS}_i = \sqrt{\frac{\sum_{j=1}^n (x_{ij} - c_i \bar{x}_j)^2}{n}} \quad (1)$$

where  $\text{RMS}_i$  is the RMS value for spectrum  $i$ ,  $x_{ij}$  is the signal for spectrum  $i$  and wavelength  $j$ ,  $c_i$  is a scaling factor obtained by a least-squares fit (“reconstructed chromatogram”),  $\bar{x}_j$  is the average signal for wavelength  $j$  and  $n$  is the number of wavelengths. This  $\text{RMS}_i$  is a measure of the difference between a single spectrum  $i$  and the average (reference) spectrum. For homogeneous peaks, where the consecutively recorded spectra change only within the noise, plotting RMS vs. analysis time (number of spectrum) will result in a more or less horizontal line. In the case of an impurity, however, such an RMS plot will indicate the magnitude and location of spectral differences. This procedure is equivalent to the results obtained with full spectral suppression of the average spectrum. To compare these RMS values more objectively with the noise of the system, an RMS threshold can be determined from the same experiment, using a region of the chromatogram where no substance elutes.

### Window evolving factor analysis (WEFA)

Evolving factor analysis (EFA) is a general method for the analysis of multivariate data with an intrinsic order [12,13]. EFA is based on the concept of factor analysis and has been applied successfully in different fields of chemistry. In principle, EFA can be used to determine the number of substances in a mixture and their concentration profiles and spectra.

For the assessment of peak homogeneity in LC–DAD, Keller and co-workers [14–16] proposed a modified version of EFA, called window EFA (WEFA). This method works as follows. Starting with the first  $k$  spectra of the recorded data, one calculates the eigenvalues (EVs) of

these  $k$  spectra. These EVs represent systematic effects in the underlying data and their magnitude. In a next step, the EVs of spectra 2 to  $k + 1$  are determined. This procedure is then repeated until the whole data table has been analysed. The results are finally visualized by plotting these EVs vs. analysis time. To make such graphs easier to interpret, the points representing the largest (first) EV are connected with a line. In the same way, lines are also drawn to connect the other EVs. In a pure sample, where the spectrum of the analyte does not change across the chromatographic peak, there is only one source of systematic variation in the data. Consequently, a single peak in the EV vs. time plot will result. In the case of an impurity, however, one will observe a second peak in the WEFA plot. In analogy to MCA, a threshold value obtained from baseline spectra can also be set, providing a means to interpret WEFA graphs more objectively.

#### *Heuristic evolving latent projections (HELP)*

Related to WEFA is the concept of the heuristic evolving latent projections (HELP) method [17,18]. HELP first performs ordinary principal component analysis (PCA) on the whole data table. PCA is a standard method for analysis of multivariate data; its main purpose is data reduction by replacing the many measured variables (different wavelengths) by a small number of new, abstract variables, which are called principal components (PCs). These PCs are a linear combination of the original variables and still contain most of the information. HELP represents the spectra by their first two PCs. In such a PC plot, those parts of the chromatogram where only one analyte elutes appear as a more or less straight line, directed towards the origin of the coordinate system. Visual inspection of PC plots will therefore indicate regions where there is only one substance present.

The second part of HELP inspects these straight lines in more detail and ensures that there is only one compound present. To do this, the abstract spectra (loadings) from those parts of the chromatogram are calculated and inspected visually. The EVs are also determined

and compared with those obtained from the baseline. An application of HELP for assessment of peak homogeneity in LC-DAD can be found in ref. 19.

In principle, neither WEFA nor HELP requires any special data pretreatment, and PCA can be performed directly on the raw data using the NIPALS algorithm [20,21]. However, to overcome instrumental or experimental difficulties, scan time correction and baseline correction may be needed, as discussed below.

It is the aim of this paper to compare the performances of these three fully multivariate methods for the assessment of peak homogeneity in LC-DAD.

#### EXPERIMENTAL SECTION

##### *Apparatus*

The liquid chromatograph was a Varian (Walnut Creek, CA, USA) LC Star system, consisting of a Model 9010 pump and a Rheodyne (Cotati, CA, USA) injection valve fitted with a 20- $\mu$ l sample loop and connected to a Model 9100 autosampler. A 100  $\times$  4.6 mm I.D. RP-18 column (Brownlee, 5  $\mu$ m) (Applied Biosystems, San Jose, CA, USA) was used at ambient temperature. Spectra were collected on a Polychrom Model 9065 diode-array detector, covering the wavelength range 220–367 nm and scanning spectra at a frequency of 16 Hz.

Instrument control, data storage and analysis were performed on a Compaq (Houston, TX, USA) Deskpro 386/25m IBM-compatible personal computer with math coprocessor.

##### *Reagents and samples*

All solvents were of HPLC grade (Rathburn, Walkerburn, UK, and Merck, Darmstadt, Germany). Water was purified using a Milli-Q system (Millipore) and analytical-reagent grade diammonium hydrogenphosphate and phosphoric acid (Merck) were used to prepare a 0.01 M phosphate buffer of pH 2.5. The sample consisted of an acidic, pharmacologically active drug (1.0  $\mu$ g on-column) and its spectrally similar isomer, used as available in the laboratory (Fig. 1).



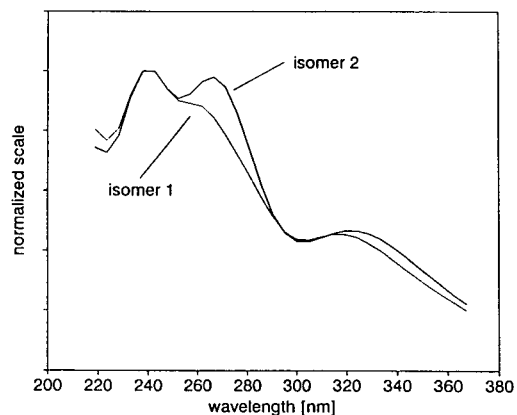


Fig. 1. Normalized spectra of the two isomers ( $r = 0.980$ ).

### Procedure

All analyses with the two isomers were carried out isocratically at a flow-rate of  $2.0 \text{ ml min}^{-1}$ . To obtain the different degrees of separation, the mobile phase consisted of 40–70% acetonitrile in  $0.01 \text{ M}$  phosphate buffer (pH 2.5). Chromatographic resolution between the two analytes could thereby be adjusted in the range of  $R_s = 0.1$ – $1.0$  (calculated on the basis of a concentration ratio of 100:1).

To separate the two isomers completely, a  $250 \times 4.6 \text{ mm}$  I.D. ODS-Hypersil column ( $5 \mu\text{m}$ ) (Bischoff, Leonberg, Germany) was used in combination with gradient elution [28–52% acetonitrile in  $0.01 \text{ M}$  phosphate buffer (pH 2.5) within 22 min at a flow-rate of  $1.5 \text{ ml min}^{-1}$ ].

### Data analysis

After collection, data were analysed with MCA using PolyView 2.0 software (Varian). A program written in-house in BASIC 7.0 (Microsoft, Redmond, WA, USA) was used for data analysis with WEFA and HELP. WEFA was performed on  $k = 7$  consecutive spectra, which was found to be appropriate for most applications studied so far.

## RESULTS AND DISCUSSION

### Results obtained from a heterogeneous peak

To illustrate the three different techniques, the results obtained from a sample containing 2% of the impurity at  $R_s = 0.6$  are given in Figs. 2 and

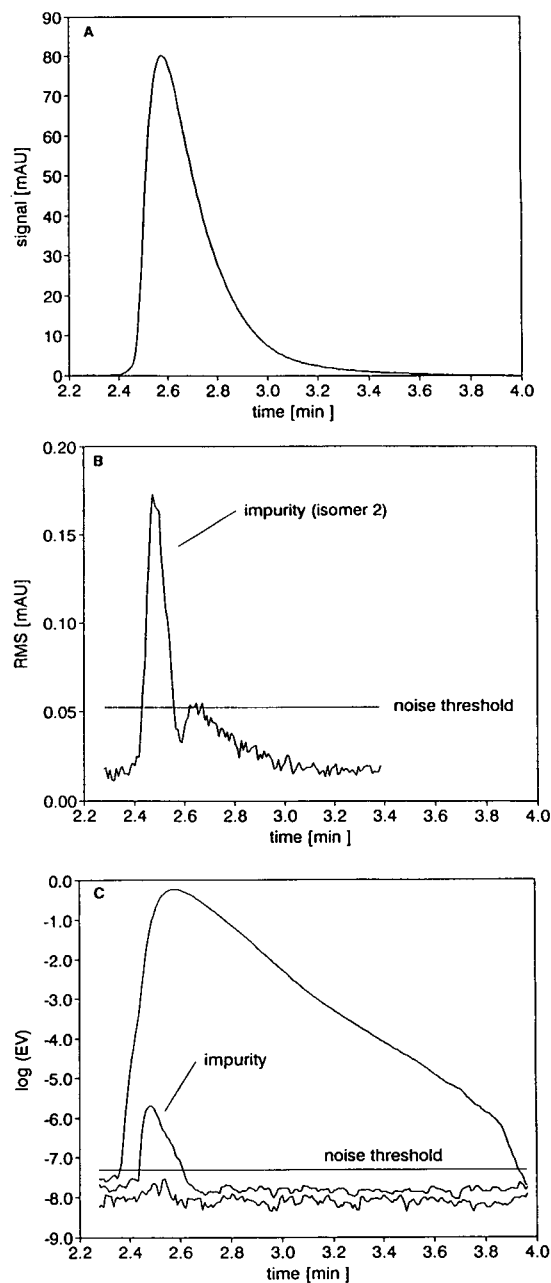


Fig. 2. Results obtained from a sample containing 2% of impurity at  $R_s = 0.6$ . (A) Chromatogram at 239 nm; (B) RMS plot of MCA; (C) WEFA plot.

3. In the MCA error plot (Fig. 2b), one observes the highest RMS values around 2.5 min. At that point on the chromatogram, the measured spectra differ most from the average spectrum. In

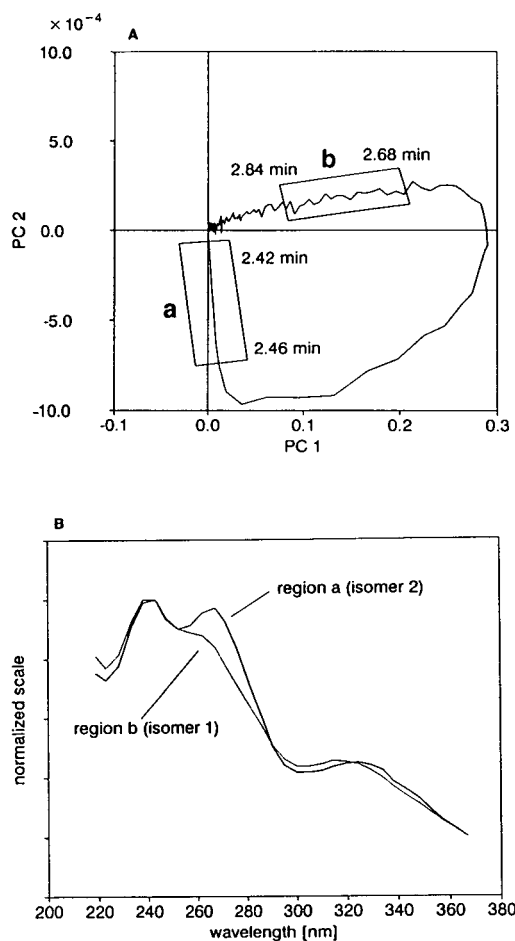


Fig. 3. HELP plots obtained from a sample containing 2% of impurity at  $R_s = 0.6$ . (A) Each point representing a spectrum is characterized by its scores on the first two PCs ( $PC_1$ ,  $PC_2$ ). Those parts of the chromatogram where only one analyte elutes appear as more or less straight lines directed towards the origin of the coordinate system (a, b). Note that  $PC_2$  is scale expanded. (B) The loadings obtained on  $PC_1$  from these two regions a and b correspond to the spectra of the two analytes.

fact, these high RMS values exceed the threshold obtained from noise and therefore indicate a significant deviation from the average spectrum. In this case, the impurity has a retention time of about 2.5 min and is situated on the upslope of the chromatographic peak (Fig. 2a). The spectra measured before and after compare with the average spectrum within the noise, which is represented by RMS values well below the threshold line.

To summarize the results of WEFA, the logarithms of the EVs are plotted vs. analysis time (Fig. 2c). Up to about 2.35 min no substance elutes from the column. The first (largest) EV,  $EV_1$ , represents noise; its level is about  $\log(EV_1) = -7.5$ . Later in the chromatogram, one observes two peaks that are caused by the two underlying substances. Owing to the tailing of the chromatographic peak and the logarithmic representation of the results,  $EV_1$  seems to be high after 3.0 min; it falls to the noise level only at 4.0 min. The second peak in the WEFA plot appears to be relatively small. Still, a comparison of the maximum of the second EV [ $\log(EV_2) = -5.7$ ] with the noise threshold [ $\log(EV_2) = -7.3$ ] shows that this  $EV_2$  is more than an order of magnitude larger than the noise.

The results obtained with HELP appear to be different, because there is no time axis (Fig. 3a). The individual spectra (points in time) are represented on the first two PCs instead. From 2.42 to 2.46 min only one isomer elutes (region a). As the spectral shape does not change in that part of the chromatogram, points representing the consecutively recorded spectra fall on a line that is directed towards the origin of the coordinate system. Thus, visual inspection of such a scores plot permits parts of the chromatogram to be selected where only one compound elutes. A second pure compound region can be found, e.g., from 2.68 to 2.84 min (region b). Comparison of regions a and b might lead to the wrong conclusion that noise is larger in b. This is not the case, however, and can be explained with the expanded scale on  $PC_2$ . In the second part of HELP, the EVs of these pure compound regions are determined and compared with those from noise. Table I shows that in the two pure compound regions  $EV_1$  is much larger than the noise. Hence the spectra change systematically. As  $EV_2$  and  $EV_3$  of the two regions a and b are comparable to the EVs of noise, only one substance is present in each of the two regions. In a last step, the abstract spectra (loadings) obtained from the two regions are plotted and visually compared with each other. Fig. 3b demonstrates that the loadings obtained from the two pure compound regions are different. Consequently, there are two analytes present in the sample.

TABLE I  
EIGENVALUES FROM NOISE AND PURE COMPOUND REGIONS

Region	Time range (min)	EV <sub>1</sub>	EV <sub>2</sub>	EV <sub>3</sub>
Baseline (noise)	2.25–2.30	$2.9 \cdot 10^{-8}$	$2.1 \cdot 10^{-8}$	$5.8 \cdot 10^{-9}$
Region a	2.42–2.46	$2.8 \cdot 10^{-4}$	$1.5 \cdot 10^{-8}$	$1.0 \cdot 10^{-8}$
Region b	2.68–2.84	$4.0 \cdot 10^{-1}$	$3.5 \cdot 10^{-8}$	$2.2 \cdot 10^{-8}$

Also, the loadings compare closely with the spectra obtained from pure samples (Fig. 1).

The main purpose of this study was to compare the performances of new multivariate techniques for the assessment of peak homogeneity in LC-DAD. Therefore, both the chromatographic separations between the analytes and the relative concentrations were changed systematically. As the third variable that is highly relevant for the performance of all methods, *i.e.*, the spectral similarity between the analytes, cannot easily be changed, it was held constant. The signal-to-noise ratio for the isocratic runs was found to be 4000.

#### Results obtained from a homogeneous peak

To demonstrate the results obtained from a homogeneous peak, an illustrative example is given below. For a homogeneous peak, the shape of the spectra varies only within the noise. Consequently, the average spectrum in MCA matches the spectra that were measured across the chromatographic peak. In such a case, the RMS values represent noise and remain below the threshold, as shown in Fig. 4b. Analogously, in WEFA there is only one peak; EV<sub>2</sub> represents noise and does not exceed the threshold either (Fig. 4c). As there is only one systematic effect present, PC<sub>1</sub> of the HELP method explains virtually all variations in the data (Fig. 5). PC<sub>2</sub> is much smaller and represents only noise. In this case, the line indicating a pure compound region is identical with PC<sub>1</sub>, while random noise causes the points representing spectra to be located to a small degree on either side of PC<sub>1</sub>. As the peak is homogeneous, a second straight line cannot be found and there is no need to determine the loadings. As completely pure reference material was not available and as a complete separation of the two isomers studied here could not be

obtained with isocratic elution, a gradient system was used to generate a homogeneous peak. Although, owing to gradient elution, the noise level was higher in the latter example, Figs. 4 and 5 clearly illustrate the results obtained from a homogeneous peak.

#### Performance of the different methods

To quantify the performance of the methods to be evaluated, we chose the detection limit of an impurity as the criterion. For MCA the criterion selected to detect the impurity was an RMS value exceeding the threshold, which was calculated as three times the noise. Analogously, the threshold value for WEFA was set to the mean EV<sub>1</sub> plus three standard deviations obtained from the noise; an EV<sub>2</sub> exceeding that threshold was considered to indicate the impurity. For the HELP method more subjective criteria were used. Two (more or less) straight lines were selected, and the loadings obtained from these regions were compared visually. Different loadings indicated an impurity.

The limits of detection of one isomer in the other are summarized in Fig. 6. Above and to the right of the line the impurity was detected. One observes for instance, that the impurity could be detected at the 0.5% level for  $R_s$  values of at least 0.3. Lower relative concentrations were not detected. Similarly, if the chromatographic separation drops below 0.3, the impurity could only be detected at a higher relative concentration. Interestingly, all three methods performed equally well in detecting one isomer under the other. One should also note that none of the tested methods makes any assumption about peak shape, chromatographic separation or similarity of the spectra. Further, the pure compound spectra need not be known in advance. It should be noted, however, that the

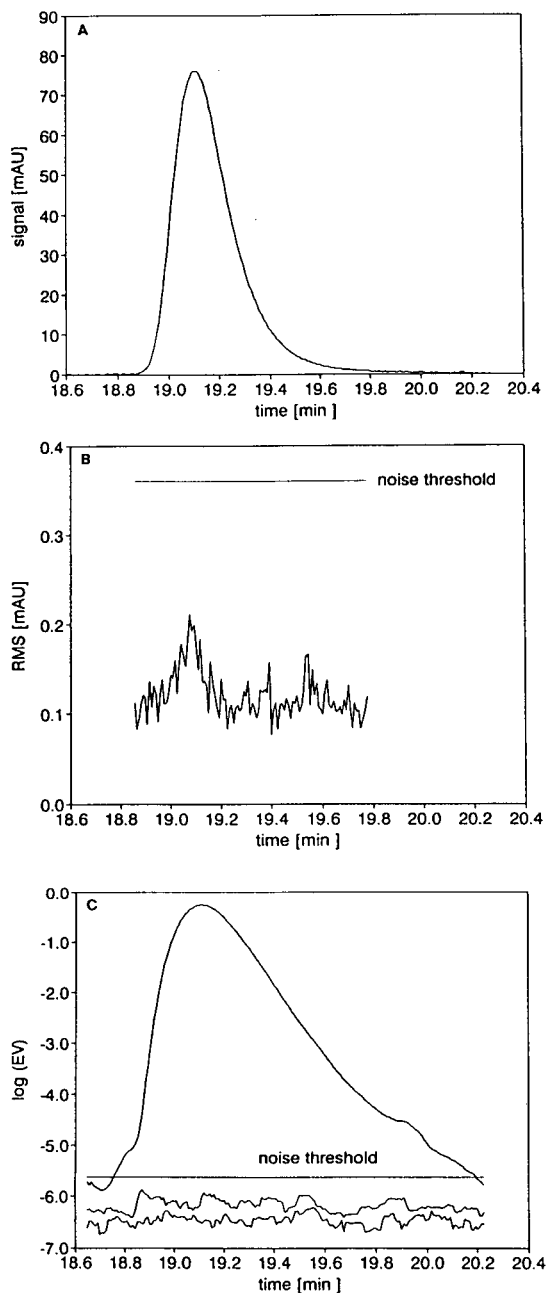


Fig. 4. Results obtained from a homogeneous peak. (A) Chromatogram at 239 nm; (B) RMS plot of MCA; (C) WEFA plot.

degree of spectral similarity will strongly affect the results obtained with the different methods. Although the influence of the similarity of the spectra cannot be quantified at present, one may

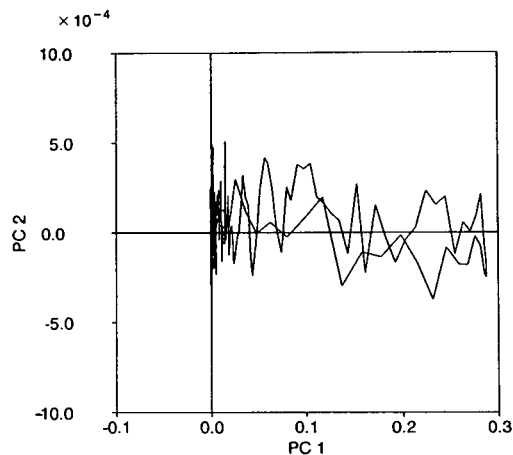


Fig. 5. HELP scores plot obtained from a homogeneous peak. Each point representing a spectrum is characterized by its scores on the first two PCs ( $PC_1$ ,  $PC_2$ ). Note that  $PC_2$  is scale expanded.

state that the methods tend to perform better the more dissimilar are the spectra, whereas the performance must be expected to decrease for more similar spectra. Still, we consider the example given here as being representative for problems observed in our laboratory. Work is in progress to understand better the effect of this parameter.

As the problem dealt with in this study is the assessment of peak homogeneity, results were shown for both a homogeneous and a heteroge-

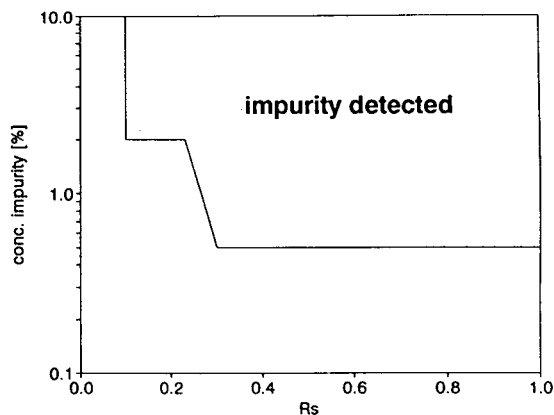


Fig. 6. Limits of detection of isomer 2 in isomer 1, obtained with all three methods and given as a function of relative concentration and chromatographic separation. Above and to the right of the line an impurity was detected with MCA, WEFA and HELP.

neous peak. The latter instance is the simplest and most representative example for a non-homogeneous peak. Very similar results are obtained for situations where more than two substances co-elute. It is important to remember, however, that detection of one or more impurities demands a (minimum) difference in both time and spectra.

#### *Possible limitations*

Generally, the smaller the chromatographic separation, the lower the relative concentration of the impurity, the more similar the spectra and the higher the noise level, the more difficult the problem is. Consequently, all methods fail to detect the very lowest concentration at  $R_s = 0.1$ .

On the other hand, instrumental and experimental difficulties must also be taken into account. MCA, WEFA and HELP all rely on linear mathematical techniques, *i.e.*, Beer's law has to be valid. Non-linearities may be due to different phenomena, such as a non-linear calibration graph, a non-zero or sloping baseline, polychromatic radiation, the DAD scan rate and noise [22].

In practice, one therefore has to be certain to work in the linear range of the calibration graph, which depends on both the instrument and the absorbance value. Non-zero or sloping baselines will seriously affect the results; adequate baseline correction before applying linear mathematical methods is therefore very important. As reported by Dose and Guiochon [23], the polychromatic radiation measured at each diode can also cause non-linearities, because Beer's law is valid for monochromatic radiation only. For cases where a spectrum changes considerably within the optical bandwidth of the diode-array detector, non-linearities can also be introduced. The time required to measure a spectrum by DAD can also lead to non-idealities, as discussed elsewhere [24]. For the system used in this study, scan time correction was performed automatically in the detector using the method reported in ref. 24. For some instruments, the noise level is a function of the signal, which is known as heteroscedasticity. This phenomenon is less obvious but can lead to serious problems in practice. A detailed discussion can be found in ref. 15.

Additionally, one should also be aware of possible pH effects and solvent effects, which could change the spectrum of a pure analyte during the chromatographic run.

For the present study, which was carried out under isocratic conditions and at relatively low concentrations of the analytes (signals not exceeding 100 milliabsorbance), the above limitations appeared not to be relevant for the instrument used. The only requirement was adequate baseline correction, implemented in the following way. First, two average spectra were calculated from the spectra measured before and after the chromatographic peak. The baseline was then estimated by linear interpolation between these two average spectra and subtracted from the raw data. After such a baseline correction there was no sign of any experimental or instrumental limitation of the methods discussed in this paper.

#### *Comparison of the different methods*

Although the three methods performed equally well, one should also note their merits and limitations. MCA has the advantage of being less complex and therefore easier to understand than the other techniques. In principle, MCA is an automated method. Still, one should bear in mind that a good peak detection algorithm is required, because inclusion of too many baseline spectra would reduce the quality of the average (reference) spectrum and thereby reduce the performance of the method.

WEFA and HELP both rely on the concept of PCA and are therefore similar. Among the three techniques WEFA can be automated most easily because no user interaction is required. A commercial example of this is Beckman's System Gold, which corresponds closely to WEFA and which can be used for the automated assessment of peak homogeneity in real time. As the selection of straight lines in the HELP method can be a difficult task in some instances, much experience and user interaction are required for this method. On the other hand, HELP is at the same time the most flexible and powerful method, because pure compound spectra can easily be found.

## CONCLUSIONS

MCA, WEFA and HELP can be applied successfully for the assessment of peak homogeneity in LC-DAD. Without making any assumption about the chromatograms or spectra, less than 1% of a spectrally similar impurity could be detected under a chromatographic peak. As could be expected, for very small amounts of the impurity and very low  $R_s$  values the methods fail. Although the tested methods worked well, one should also be aware of possible instrumental and experimental difficulties.

## ACKNOWLEDGEMENT

The authors thank O.M. Kvalheim for his collaboration.

## REFERENCES

- 1 A.C.J.H. Drouen, H.A.H. Billiet and L. de Galan, *Anal. Chem.*, 56 (1984) 971.
- 2 F.V. Warren, Jr., B.A. Bidlingmeyer and M.F. Delaney, *Anal. Chem.*, 59 (1987) 1897.
- 3 G.T. Carter, R.E. Schiesswohl, H. Burke and R. Yang, *J. Pharm. Sci.*, 71 (1982) 317.
- 4 A.F. Fell, H.P. Scott, R. Gill and A.C. Moffat, *J. Chromatogr.*, 282 (1983) 123.
- 5 B.J. Clark, A.F. Fell, H.P. Scott and D. Westerlund, *J. Chromatogr.*, 286 (1984) 261.
- 6 T. Alfredson and T. Sheehan, *J. Chromatogr. Sci.*, 24 (1986) 473.
- 7 J.B. Castledine, A.F. Fell, R. Modin and B. Sellberg, *Anal. Proc.*, 29 (1992) 100.
- 8 J.B. Castledine, A.F. Fell, R. Modin and B. Sellberg, *J. Chromatogr.*, 592 (1992) 27.
- 9 R.P. Bauman, *Appl. Spectrosc.*, 13 (1959) 156.
- 10 M.J. Milano, S. Lam, M. Savonis, D.B. Pautler, J.W. Pav and E. Grushka, *J. Chromatogr.*, 149 (1978) 599.
- 11 J.L. Excoffier, M. Joseph, J.J. Robinson and T.L. Sheehan, *J. Chromatogr.*, 631 (1993) 15.
- 12 M. Maeder, *Anal. Chem.*, 59 (1987) 527.
- 13 H.R. Keller and D.L. Massart, *Chemometr. Intell. Lab. Syst.*, 12 (1992) 209.
- 14 H.R. Keller and D.L. Massart, *Anal. Chim. Acta*, 246 (1991) 379.
- 15 H.R. Keller, D.L. Massart, Y.Z. Liang and O.M. Kvalheim, *Anal. Chim. Acta*, 263 (1992) 29.
- 16 H.R. Keller, D.L. Massart, J.O. de Beer, *Anal. Chem.*, 65 (1993) 471.
- 17 O.M. Kvalheim and Y.Z. Liang, *Anal. Chem.*, 64 (1992) 936.
- 18 Y.Z. Liang, O.M. Kvalheim, H.R. Keller, D.L. Massart, P. Kiechle and F. Erni, *Anal. Chem.*, 64 (1992) 946.
- 19 H.R. Keller, D.L. Massart, Y.Z. Liang and O.M. Kvalheim, *Anal. Chim. Acta*, 267 (1992) 63.
- 20 S. Wold, K. Esbensen and P. Geladi, *Chemometr. Intell. Lab. Syst.*, 2 (1987) 37.
- 21 B.G.M. Vandeginste, C. Sielhorst and M. Gerritsen, *Trends Anal. Chem.*, 7 (1988) 286.
- 22 H.R. Keller and D.L. Massart, *Anal. Chim. Acta*, 263 (1992) 21.
- 23 E.V. Dose and G. Guiochon, *Anal. Chem.*, 61 (1989) 2571.
- 24 H.R. Keller, D.L. Massart, P. Kiechle and F. Erni, *Anal. Chim. Acta*, 256 (1992) 125.



## Chiral stationary phase design

# Use of intercalative effects to enhance enantioselectivity

William H. Pirkle\* and Patrick G. Murray

*School of Chemical Sciences, University of Illinois, Box 44, Roger Adams Laboratory, 1209 West California Street, Urbana, IL 61801 (USA)*

(Received January 19th, 1993)

---

### ABSTRACT

Two new chiral stationary phases derived from L-proline were designed specifically to separate the enantiomers of N-(3,5-dinitrobenzoyl) amino acid esters and amides and related analytes. The incorporation of structural features which diminish the retention of the first eluting enantiomers has led to the observation of separation factors as high as eighty for selected N-(3,5-dinitrobenzoyl)leucine amides using a normal mobile phase and as high as seven using a reversed mobile phase. The mechanistic rationale by which these chiral stationary phases were designed and the underlying reasons for the high levels of enantioselectivity are discussed.

---

### INTRODUCTION

Owing to the increasingly common need to determine enantiomeric purity, the development of chiral stationary phases for the gas and liquid chromatographic separation of a wide range of enantiomers has been rapid (see, for example, ref. 1). Accompanying this development has been a growing understanding of the mechanisms by which enantioselectivity occurs. For the chemist, the challenge now lies in collecting observations and making deductions relevant to the improvement of existing chiral selectors and the development of new chiral selectors for targeted classes of molecules. Synthetic brush-type chiral phases are particularly suited to these activities.

For example, in endeavoring to design effective chiral stationary phases, one wishes to tailor the chiral stationary phase (CSP) so as to afford

high affinity for one enantiomer while reducing affinity for the other. The latter, often more difficult than the former, basically requires that one restrict access of the least retained enantiomer to polar binding sites in the CSP. Polar functionality in the CSP which is not essential to the chiral recognition process is best eliminated, for it is deleterious to enantioselectivity [2]. Additionally, the quasi-membrane-like structure of brush-type phases can introduce subtle, second-order perturbations of the primary chiral recognition mechanism(s). These can often be used to advantage in increasing enantioselectivity. For instance, should one analyte enantiomer intercalate a portion of its structure (*e.g.* a long alkyl group) between the strands of bonded phase, enantioselectivity can be influenced dramatically [3]. Control of the conformational mobility of the CSP can also enhance chiral recognition if properly applied. Clearly, one wishes to populate a conformation which permits only the more retained enantiomer access to sites where bonding interactions occur. Mechanistic

---

\* Corresponding author.



insights such as these, combined with a growing understanding of chiral recognition processes, are beginning to enable us to design chiral phases specifically intended to separate the enantiomers of particular classes of substrates [4,5].

Various derivatives of proline have been used as the chiral sorbent in the gas chromatographic separation of enantiomers [6]. Likewise, proline and hydroxyproline have served as selectors in the separation of a number of bidentate-like enantiomers by ligand-exchange chromatography [7]. However, other attempts to utilize a proline-based chiral selector for the liquid chromatographic separation of enantiomers have met with but modest success [8–11].

We had reason to believe that the conformational rigidity of proline could be used to advantage in designing a chiral stationary phase capable of rendering high levels of enantioselectivity for specifiable analytes. We report herein two such chiral phases, discuss the implications of the design, and demonstrate the levels of enantioselectivity which can be realized when one applies those principles of CSP design which are thus far understood.

## EXPERIMENTAL

### Chromatography

Chromatography was performed with an Aspec-Bischoff Model 2200 isocratic HPLC pump, a Rheodyne Model 7125 injector equipped with a 20- $\mu$ l sample loop, a Milton-Roy LDC UV Monitor D fixed-wavelength detector operating at 254 nm, and a Hewlett-Packard 3394A recording integrator. A Euromark HPLC column oven was used to maintain a constant temperature of 20°C. Normal-phase void volumes were determined using 1,3,5-tri-*tert*-butylbenzene, and reversed-phase void volumes were determined using NaI in methanol.

The olefinic precursors to CSPs I and II were prepared according to the scheme shown in Fig. 1.

### *N*-Benzyloxycarbonyl-*L*-proline (A)

In a 250-ml flask equipped with a magnetic stir bar 11.5 g (0.099 mol) of *L*-proline was dissolved

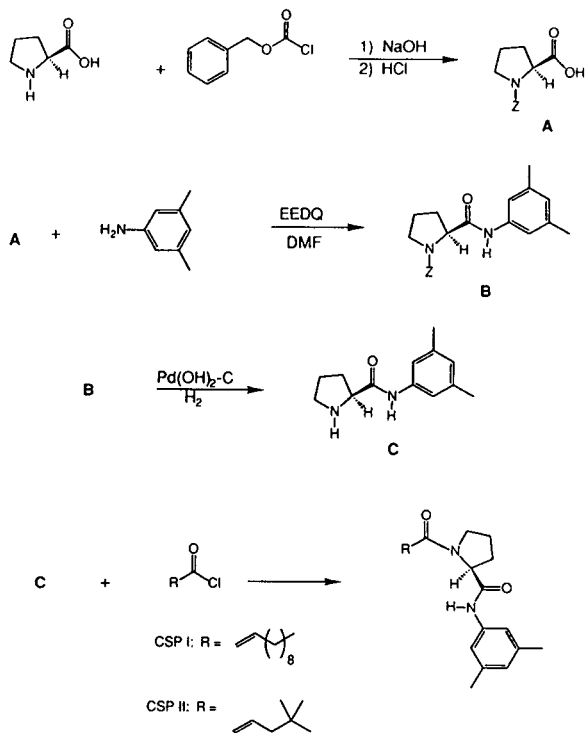


Fig. 1. Synthesis of olefinic precursors to CSPs I and II. EEDQ = 2-Ethoxy-1-ethoxy-carbonyl-1,2-dihydroquinoline; DMF = dimethylformamide.

in 50 ml of 2 M NaOH. The mixture was cooled to 0°C and 16 ml (0.105 mol) of benzyl chloroformate and 50 ml of 2N NaOH were added in portions with stirring over the course of 1 h. When the additions were complete, the reaction mixture was stirred for an additional 30 min at 0°C, and then allowed to warm to room temperature and stirred for another 30 min. The alkaline reaction mixture was extracted twice with 75-ml portions of diethyl ether, and the ether extracts discarded. The aqueous layer was acidified to Congo blue with 6 M HCl, and extracted three times with diethyl ether. The ether extracts were combined, dried with MgSO<sub>4</sub>, and concentrated under reduced pressure to give 23.4 g of a colorless solid, yield 95%, m.p. 75–76°C. <sup>1</sup>H NMR (C<sup>2</sup>HCl<sub>3</sub>) 200 MHz  $\delta$  7.30 (s, 5H); 5.10 (s, 2H); 4.40 (m, 1H); 3.50 (m, 2H); 2.30–1.80 (m, 4H). IR (mull) cm<sup>-1</sup> 2980, 2886, 1741, 1358, 1176, 1122, 1089.

*N*-(Benzyloxycarbonyl)-*L*-proline-3,5-dimethylanilide (**B**)

*N*-Benzyloxycarbonyl-*L*-proline, 6.91 g (0.027 mol), 7.34 g (0.030 mol) of 2-ethoxy-1-ethoxycarbonyl-1,2-dihydroquinoline (EEDQ), and 50 ml of dry dimethylformamide were placed in a 100-ml flask equipped with a magnetic stir bar. The mixture was stirred until homogeneous, and then 3.70 g (0.030 mol) of freshly distilled 3,5-dimethylaniline was added. The reaction mixture was stirred overnight, and the contents of the flask were poured into a 250-ml separatory funnel containing 75 ml of ethyl acetate. A 75-ml volume of water was added to the separatory funnel and the layers were separated. The organic layer was washed sequentially with two more 75-ml portions of water, two 50-ml portions of 2 *M* HCl, and two 50-ml portions of 5% NaHCO<sub>3</sub>. The ethyl acetate layer was dried with MgSO<sub>4</sub>, filtered, concentrated under reduced pressure, and dried *in vacuo* to give 8.08 g of a white solid, 85% yield, m.p. 138–140°C. <sup>1</sup>H NMR (C<sup>2</sup>HCl<sub>3</sub>) 200 MHz δ 9.00 (br s, 1H), 7.40 (br s, 5H), 7.10 (s, 2H); 6.80 (s, 1H), 5.20 (s, 2H), 4.50 (m, 1H), 3.50 (m, 2H), 2.60–2.40 (m, 2H); 2.30 (s, 6H), 1.90 (m, 2H). Analysis for C<sub>21</sub>H<sub>24</sub>O<sub>3</sub>N<sub>2</sub>: calculated C 71.57; H 6.86; N 7.95; found C 71.13; H 6.90; N 7.84.

*L*-Proline-3,5-dimethylanilide hydrochloride (**C**)

*N*-(Benzyloxycarbonyl)-*L*-proline-3,5-dimethylanilide, 6.0 g (0.017 mol), was dissolved with gentle heating in 50 ml dry ethanol, placed in a heavy walled pressure bottle, and 600 mg of 20% Pd(OH)<sub>2</sub> on carbon (Pearlman's catalyst) was added along with 2 drops of glacial acetic acid. The pressure bottle was installed in a Parr hydrogenator, flushed with nitrogen, and rocked under 20 p.s.i. (1 p.s.i. = 6894.76 Pa) of hydrogen for 12 h. After this time, the pressure bottle was removed from the apparatus, and the contents of the bottle filtered through Celite. The filtrate was concentrated under reduced pressure to give 3.71 g of a pasty white solid (100% yield). The residue was dissolved in dry dichloromethane and converted to the hydrochloride salt with gaseous HCl. m.p. 245°C (decomp). <sup>1</sup>H NMR ([<sup>2</sup>H<sub>6</sub>]dimethyl sulfoxide) 200 MHz δ 10.90 (s, 1H); 7.40 (s, 2H); 6.80 (s, 1H); 4.50 (t,

1H); 3.50 (s, 2H); 3.30 (m, 2H); 2.50 (m, 2H); 2.30 (s, 6H); 200 (br s, 2H). Analysis for C<sub>13</sub>H<sub>19</sub>O<sub>2</sub>N<sub>2</sub>Cl: calculated: C 61.29; H 7.52; N 11.00; found: C 61.04; H 7.48; N 11.07.

*2,2-Dimethyl-4-pentenoic acid*

*2,2-Dimethyl-4-pentenoic acid* was prepared by oxidation of the corresponding aldehyde [12] using the following variation of a reported procedure [13]. Silver(II) oxide, 10.32 g (0.045 mol), was placed in a 250-ml flask equipped with a magnetic stir bar and covered with 75 ml of water. Sodium hydroxide, 8.91 g (0.223 mol), was added and the reaction mixture heated to 60°C. *2,2-Dimethyl-4-pentenal*, 5.0 g (0.045 mol), was added and the reaction mixture was stirred for 15 min at this temperature. Metallic silver forms and coats the walls of the reaction vessel. The mixture was then immediately filtered and the filter cake washed with two 25-ml portions of hot water. The filtrate was acidified with concentrated HCl and extracted 3 times with 75-ml portions of diethyl ether. The ether extracts were combined, dried with MgSO<sub>4</sub>, concentrated, and dried *in vacuo* to give 4.30 g of a pale yellow oil, yield 75%. <sup>1</sup>H NMR (C<sup>2</sup>HCl<sub>3</sub>) 200 MHz δ 12.00 (br s, 1H); 5.80 (m, 1H); 5.10 (dd, 2H); 2.30 (d, 2H); 1.10 (s, 6H). IR (neat) cm<sup>-1</sup> 2926, 1716, 1684, 1651, 1448, 1379, 1329, 1269, 908.

*2,2-Dimethyl-4-pentenoyl chloride*

*2,2-Dimethyl-4-pentenoic acid*, 4.0 g (0.031 mol), was dissolved in 20 ml dry dichloromethane and placed in a 50-ml round-bottom flask equipped with a magnetic stir bar. Oxalyl chloride, 5.9 g (0.047 mol) was added carefully, and the mixture was stirred under nitrogen for 40 min, after which time all gas evolution had ceased. The reaction mixture was then concentrated under reduced pressure to afford a yellow oil, 4.60 g, (quantitative yield). This material was used directly, without further purification.

*N*-(10-Undecenoyl)-*L*-proline-3,5-dimethylanilide

*L*-Proline-3,5-dimethylanilide, 1.98 g (0.009 mol), and 1.25 ml (0.009 mol) of triethylamine were dissolved in dry tetrahydrofuran in a 100-ml

flask equipped with a magnetic stir bar and cooled to 0°C. 2.02 g (0.010 ml) of 10-undecenoyl chloride was added in portions over 15 min. When the additions were complete, the reaction mixture was allowed to warm to room temperature and was stirred under nitrogen for 2 h. After this time, the triethylamine hydrochloride precipitate was removed by filtration, and the reaction mixture was concentrated to dryness on a rotary evaporator. The residue was taken up in 75 ml of diethyl ether, and washed with successive 50-ml portions of 5% NaHCO<sub>3</sub> and 2 M HCl. The organic layer was dried with MgSO<sub>4</sub>, concentrated, and dried *in vacuo* to yield 3.40 g of a pale yellow syrup (98% yield). <sup>1</sup>H NMR (C<sup>2</sup>HCl<sub>3</sub>) 200 MHz δ 9.60 (br s, 1H); 7.15 (s, 2H); 6.70 (s, 1H); 5.80 (m, 1H); 4.95 (m, 2H); 4.80 (d, 1H); 3.50 (m, 2H); 2.30 (m, 2H); 2.20–1.60 (messy, 6H); 2.25 (s, 6H); 1.30 (br s, 14H). Analysis for C<sub>24</sub>H<sub>36</sub>N<sub>2</sub>O<sub>2</sub>: calculated: C 74.96; H 9.44; N 7.28; found: C 74.97; H 9.46; N 7.29.

*N*-(2,2-Dimethyl-4-pentenoyl)-L-proline-3,5-dimethylanilide

L-Proline-3,5-dimethylanilide hydrochloride, 1.85 g (0.0073 mol), was placed in a 100-ml flask, and 30 ml of 5% NaOH and 30 ml of dichloromethane was added. The biphasic reaction mixture was stirred vigorously to dissolve the amine hydrochloride. 2,2-Dimethyl-4-pentenoyl chloride, 3.20 g (0.022 mol), was added in portions to the dichloromethane layer. The reaction mixture was stirred vigorously for 1 h. After this time, the layers were separated, the organic layer was washed with two 25-ml portions of 2 M HCl, dried with MgSO<sub>4</sub>, and concentrated under reduced pressure to give 2.00 g of a white solid, yield 84%. The product was purified by flash chromatography using a mobile phase consisting of an ethyl acetate–hexane (1:4) mixture to elute early running impurities, and then dichloromethane to elute the product. Yield after chromatography 1.5 g, 63%. m.p. 128–130°C. <sup>1</sup>H NMR (C<sup>2</sup>HCl<sub>3</sub>) 200 MHz δ 9.20 (br s, 1H); 7.10 (s, 2H); 6.70 (s, 1H); 5.60–5.90 (m, 1H); 5.00 (m, 2H); 4.80 (dd, 1H); 3.70 (m, 2H); 2.40 (d, 2H); 2.30 (s, 6H); 2.20–1.70 (m, 4H); 1.30 (s, 6H). Analysis for C<sub>20</sub>H<sub>28</sub>O<sub>2</sub>N<sub>2</sub>: calcu-

lated: C 73.14; H 8.59; N 8.53; found: C 73.25; H 8.52; N 8.26.

*N*-[11-(Dimethylethoxysilyl)undecanoyl]-L-proline-3,5-dimethylanilide

An oven-dried 100-ml flask equipped with a stir bar, condenser and a nitrogen inlet was charged with 5 ml of (CH<sub>3</sub>)<sub>2</sub>SiHCl, 2.9 g of N-(10-undecenoyl)-L-proline-3,5-dimethylanilide dissolved in 10 ml of dry dichloromethane, and about 30 mg of H<sub>2</sub>PtCl<sub>6</sub>. The mixture was refluxed for 6 h and then concentrated to dryness under reduced pressure. Residual (CH<sub>3</sub>)<sub>2</sub>SiHCl was chased with two 25-ml portions of dry dichloromethane. The resulting dark oil was taken up in 30 ml of anhydrous diethyl ether and treated with 10 ml of triethylamine–absolute ethanol (1:1). This mixture was heated to reflux for 10 min, filtered to removed the precipitated triethylamine hydrochloride, the filter cake was washed with two 15-ml portions of diethyl ether, and the filtrate and washings were combined and concentrated under reduced pressure. The residue was chromatographed on silica using 1.5% methanol in dichloromethane. The product was isolated as a pale yellow oil, 1.67 g (47% yield). <sup>1</sup>H NMR (C<sup>2</sup>HCl<sub>3</sub>) 200 MHz δ 9.2 (br s, 1H); 7.15 (s, 2H); 6.70 (s, 1H); 4.80 (d, 1H); 3.65 (q, 2H); 3.50 (m, 2H); 2.30 (m, 2H); 2.20–1.60 (m, 4H); 2.25 (s, 6H); 1.30 (br s, 16H); 1.00 (t, 3H); 0.50 (t, 2H); 0.00 (s, 6H).

*Preparation of CSP I*

The purified silane was dissolved in dichloromethane and added to a flask containing 5.0 g of 5 μm, 100 Å Rexchome silica (Regis, Morton Grove, IL, USA) which had been azeotropically dried with benzene. The slurry was sonicated for several minutes to insure complete coverage of the silica gel with the silane and the solvent was removed under reduced pressure. This procedure was repeated twice, with 1 ml of dimethylformamide being added the last time. The silica and the silane were then heated at 100°C under reduced pressure (1.0 mm Hg = 133.322 Pa) in a Kugelrohr apparatus for 24 h. After cooling, the modified silica gel was washed with several 50-ml portions of methanol and slurry packed into a 250 × 4.6 mm I.D. stainless-steel HPLC column

using methanol. After washing with 100 ml of dichloromethane, CSP I was endcapped using 2 ml of hexamethyldisilazane in 50 ml of dichloromethane. Elemental analysis of residual CSP from the packing procedure showed a loading of 0.22 mmol/g based on C and 0.21 mmol/g based on N.

*N*-[5-(Dimethylethoxysilyl)-2,2-dimethylpentanoyl]-*L*-proline-3,5-dimethylanilide

*N*-[5-(Dimethylethoxysilyl)-2,2-dimethylpentanoyl]-*L*-proline-3,5-dimethylanilide was prepared using a procedure similar to that described for *N*-[11-(dimethylethoxysilyl)undecanoyl]-*L*-proline-3,5-dimethylanilide. After chromatography, 1.5 g (52% yield) of a pale yellow oil was obtained.  $^1\text{H NMR}$  ( $\text{C}^2\text{HCl}_3$ ) 200 MHz  $\delta$  9.20 (br s, 1H); 7.10 (s, 2H); 6.70 (s, 1H); 4.80 (dd, 1H); 3.70 (m, 2H); 3.60 (q, 2H); 2.30 (s, 6H); 2.00–1.40 (m, 6H); 1.30 (s, 6H); 1.10 (t, 3H); 0.50 (m, 2H); 0.00 (s, 6H).

*Preparation of CSP II*

CSP II was prepared using a procedure similar to that described for the preparation of CSP I. Elemental analysis of residual CSP from the packing procedure showed a loading of 0.23 mmol/g based on C and 0.20 mmol/g based on N.

*The analytes*

All analytes reported herein were available from previous experiments conducted in these laboratories. The synthesis and characterization of these analytes is reported elsewhere [14,15].

RESULTS AND DISCUSSION

From prior studies in these laboratories, we were aware that the enantiomers of *N*-protected amino acid anilides can be separated on several  $\pi$ -acidic CSPs [16]. Keeping the aforementioned considerations in mind, Corey Pauling Koltung (CPK) space filling molecular models (Harvard Apparatus, South Natick, MA, USA) were used to aid in the design of a (*S*)-proline-derived chiral stationary phase intended to retain the (*S*)-enantiomers of *N*-(3,5-dinitrobenzoyl)amino

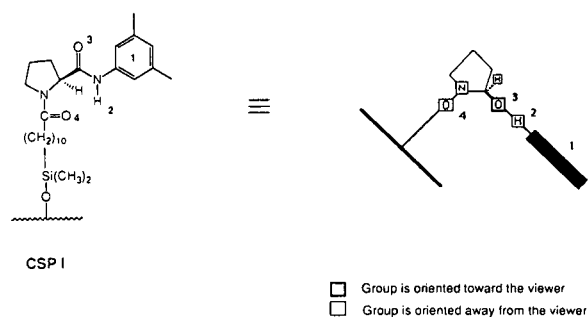


Fig. 2. CSP I and a cartoon-like representation of CSP I.

acids (and their ester and amide derivatives). The structure of this CSP is shown in Fig. 2, along with a cartoon-like representation intended to simplify aspects of the chiral recognition mechanism to be subsequently discussed. The analytes to be discussed are represented using the convention shown in Fig. 3.

The conventions introduced in Figs. 2 and 3 are used in Fig. 4 in an attempt to convey, in two dimensions, our view of the three-dimensional structure of the more stable 1:1 diastereomeric adsorbate expected to result from interaction of the *N*-(10-undecenoyl)-*L*-proline-3,5-dimethylanilide-derived CSP with esters or amides of (*S*)-*N*-(3,5-dinitrobenzoyl)leucine. The important bonding interactions are shown using a double-headed arrow.

The essential bonding interactions, as shown in Fig. 4, were expected to be a face-to-face  $\pi$ - $\pi$  interaction between the 3,5-dinitrobenzoyl group and the 3,5-dimethylanilide moiety, a hydrogen bond between the relatively acidic 3,5-dinitrobenzamide proton and the carbonyl oxygen in the CSP's tether to silica, and a hydrogen bond between the 3,5-dimethylanilide amide proton

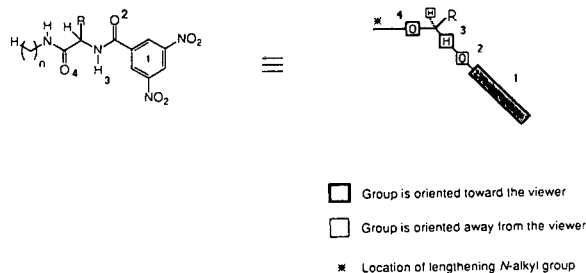


Fig. 3. Analytes and convention used to represent analytes in Figs. 4 and 5.

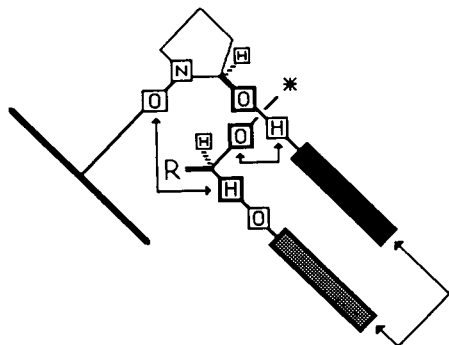


Fig. 4. Representation of the more stable diastereomeric adsorbate expected to form between CSP I and amides of N-(3,5-dinitrobenzoyl) amino acids.

and the carbonyl oxygen in the analyte C-terminal ester or amide. Although conceptually similar CSPs could be derived from other amino acids, proline was selected since, as a secondary amine, nitrogen acylation leaves no extraneous amide N–H. This amide hydrogen is not considered essential to the retention of the more retained enantiomer and its omission was expected to reduce the extent of achiral retention and thus improve enantioselectivity. The conformation imposed by the 5-member ring and the planarity of the 3,5-dimethylanilide system was expected to impart strong affinity for the (*S*)-enantiomers of the target analytes, while the proline ring itself was expected to discourage approach of the analytes' (*R*)-enantiomer from the “backside” of the CSP. By further reducing retention of the (*R*)-enantiomer, enantioselectivity might be enhanced.

A final inference drawn from the models is noteworthy. In the complex containing the more retained enantiomer, the alkoxy group of the C-terminal ester (or the alkyl group(s) of a C-terminal amide) is directed away from the tether and the silica support. Should the least retained enantiomer bind to the CSP in a similar fashion, so as to enjoy the face-to-face  $\pi$ – $\pi$  interaction and the hydrogen bond from the 3,5-dinitrobenzamide N–H to the carbonyl oxygen in the tethering arm of the CSP, its alkoxy group (if an ester) or its N-alkyl group(s) (if an amide) would then be directed between the adjacent strands of bonded phase and toward the silica

support. In a non-polar mobile phase, any alkyl group so directed should exert a destabilizing effect on the complex. This intercalative interaction with the neighboring strands of bonded phase and with the underlying silica support was expected to selectively reduce the retention of the less retained enantiomer, the effect increasing with an increase in the length of the alkoxy or alkyl group. A representation of this arrangement is shown in Fig. 5.

Chromatographic data for the normal-phase separation of the enantiomers of amides of N-(3,5-dinitrobenzoyl)leucine on CSP I are shown in Table I.

As can be seen, the enantioselectivities encountered are substantial and increase as the length of the N-alkyl amide is increased incrementally, particularly in a dichloromethane mobile phase. This suggests that an intercalative hypothesis is valid. Little retention is observed for the initially eluted enantiomer, this being a major factor in the high levels of enantioselectivity noted for these analytes.

From the foregoing mechanistic rationale, it was expected that shortening the tether which connects the selector to silica would afford still higher levels of enantioselectivity since this would exacerbate the intercalation difficulty encountered by the least retained enantiomers. Adding geminal dimethyl groups on the  $\alpha$  carbon of the tether was expected to further compound the difficulty of intercalation. The structure of this modified CSP, II, is shown in Fig. 6.

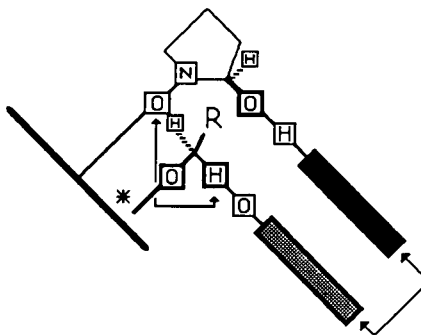
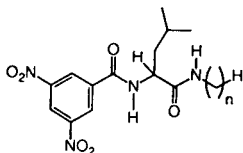


Fig. 5. Representation of the less stable diastereomeric adsorbate expected to form between CSP I and amides of N-(3,5-dinitrobenzoyl) amino acids.

TABLE I

NORMAL-PHASE SEPARATION OF THE ENANTIOMERS OF N-(3,5-DINITROBENZOYL)LEUCINE AMIDES ON CSP I



$k'_1$  = Capacity factor for the first eluting enantiomer;  $\alpha$  = chromatographic separation factor; flow-rate 2 ml/min.

n	2-Propanol–hexane (15:85, v/v)		100% Dichloromethane	
	$k'_1$	$\alpha$	$k'_1$	$\alpha$
1	1.73	18.4	1.26	16.8
2	1.39	23.7	0.88	21.1
3	1.28	26.6	0.70	26.6
6	1.04	26.5	0.53	28.3
10	0.85	26.8	0.49	26.5
14	0.78	25.2	0.36	30.41
18	0.62	28.2	0.31	31.0

When CSP II was prepared and evaluated, it was found to afford greater enantioselectivities than CSP I for all analytes examined. Normal-phase separation factors range from 27 to 50 for the enantiomers of the homologous series of N-(3,5-dinitrobenzoyl)leucine amides shown in Table I. As the analytes' C-terminal amide N–H is not invoked as essential to the retention of the more retained enantiomer, amides derived from secondary amines or bulky primary amines (which are thought to sterically restrict access to the amide N–H) were expected to show even higher levels of enantioselectivity. This is the case, as the data in Table II attest.

Data from the normal- and reversed-phase chromatographic separation of the enantiomers of a homologous series of N-(3,5-dinitrobenzoyl)- $\alpha$ -amino-alkyl phosphonates are presented in Table III.

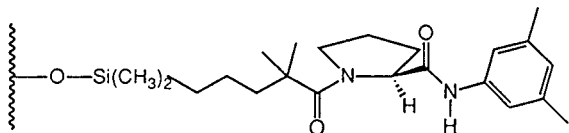
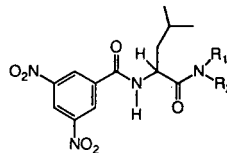


Fig. 6. Structure of CSP II.

TABLE II

NORMAL-PHASE SEPARATION OF THE ENANTIOMERS OF N-(3,5-DINITROBENZOYL)LEUCINE AMIDES ON CSP II



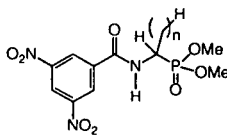
Mobile phase consisting of 20% (v/v) 2-propanol–hexane (20:80, v/v);  $k'_1$  = capacity factor for the first eluting enantiomer;  $\alpha$  = chromatographic separation factor; flow-rate 2 ml/min.

$R_1$	$R_2$	$k'_1$	$\alpha$
CH <sub>3</sub>	CH <sub>3</sub>	0.61	30.4
C <sub>8</sub> H <sub>17</sub>	C <sub>8</sub> H <sub>17</sub>	0.16	48.7
H	Adamantyl	0.32	64.4
H	<i>tert.</i> -Butyl	0.22	86.3

From the chiral recognition process shown in Fig. 3, the alkyl group on the stereogenic center of the more retained enantiomer of an N-(3,5-dinitrobenzoyl)- $\alpha$ -amino-alkylphosphonate was

TABLE III

NORMAL- AND REVERSED-PHASE SEPARATION OF THE ENANTIOMERS OF N-(3,5-DINITROBENZOYL)- $\alpha$ -AMINO-ALKYLPHOSPHONATE ESTERS ON CSP I



$k'_1$  = Capacity factor for the first eluting enantiomer;  $\alpha$  = chromatographic separation factor; flow-rate 2 ml/min.

n	Normal phase, 2-propanol–hexane (20:80)		Reversed phase, water–methanol (20:80)	
	$k'_1$	$\alpha$	$k'_1$	$\alpha$
1	3.07	4.57	1.09	1.52
2	2.84	4.31	1.26	1.60
3	2.61	4.31	1.60	1.63
4	2.44	4.31	1.83	1.77
5	2.22	4.35	2.11	1.86
6	2.04	4.28	2.59	1.92
7	1.92	4.15	3.19	1.98
9	1.60	3.95	4.98	2.06

expected to be intercalated between the strands of bonded phase. Should this group be long enough to experience intercalation difficulties under normal phase conditions, enantioselectivity seemed likely to be reduced as a consequence of reduced retention of the more retained enantiomer relative to its non-intercalating antipode. Were a reversed mobile phase used, this trend might be reversed, owing to a hydrophobic incentive for intercalation of alkyl groups between strands of bonded phase. As documented in Table III, these trends are observed. Such trends provide compelling support for the intercalation hypothesis.

## CONCLUSIONS

The design, synthesis and chromatographic evaluation of two chiral stationary phases derived from (*S*)-proline has been described. These chiral stationary phases have been used in an ongoing investigation into the effect of intercalative processes on chiral recognition. A mechanistic rationale was used for the *a priori* design of these chiral stationary phases, both of which show unusually high levels of enantioselectivity for the enantiomers of the targeted class of analytes. The elution order of the analyte enantiomers is as expected from the rationale.

While CSPs which afford high levels of enantioselectivity are unnecessary and even undesirable for most analytical determinations of enantiomeric purity, one can utilize a CSP of intentionally lowered enantiomeric purity to reduce run times, perform the chromatography at elevated temperatures, or use a suboptimal mobile phase to reduce enantioselectivity and run time. There are, however, several advantages in having access to high levels of enantioselectivity. A CSP capable of high enantioselectivity will often resolve the enantiomers of compounds which, when chromatographed on CSPs of lesser ability, are either inseparable or of marginal separability. Moreover, the proline-derived chiral phases described herein are not restricted to the separation of the enantiomers of  $\alpha$ -amino acid derivatives but suffice to separate the enantiomers of the 3,5-dinitrobenzamides of various chiral amines and the 3,5-dinitrophenyl carbamates of

many chiral alcohols. High levels of enantioselectivity are desirable for preparative applications and are essential to new process scale technology using hollow-fiber membranes [17,18]. Finally, high levels of enantioselectivity permit the design of chromatographic and spectroscopic experiments, the results of which can yield unambiguous information concerning the nature of the chiral recognition processes involved. Such information can be instrumental in the design of even better chiral selectors.

## ACKNOWLEDGEMENTS

The authors gratefully acknowledge financial support from the NSF, Eli Lilly and Company, and Glaxo Research Laboratories. Solvents employed for the chromatography were generously supplied by EM Science, a Division of EM Merck. The Euromark HPLC column oven was generously supplied by Euromark Industries in Melrose Park, IL, USA.

## REFERENCES

- 1 S. Allenmark, *Chromatographic Enantioseparation*, Ellis Horwood, New York, 2nd ed., 1991.
- 2 W.H. Pirkle and C.J. Welch, *J. Chromatogr.*, 589 (1992) 45.
- 3 W.H. Pirkle and P.G. Murray, *J. Chromatogr.*, 641 (1993) 21.
- 4 W.H. Pirkle and J.A. Burke, *J. Chromatogr.*, 557 (1991) 173.
- 5 W.H. Pirkle, C.J. Welch and B. Lamm, *J. Org. Chem.*, 57 (1992) 3854.
- 6 N. Oi, H. Kitahara, Y. Inada and T. Doi, *J. Chromatogr.*, 237 (1982) 297.
- 7 V. Davankov, A.S. Bochkov, A.A. Kurganov, P. Roumeliotis and K.K. Unger, *Chromatographia*, 13 (1980) 677.
- 8 J.N. Akanya, S.M. Hitchen and D.R. Taylor, *Chromatographia*, 16 (1982) 224.
- 9 P. Pescher, M. Claude, R. Rosset, A. Tambute and L. Oliveros, *Nouv. J. Chim.*, 9 (1985) 621.
- 10 C.D. Haurou, G. Declercq, P. Ramiandrasoa and J.L. Millet, *J. Chromatogr.*, 547 (1991) 31.
- 11 M. Ohwa, M. Akiyoshi and S. Mitamura, *J. Chromatogr.*, 521 (1990) 122.
- 12 R. Salomon and J. Ghosh, *Org. Synth.*, 62 (1984) 125.
- 13 I.A. Pearl, *Org. Synth. Coll. Vol. IV*, (1963) 972.
- 14 C.J. Welch, *Ph.D. Thesis*, University of Illinois, Urbana, IL, 1992.

- 15 J.A. Burke, *Ph.D. Thesis*, University of Illinois, Urbana, IL, 1992.
- 16 W.H. Pirkle and J.E. McCune, *J. Chromatogr.*, 479 (1989) 419.
- 17 W.H. Pirkle and E.M. Doherty, *J. Am. Chem. Soc.*, 111 (1989) 4113.
- 18 W.H. Pirkle and W.E. Bowen, presented at the *204th National Meeting of the American Chemical Society, Washington, DC, August 1992*, paper ORGN 357.





# Use of homologous series of analytes as mechanistic probes to investigate the origins of enantioselectivity on two chiral stationary phases

William H. Pirkle\*, Patrick G. Murray and J. Andrew Burke

*School of Chemical Sciences, University of Illinois, Box 44, Roger Adams Laboratory, 1209 West California Street, Urbana, IL 61801 (USA)*

(Received January 19th, 1993)

---

## ABSTRACT

The normal-phase liquid chromatographic behavior of two homologous series of racemic carbamate derivatives of leucine anilides was examined on two chiral stationary phases, one of which has not been described heretofore. These chiral stationary phases are related structurally to the N-(3,5-dinitrobenzoyl)leucine chiral stationary phases originally developed in these laboratories, but differ from each other principally in the manner in which the chiral selector is attached to the silica gel support. While these selectors utilize the same interaction sites for bonding, the length of the analyte's linear alkoxy substituent strongly influences enantioselectivity on only one of the chiral stationary phases. Similar but substantially less severe trends are noted as the length of a *p*-alkyl substituent on the second series of anilides is increased. Inferences concerning possible chiral recognition mechanisms are drawn from these observations.

---

## INTRODUCTION

The use of chiral stationary phases (CSPs) to effect separation of the enantiomers of organic compounds has increased dramatically in the last decade (see, for example, ref. 1). For analytical applications, one desires a chiral selector which has a broad range of applicability but not necessarily a high degree of enantioselectivity. This will become increasingly the case as high-efficiency separation techniques (*e.g.* capillary electrophoresis) become more widespread. However, chiral selectors for preparative applications should show appreciable levels of enantioselectivity as well as broad applicability. The development of such chiral selectors is greatly facilitated by an understanding of the interactions involved in chiral recognition processes. Several of the

broad-spectrum CSPs now available commercially have resulted from detailed investigations into the mechanistic basis for enantiodiscrimination. For example, the mechanism of chiral recognition between N-(3,5-dinitrobenzoyl)leucine derivatives and the esters and amides of N-(2-naphthyl)alanine (and related analytes) is believed to be fairly well understood, the proposed mechanism being supported by <sup>1</sup>H nuclear Overhauser effect studies [2] as well as by X-ray crystallographic data [3]. Guided by the mechanistic hypothesis, N-(aryl)amino acid-derived CSPs have been developed which show extremely high levels of enantioselectivity. In fact, separation factors exceeding one hundred have been observed in some cases.

To achieve high degrees of enantioselectivity, the selector must be tailored to have a high affinity for the more strongly complexed analyte enantiomer. In addition, the affinity of the selector for the less strongly complexed enan-

---

\* Corresponding author.

tiomer should be minimal. This can be done, in part, by appropriate design of the selector. However, the enantioselectivity demonstrated by a particular selector is often influenced markedly by subtle factors. For example, we have previously demonstrated that the manner in which a chiral selector is linked to the underlying silica gel support can effect both retention and enantioselectivity [4,5].

Within a homologous series of analytes, enantioselectivity can be strongly dependent upon the length of a simple alkyl group in the analyte molecule. This is a clear demonstration that the alkyl group differentially influences the adsorption of the enantiomers. While relatively few such studies have been reported, we encounter this type of behavior fairly frequently. Mechanistic rationales accounting for this behavior can in many cases be tested by utilizing a modified version of the chiral stationary phase in which the selector presents the same interaction sites to the analyte enantiomers, but is "reoriented" so as to either exacerbate or relieve the interaction which causes enantioselectivity to be influenced by the length of the substituent in the analyte. Herein, we describe an instance of this type of behavior, offer a mechanistic rationale, and design a modified CSP to test the rationale.

## EXPERIMENTAL

### Chromatography

Chromatography was performed with an Anspec-Bischoff Model 2200 isocratic HPLC pump, a Rheodyne Model 7125 injector equipped with a 20- $\mu$ l sample loop and two Milton Roy-LDC UV Monitor D fixed-wavelength detectors (254 and 280 nm) connected in series. The data was acquired using both a Kipp & Zonen BD 41 dual-pen chart recorder and a Hewlett-Packard 3394A recording integrator. Void volumes were determined using 1,3,5-tri-*tert*.-butylbenzene [6].

### Chiral stationary phases

CSP I was prepared by a slight modification of a described procedure [7]. CSP II was prepared according to the scheme outlined in Fig. 1.

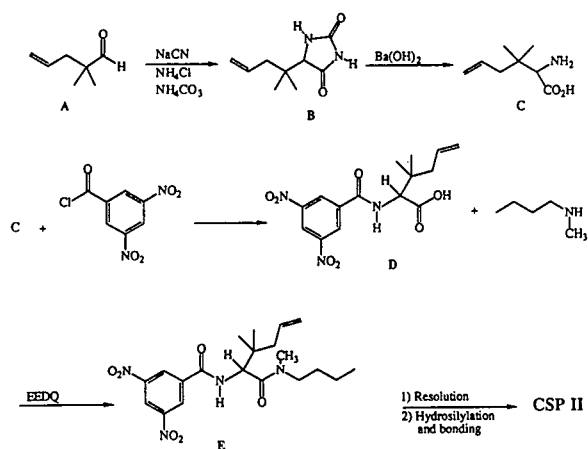


Fig. 1. Preparation of chiral stationary phase II.

### 2,2-Dimethyl-4-pentenylhydantoin (B)

To a solution of 1.15 g (23.4 mmol) of NaCN (poison!) and 1.26 g (23.5 mmol) of NH<sub>4</sub>Cl in 10 ml of water, a solution of 2.50 g (22 mmol) of aldehyde A in 10 ml of methanol was added dropwise over 10 min. The addition funnel was rinsed with two 5-ml portions of methanol and the rinses were added to the reaction mixture. After 20 min, the reaction mixture was poured into a pressure bottle containing 10 g of NH<sub>4</sub>CO<sub>3</sub> and sealed. The solution was heated on a steam bath and the progress of the reaction monitored by TLC using dichloromethane–diethyl ether (4:1). The *R<sub>F</sub>* for the cyanohydrin is 0.80 and for the hydantoin is 0.10. After heating the reaction mixture for 6 h, it was cooled, and then concentrated under reduced pressure, diluted with 20 ml of water, and extracted with three 50-ml portions of dichloromethane. The combined organic layers were washed with two 20-ml portions of water, dried over MgSO<sub>4</sub>, filtered and concentrated under reduced pressure. The residue was recrystallized from ethyl acetate:hexane to give 3.65 g of a white solid, yield 85%, m.p. 157–158°C. <sup>1</sup>H NMR (C<sup>2</sup>HCl<sub>3</sub>-[<sup>2</sup>H<sub>6</sub>]dimethyl sulfoxide, 6:1) 360 MHz  $\delta$  1.00 (m, 6H); 2.18 (m, 2H); 3.75 (s, 1H); 5.05–5.20 (m, 2H); 5.70–5.90 (m, 1H); 7.40 (br s, 1H); 10.20 (br s, 1H). <sup>13</sup>C NMR (C<sup>2</sup>HCl<sub>3</sub>-[<sup>2</sup>H<sub>6</sub>]dimethyl sulfoxide, 6:1) 75 MHz  $\delta$  21.85, 22.08, 42.07, 64.65, 117.72, 132.20, 157.60, 174.10. Mass spectrum 70 eV *m/z* (relative intensity) 182(0.7), 100(100), 83(75), 55(96), 41(47). Analysis for C<sub>9</sub>H<sub>14</sub>N<sub>2</sub>O<sub>2</sub>:

calculated: C 59.32; H 7.74; N 15.37; found C 59.31; H 7.78; N 15.38.

#### 2-Amino-3,3-dimethyl-5-hexenoic acid (C)

A stainless-steel tube was charged with 4.0 g (22 mmol) of **B**, 16 g (51 mmol) of Ba(OH)<sub>2</sub> octahydrate and 60 ml of water and sealed. The tube was placed in a tube furnace and heated to 145°C for 16 h. The tube was allowed to cool thoroughly, opened, and the contents were poured into a 500-ml beaker. The tube was rinsed with 100 ml of water, and the water rinses were added to the 500-ml beaker. Solid NH<sub>4</sub>CO<sub>3</sub> was added until the precipitation of BaCO<sub>3</sub> was complete. The mixture was heated on a steam bath until gas evolution ceased, about 30 min. Celite was added to the warm reaction mixture and the solution was filtered. The filter cake was washed with two 20-ml portions of water and the combined filtrates were concentrated under reduced pressure. The residue was taken up in 100 ml of absolute ethanol and concentrated to dryness. Recrystallization from water–ethanol gave 2.80 g of a white solid, yield 80%. m.p. > 250°C. <sup>1</sup>H NMR ([<sup>2</sup>H<sub>6</sub>]dimethyl sulfoxide) 360 MHz δ 0.96 (s, 3H); 0.98 (s, 3H); 2.14 (m, 2H); 3.64 (d, 1H); 5.05–5.20 (m, 2H); 5.70–5.90 (m, 1H); 8.2 (br s, 2H); 14.00 (br s, 1H). Mass spectrum 70 eV *m/z* (relative intensity) 112(16.7), 83(25), 75(100), 55(61), 41(36). Analysis for C<sub>8</sub>H<sub>15</sub>NO<sub>2</sub>: calculated: C 61.62; H 9.62; N 8.91; found C 60.94; H 9.68; N 9.08.

#### *N*-(3,5-Dinitrobenzoyl)-2-amino-3,3-dimethyl-5-hexenoic acid (D)

A 300-ml flask equipped with stir bar and nitrogen inlet was charged with 4.68 g (20 mmol) of 3,5-dinitrobenzoyl chloride, 3.10 g (19.5 mmol) of amino acid **C**, and 100 ml of dry tetrahydrofuran (THF). A solution of 1.6 ml (23 mmol) of propylene oxide in 40 ml of dry THF was added dropwise over a 30 min period to the cooled (0°C) heterogeneous reaction mixture. After an additional 30 min, the homogeneous reaction mixture was concentrated under reduced pressure and triturated with 50 ml of dichloromethane at 0°C to give 5.63 g of a white solid. A second crop of 0.53 g was obtained from the filtrate, yield 89%, m.p. 181–183°C. <sup>1</sup>H

NMR (C<sup>2</sup>HCl<sub>3</sub>-[<sup>2</sup>H<sub>6</sub>]dimethyl sulfoxide, 20:1) 360 MHz δ 1.09 (s, 6H); 2.20 (m, 2H); 4.76 (d, 1H); 5.05–5.20 (m, 2H); 5.80–6.00 (m, 1H); 7.88 (m, 1H); 9.10 (m, 2H); 9.13 (m, 1H). Mass spectrum 70 eV *m/z* (relative intensity) 351(0.6), 251(10), 195(20), 149(15), 83(100), 55(93). Analysis for C<sub>15</sub>H<sub>17</sub>N<sub>3</sub>O<sub>7</sub>: calculated: C 51.28; H 4.88; N 11.96; found C 51.27; H 4.98; N 11.71.

#### *N*-(3,5-Dinitrobenzoyl)-2-amino-3,3-dimethyl-5-hexenoic acid methyl butyl amide (E)

A flask equipped with stir bar and nitrogen inlet was charged with 50 ml of dry dichloromethane, 1.44 g (5.8 mmol) of 2-ethoxy-1-ethoxycarbonyl-1,2-dihydroquinoline (EEDQ), and 1.50 g (4.3 mmol) of **D**. After stirring for 20 min at ambient temperature, 6 ml (58 mmol) of *N*-methyl butyl amine was added in one portion. A dark purple color developed, but faded to a pale yellow after 20 min. After this time, the reaction mixture was poured into a separatory funnel containing 100 ml of dichloromethane. The organic layer was washed sequentially with four 30-ml portions of 1 M HCl, 40 ml of water, and 40 ml of water–saturated NH<sub>4</sub>Cl (3:1). The organic layer was dried with MgSO<sub>4</sub>, filtered, concentrated under reduced pressure and dried *in vacuo* to give 1.65 g of colorless oil, 92% yield. Two amide rotamers are observed in the <sup>1</sup>H NMR in approximately a 60:40 ratio. <sup>1</sup>H NMR (C<sup>2</sup>HCl<sub>3</sub>) 200 MHz δ 0.90–1.70 (m, 14 H); 2.00–2.10 (m, 1H); 2.20–2.40 (m, 1H); 2.94 (s, 1.3H); 3.10–3.40 (2.7H); 3.40–3.80 (m, 1H); 5.10–5.30 (m, 3H); 5.80–6.10 (m, 1H); 7.40 (m, 1H); 9.00 (m, 2H); 9.20 (m, 1H). Mass spectrum 70 eV *m/z* (relative intensity) 420(4.9), 306(56), 195(59), 114(67), 95(100), 57(84), 44(68). Analysis for C<sub>20</sub>H<sub>28</sub>N<sub>4</sub>O<sub>6</sub>: calculated: C 57.13; H 6.71; N 13.32; found C 57.09; H 6.70; N 13.09.

#### Resolution of the enantiomers of E

The enantiomers of **E** were separated by preparative chromatography on a 75 × 2.5 cm column containing the (*S*)-*N*-(1-naphthyl)leucine CSP bonded to 40 μm silica gel. A 2-propanol–hexane (30:70) mixture was used as the mobile phase. From mechanistic considerations, the first eluted enantiomer is assigned as (*R*)-**E**, and the second as (*S*)-**E**. Each enantiomer was obtained

as a colorless oil, and shown to be of greater than 99% enantiomeric purity by analytical HPLC. Each has a  $^1\text{H}$  NMR spectrum identical to that of the racemate.

### Preparation of CSP 3

An oven-dried 100-ml flask equipped with a stir bar, condenser and nitrogen inlet was charged with 10 ml of  $(\text{CH}_3)_2\text{SiHCl}$ , 10 ml of dry dichloromethane, 0.70 g of (*S*)-**E** and 30 mg of  $\text{H}_2\text{PtCl}_6$ , and the mixture was refluxed for 4 h. After this time, the mixture was concentrated to dryness and any residual  $(\text{CH}_3)_2\text{SiHCl}$  was chased with two additional 30-ml portions of dry dichloromethane. The dark oil was diluted with 50 ml of dry ethyl ether and treated with 4 ml of triethylamine–absolute ethanol (1:1). The triethylamine hydrochloride which precipitated was removed by filtration using Celite. The filter cake was washed with two 10-ml portions of dry ethyl ether, the filtrate was concentrated and chromatographed on silica using dichloromethane–diethyl ether (10:1). The purified silane in 20 ml of dichloromethane was poured into a 100-ml flask containing 4.30 g of 5  $\mu\text{m}$  silica which had been azeotropically dried with benzene. The solvents were removed under reduced pressure, and the silica and silane were heated at 110°C for 12 h with rocking on a Kugelrohr apparatus. After cooling, the modified silica was washed sequentially with 50 ml of methanol, 30 ml of ethyl acetate, 30 ml of dichloromethane and 30 ml of diethyl ether. The washed silica was slurry packed using methanol into a 250  $\times$  4.6 mm I.D. stainless-steel HPLC column. After washing with 100 ml of dichloromethane, the CSP was endcapped using 2 ml of hexamethyldisilazane in 20 ml of dichloromethane. Elemental analysis of the residual CSP from the packing procedure showed a loading of 0.20 mmol/g based on C and 0.18 mmol/g based on N.

### Synthesis of racemic analytes

All N-carbamoyl protected leucine derivatives were prepared by reaction of the racemic amino acid with the appropriate chloroformate using standard conditions [8]. In cases where the chloroformates were not commercially available,

they were prepared by allowing phosgene to react with the appropriate alcohol in toluene [9].

All anilides were prepared from the corresponding N-carbamoyl protected amino acids by allowing the corresponding aniline to react with the amino acid in the presence of dicyclohexylcarbodiimide (DCC) in dry dichloromethane. All products were characterized at the N-protected amino acid stage by  $^1\text{H}$  NMR and IR, and at the anilide stage by  $^1\text{H}$  NMR and combustion analysis. All spectroscopic and elemental analysis data are in accord with the structures of the expected products.

### RESULTS AND DISCUSSION

Linear series of racemic N-(*n*-alkoxycarbonyl)leucine-3,5-dimethylanilides and racemic N-(ethoxycarbonyl)leucine-*p*-alkylanilides were prepared (shown in Fig. 2), and their chromatographic behavior investigated on CSP I, an N-(3,5-dinitrobenzoyl)leucine-derived phase, and CSP II, an N-(3,5-dinitrobenzoyl)-“*tert.*-leucine”-like CSP, both shown in Fig. 3. Notice that while CSP II contains the same functional groups (interaction sites) as CSP I, CSP II is linked to the silica support via the amino acid alkyl sidechain and not through the C-terminal carboxamide, as is CSP I.

Plots of the chromatographic separation factor ( $\alpha$ ) versus *n* (the number of methylene units in the alkoxy or alkyl substituent) are shown in Fig. 4 for the normal-phase separation of enantiomers of the N-(*n*-alkoxycarbonyl)leucine-3,5-dimethylanilides (Type 1 analytes) and the N-(ethoxycarbonyl)leucine-*p*-alkylanilides (Type 2 analytes) on CSP I.

On CSP I, the degree of enantioselectivity (*i.e.*  $\alpha$ ) afforded the enantiomers of the N-(*n*-alkoxycarbonyl)leucine-3,5-dimethylanilide analytes is highly dependent upon the length of the carba-

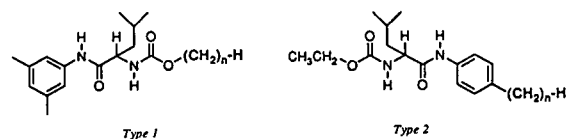


Fig. 2. Analytes prepared for use in the study with CSPs I and II.

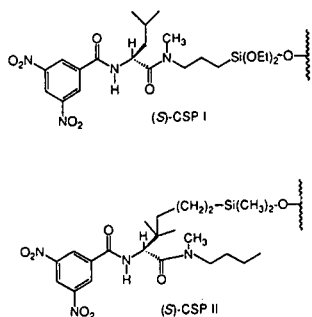


Fig. 3. Chiral stationary phases used in the investigation.

mate alkoxy group, and is greatest when this group is long. Retention of both enantiomers decreases as the alkoxy substituent is lengthened, but does so more quickly for the least retained enantiomer. Plots of the natural logarithm of the capacity factors,  $k'$ , versus  $n$  (Fig. 5) show the hastened elution of the least retained enantiomer relative to the more retained enantiomer as  $n$  increases. In the non-polar mobile phase used, this behavior suggests that unfavorable steric interactions are occurring to a greater extent for the least retained enantiomer, presumably as a consequence of the carbamate alkoxy group having to intercalate between adjacent strands of bonded phase.

The use of Corey Pauling Koltung (CPK) space filling molecular models (Harvard Ap-

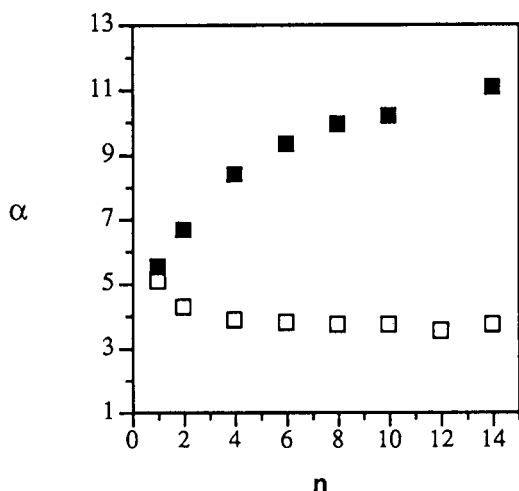


Fig. 4. Enantioselectivity ( $\alpha$ ) versus alky chain length ( $n$ ) on CSP I; mobile phase consisting of 2-propanol–hexane (5:95, v/v). ■ =  $n$ -Alkoxy carbamates; □ =  $p$ -alkyl anilides.

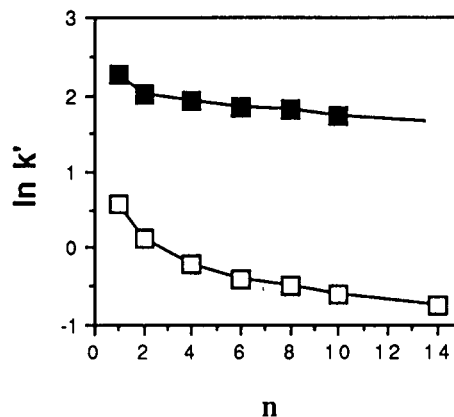


Fig. 5. Natural logarithm of  $k'$  (capacity factor) versus the number of methylene units in the alkoxy substituent ( $n$ ) for the Type 1 analytes on CSP I; mobile phase consisting of 2-propanol–hexane (5:95, v/v). □ =  $\ln k'_1$ ; ■ =  $\ln k'_2$ .

paratus, South Natick, MA, USA) to explore possible structures of the more stable diastereomeric complex(es) between the CSP and the analyte [the ( $S$ )–( $S$ ) or ( $R$ )–( $R$ ) complex] leads one to conclude that interactions making the dominant contribution to the retention of the more retained enantiomer are similar to those postulated earlier for a different analyte–selector combination [2]. The essential bonding interactions are believed to be a face-to-face  $\pi$ – $\pi$  interaction between the 3,5-dimethylanilide and the 3,5-dinitrobenzoyl systems, a hydrogen bond between the 3,5-dimethylanilide N–H and the C-terminal amide carbonyl oxygen of the CSP, and a hydrogen bond between the acidic 3,5-dinitrobenzamide N–H and the carbamate carbonyl oxygen. Cartoon-like representations of the selector and the analyte, intended to simplify aspects of the chiral recognition mechanism to be developed later, are introduced in Fig. 6.

From this model, depicted in Fig. 7, it may be seen that for the more retained enantiomer neither the alkoxy groups of the Type 1 analytes nor the  $p$ -alkyl substituents of the Type 2 analytes are intercalated between the adjacent strands of the bonded phase.

In considering chiral recognition mechanisms, we have seldom made attempts to describe the structures of adsorbates which contribute to the retention of the least retained enantiomer. Often, these adsorbates are populated but a

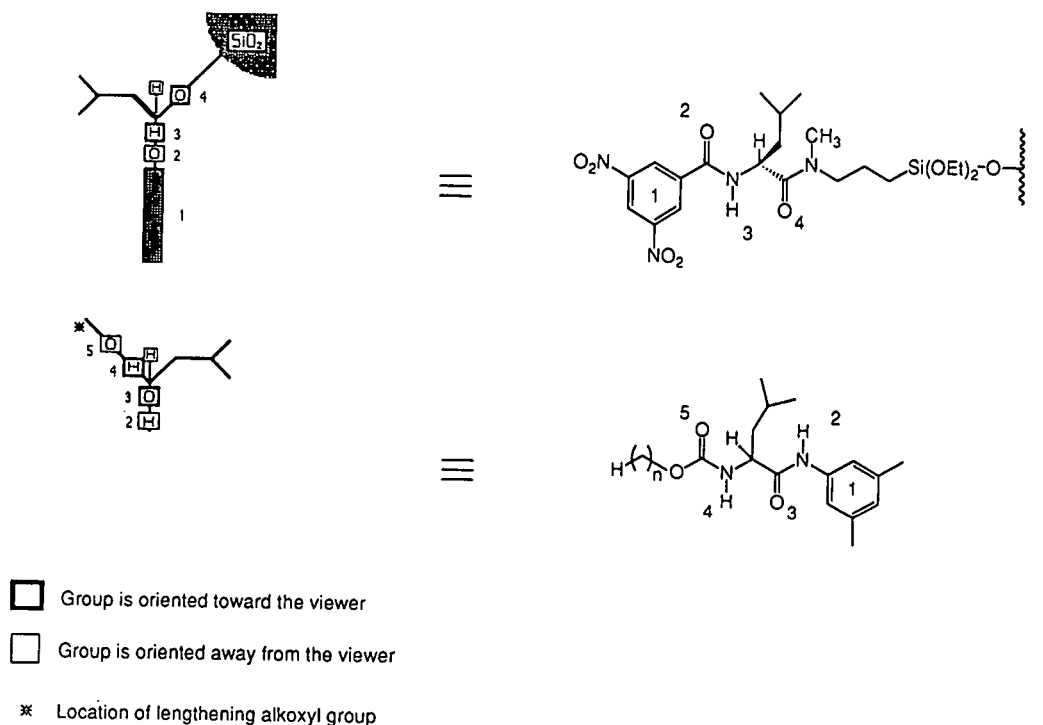


Fig. 6. Legend to accompany Figs. 7 and 8.

small fraction of the time and are difficult to describe with confidence. While it has been suggested that the least retained enantiomer may utilize the same simultaneous bonding interactions as does its antipode [10], this is deemed unlikely when substantial enantioselectivity is encountered. If a retention mechanism (or combination of mechanisms) requires that the

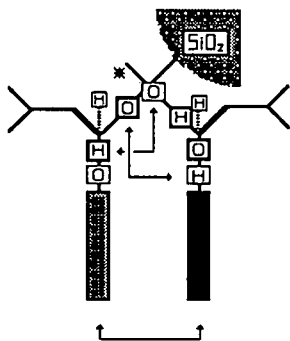


Fig. 7. Proposed chiral recognition mechanism for the more stable (*S,S*) diastereomeric complex between CSP I and the Type 1 and Type 2 analytes.

alkoxy group of the least retained enantiomer be directed between adjacent strands of bonded phase and toward the silica support, this intercalation is expected, for steric reasons, to become increasingly unfavorable as the alkoxy group is lengthened. This intercalation would be expected to hasten elution of the least retained enantiomer relative to its antipode, and likewise to do so to an increasing extent as the alkoxy group becomes longer. The bonding interactions just invoked to explain the principle sources of retention for the more retained enantiomer do not, from study of the CPK models, seem to require any intercalation. Moreover, these bonding interactions do not appear to be simultaneously available to the least retained enantiomer. However, several alternate combinations of bonding interactions between the CSP and the least retained enantiomer can be envisioned, and some of these seemingly require intercalation of the alkoxy group. Two conceivable structures for these least stable diastereomeric adsorbates which may arise from interaction of the least

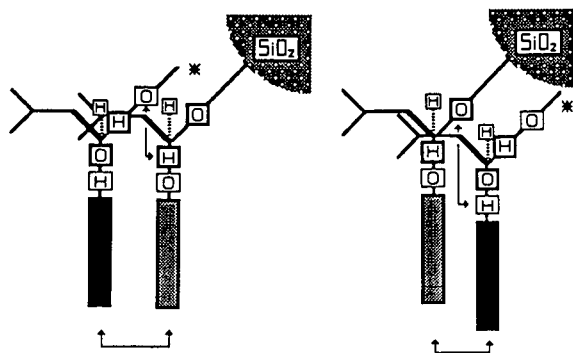


Fig. 8. Two hypothetical structures (chiral recognition mechanisms) for the less stable diastereomeric complex between CSP I and Type 1 and Type 2 analytes.

retained enantiomer with the CSP are depicted in Fig. 8. None of these combinations seem to entail intercalation of the *p*-alkyl substituents of the Type 2 analytes, consistent with the comparatively small effect the length of this substituent exerts on enantioselectivity. In the cases under discussion, the least stable diastereomeric adsorbates are heterochiral. That is, the analyte and the CSP bear dissimilar stereochemical descriptors [e.g. (*R*) and (*S*)].

In the first of the two bonding schemes depicted in Fig. 8, the carbamate alkoxy group is directed alongside the tether and toward the silica support, an intercalative situation. In this representation, the least retained enantiomer is shown to approach the hindered face of the CSP, and in doing so undergoes two simultaneous bonding interactions (a face-to-face  $\pi$ - $\pi$  interaction, and a hydrogen bond involving the di-nitrobenzamide N-H and the carbamate carbonyl oxygen). In the second representation, a face-to-face  $\pi$ - $\pi$  interaction and a hydrogen bond involving the anilide N-H and the carbonyl oxygen in the tether of the phase are invoked as bonding interactions. The strength of these interactions will be reduced since, owing to the difficulty of intercalation, the two components cannot approach one another as closely as in the case of the more stable complex. We hasten to point out that there is no experimental evidence that complexes like those depicted in Fig. 8 actually exist, and that these hypothetical bonding schemes are postulated to rationalize the

experimental results. One must remember that the observed retention stems from a composite of many processes, some no doubt quite subtle. The relative importance of chiral recognition schemes like those represented in Fig. 8, and their respective contributions to the overall observed retention, is difficult to assess.

Retention for the Type 2 analytes falls off at more or less the same rate for both enantiomers throughout the series and  $\alpha$  remains relatively constant as a consequence. The *p*-alkyl group in either enantiomer is directed away from the silica support and, consistent with the mechanistic picture developed, its length does not dramatically influence enantioselectivity.

To the extent that the proposed models represent reality, a chiral stationary phase which presents the same interaction sites to these analytes without requiring intercalation of any substituent should demonstrate enantioselectivity which is independent of the length of the substituent. CSP II was expected to be such a phase. Using the prior interaction schemes, neither enantiomer of the Type 1 analytes would be expected to intercalate its alkoxy substituent between the strands of bonded phase and enantioselectivity should thus be rather constant throughout the homologous series. Considerations of the effect of the length of the *p*-alkyl substituent of the Type 2 analytes on enantioselectivity lead to similar expectations.

Plots of enantioselectivity ( $\alpha$ ) versus substituent length (*n*) for both homologous series of analytes on CSP II are shown in Fig. 9.

The chromatographic separation factor,  $\alpha$ , for the enantiomers of the Type 1 analytes is always smaller on CSP II than on CSP I, and remains relatively constant throughout the series. Retention diminishes at more or less equal rates for both enantiomers as the carbamate alkoxy substituent is lengthened. Elution order of the enantiomers of both types of analytes is the same on both CSP I and CSP II. These are precisely the observations expected on the basis of the preceding mechanistic rationale. CSP II affords less enantioselectivity for the Type 1 analytes than does CSP I because, in the absence of intercalation difficulties, the least retained enantiomers are retained longer and enantioselectivi-



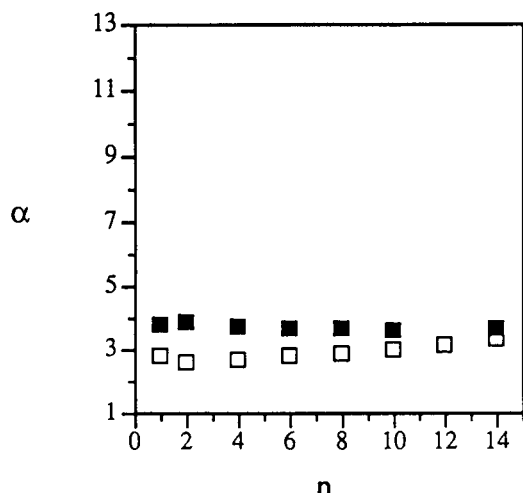


Fig. 9. Enantioselectivity ( $\alpha$ ) versus alkyl chain length ( $n$ ) on CSP II; mobile phase consisting of 2-propanol–hexane (5:95, v/v). ■ =  $n$ -Alkoxy carbamates; □ =  $p$ -alkyl anilides.

ity is thus diminished. As predicted, enantioselectivity does not change appreciably throughout the homologous series of Type 2 analytes, since the  $p$ -alkyl substituents, according to the rationale, are intercalated on neither CSP I nor CSP II.

Note that the enantiomers of the Type 1 analyte having  $n=2$  show a greater separation factor on CSP 2 than do the enantiomers of the Type 2 analytes having  $n=1$  or 2. This is ascribed to the greater  $\pi$ -basicity of a 3,5-dimethylanilide relative to a  $p$ -toluamide or a  $p$ -ethylanilide. One expects, and typically finds, that similar amides derived from more  $\pi$ -basic arylamines (e.g. naphthylamines) show greater retention and enantioselectivity on CSPs I and II.

## CONCLUSIONS

The enantiomers of homologous series of  $N$ -( $n$ -alkoxycarbonyl)leucine-3,5-dimethylanilides and  $N$ -(ethoxycarbonyl)leucine- $p$ -alkylanilides were separated on similar chiral stationary phases which differ principally in their respective modes of attachment to the silica gel support.

While the retention of each enantiomer results from the contributions of many different analyte-adsorbant interactions, the overall chromatographic behavior is rationalized in terms of one or two of the more important contributing mechanisms of retention. Different retention processes are proposed for each enantiomer. On CSP I, the most retained enantiomers of the  $N$ -(alkoxycarbonyl)leucine-3,5-dimethylanilides do not appear to intercalate the alkoxy substituents between neighboring strands of bonded phase to as great an extent as do the less retained enantiomers. The longer the alkoxy substituent, the more difficult the intercalation becomes. Consequently, the least retained enantiomer has its retention reduced relative to its antipode. This causes enantioselectivity to increase as the alkoxy group becomes longer. On CSP II, neither enantiomer is thought to intercalate its alkoxy group to any significant extent and enantioselectivity is essentially independent of the length of this substituent.

For the  $p$ -alkylanilide series, the length of the  $p$ -alkyl group has a modest effect on enantioselectivity on CSP I (long substituents diminish enantioselectivity slightly) and little effect on CSP II. In the former instance, one might assume that the  $p$ -alkyl substituents of the most retained enantiomers undergo some modest steric difficulty through encounter with neighboring strands of bonded phase. However, nothing more definite can be said about these interactions at present.

In principle, it should be possible to engineer a chiral stationary phase which, by virtue of its design, can use intercalative processes to advantage in enhancing enantioselectivity. Such investigations are currently underway.

## ACKNOWLEDGEMENTS

Financial support from the National Science Foundation, Eli Lilly and Company, and Glaxo Research Laboratories is gratefully acknowledged. HPLC solvents were generously supplied by EM Science, a division of EM Industries, Inc.

REFERENCES

- 1 W.J. Lough (Editor), *Chiral Liquid Chromatography*, Chapman & Hall, New York, 1989.
- 2 W.H. Pirkle and T.C. Pochapsky, *J. Am. Chem. Soc.*, 108 (1986) 5627.
- 3 W.H. Pirkle, J.A. Burke and S.R. Wilson, *J. Am. Chem. Soc.*, 111 (1989) 9222.
- 4 W.H. Pirkle, M.H. Hyun and B. Banks, *J. Chromatogr.*, 316 (1984) 585.
- 5 W.H. Pirkle and R.J. Dappen, *J. Chromatogr.*, 404 (1987) 107.
- 6 W.H. Pirkle and C.J. Welch, *J. Liq. Chromatogr.*, 14 (1991) 1.
- 7 W.H. Pirkle, A. Tsipouras and T.J. Sowin, *J. Chromatogr.*, 319 (1985) 392.
- 8 M. Bodansky and A. Bodansky, *The Practice of Peptide Synthesis*, Springer, New York, 1984.
- 9 H.E. Carter, R.L. Frank and H.W. Johnson, *Org. Synth.*, 23 (1943) 13.
- 10 S. Topial and M. Sabio, *Chirality*, 3 (1991) 56.



# High-performance chiral displacement chromatographic separations in the normal-phase mode

## I. Retention and adsorption studies of potential displacers developed for the Pirkle-type naphthylalanine silica stationary phase

Pearle L. Camacho-Torralba<sup>☆</sup> and Gy. Vigh<sup>\*</sup>

*Chemistry Department, Texas A&M University, College Station, TX 77843-3255 (USA)*

David H. Thompson

*Oregon Graduate Institute of Science & Technology, Beaverton, OR 97006 (USA)*

(First received December 29th, 1992; revised manuscript received February 23rd, 1993)

---

### ABSTRACT

Three families of potential displacers have been designed and synthesized for use with the Pirkle-type naphthylalanine silica stationary phases operated in the normal-phase mode. The displacers contain a  $\pi$ -acid head group (3,5-dinitrobenzoate, 3,5-dinitrobenzamide or 3,5-dinitrophenylcarbamate groups), an H-bonding mid-section (C=O and/or NH groups) and a solubility adjusting tail section (*n*-alkyl groups). By varying the length of the alkyl chain between methyl and tetracosanyl, a large number of homologous compounds were synthesized in each family. The capacity factors of the homologues were measured in *n*-hexane–tetrahydrofuran eluents; the *k'* values vary regularly with both the tetrahydrofuran concentration of the eluent and the length of the alkyl chain. The individual excess adsorption isotherms of the homologues were also determined and the isotherm parameters were correlated with the length of the alkyl chain. Because the capacity factors and the adsorption strengths of these compounds cover a broad range, they can serve as displacers in a variety of normal-phase chiral displacement chromatographic separations.

---

### INTRODUCTION

The N-(2)-naphthyl-alaninate silica, a  $\pi$ -electron donor stationary phase developed by Pirkle and co-workers [1–5] is commonly used for

chiral separations, which are accomplished in the normal-phase mode with *n*-hexane–tetrahydrofuran eluents. In accordance with Dalglish's three-points-of-interaction rule [6], this stationary phase can be used to separate the enantiomers of solutes which contain a  $\pi$ -acid functional group (most often a 3,5-dinitrobenzoyl or 3,5-dinitrophenylcarbamoyl group) and an H-donor or H-acceptor group. Earlier, we published an HPLC method [7] for the analytical-scale separation of the enantiomers of platelet-aggregating

---

<sup>\*</sup> Corresponding author.

<sup>☆</sup> Present address: Lyphomed, Division of Fujisawa USA, Inc., Melrose Park, IL 60160, USA.

factor analogues and 1,2-*O*-dihexadecyl-*rac*-glycerol ether derivatives which used the N-(2)-naphthyl-alaninate silica Pirkle-type phase. The success of this analytical separation prompted us to try to develop an analogous preparative-scale displacement chromatographic separation method to produce the individual glycerol ether enantiomers in quantities sufficient for the determination of their respective physico-chemical and pharmaco-chemical properties.

Because the principles of chiral displacement chromatographic separations have been recently discussed [8–10], they are not repeated here and the reader is referred to them for an in-depth review. The greatest hindrance to the development of any displacement chromatographic separation is the lack of readily available displacers and the paucity of the relevant adsorption isotherm data. Therefore, we have synthesized a large number of potential displacers to be used for chiral separations in the normal-phase mode and characterized their retention and adsorption behavior on the naphthylalanine silica stationary phase. The results of these studies are summarized in the present paper. The displacers were then used to develop a displacement chromatographic method for the separation of the enantiomers of the glycerol ether derivatives, the results of which will be discussed in Part II [11].

## EXPERIMENTAL

### Materials

A 250 mm × 4.6 mm I.D. Rexchrom column, packed with a 5- $\mu$ m D-naphthylalanine silica (DNAS) was obtained from Regis (Morton Grove, IL, USA) and used for the retention studies. Another, 100 mm × 2.6 mm I.D. column was slurry-packed in our laboratory [12] using another batch of the 5- $\mu$ m DNAS stationary phase (a gift by Dr. J. Perry of Regis). This small column was used for the adsorption isotherm determinations using the frontal chromatographic technique [13]. Both columns were equipped with water jackets and thermostatted by a UF-3 type recirculating water bath (Science and Electronics, Dayton, OH, USA) at 30°C, unless indicated otherwise.

HPLC-grade *n*-hexane (Baxter, Muskegon,

MI, USA) and tetrahydrofuran (Fisher Scientific, Fair Lawn, NJ, USA) were used for eluent preparation. Reagent-grade 3,5-dinitrobenzoyl chloride (DNB) was obtained from Aldrich (Milwaukee, WI, USA) and used as received. The mixtures of *n*-alcohols (ALFOL C<sub>16</sub>–C<sub>28</sub>) were obtained from Vista Chemical Co. (Houston, TX, USA); the other chemicals used were obtained from Aldrich, Eastman-Kodak (Rochester, NY, USA), Fisher Scientific or Wiley Organic (Cochocton, OH, USA), and used without further purification.

### Apparatus

An isocratic liquid chromatograph consisting of a Type 2020 pump, a Type 2050 variable-wavelength UV detector (all from Varian, Walnut Creek, CA, USA), a pneumatically activated, computer-controlled Type 7000 injection valve (Rheodyne, Cotati, CA, USA) equipped with 10- and 50- $\mu$ l sample loops, and a Maxima 820 chromatographic work station (Millipore, Bedford, MA, USA) was used for the retention studies. A custom-built displacement chromatograph consisting of two Type 2020 pumps, a Type 2050 variable-wavelength UV detector and a Type RI-3 differential refractive index detector (all from Varian), as well as a pneumatically activated, computer-controlled Type 7000 injection valve (Rheodyne) equipped with 100- $\mu$ l to 5-ml sample loops, and a Type 7010 switching valve (Rheodyne) as described in ref. 12, was used for the adsorption isotherm determinations. A Type 4270 integrator (Varian), connected to a NEC Powermate I AT-compatible computer (Computer Access, College Station, TX, USA) and running the Chromplot-1 program developed in our laboratory [12], was used for system control, data collection and analysis.

### Synthetic procedures

The details of displacer synthesis are described elsewhere [10]. Briefly, ester and amide-type displacers were synthesized according to the general Schotten–Baumann reaction schemes, while the carbamate-type displacers were obtained by reacting alcohols with 3,5-dinitrophenylisocyanate, generated *in situ* by thermal decomposition of the corresponding azide [5].

### Adsorption isotherm measurements

The adsorption isotherms of the potential displacers were determined by frontal analysis using the small packed column. All isotherms were measured up to the solubility limit of the particular compound. In each successive step, the amount of displacer adsorbed on the stationary phase was calculated by the following equation:

$$q_i = [C_{mi}(V_m - V_0)] + q_{i-1} \quad (1)$$

where  $q_{i-1}$  is the amount of the compound adsorbed through the  $(i-1)$ th step ( $\mu\text{mole}/\text{column}$ ),  $C_{mi}$  is the mobile phase concentration ( $\text{mM}$ ) of the compound in the  $i$ th step,  $V_m$  is the breakthrough volume ( $\text{ml}$ ) of the concentration front in the  $i$ th step, and  $V_0$  is the column hold-up volume ( $\text{ml}$ ). The hold-up volume of the column was determined at  $30^\circ\text{C}$  by injecting an *n*-heptane solution into the eluent and recording the signal of the differential refractive index detector: it was  $0.4 \text{ ml}$ . The geometrical volume and the void volume were then used to calculate the void volume fraction and the nominal stationary phase volume [14] and resulted in a void volume fraction of  $\varepsilon = 0.75$ , a calculated phase ratio of  $F = 0.333$  ( $F = (1 - \varepsilon)/\varepsilon$ ), and a nominal stationary phase volume of  $V_s = 0.133 \text{ ml}$ . With these values, both the mobile phase concentrations and the stationary phase concentrations could be expressed in  $\text{mmol}/\text{l}$  units.

## RESULTS AND DISCUSSION

### Retention studies of the potential displacers

The single most important factor that precludes the more widespread use of displacement chromatography is the lack of universally applicable displacers. The displacers must meet several contradictory criteria: they must have convex adsorption isotherms, be adsorbed more strongly on the stationary phase than the compounds to be separated, and be reasonably soluble in the carrier solvent to allow the preparation of concentrated displacer solutions. Furthermore, their chromatographic characteristics should, preferably, be similar to those of a large number of

different solutes over a wide range of experimental conditions.

Unfortunately, no single compound possesses all these characteristics. However, in the case of a Pirkle-type stationary phase, one can identify the intermolecular interactions that lead to the desired adsorption characteristics: carefully balanced  $\pi$ - $\pi$  interactions, hydrogen bonding interactions and Van der Waals-type interactions. Thus, the generic structure of a displacer to be used on a Pirkle-type phase can be deduced: it should contain a  $\pi$ -acid (e.g. a 3,5-dinitrophenyl-) or  $\pi$ -base (e.g. a naphthylamine-) anchor group, a hydrogen-donor/acceptor group (e.g. an amide group), and a hydrophobic, solubility adjusting group (e.g. a long-chain alkyl group). Preferably, these groups should be readily attachable to a common core structure using inexpensive reagents and simple preparative methods.

In order to find broadly applicable displacers for the Pirkle-type phase, three series of homologous compounds were synthesized and studied in detail: the 3,5-dinitrobenzoyl esters of alcohols (DNB esters), the 3,5-dinitrophenylcarbamates of alcohols (DNP carbamates), and the *N*-3,5-dinitroamidoethyl-1-alkanoates (DNB amides).

The DNB esters with carbon numbers ranging from 1 to 28 were synthesized and their capacity factors were determined in tetrahydrofuran (THF)-*n*-hexane eluents at  $30^\circ\text{C}$ . The  $k'$  values are shown in Fig. 1 as a function of the alkyl

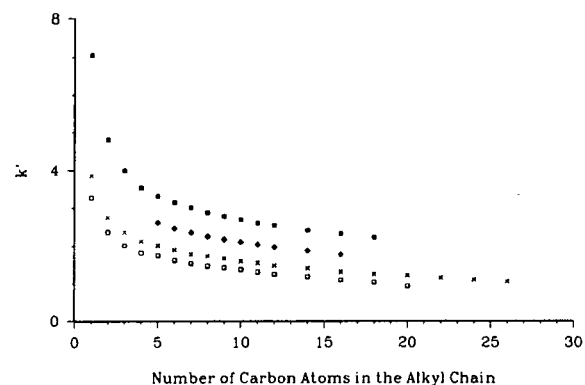


Fig. 1. The  $k'$  values of the DNB esters of *n*-alcohols as a function of the number of carbon atoms in their alkyl chain in different THF-*n*-hexane eluents at  $30^\circ\text{C}$ . Symbols: ■ = 2.5% THF; ◆ = 5% THF; × = 7.5% THF; □ = 10% THF.

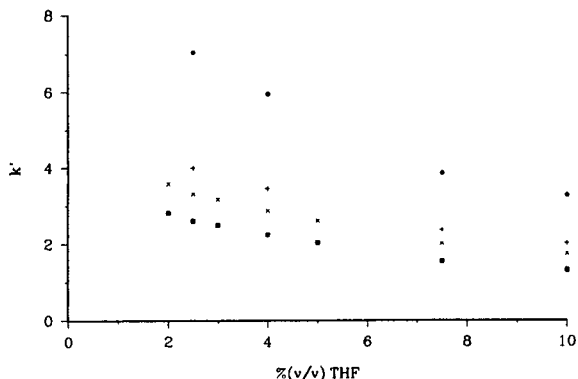


Fig. 2. The  $k'$  values of the DNB esters of  $n$ -alcohols with odd carbon numbers as a function of the % (v/v) THF concentration in different THF- $n$ -hexane eluents at 30°C. Symbols: ● =  $C_1$ ; + =  $C_3$ ; × =  $C_5$ ; ■ =  $C_{11}$ .

chain length. Initially,  $k'$  decreases very rapidly with the chain length. However, once the alkyl group becomes larger than hexyl, the change in  $k'$  becomes very small. This indicates that the first ten or so members of the DNB ester homologous series cover almost the entire of  $k'$  range that one can expect to see for these compounds. Therefore, the derivatives which have a very long alkyl chain will be of a lesser practical significance as displacers, and the disproportionately greater difficulties which are encountered when one tries to synthesize them in sufficiently high purity can be avoided.

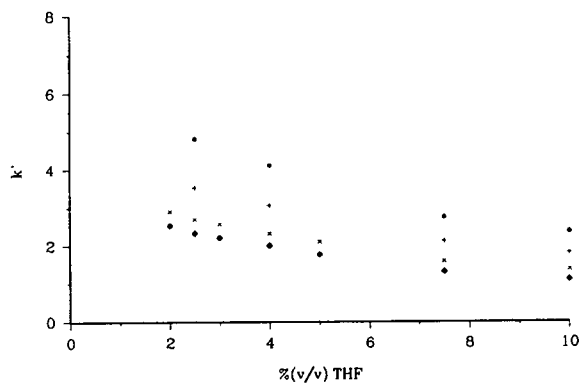


Fig. 3. The  $k'$  values of the DNB esters of  $n$ -alcohols with even carbon numbers as a function of the % (v/v) THF concentration in different THF- $n$ -hexane eluents at 30°C. Symbols: ● =  $C_2$ ; + =  $C_4$ ; × =  $C_{10}$ ; ◆ =  $C_{16}$ .

The  $k'$  values of the DNB esters are shown as a function of the THF concentration in Figs. 2 and 3 for the odd carbon number esters and the even carbon number esters, respectively. The  $k'$  values do not decrease with the THF concentration very rapidly, and the largest extrapolated capacity factor is less than about 20 (for the methanol derivative in pure  $n$ -hexane) indicating that the DNB esters do not form strong hydrogen bonds with the stationary phase.

DNP carbamate derivatives of  $n$ -alcohols were synthesized to produce more strongly retained displacers by increasing the hydrogen bonding opportunities with the additional NH group. The  $k'$  values of the DNP carbamates are shown in Fig. 4 as a function of the number of carbon atoms in the alkyl chain. A comparison of Figs. 1 and 4 shows that the DNP derivatives are indeed more strongly retained than the corresponding DNB esters, especially at low THF concentrations. Just as with the DNB esters, the capacity factor decreases very rapidly as the chain length increases from methyl to amyl, but from then on the decrease is slow, indicating that the promising displacer candidates are the methyl to decyl derivatives which can be synthesized in sufficiently high purity relatively easily. The  $k'$  values of the DNP carbamates are shown as a function of the THF concentration in Figs. 5 (odd number of carbon atoms) and 6 (even number of carbon atoms). A comparison of Figs. 2 and 5, and 3

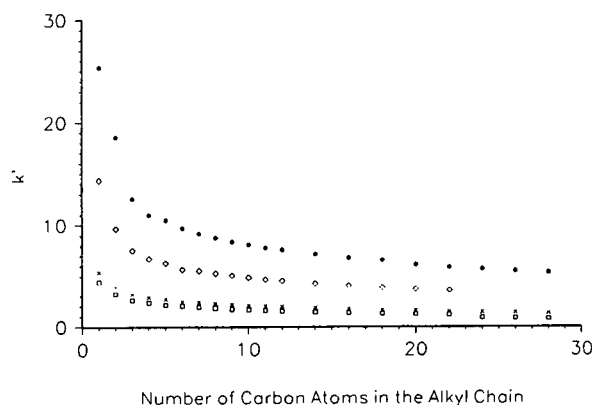


Fig. 4. The  $k'$  values of the DNP carbamates of  $n$ -alcohols as a function of the number of carbon atoms in their alkyl chain in different THF- $n$ -hexane eluents at 30°C. Symbols: ● = 2.5% THF; ◇ = 4% THF; × = 7.5% THF; □ = 10% THF.

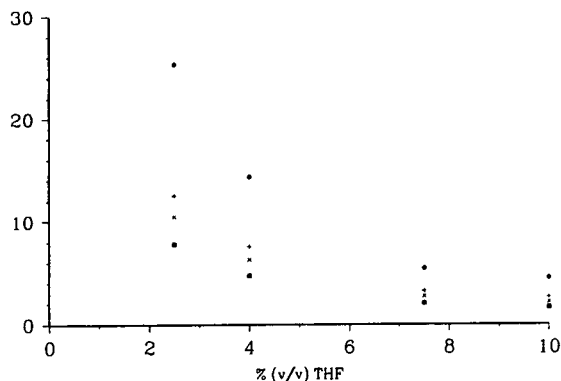


Fig. 5. The  $k'$  values of the DNP carbamates of  $n$ -alcohols with odd carbon numbers as a function of the % (v/v) THF concentration in different THF- $n$ -hexane eluents at 30°C. Symbols: ● = C<sub>1</sub>; + = C<sub>3</sub>; × = C<sub>5</sub>; ■ = C<sub>11</sub>.

and 6 shows that the retention of the DNP carbamates decreases with the THF concentration much more rapidly than that of the DNB esters. The largest extrapolated capacity factor is about 50 (for the methanol derivative in pure  $n$ -hexane) indicating that the DNP carbamates do form strong hydrogen bonds with the stationary phase. The rapid decrease of the  $k'$  values brought about by the THF is quite understandable, considering that both the stationary phase and the THF covet the additional polar bonding site which is present in the DNP carbamates.

A third family of even more polar compounds was synthesized based on the bifunctional start-

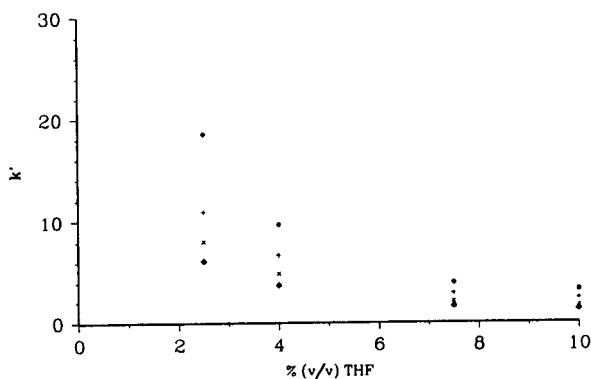


Fig. 6. The  $k'$  values of the DNP carbamates of  $n$ -alcohols with even carbon numbers as a function of the % (v/v) THF concentration in different THF- $n$ -hexane eluents at 30°C. Symbols: ● = C<sub>2</sub>; + = C<sub>4</sub>; × = C<sub>10</sub>; ◆ = C<sub>16</sub>.

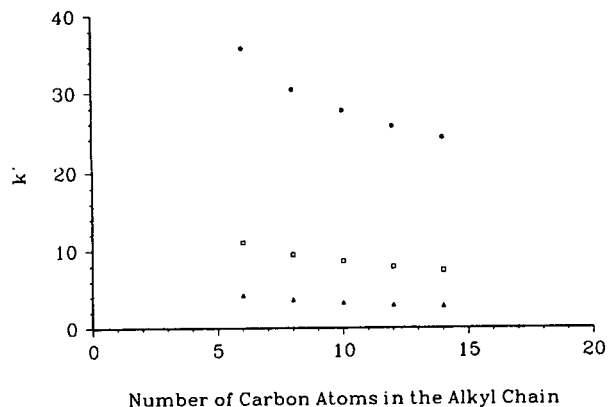


Fig. 7. The  $k'$  values of the N-3,5-dinitrobenzamidoethyl alkanooates as a function of the number of carbon atoms in their alkyl chain in different THF- $n$ -hexane eluents at 30°C. Symbols: ● = 5% THF; □ = 10% THF; ▲ = 15% THF.

ing material, ethanolamine. The amino group was reacted with 3,5-dinitrobenzoyl chloride at subambient temperatures (0–4°C), followed by esterification of the hydroxyl group with  $n$ -alkanoyl chlorides (6–14 carbon atoms). The capacity factors of these compounds, measured in 5, 10 and 15% (v/v) THF in  $n$ -hexane eluents, are plotted in Fig. 7 as a function of the alkyl chain length, and in Fig. 8 as a function of the % (v/v) THF concentration. Much more than with the other homologous series, the  $k'$  values decrease rapidly with both the chain length and the THF concentration. These compounds are much more retained than either the DNB esters or the

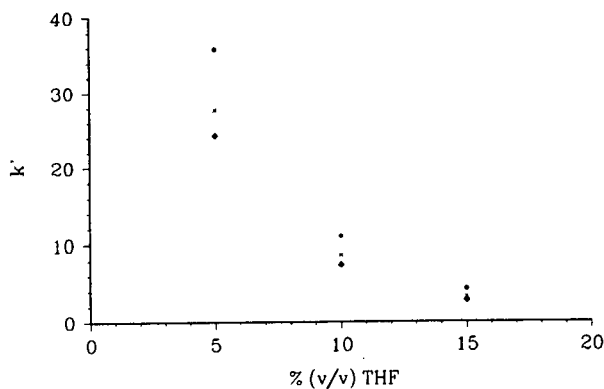


Fig. 8. The  $k'$  values of the N-3,5-dinitrobenzamidoethyl alkanooates as a function of the % (v/v) THF concentration in the THF- $n$ -hexane eluents at 30°C. Symbols: ● = C<sub>6</sub>; × = C<sub>10</sub>; ◆ = C<sub>14</sub>.



DNP carbamates: the largest extrapolated capacity factor is around 100 (for the methanol derivative in pure *n*-hexane).

Since all members of these three homologous series display regular retention behavior and their  $k'$  values cover a sufficiently broad range, their adsorption isotherms were investigated to determine their utility as potential displacers for normal-phase chiral separations.

#### Determination of the adsorption isotherms

The individual excess adsorption isotherms of the DNB esters were determined by the breakthrough method using a carrier solution of 7.5% (v/v) THF in *n*-hexane at 30°C. Because the DNB esters are very soluble in this carrier solvent, quite high mobile phase concentrations could be tested. Some of the measured individual excess adsorption isotherms are shown in Fig. 9. The single-component, simple Langmuir isotherm equation was fitted to the measured data and the  $a$  and  $b$  isotherm parameters were evaluated using the least-squares method. The isotherm parameters were used to recalculate the individual excess adsorption isotherms, which are shown as solid lines in Fig. 9. There is a reasonably good fit between the measured isotherms (symbols) and the calculated isotherms (lines).

The logarithms of the isotherm parameters are linearly related to the number of carbon atoms in

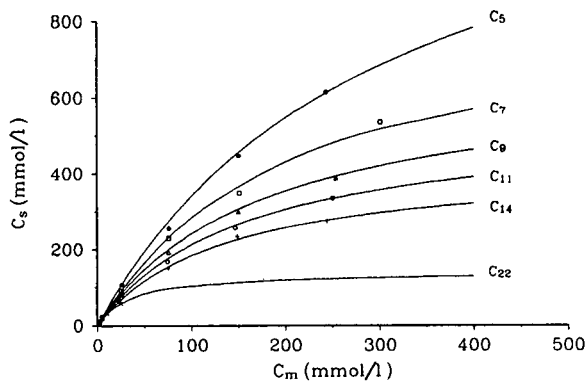


Fig. 9. Individual excess adsorption isotherms of the 3,5-dinitrobenzoyl esters of *n*-alcohols. Carrier: 7.5% (v/v) THF in *n*-hexane at 30°C. Symbols: ● = C<sub>5</sub>; □ = C<sub>7</sub>; △ = C<sub>9</sub>; ○ = C<sub>11</sub>; + = C<sub>14</sub>; × = C<sub>22</sub>.

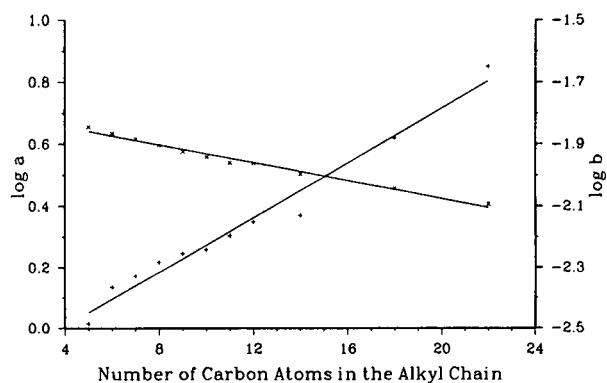


Fig. 10. The logarithm of the isotherm parameters  $a$  and  $b$  as a function of the length of the alkyl chain for the 3,5-dinitrobenzoyl esters of *n*-alcohols. Carrier: 7.5% (v/v) THF in *n*-hexane at 30°C. Symbols: × = log  $a$ ; + = log  $b$ .

the alkyl chain, as shown in Fig. 10, and to each other, as shown in Fig. 11. This suggests that the adsorption strength in the family of DNB esters varies regularly with the structure of the compounds, and that quantitative structure–adsorption relationships, similar to the familiar quantitative structure–retention relationships [15] can be derived from these data.

The individual excess adsorption isotherms of the most polar displacer candidates, the DNB amides, are shown in Fig. 12. The measurements were limited to the 0 to 15 mM concentration range, because the solubilities of the DNB amides are low at 30°C in the 10% (v/v) THF in

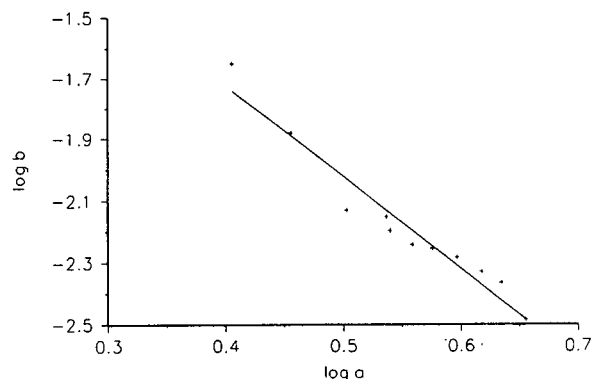


Fig. 11. Log  $a$  as a function of log  $b$  for the the 3,5-dinitrobenzoyl esters of *n*-alcohols. Carrier: 7.5% (v/v) THF in *n*-hexane at 30°C.

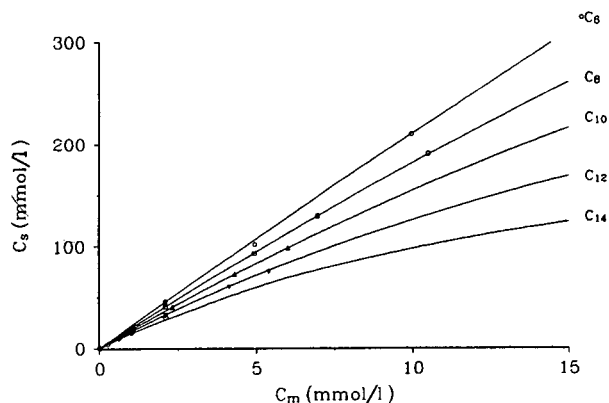


Fig. 12. Individual excess adsorption isotherms of the N-3,5-dinitrobenzamidoethyl alkanates. Carrier: 10% (v/v) THF in *n*-hexane at 30°C. Symbols: ○ = C<sub>6</sub>; □ = C<sub>8</sub>; △ = C<sub>10</sub>; ▽ = C<sub>12</sub>; ◇ = C<sub>14</sub>.

*n*-hexane solvent. The adsorption isotherm parameters, *a* and *b*, were determined as before and are shown in Figs. 13 and 14. It can be seen from Fig. 12 that the fit between the measured isotherms (symbols) and the calculated isotherms (solid line) is again reasonably good. The isotherm parameters, log *a* and log *b*, are linearly related to the number of carbon atoms in the alkyl chain, as shown in Fig. 13, and to each other, as shown in Fig. 14. It can be seen by comparing the *a* parameters in Figs. 10 and 13 that the adsorption strength of the DNB amides is about five times higher than that of the DNB esters, and that the adsorption strength of the

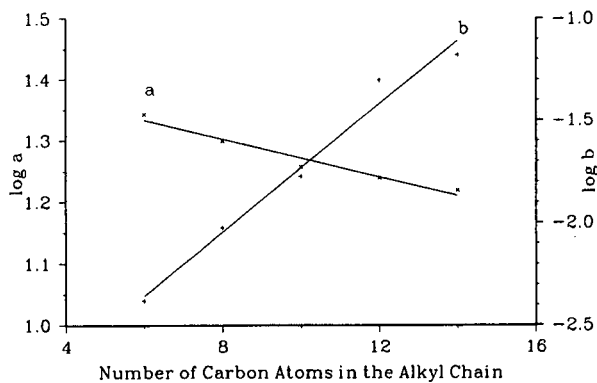


Fig. 13. The logarithm of the isotherm parameters *a* and *b* as a function of the length of the alkyl chain for the N-3,5-dinitrobenzamidoethyl alkanates. Carrier: 10% (v/v) THF in *n*-hexane at 30°C. Symbols: × = log *a*; + = log *b*.

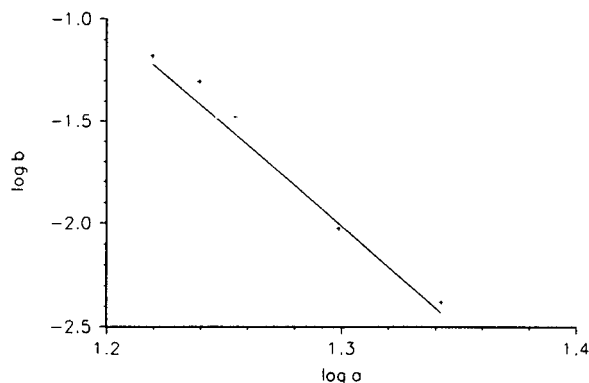


Fig. 14. Log *a* as a function of log *b* for the N-3,5-dinitrobenzamidoethyl alkanates. Carrier: 10% (v/v) THF in *n*-hexane at 30°C.

DNB amides decreases with the increasing carbon number more rapidly than the adsorption strength of the DNB esters.

Some of these displacers were successfully used for the development of chiral displacement chromatographic separations on Pirkle-type stationary phases, cyclodextrin-based stationary phases, and cellulose-based stationary phases [16]. These results will be discussed in Part II of this series.

## CONCLUSIONS

Several displacer families covering a broad range of polarities (DNB esters, DNP carbamates and DNB amides) were designed and synthesized according to the concept of generic displacers. These displacers contain at least one anchoring group, one hydrogen bonding group and a solubility adjusting group. The retention and the adsorption properties of these displacers were determined and found to follow very regular patterns as a function of the length of their alkyl chain: longer chains result in smaller capacity factors and weaker adsorption. This regular adsorption behavior permits straightforward selection of a displacer for a Pirkle-type chiral stationary phase and eliminates most of the trial-and-error effort traditionally involved in the development of a displacement chromatographic separation.

## ACKNOWLEDGEMENT

Partial financial support by the National Science Foundation (CH-8919151), the Texas Coordinating Board of Higher Education TATR Program (Grant No. 3376) and the Dow Chemical Company, Midland, MI to Gy.V., and by the Department of Energy, Office of Basic Energy Sciences (DE-FG 06-88 ER13963) to D.H.T. is gratefully acknowledged.

## REFERENCES

- 1 W.H. Pirkle, J.M. Finn, J.L. Schreiner and B.C. Hamper, *J. Am. Chem. Soc.*, 103 (1981) 3964.
- 2 W.H. Pirkle and T.C. Pochapsky, *J. Org. Chem.*, 51 (1986) 102.
- 3 W.H. Pirkle and T.C. Pochapsky, *J. Am. Chem. Soc.*, 108 (1986) 352.
- 4 W.H. Pirkle and T.C. Pochapsky, *J. Am. Chem. Soc.*, 108 (1986) 5267.
- 5 W.H. Pirkle, T.C. Pochapsky, G.S. Mahler, D.E. Corey, D.S. Reno and D.M. Alessi, *J. Org. Chem.*, 51 (1986) 102.
- 6 C.E. Dalglish, *J. Am. Chem. Soc.*, 137 (1952) 3940.
- 7 P.L. Camacho, E. Geiger, Gy. Vigh, R. Webster and D.H. Thompson, *J. Chromatogr.*, 506 (1990) 611.
- 8 Gy. Vigh, G. Quintero and Gy. Farkas, *J. Chromatogr.*, 484 (1989) 256.
- 9 Gy. Vigh, L.H. Irgens and Gy. Farkas, *J. Chromatogr.*, 502 (1990) 11.
- 10 P.L. Camacho, *Dissertation*, Texas A&M University, College Station, TX, 1991.
- 11 P.L. Camacho, Gy. Vigh and D.H. Thompson, *J. Chromatogr.*, submitted for publication.
- 12 Gy. Vigh, G. Quintero and Gy. Farkas, *J. Chromatogr.*, 484 (1989) 251.
- 13 A. Bartha and Gy. Vigh, *J. Chromatogr.*, 260 (1983) 337.
- 14 S. Golshan-Shirazi and G. Guiochon, *Anal. Chem.*, 60 (1988) 2364.
- 15 R. Kaliszan, *Quantitative Structure–Chromatographic Retention Relationships*, Wiley, New York, 1987.
- 16 Gy. Vigh, P.L. Camacho, C. Piggee and M.D. Beeson, presented at the 16th International Symposium on Column Liquid Chromatography, Baltimore, MD, June 14–19, 1992.

# Liquid chromatographic chiral separations of the N-6-(*endo*-2-norbornyl)-9-methyladenine enantiomers

D.T. Witte\*

University Centre for Pharmacy, A. Deusinglaan 2, 9713 AW Groningen (Netherlands)

M. Ahnoff and K.-E. Karlsson

Astra Hässle AB, 431 83 Mölndal (Sweden)

J.-P. Franke and R.A. de Zeeuw

University Centre for Pharmacy, A. Deusinglaan 2, 9713 AW Groningen (Netherlands)

(First received January 7th, 1993; revised manuscript received March 2nd, 1993)

## ABSTRACT

Attempts to separate the enantiomers of the novel adenosine antagonist N-0861, the racemic mixture of N-6-(*endo*-2-norbornyl)-9-methyladenine, by high-performance liquid chromatography are described. Owing to the very low efficiency and the lack of selectivity of the  $\alpha$ -AGP column, the direct separation method did not give satisfactory results. The indirect separation method involved derivatization of N-0861 with (+)-1-(9-fluorenyl)ethylchloroformate. The method is easy to perform and aqueous solutions can be used. The calibration graphs showed that the reaction is linear. A resolution between the formed diastereoisomers of 1.13 within 30 min was obtained on a  $C_8$  column with an acetonitrile–water eluent. The identities of the reaction products were checked by LC–MS.

## INTRODUCTION

The racemic mixture of N-6-(*endo*-2-norbornyl)-9-methyladenine (N-0861), (Whitby Research, Richmond, VA, USA), the structure of which is depicted in Fig. 1, is under study as a novel adenosine antagonist. The adenosine receptor can be divided into several subtypes [1]. Although it is known that biologically active molecules, such as receptors and enzymes, tend to be stereoselective in their binding to, and activation by, *e.g.* drugs [2], N-0861 is under study as a racemate.

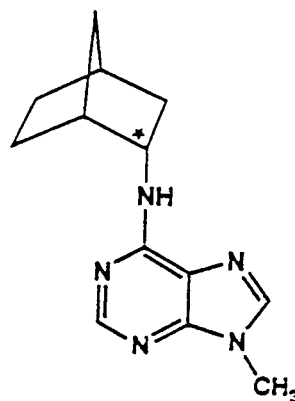


Fig. 1. Structure of N-0861. The asterisk denotes the chiral centre.

\* Corresponding author. Present address: Astra Hässle AB, Bioanalytical Chemistry, 431 83 Mölndal, Sweden.

This paper describes a direct and an indirect high-performance liquid chromatographic (HPLC) method for the separation of the enantiomers of N-0861. As N-0861 seemed to have no suitable functional groups close to the chiral centre that may facilitate an interaction with a particular chiral stationary phase, the choice of a suitable stationary phase was difficult. For protein-based chiral columns the enantioselective properties are based on principles of bioaffinity towards the protein [3]. A protein-based column was chosen because this bioaffinity involves a combination of hydrogen bonding, electrostatic interaction and hydrophobic interaction [4].

The indirect separation method [5] involved a derivatization reaction with (+)-1-(9-fluorenyl)ethylchloroformate [(+)-Flec]. Chloroformates are known for their reactivity towards amino acids [6], primary and secondary amines [6–8] and tertiary amines [9,10]. The supposed reaction scheme is depicted in Fig. 2 as reaction A.

The influences of pH and buffer on the derivatization reaction were studied together with the reaction time. The formation of the hydroxy product of (+)-Flec, which is shown as reaction

B in Fig. 2, needs to be controlled by appropriate pH adjustment of the reaction mixture.

To check the linearity of the derivatization reaction, calibration graphs were constructed for both diastereoisomers in the range 80–0.625  $\mu\text{g/ml}$  of racemic N-0861. The influence of concentration on the resolution of the diastereoisomers was studied using the same calibration graphs.

## EXPERIMENTAL

### HPLC equipment

Unless indicated otherwise, the solvent-delivery system was a Model 9010 HPLC pump and 20- $\mu\text{l}$  injections were made with a Model 9095 autosampler, both purchased from Varian (Walnut Creek, CA, USA). Detection at 270 nm was carried out with a Model 1000 S diode-array detector from Applied Biosystems (Foster City, CA, USA). Integration of the chromatograms was effected with an SP-4270 integrator (Spectra-Physics, San Jose, CA, USA). The experiments to improve the separation and to prepare the calibration graphs were carried out with a Model 2150 LKB HPLC solvent-delivery system (Pharmacia-LKB Biotechnology, Uppsala, Sweden).

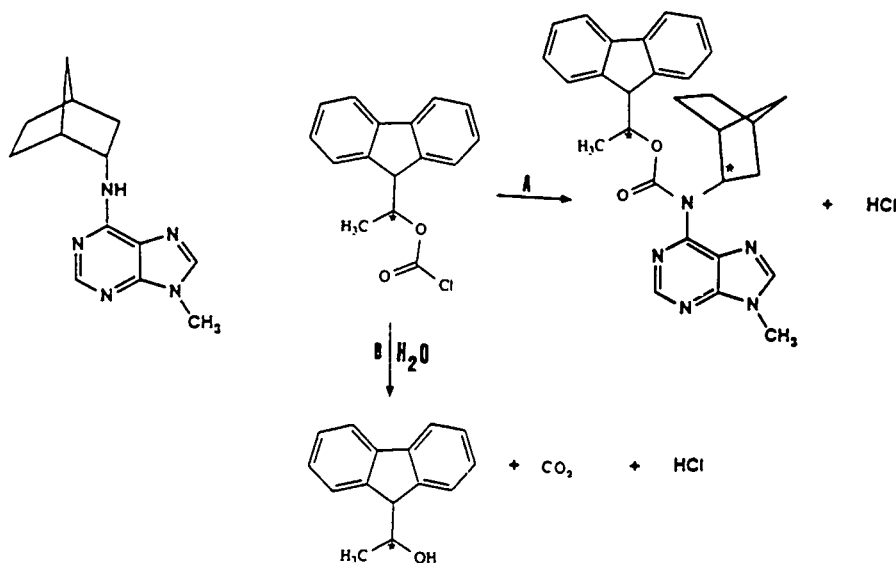


Fig. 2. (A) The expected reaction between N-0861 and (+)-Flec; (B) the hydrolysis of (+)-Flec resulting in (+)-Flec-OH. The asterisks denote the chiral centres.

This pump was used in combination with a Model 710 A WISP (Waters, Milford, MA, USA) and detection was carried out with a Model 770 spectrophotometric detector at 270 nm (Spectra-Physics, Santa Clara, CA, USA). For integrating the chromatograms a C-R3A Chromatopac (Shimadzu, Kyoto, Japan) and for recording a BD 40 recorder (Kipp, Delft, Netherlands) was used. If the column temperature was controlled the column was immersed in a water-bath. A combination of a Thermomix 1442 D thermostat (Braun, Rijswijk, Netherlands) and a cooling device (HETO, Birkerød, Denmark) was used to regulate the temperature the bath.

#### Mass spectrometers

Two types of liquid chromatographic–mass spectrometric (LC–MS) apparatus were used. In the following they will be referred to as LC–MS-I and LC–MS-II, respectively.

*LC–MS-I.* An API III triple quadrupole from Perkin-Elmer Sciex (Thornhill, Ontario, Canada) with an ion-spray interface was used. The repeller potential was +50 V for positive ions. The liquid chromatographic system used in combination with the Perkin-Elmer Sciex spectrometer consisted of a Hewlett-Packard (Palo Alto, CA, USA) Series 1050 pump and an autosampler, in combination with a Hewlett-Packard Series 1050 variable-wavelength UV detector. A 33 × 4 mm I.D. C<sub>18</sub> column with 5- $\mu$ m particles (Supelco, Bellefonte, PA, USA) was used for LC–MS-I.

*LC–MS-II.* A Finnigan MAT (San Jose, CA, USA) TSQ-700 mass spectrometer with an electrospray LC–MS interface was used. The mass detector was in the positive-ion mode. The eluent-delivery system was a Phoenix from Carlo Erba (Milan, Italy). A 900 × 0.25 mm column filled with 5- $\mu$ m particles of Kromasil C<sub>8</sub> (Eka Nobel, Bohus, Sweden) was used for LC–MS-II.

#### Chemicals

Racemic N-6-(endo-2-norbornyl)-9-methyladenine was a gift from Whitby Research, according to whom the drug was an optically neutral mixture of the (+)- and (–)-enantiomers. (+)-1-(9-Fluorenyl)ethyl chloroformate,

which was a 18 mM solution in acetone, was obtained from Aldrich Chemie (Steinheim, Germany). Deuterium oxide was purchased from Dr. Glaser (Basle, Switzerland), acetonitrile of HPLC grade from Rathburn (Walkerburn, UK) and acetic acid, sodium acetate, sodium borate and sodium phosphate, all of analytical-reagent grade, from Merck (Darmstadt, Germany). Four different buffer solutions were prepared in distilled water, namely 0.25 M borate (pH 8.1), 0.2 M phosphate (pH 7.0 and 6.3) and 0.2 M acetate (pH 5.2). These four buffers will be referred to as buffers a, b, c and d, respectively.

#### Direct separation method

For the direct separation a Chiral-AGP ( $\alpha$ -AGP) column (100 × 4 mm I.D.) (ChromTech, Stockholm, Sweden) with 5- $\mu$ m particles was used. The eluents studied consisted of different ratios of an organic modifier with 0.01 M phosphate buffer. Two phosphate buffers with corresponding pH values of 6.95 and 5.30 were used. The organic modifiers tested were methanol, ethanol, acetonitrile and 2-propanol. Both phosphate buffers were also tested without the addition of an organic modifier. Chromatographic runs were carried out with all eluent combinations at various temperatures in the range 0–50°C. The eluent flow-rate for all experiments was 0.5 ml/min. Injections of 20  $\mu$ l from a solution of 5  $\mu$ g/ml of N-0861 in the corresponding eluent were made.

#### Indirect separation method

Indirect separations, unless indicated otherwise, were carried out with a 150 × 4 mm I.D. Nucleosil C<sub>18</sub> column with 5- $\mu$ m particles (Macherey–Nagel, Düren, Germany) in combination with a gradient. The gradient started at 50% acetonitrile–50% 0.1 M acetic acid (pH 2.9) for the first 22 min, and from 22 to 40 min it was increased linearly to 100% acetonitrile. After each run the starting conditions were equilibrated for at least 15 min.

#### General derivatization procedure

The derivatization reactions were performed in 250- $\mu$ l autosampler microvial inserts. These inserts were placed in larger vials, which were

then sealed with Teflon seals. To 80  $\mu\text{l}$  of a solution of 200  $\mu\text{g}/\text{ml}$  of N-0861 in acetonitrile were added 80  $\mu\text{l}$  of one of the four buffers and 40  $\mu\text{l}$  of an 18 mM (+)-Flec solution in acetone. The vial was closed and the reaction was allowed to take place at room temperature for different time periods. The percentage of N-0861 still present in the sample was related to a reference solution of N-0861. This reference solution consisted of 80  $\mu\text{l}$  of 200  $\mu\text{g}/\text{ml}$  of N-0861 in acetonitrile, 80  $\mu\text{l}$  of the corresponding buffer and 40  $\mu\text{l}$  acetone. Because of the absence of (+)-Flec, this sample was considered to contain 100% N-0861. The mean value of the chromatographic peak area from these reference samples was used for further calculations.

#### *Procedure for studying the influence of type of buffer and pH on the derivatization reaction*

To study the influence of the type of buffer and the pH on the reaction rate, four different buffers (a, b, c and d) were studied. Injections were made 2 h after the reaction mixture was prepared. These experiments were carried out in duplicate on different days. The HPLC conditions are given under *Indirect separation method* and the detailed procedure for the derivatization reaction is outlined under *General derivatization procedure*.

#### *Procedure for studying the derivatization reaction*

To study the reaction time, samples were prepared as described under *General derivatization procedure*. The 0.2 M phosphate buffer of pH 7.0 was used. Injections were made at different times after the reaction had started. The corresponding derivatization times were in the range 1–1440 min. The HPLC conditions and the column were the same as those given under *Indirect separation method*, except that the acetic acid was omitted from the eluent, resulting in an eluent containing acetonitrile and water.

#### *Procedure for preparing the calibration graphs and studying the influence of different concentrations of N-0861 on the resolution between the diastereoisomers*

The solutions used to prepare the calibration graphs were prepared by adding 40  $\mu\text{l}$  of 18 mM

(+)-Flec in acetone to 80  $\mu\text{l}$  of phosphate buffer b and to 80  $\mu\text{l}$  of an N-0861 solution in acetonitrile. The concentration of racemic N-0861 in acetonitrile varied from 200 to 1.56  $\mu\text{g}/\text{ml}$ , which corresponds to a concentration range of racemic N-0861 in the reaction vial of 80–0.625  $\mu\text{g}/\text{ml}$ . The concentration range for each enantiomer therefore ranged from 40 to 0.313  $\mu\text{g}/\text{ml}$ . The HPLC system used is described under *Improvement of the separation*. Injections of 20  $\mu\text{l}$  were made more than 2 h after the preparation of the derivatization mixture. Calibrations graphs were constructed twice on different days. The mean peak area on the chromatogram of each diastereoisomer was used to prepare the calibration graph. The influence of different concentrations N-0861 on the resolution between the diastereoisomers was also studied.

#### *Liquid chromatographic–mass spectrometric procedure*

For the LC–MS experiments, derivatization samples were prepared using 0.2 M phosphate buffer (pH 7.0). Injections were made more than 2 h after the start of the derivatization reaction.

*LC–MS-I.* The eluent used was a gradient of a mixture of A (50% acetonitrile–50% 2 mM ammonium acetate–0.1% formic acid) and B (100% acetonitrile–0.1% formic acid). The gradient started at 100% A for 5 min, from 5 to 10 min it was changed to 10% A–90% B, this ratio was kept constant from 10 to 15 min, then from 15 to 20 min the gradient was returned to its starting point. The eluent flow-rate was 1.0 ml/min and 20- $\mu\text{l}$  injections from the derivatization mixture were made. The above conditions are further referred to as LC–MS-I.

*LC–MS-II.* The eluent used for these experiments was 70% acetonitrile–30% 5 mM ammonium acetate in  $\text{D}_2\text{O}$ . The flow-rate with this narrow-bore column was ca. 1  $\mu\text{l}/\text{min}$ . The amount injected was 100 nl.

## RESULTS AND DISCUSSION

### *Direct separation*

The direct method using the  $\alpha$ -AGP column for the separation of the N-0861 enantiomers was not satisfactory. The best results obtained with the tested eluents and temperatures are depicted

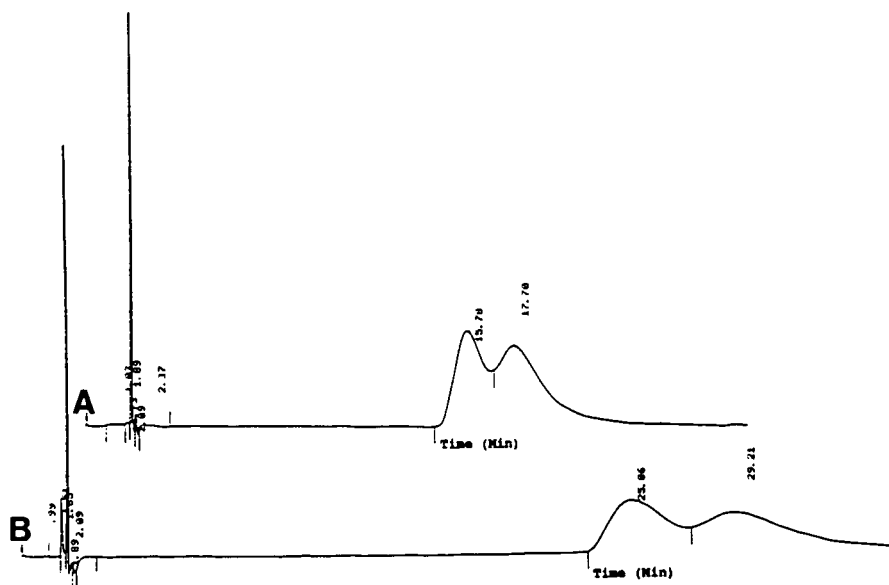


Fig. 3. Separation of the N-0861 enantiomers on an  $\alpha$ -AGP column. (A) Eluent acetonitrile–0.01 M phosphate buffer (pH 6.95) (3:97). Temperature, 20°C. (B) Eluent acetonitrile–0.01 M phosphate buffer (pH 6.95) (1:99). Temperature, 20°C.

in Fig. 3. With an eluent of 1% acetonitrile–99% 0.01 M phosphate buffer (pH 6.95) and a column temperature of 20°C, a resolution of 0.78 could be obtained.

#### Indirect separation

Fig. 4 shows a chromatogram obtained from a derivatized sample during the initial phase of the

studies. Peak 1 is the N-0861 still present in the sample, peak 2 the hydrolysis product of (+)-Flec, denoted as Flec-OH, peaks 3 the diastereoisomeric derivatization products and peak 4 the remaining (+)-Flec. These peaks were tentatively identified by comparing this chromatogram with reference chromatograms of the different solutions used for the derivatization. It should be

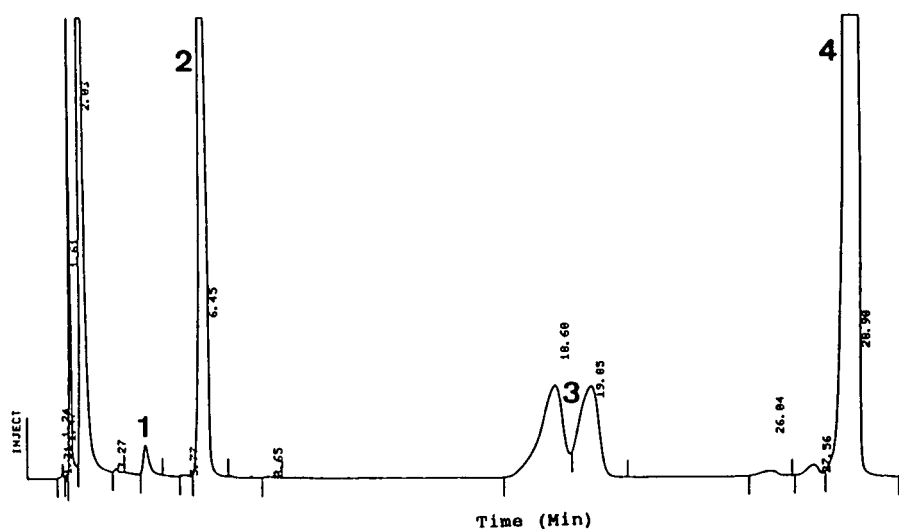


Fig. 4. Chromatogram obtained on a  $C_{18}$  column after derivatization of N-0861 with (+)-Flec. Conditions as given under Indirect separations. 1 = N-0861; 2 = (+)-Flec-OH; 3 = the two diastereoisomers resulting from the derivatization reaction; 4 = (+)-Flec.



noted that peaks number 3 and 4 exhibit pronounced fronting which does not occur in the other peaks; we have no explanation for this phenomenon. To be certain about the structure of the eluted compounds, LC-MS experiments were performed. The improvement of the initial separation is described later.

#### Liquid chromatography-mass spectrometry

The structures of three of the main peaks in the chromatogram in Fig. 4 could be elucidated with LC-MS-I. The resulting mass/charge ( $m/z$ ) ratios from LC-MS-I together with the molecular masses ( $M_r$ ) of the expected products are given in Table I.

Peak 1, which is underivatized N-0861, could not be detected with LC-MS-I because the derivatization reaction was almost complete. The  $m/z$  ratios of the ions of peaks 2 and 4 correspond to the ammonium adducts of the hydrolysis product of (+)-Flec and unchanged (+)-Flec, respectively. The ions found at peak 3 were different from the  $M_r + 1$  of the expected products, and they did not correspond to the ammonium adducts of the expected products. The ion of  $m/z$  498 suggest the addition of  $H_2O$  during the experiment. Under the influence of

TABLE I

MOLECULAR MASSES ( $M_r$ ) OF THE EXPECTED PRODUCTS FROM THE DERIVATIZATION REACTION AND THE ACTUALLY FOUND  $m/z$  RATIOS OF THE IONS DETECTED BY THE MASS SPECTROMETER CORRESPONDING TO THREE OF THE FOUR PEAKS IN FIG. 4

Parameter	Peak 1	Peak 2	Peak 3	Peak 4
$M_r$	243	210	479	272
$m/z$	n.d. <sup>a</sup>	228	498	290

<sup>a</sup> Not detected.

the chloroformate, the methyladenine ring structure present in N-0861 may have opened on addition of  $H_2O$ . The addition of  $H_2O$  will increase the  $M_r$  by 18. If the resulting molecule is protonated, the  $m/z$  will be 498. This supposed mechanism results in two possible products, as can be seen in Fig. 5, routes A and B. To verify this mechanism and to be able to distinguish between the products of routes A and B, LC-MS-II studies with an eluent containing  $^2H_2O$  instead of  $H_2O$  were performed [11]. With this eluent the number of protons linked to heteroatoms in the molecule can be determined. These protons will be exchanged with the

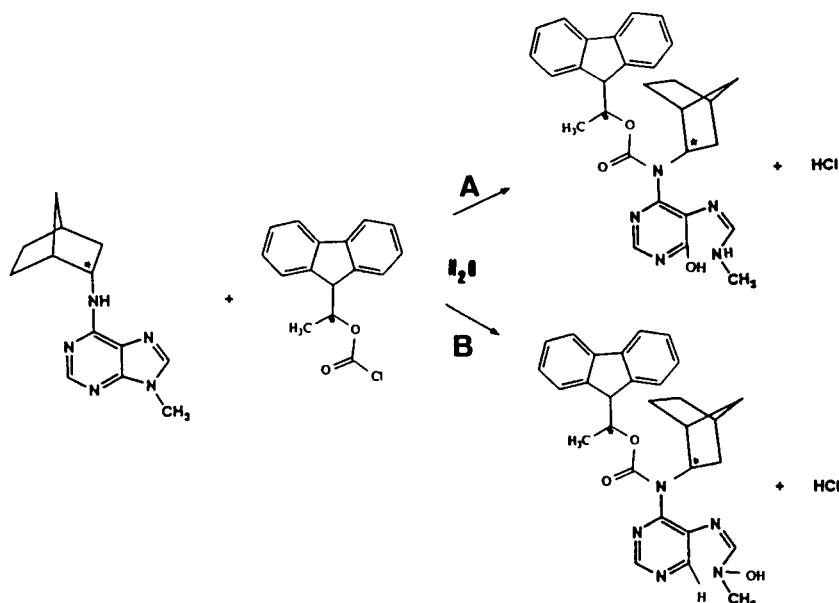


Fig. 5. The two possible derivatization reactions resulting in products that will yield  $m/z$  501 (route A) and 500 (route B) in LC-MS-II. The asterisks denote the chiral centres.

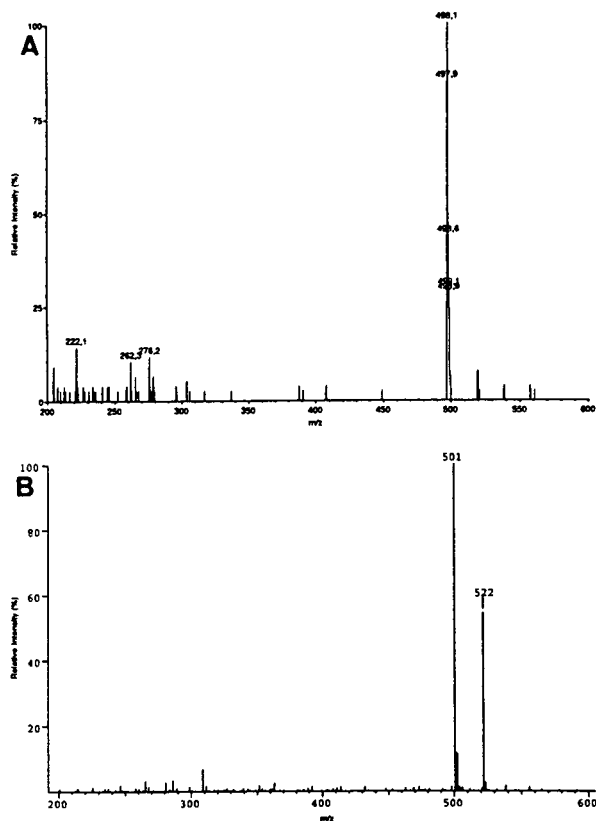


Fig. 6. Mass spectra of peak 3 in Fig. 4. (A) LC-MS-I with  $\text{H}_2\text{O}$  in the eluent; (B) LC-MS-II with  $^2\text{H}_2\text{O}$  in the eluent instead of  $\text{H}_2\text{O}$ .

deuterium ions present in the eluent, resulting in an increase in the  $m/z$  of 1 for each exchangeable proton present in the molecule. The proton which gives the molecule its charge will also be exchanged by a deuterium ion. The LC-MS-I

results showed an  $m/z$  of 498 for peak 3, as can be seen in Table I and Fig. 6A. Deuterium for the charge instead of a proton gives  $m/z$  499. If there is one exchangeable proton in the molecule as in the product of route B in Fig. 5, the  $m/z$  will be 500, and if there are two exchangeable protons the  $m/z$  must be 501. Fig. 6B shows the ions corresponding to peak 3 found in the LC-MS-II experiment. The ion of  $m/z$  501 suggests that there are two protons linked to heteroatoms (OH and NH) present in the derivative. Hence it can be concluded that the structure of the derivative is that depicted in Fig. 5, route A.

The ions of  $m/z$  520 and 522 in Fig. 6A and B, respectively, may result from complexation with sodium instead of protonation. Traces of sodium may have been present in the mobile phase even without it having been added.

#### *Influence of type of buffer and pH on the derivatization reaction*

Table 2 shows the results of the derivatization reaction in different buffers at various pH values. The use of a phosphate buffer of pH 6.3 or 7.0 gives the highest yield after 2 h. There is no significant difference between the reaction yields with these two buffers.

When the acetate buffer was used, an extra peak was observed in the chromatogram, as can be seen in Fig. 7. LC-MS-I showed that this peak contained an ion of  $m/z$  314. This  $m/z$  suggests the formation of an ammonium adduct with the product from the reaction between acetate and (+)-Flec. The reaction between

TABLE II

EFFECT OF THE BUFFER AND pH ON THE DERIVATIZATION REACTION AND ON THE CONVERSION OF (+)-FLEC TO (+)-FLEC-OH ( $n = 2$ )

Buffer	pH	N-0861 left (%)	Total area of the two diastereoisomers formed ( $n = 2$ )	(+)-Flec-OH formed (%) ( $n = 2$ ) <sup>a</sup>
(a) borate	8.1	5.7	3 690 240, 3 442 788	93, 82
(b) phosphate	7.0	1.0	4 387 925, 3 952 745	28, 30
(c) phosphate	6.3	1.1	4 329 186, 400 895	31, 23
(d) acetate	5.2	46.1	n.d. <sup>b</sup>	77, 80

<sup>a</sup> % (+)-Flec-OH = [area (+)-Flec-OH/area (+)-Flec-OH + area (+)-Flec] · 100.

<sup>b</sup> Not detected; see text.

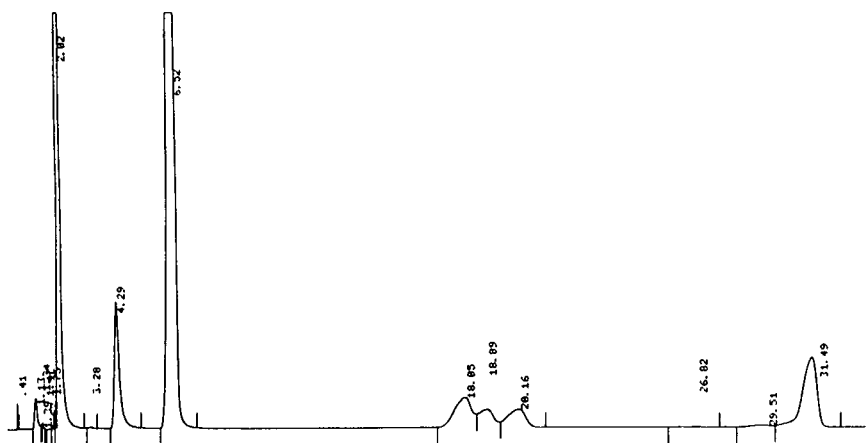


Fig. 7. Chromatogram obtained from the product of the derivatization reaction in the acetic acid buffer (pH 5). The disturbing peak elutes at 18 min.

acetate and (+)-Flec may result in the formation of an anhydride [12]. This anhydride, which is unstable in an aqueous environment, co-elutes with the diastereoisomers with a retention time of 18 min. The degradation product of the anhydride in aqueous solution is probably Flec-OH. This explains the high percentage of Flec-OH in Table II for the experiment with the acetate buffer. Acetate present in the reaction medium reacts with the Flec before the desired reaction between Flec and N-0861 is complete, and the resulting anhydride gives a disturbing peak in the chromatogram. With the knowledge of the reaction between the acetate and the (+)-Flec in mind, it was checked whether the acetate in the eluent reacts with (+)-Flec during the chromatographic run. A reference (+)-Flec, namely a solution of 80  $\mu$ l of acetonitrile with 80  $\mu$ l of phosphate buffer (pH 7) and 40  $\mu$ l of a 18 mM (+)-Flec solution in acetone, was injected into the chromatographic system. A small peak eluted at the same time as the product between acetate and (+)-Flec. Therefore, to avoid this reaction, the acetic acid was removed from the eluent. This had no effect on the retention and/or peak shape of the diastereoisomers, (+)-Flec and (+)-Flec-OH, but the retention of N-0861 was delayed by 1.5 min to 6 min and the disturbing peak had disappeared.

#### Output of the derivatization reaction

Fig. 8 shows the results after different reaction times. It can be seen that the reaction is more than 90% complete after 1 h. The variation in the percentage of the diastereoisomers formed after a reaction time of more than 1 h may be an indication for the precision of the method. The average percentage of the formed diastereoisomers after a reaction time of more than 59 min was 94% with a relative standard deviation of 3%

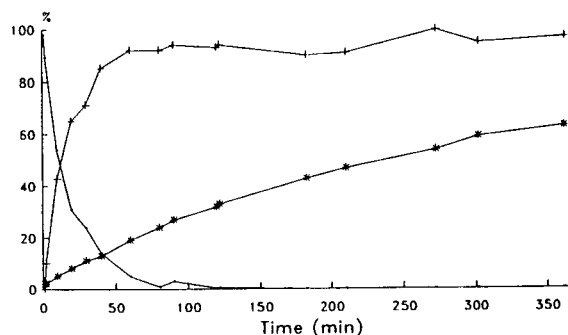


Fig. 8. Influence of reaction time on the derivatization yield. (●) % N-0861 = (area N-0861 after derivatization/area of the reference N-0861) · 100. (+) % derivatives = (total area of the two diastereoisomers at a certain time/total area of the two diastereoisomers after a time of 272 min) · 100. (\*) % Flec-OH = [area (+)-Flec-OH/area (+)-Flec-OH + area (+)-Flec] · 100.

( $n = 11$ ). After 1 h N-0861 was no longer detectable and differences in the amount of the reaction product will reflect the random errors in the procedure. The reaction product is stable for at least 1 day.

#### Improvement of the separation

The highest resolution within acceptable retention times,  $t_{R_1}$  and  $t_{R_2}$  of 27 and 30 min respectively, was obtained with a  $125 \times 4$  mm I.D. LiChrospher RP Select B  $C_8$  column with  $5\text{-}\mu\text{m}$  particles (Merck). The combination of this  $C_8$  column, which was thermostated at  $30^\circ\text{C}$ , with an eluent of water–acetonitrile (60:40, v/v) and a flow-rate of 1 ml/min resulted in a resolution ( $R_s$ ) of 1.13. A chromatogram obtained under these conditions is shown in Fig. 9. Underivatized N-0861 could not be detected because the derivatization reaction was almost complete at the time the sample was injected into the HPLC system. The long run time is necessary to allow the unreacted (+)-Flec to elute from the column. If the remaining (+)-Flec could be removed before the injection, the run time could be decreased substantially. The disadvantage of removing anything from the reaction sample is the risk that some of the diastereoisomers will also be removed. If the latter happens it will

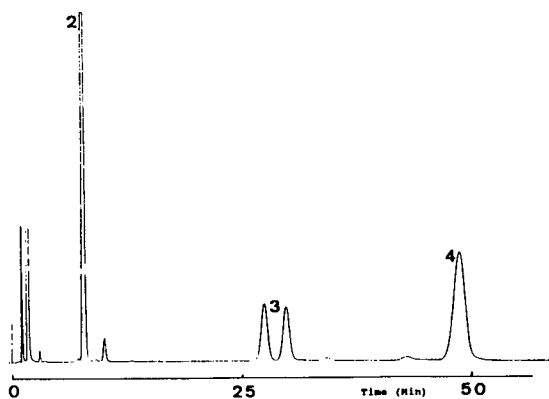


Fig. 9. Chromatogram obtained on a  $C_8$  column, after derivatization of N-0861 with (+)-Flec. Conditions as given under Improvement of the separation. 2 = (+)-Flec-OH; 3 = the two diastereoisomers resulting from the derivatization reaction; 4 = (+)-Flec.

decrease the sensitivity of the method. Another method to decrease the run time may be to use gradient elution after the diastereoisomers have eluted from the column. However, the easiest way to remove Flec is to inject samples one day after the derivatization. The derivatization products are sufficiently stable but Flec will be converted completely into Flec-OH, which elutes at about 7 min.

#### Calibration graphs and influence of different concentrations of N-0861 on the resolution between the diastereoisomers

The calibration graphs are described by the equation

$$y = Ax + B \quad (1)$$

where for the first-eluting isomer  $A = 7.64 \cdot 10^{10}$ ,  $B = 432$  and the correlation coefficient  $r = 0.9999$  and for the second-eluting isomer  $A = 8.54 \cdot 10^{10}$ ,  $B = 5659$  and  $r = 0.9999$ . As the individual enantiomers of N-0861 were not available, the calibration graphs were prepared using racemic N-0861. The elution order therefore could not be established. The calibration graphs for the single diastereoisomers show good linearity with  $r = 0.9999$  in each instance. This shows that the derivatization reaction resulting in the formation of the diastereoisomers is linear, at least in the concentration range studied. The lowest concentration studied corresponds to a total amount injected of 6 ng for each N-0861 enantiomer.

It should be noted that there is no significant influence of concentration on the resolution. Nevertheless, for enantiomeric purity studies, calibration graphs with different ratios of the enantiomers should be prepared because a large amount of the first-eluting diastereoisomer can easily disturb the measurement of a small peak of the second-eluting diastereoisomer.

#### CONCLUSIONS

Owing to the very low efficiency and the lack of selectivity of the  $\alpha$ -AGP column for the enantiomers of N-0861, the direct separation

method did not give satisfactory results. On the other hand, even if a better separation had been possible, applications to biological samples might have been limited because  $\alpha$ -AGP stationary phases may easily be ruined by a biological matrix if not properly removed.

For the enantiomeric separation of N-0861, derivatization with (+)-Flec showed good potential. The method is easy to perform and aqueous solutions can be used. This, in combination with the use of a reversed-phase HPLC system, may make the method suitable for biological samples to study enantioselectivity in the kinetics of N-0861. However, for bioanalytical work an exhaustive clean-up step of the sample will remain necessary before the derivatization reaction can take place. The calibration graphs showed that the reaction is linear. A resolution between the formed diastereoisomers of 1.13 within 30 min was obtained on a C<sub>8</sub> column with an acetonitrile–water eluent.

The identities of the reaction products were checked by LC–MS. The derivatization product appeared to be different from the expected product. Under the influence of the chloroformate the methyladenine ring structure present in N-0861 opened on addition of H<sub>2</sub>O. This was established by LC–MS experiments in which the H<sub>2</sub>O in the eluent was replaced with <sup>2</sup>H<sub>2</sub>O. With this eluent the number of protons linked to heteroatoms, such as nitrogen and/or oxygen, could be calculated. This allowed the exact structure of the derivatization product to be elucidated.

As the individual enantiomers of N-0861 were not available, the elution order of the enantiom-

ers could not be established. However, it should be noted that if enantiomeric purity studies require a reversal of the elution order, this can easily be achieved because the individual enantiomers of Flec are commercially available.

A drawback of the indirect method is the relatively high price of the optically pure derivatization reagent.

#### ACKNOWLEDGEMENTS

Most of this work was carried out at Astra Hassle (Mölndal, Sweden) during a research stay by D.T. W., which was financially supported by the Dutch Organization of Scientific Research, NWO.

#### REFERENCES

- 1 J. Linden, *Faseb J.*, 5 (1991) 2668.
- 2 E.J. Ariëns, *Adv. Drug Res.*, 3 (1966) 235.
- 3 S.R. Narayanan, *J. Pharm. Biomed. Anal.*, 10 (1992) 251.
- 4 J. Hermansson, *Trends Anal. Chem.*, 8 (1989) 251.
- 5 N.R. Srinivas and L.N. Igwemezie, *Biomed. Chromatogr.*, 6 (1992) 163.
- 6 S. Einarsson, B. Josefsson, P. Moller and D. Sanchez, *Anal. Chem.*, 59 (1987) 1191.
- 7 A. Roux, G. Blanchot, A. Baglin and B. Fluovat, *J. Chromatogr.*, 579 (1991) 453.
- 8 M.T. Rosseel, A.M. Vermeulen and F.M. Belpaire, *J. Chromatogr.*, 568 (1991) 239.
- 9 D.T. Witte, R.A. De Zeeuw and B.F.H. Drenth, *J. High Resolut. Chromatogr.*, 13 (1990) 569.
- 10 D.T. Witte, J. Bosman, T. De Boer, B.F.H. Drenth, K. Ensing and R.A. De Zeeuw, *J. Chromatogr.*, 553 (1991) 365.
- 11 K.-E. Karlsson, *J. Chromatogr.*, in press.
- 12 S. Björkman, *J. Chromatogr.*, 339 (1985) 339.

CHROM. 25 071

# Shape-selective separation of polycyclic aromatic hydrocarbons by reversed-phase liquid chromatography on tetraphenylporphyrin-based stationary phases

Chris E. Kibbey and Mark E. Meyerhoff\*

Department of Chemistry, University of Michigan, Ann Arbor, MI 48109 (USA)

(First received December 18th, 1992; revised manuscript received March 9th, 1993)

---

## ABSTRACT

The reversed-phase chromatographic behavior of planar and non-planar polycyclic aromatic hydrocarbons (PAHs) is investigated on tetraphenylporphyrin and two metallotetraphenylporphyrin [Sn(IV), In(III)] bonded stationary phases using methanol–water and acetonitrile–water as mixed solvent mobile phases. Large differences in the capacity factors of aromatic solute pairs having the same number of carbon atoms, but differing in three-dimensional shape (*e.g.*, triphenylene/*o*-terphenyl and perylene/ $\alpha$ ,  $\alpha'$ -binaphthyl), suggest that the three tetraphenylporphyrin-based supports possess shape selectivity toward small planar aromatic solutes. Capacity factors for planar PAH solutes on these supports are significantly greater than for non-planar polyaryls having the same number of carbon atoms.

---

## INTRODUCTION

Polycyclic aromatic hydrocarbons (PAHs) are ubiquitous in the environment, as they are formed readily by the combustion of virtually any organic material. Within the general class of PAHs, the most virulent carcinogens are those planar PAHs which possess potent bay region activity [1]. While the link between the angular arrangement of a PAH's fused rings and its carcinogenic activity has been well established [2], the development of chromatographic stationary phases having adequate shape selectivity to discriminate between planar and non-planar PAHs remains a challenge.

Reversed-phase liquid chromatography is the method of choice for the separation and quantitation of PAHs. Reversed-phase separations of PAHs typically are performed on chemically bonded octadecylsilyl (ODS) phases [3]. The

morphology of bonded ODS groups on the surface of these supports varies depending on the functionality of the alkyl silane used. Commercial ODS phases prepared from monofunctional silanes yield a brush-like monomeric coverage of octadecyl chains on the silica surface, while polyfunctional silanes are used to prepare ODS phases with a comparatively more rigid network of octadecyl chains.

The morphology of the bonded ODS groups plays a significant role in PAH planarity recognition on these supports. The greater shape selectivity of polymeric ODS phases makes these supports better suited than monomeric ODS-silicas for PAH separations [4]. Shape selectivity on polymeric ODS supports is attributed to the ability of planar solutes to slide more readily into "slots" formed by the rigid network of ordered alkyl chains than do non-planar solutes [5,6]. The alkyl chains of monomeric ODS phases are able to adopt a more random orientation on the silica surface; hence these supports are less able to discriminate between planar and non-planar

---

\* Corresponding author.

solutes on the basis of shape. Additional evidence that solute shape selectivity is influenced by the morphology of alkyl chains on the stationary phase comes from the observation that the chromatographic properties of solutes on monomeric straight-chain alkyl phases become more like those of polymeric stationary phases as the chain lengths of the bonded alkanes are increased [7,8], the bonding density of alkyl chains on the silica surface is increased [9], or the stationary phase temperature is decreased [10]. In the latter case, alkyl chain mobility decreases with decreasing temperature, resulting in a bonded phase morphology that resembles that of a crystalline solid [10]. Long alkyl chains adopt a more ordered arrangement on the silica surface due to configurational constraints than short alkyl chains [7]; yielding a surface morphology for the former characterized by a comparatively rigid network of deep slots. In addition, the alkyl chain packing structure on the silica surface becomes more ordered as the surface bonding density is increased [9].

Several sets of PAH solutes have been used to characterize the shape selectivity of reversed-phase supports [4,11]. Among these are the set consisting of phenanthro[3,4-*c*]phenanthrene (PhPh), a helically shaped PAH; benzo[*a*]pyrene (BaP), a planar solute; and dibenzo[*g,p*]chrysene (TBN), which is saddle shaped. The elution order of these three solutes on a monomeric ODS support is: TBN > PhPh > BaP; while on a polymeric ODS support the order of elution is: BaP > TBN > PhPh [4]. Other investigators have used aromatic solute pairs, which have the same number of carbon atoms, but differ in three-dimensional shape (*i.e.*, triphenylene/*o*-terphenyl), to assess the shape selectivity of reversed-phase supports [11].

Separations of small PAHs (2–5 rings) on a number of aromatic hydrocarbon bonded stationary phases, including phenyl, *p*-bis(dimethylphenyl), 1,3,5-tris(trimethylphenyl), naphthylethyl, and pyrenylethyl, have also been reported [11–13]. The dominant factors affecting retention on these supports are the size and shape of the PAH solute. Retention on these supports is believed to result from a combination of  $\pi$ – $\pi$  and shape interactions between the

solute PAHs and the surface-bonded aromatic groups. PAH retention and stationary phase shape selectivity increase with the size of the chemically bonded aromatic system [11]. In contrast to the usual shape selectivity observed with polymeric ODS phases, both the *p*-bis(dimethylphenyl) and the 1,3,5-tris(trimethylphenyl) bonded phases displayed greater selectivity for non-planar *versus* planar solutes due to an apparent steric constraint between planar solutes and pendant methyl groups on the bonded phenyl moiety [12].

Recently, we reported the synthesis and characterization of silica gel stationary phases possessing immobilized tetraphenylporphyrin and metallotetraphenylporphyrins [Sn(IV) and In(III)] [14]. The two chemically bonded metallotetraphenylporphyrin-silicas proved useful for the anion-exchange separation of aromatic sulfonates and carboxylates. The presence of a macrocyclic aromatic system in tetraphenylporphyrin [15] prompted preliminary investigations into the possible application of these stationary phases to the separation of PAHs [14]. We report here, in more detail, our observations regarding the reversed-phase separation of several small PAHs (2–4 rings) on 5-*para*-carboxyphenyl 10,15,20-phenylporphyrin- ( $H_2$ TPP), and In(III) and Sn(IV) metallated 5-*para*-carboxyphenyl 10,15,20-tri-phenylporphyrin- [In(TPP) and Sn(TPP), respectively] bonded stationary phases. For small PAHs, these three tetraphenylporphyrin-silicas yield a linear relationship between the logarithm of the capacity factor ( $k'$ ) and the correlation factor ( $F$ ). Differences in aromatic solute retention between the tetraphenylporphyrin and polymeric ODS supports as a function of temperature are also discussed.

## EXPERIMENTAL

### Equipment

The HPLC system used in this work consisted of a Spectra-Physics (San Jose, CA, USA) SP 8700 solvent-delivery system, a Spectra-Physics SP 4290 computing integrator, a Kratos (Ramsey, NJ, USA) Spectroflow 773 variable-wavelength UV–Vis detector, an ISCO (Lincoln, NE, USA) ISIS autosampler and a Rheodyne

(Cotati, CA, USA) model 7010 sample valve with a 20- $\mu$ l loop. The columns were thermostated using a Fisher Scientific (Pittsburgh, PA, USA) water jacket connected to a Fisher Scientific Model 80 Isotemp constant-temperature circulator.

### Materials

The preparation of the H<sub>2</sub>TPP, In(TPP) and Sn(TPP) stationary phases used in this work is described elsewhere [14]. The three tetraphenylporphyrin silicas were slurry packed in methanol–water (50:50, v/v) by the down-fill method [16] into separate 10 cm  $\times$  4.6 mm I.D. stainless-steel columns (Alltech, Deerfield, IL, USA). The aromatic solutes were of reagent grade or better and purchased from Aldrich (Milwaukee, WI, USA); with the exception of  $\alpha, \alpha'$ -binaphthyl, which was obtained from ICN (Irvine, CA, USA). The mobile phases used in this work were made up by volume from LC-grade solvents (Mallinckrodt, Paris, KY, USA) and 16 M $\Omega$  deionized water.

## RESULTS AND DISCUSSION

The porphyrin coverage on the H<sub>2</sub>TPP, In(TPP) and Sn(TPP) supports was determined from the increase in nitrogen content of the aminopropyl silica starting material following tetraphenylporphyrin immobilization, acetylation with acetic anhydride, and metallation of the immobilized tetraphenylporphyrin with either tin(IV) or indium(III) [14]. The nitrogen content and porphyrin coverage of the three supports are shown in Table I. Both the H<sub>2</sub>TPP and the In(TPP) phases have similar porphyrin coverages (0.35 and 0.32  $\mu$ mol/m<sup>2</sup>, respectively), while the

porphyrin coverage on the Sn(TPP)-silica (0.18  $\mu$ mol/m<sup>2</sup>) is lower. The Sn(TPP) phase was prepared from an aminopropyl silica with a smaller pore size and larger surface area than that used to prepare the H<sub>2</sub>TPP and In(TPP) supports. Consequently, in the preparation of the Sn(TPP)-silica, the porphyrin may have been excluded from access to the amine sites on the interior surface of the aminopropyl silica.

The efficiencies of the three columns packed with the tetraphenylporphyrin-silicas were determined from the elution of a toluene band with a mobile phase consisting of methanol–water (50:50, v/v). Column efficiency was calculated from the retention time of the toluene peak ( $t_R$ ) and its peak width at baseline ( $t_w$ ) as follows:

$$N = 16 \left( \frac{t_R}{t_w} \right)^2 \quad (1)$$

The H<sub>2</sub>TPP, In(TPP) and Sn(TPP) columns had average ( $n = 4$ ) efficiencies of 2100, 2200 and 2900 theoretical plates, respectively. While these column efficiencies are poorer than those of commercially packed columns, the efficiencies obtained here were sufficient for evaluating the separation of PAHs. Further, the slight asymmetry of the solute bands eluting from these columns is attributed to poor stationary phase packing (see Fig. 4).

The capacity factors of nine PAH solutes on the three tetraphenylporphyrin-based supports using methanol–water and acetonitrile–water mobile phases of different composition are presented in Table II. While the In(TPP) stationary phase exhibits slightly greater retention of triphenylene, chrysene and perylene than the H<sub>2</sub>TPP and the Sn(TPP) silicas, there is no difference in the elution order of the aromatic solutes on the three tetraphenylporphyrin-silica stationary phases. It is important to note that the capacity factors of the PAHs were negligible on a column packed with acetylated aminopropyl silica alone (data not shown). Interactions between these aromatic solutes and acetylated aminopropyl groups or residual silanol sites on the support surface do not appear to play a role in solute retention on the three tetraphenylporphyrin-silicas.

TABLE I  
SURFACE PORPHYRIN COVERAGE ON THE THREE PORPHYRIN-SILICAS

Porphyrin phase	Nitrogen (%)	Porphyrin coverage ( $\mu$ mol/m <sup>2</sup> )
H <sub>2</sub> TPP	0.98	0.35
InTPP	0.93	0.32
SnTPP	1.48	0.18



TABLE II

PAH CAPACITY FACTORS ON THE THREE PORPHYRIN-SILICAS UNDER THE MOBILE PHASE CONDITIONS INDICATED

PAH solute	Capacity factor ( $k'$ )											
	Methanol–water (80:20)			Methanol–water (70:30)			Acetonitrile–water (60:40)			Acetonitrile–water (50:50)		
	H <sub>2</sub> TPP	InTPP	SnTPP	H <sub>2</sub> TPP	InTPP	SnTPP	H <sub>2</sub> TPP	InTPP	SnTPP	H <sub>2</sub> TPP	InTPP	SnTPP
Naphthalene	0.75	0.72	0.74	1.26	1.13	1.40	0.87	0.73	0.73	1.66	1.53	1.62
Phenanthrene	1.80	1.76	1.76	3.71	3.58	3.99	1.59	1.54	1.38	3.56	3.73	3.40
Anthracene	1.94	1.90	1.85	4.12	3.94	4.24	1.69	1.64	1.49	3.85	4.04	3.56
Pyrene	3.17	3.27	3.14	7.03	7.32	7.53	2.56	2.98	2.22	6.08	7.49	5.41
Chrysene	5.16	5.79	4.96	12.74	15.34	13.24	3.49	4.20	3.08	9.09	11.68	8.02
<i>o</i> -Terphenyl	1.54	1.31	1.58	3.46	2.83	3.97	1.59	1.26	1.37	4.04	3.49	3.73
Triphenylene	4.84	5.62	4.76	12.04	14.49	12.48	3.24	3.85	2.94	8.24	10.52	7.64
$\alpha,\alpha'$ -Binaphthyl	3.03	2.40	3.09	–	–	–	2.42	2.44	2.28	–	–	–
Perylene	11.87	15.46	10.56	–	–	–	6.40	6.42	5.73	–	–	–

There are, however, significant differences in PAH retention observed on all three supports as the mobile phase is changed from one that is methanol based to one that is based on acetonitrile. A lower mobile phase concentration of acetonitrile is needed to achieve a given PAH capacity factor on the tetraphenylporphyrin-based supports compared to a methanol-based mobile phase. Acetonitrile generally is regarded as a stronger eluent than methanol, as at a given composition, solute retention on reversed-phase supports is greater with methanol–water than with acetonitrile–water eluents. However, when dealing with stationary phases and solutes possessing unsaturated sites, the influence of  $\pi$ – $\pi$  interactions (between the cyano group of acetonitrile and the double bonds of the solute and stationary phase) on solute retention must be considered in addition to solvophobic effects [17].

The appreciable difference in capacity factors between *o*-terphenyl/triphenylene and  $\alpha,\alpha'$ -binaphthyl/perylenes on the three porphyrin-silicas (Table II) indicates that these stationary phases possess selectivity for planar *versus* non-planar solutes. These aromatic solute pairs were chosen for study based on their commercial availability and prior use as probes for assessing shape selectivity [11]. The ratio of the capacity factors of triphenylene and *o*-terphenyl ( $\alpha_{\text{trip}/o\text{-ter}}$ ) on the H<sub>2</sub>TPP and Sn(TPP) columns is approximately 3 when methanol-based mobile phases

are used, while on the In(TPP) column, this ratio is approximately 4. The selectivity factors for the perylene/ $\alpha,\alpha'$ -binaphthyl pair ( $\alpha_{\text{pery}/\alpha,\alpha'}$ ) on the H<sub>2</sub>TPP-, In(TPP)- and Sn(TPP)-based supports with a methanol–water (80:20) mobile phase (3.9, 6.4 and 3.4, respectively) are even greater than those for the triphenylene/*o*-terphenyl pair on the three tetraphenylporphyrin-silicas. On a typical monomeric ODS stationary phase the selectivity factor ( $\alpha_{\text{trip}/o\text{-ter}}$ ) ranges from 1.0 to 1.7 [13], while the value of  $\alpha_{\text{trip}/o\text{-ter}}$  on a polymeric ODS phase lies between 2.0 and 2.7 [6]. Jinno *et al.* [13] suggest that a selectivity factor ( $\alpha_{\text{trip}/o\text{-ter}}$ ) of 2.0 or greater is an indication of significant solute planarity recognition. Based on this latter criterion, the three tetraphenylporphyrin-silicas possess a high degree of shape selectivity for small aromatic solutes.

While both polymeric ODS and tetraphenylporphyrin-silica phases display selectivity for planar solutes, we believe that the retention mechanisms that lead to shape selectivity on these two types of support may be different. According to the “slot model”, interactions with polymeric ODS supports that result in increased retention of planar solutes are primarily physical in nature [5]. Shape selectivity on the tetraphenylporphyrin-silicas, however, may reflect differences in the magnitudes of  $\pi$ – $\pi$  overlap of aromatic solutes with the tetraphenylporphyrin macrocycle. For example, the aromatic macrocycle of tetraphenylporphyrin is large enough to

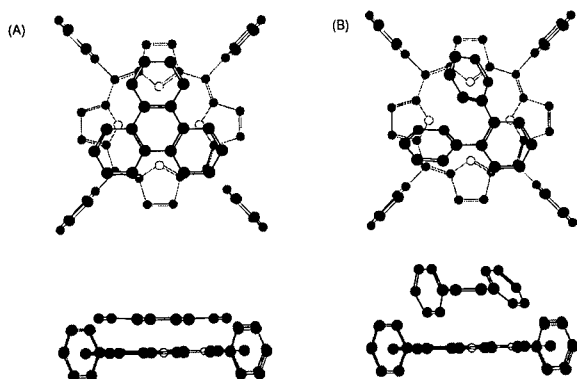


Fig. 1. Idealized interactions of (A) triphenylene and (B) *o*-terphenyl with the tetraphenylporphyrin macrocycle.

accommodate both triphenylene and *o*-terphenyl (Fig. 1). However, the non-planar geometry of the latter prevents it from attaining as strong an interaction with the tetraphenylporphyrin macrocycle as triphenylene. A similar argument can be made to account for the greater retention of perylene compared to  $\alpha,\alpha'$ -binaphthyl on the three tetraphenylporphyrin-silicas (Table II). Of course, a more thorough examination of the retention of PAH solutes differing in three-dimensional shape (*e.g.*, PhPh, TBN and BaP) will be required before more definitive conclusions regarding shape selectivity on these supports can be drawn. It should also be noted that Fig. 1 is meant to convey the idealized differences in  $\pi$ - $\pi$  interaction of the two solutes with the tetraphenylporphyrin macrocycle, and not necessarily an accurate model of such interactions.

Shape selectivity on pyrenylethyl-silica has been attributed to the ability of planar solutes to partition into slots formed from the closely spaced arrangement of aggregated pyrenylethyl groups on the silica surface [11]. The likelihood of a similar closely spaced arrangement of tetraphenylporphyrin groups on the three tetraphenylporphyrin-silicas used here seems unlikely for two reasons. First, the bonding density of aminopropyl groups on the starting silica phase was approximately one half of its theoretical maximum value [14]. Consequently, the density of tetraphenylporphyrins immobilized on the surface of these supports is low. Furthermore, tetraphenylporphyrins generally do not aggregate due

to the near perpendicular orientation of their *meso*-phenyl rings to the porphyrin macrocycle [18].

Increasing the temperature at which a particular separation is carried out in LC generally results in a decrease in the separation factor ( $\alpha$ ) between pairs of solutes, but does not change the solute elution order. Snyder refers to such behavior as a "regular" temperature effect [19]. However, "irregular" temperature effects have been observed for solutes differing in three-dimensional shape on ODS supports. That is, changes in the separation temperature of "irregular" systems not only result in changes in  $\alpha$ , but in changes in the elution order of the solutes as well. For example, the elution order of the solute pairs *o*-terphenyl/anthracene and  $\alpha,\alpha'$ -binaphthyl/triphenylene is reversed on an ODS support as the column temperature is increased [20]. In addition, the elution order of the three PAH probes (PhPh, TBN and BaP) is influenced by column temperature on polymeric ODS supports [10]. Snyder [19] argues that at higher temperatures solute retention on ODS supports is favored by solutes that are more compact and near-spherical in three-dimensional shape.

Dissimilarities between ODS and the new tetraphenylporphyrin-silica supports are apparent from differences in the effects of column temperature on the elution order of small aromatic solutes. Four aromatic solutes (*o*-terphenyl, triphenylene, anthracene and  $\alpha,\alpha'$ -binaphthyl) were eluted from the In(TPP)-silica support with methanol-water (70:30) at column temperatures ranging from 25 to 65°C. A plot of  $\ln k'$  versus reciprocal temperature ( $1/T$ ) for these four aromatic solutes is shown in Fig. 2. The linear variation in  $\ln k'$  as a function of  $1/T$  for these four solutes indicates that their individual retentions are governed by a single sorption mechanism. Furthermore, it is apparent that the selectivity factor ( $\alpha$ ) between pairs of solutes decreases as the temperature is increased, but their elution order on In(TPP)-silica does not change (Fig. 2). Thus, "regular" temperature effects are observed with these aromatic solutes on In(TPP)-silica whereas the elution of these solutes on ODS-silica is "irregular" with respect to temperature [20].

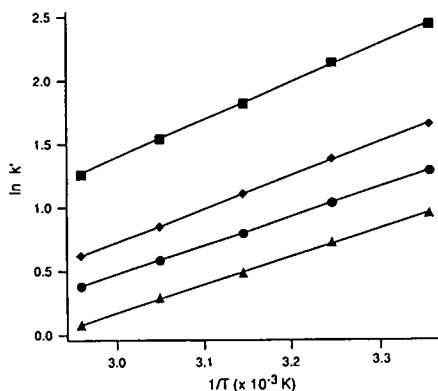


Fig. 2. Plot of  $\ln k'$  versus  $1/T$  for (■) triphenylene, (▲) *o*-terphenyl, (◆)  $\alpha,\alpha'$ -binaphthyl and (●) anthracene on In(TPP)-silica. Mobile phase: methanol–water (70:30).

The linear correlation between  $\log k'$  and the number of double bonds in an unsubstituted PAH [correlation factor ( $F$ )] is well established for ODS supports [21]. A plot of  $\log k'$  versus correlation factor for the elution of naphthalene ( $F = 5$ ), anthracene ( $F = 7$ ), pyrene ( $F = 8$ ) and chrysene ( $F = 9$ ) from the three tetraphenylporphyrin-silica packed columns with a methanol–water (70:30) mobile phase is shown in Fig. 3. A linear relationship between  $\log k'$  and  $F$  is also apparent for these PAH solutes on the three tetraphenylporphyrin-silicas.

Separation of five PAHs on the three porphyrin-silicas are shown in the three chromatograms of Fig. 4. The five solutes are reasonably well separated on all three stationary phases using a mobile phase of methanol–water (70:30). The elution order is similar to the elution order of these solutes on conventional ODS bonded phases. The separation of phenanthrene and anthracene on the three tetraphenylporphyrin-silicas could be improved through more efficient stationary phase packing and through the use of columns longer than the 10-cm analytical columns used in this work. The macrocyclic ring of the tetraphenylporphyrin system is wide enough to accommodate most PAHs containing up to 4 or 5 rings (Fig. 1). Allowing for rotation of the immobilized tetraphenylporphyrin's four *meso*-phenyl rings from their near perpendicular orientation to the porphyrin macrocycle, PAHs

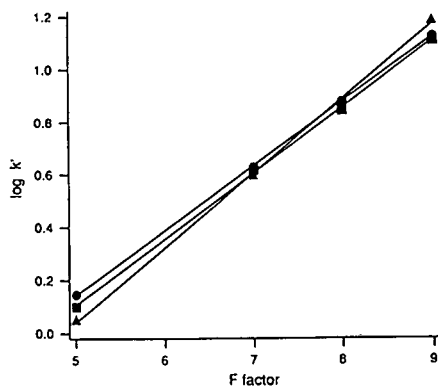


Fig. 3. Plots of  $\log k'$  versus correlation factor ( $F$ ) for PAHs on the (■) H<sub>2</sub>TPP, (▲) InTPP and (●) SnTPP bonded supports. Linear regression analysis: H<sub>2</sub>TPP (slope: 0.25, intercept: -1.14); InTPP (slope: 0.28, intercept: -1.36); and SnTPP (slope: 0.24, intercept: -1.08).

grams of Fig. 4. The five solutes are reasonably well separated on all three stationary phases using a mobile phase of methanol–water (70:30). The elution order is similar to the elution order of these solutes on conventional ODS bonded phases. The separation of phenanthrene and anthracene on the three tetraphenylporphyrin-silicas could be improved through more efficient stationary phase packing and through the use of columns longer than the 10-cm analytical columns used in this work. The macrocyclic ring of the tetraphenylporphyrin system is wide enough to accommodate most PAHs containing up to 4 or 5 rings (Fig. 1). Allowing for rotation of the immobilized tetraphenylporphyrin's four *meso*-phenyl rings from their near perpendicular orientation to the porphyrin macrocycle, PAHs

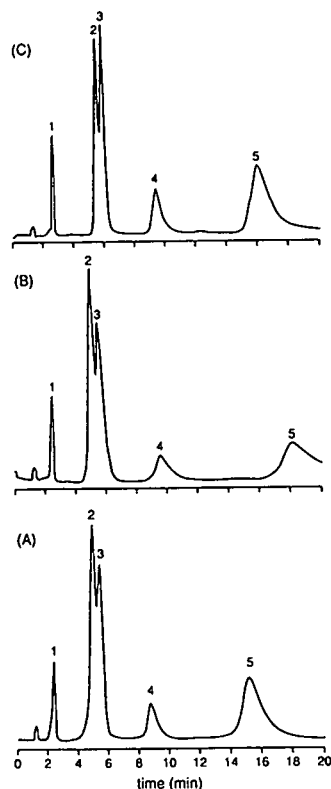


Fig. 4. Separation of five PAHs on the (A) H<sub>2</sub>TPP, (B) InTPP and (C) SnTPP columns. Peaks: 1 = naphthalene; 2 = phenanthrene; 3 = anthracene; 4 = pyrene; 5 = chrysene. Mobile phase: methanol–water (70:30). Flow-rate: 1.0 ml/min. Column temperature: 25°C. Detection: 254 nm (0.100 AUFS).

made up of more than 5 aromatic rings conceivably could also be separated on these tetraphenylporphyrin-silicas via preferential  $\pi$ - $\pi$  interaction with the porphyrin macrocycle.

#### CONCLUSIONS

Tetraphenylporphyrins chemically bonded onto silica yield stationary phases with novel shape selectivity toward PAHs. The greater retention of planar (*versus* non-planar) aromatic solutes on these supports may reflect greater  $\pi$ - $\pi$  overlap between the former and the porphyrin macrocycle. We are currently evaluating the chromatographic behavior of larger PAH solutes on these supports. In addition, we plan on studying the elution of other PAHs having dissimilar three-dimensional shape in order to gain a better understanding of the apparent shape selectivity of these supports. Performing these separations with normal-phase eluents (*e.g.*, hexane-dichloromethane) may help to distinguish between solute retention based on solvophobic *versus*  $\pi$ - $\pi$  interactions. Further, there are other classes of macrocyclic aromatic compounds, such as phthalocyanine, sapphyrin and rubyrin, that also may be used to prepare LC stationary phases with interesting solute shape selectivities.

#### ACKNOWLEDGEMENTS

The authors gratefully acknowledge partial financial support for this work from the National Institutes of Health (GM 28882). C.E.K. also acknowledges financial support from Amoco and Sokol funded Department of Chemistry fellowships. In addition, we thank the Anspec Co. (Ann Arbor, MI, USA) for use of their column packing equipment.

#### REFERENCES

- 1 G.H. Loew, J. Phillips, J. Wong, L. Hjelmeland and G. Pack, *Cancer Biochem. Biophys.*, 2 (1978) 113–122.
- 2 R.G. Harvey, *Polycyclic Aromatic Hydrocarbons: Chemistry and Carcinogenicity*, Cambridge University Press, New York, 1991, Ch. 3.
- 3 K. Ogan, E. Katz and W. Slavin, *Anal. Chem.*, 51 (1979) 1315–1320.
- 4 L.C. Sander and S.A. Wise, *Anal. Chem.*, 56 (1984) 504–510.
- 5 S.A. Wise and L.C. Sander, *J. High Resolut. Chromatogr. Chromatogr. Commun.*, 8 (1985) 248–255.
- 6 K. Jinno, T. Ibuki, N. Tanaka, M. Okamoto, J.C. Fetzer, W.R. Biggs, P.R. Griffiths and J.M. Olinger, *J. Chromatogr.*, 461 (1989) 209–227.
- 7 L.C. Sander and S.A. Wise, *Anal. Chem.*, 59 (1987) 2309–2313.
- 8 N. Tanaka, K. Sakagami and M. Araki, *J. Chromatogr.*, 199 (1980) 327–337.
- 9 K.B. Sentell and J.G. Dorsey, *J. Chromatogr.*, 461 (1989) 193–207.
- 10 L.C. Sander and S.A. Wise, *Anal. Chem.*, 61 (1989) 1749–1754.
- 11 N. Tanaka, Y. Tokuda, K. Iwaguchi and M. Araki, *J. Chromatogr.*, 239 (1982) 761–772.
- 12 K. Jinno, T. Nagoshi, N. Tanaka, M. Okamoto, J.C. Fetzer and W.R. Biggs, *J. Chromatogr.*, 386 (1987) 123–135.
- 13 K. Jinno, K. Yamamoto, H. Nagashima, T. Ueda and K. Itoh, *J. Chromatogr.*, 517 (1990) 193–207.
- 14 C.E. Kibbey and M.E. Meyerhoff, *Anal. Chem.*, in press (1993).
- 15 S.J. Silvers and A. Tulinsky, *J. Am. Chem. Soc.*, 89 (1967) 3331–3337.
- 16 C.F. Poole and S.A. Schuette, *Contemporary Practice of Chromatography*, Elsevier, New York, 1984, Ch. 4.
- 17 G. Thévenon-Emeric, A. Tchaplal and M. Martin, *J. Chromatogr.*, 550 (1991) 267–283.
- 18 W.I. White, in D. Dolphin (Editor), *The Porphyrins*, Academic Press, New York, 1978, Vol. V, Part C, Ch. 7.
- 19 L.R. Snyder, *J. Chromatogr.*, 179 (1979) 167–172.
- 20 J. Chmielowiec and H. Sawatzky, *J. Chromatogr. Sci.*, 17 (1979) 245–252.
- 21 J.F. Schabron, R.J. Hurtubise and H.F. Silver, *Anal. Chem.*, 49 (1977) 2253–2260.



# Solid-phase extraction of phenols using membranes loaded with modified polymeric resins

Luther Schmidt, Jeffrey J. Sun and James S. Fritz\*

*Ames Laboratory, US Department of Energy and Department of Chemistry, Iowa State University, 332 Wilhelm Hall, Ames, IA 50011 (USA)*

Donald F. Hagen, Craig G. Markell and Eric E. Wisted

*3M Co. Research Center, St. Paul, MN 55144 (USA)*

(First received October 20th, 1992; revised manuscript received March 5th, 1993)

---

## ABSTRACT

Membranes impregnated with polystyrene–divinylbenzene (PS–DVB) or acetyl–PS–DVB resin beads were used for solid-phase extraction of ppm (w/w) concentrations of phenols from aqueous samples. A macro procedure uses  $47 \times 0.5$  mm disks with 200–500 ml sample volumes at ca. 200 ml/min flow-rates. A smaller-scale procedure uses a thicker disk (3 mm) packed into a conventional solid-phase extraction column (7 mm I.D.). The retained phenols are eluted from the disk with organic solvent, and the individual phenols are determined quantitatively by GC or HPLC. Recoveries for 16 different phenols, including those included in the US Environmental Protection Agency list of priority pollutants, averaged 98% with a standard deviation of  $\pm 2\%$ .

---

## INTRODUCTION

In 1989 a new family of materials for solid-phase extraction (SPE) was introduced [1]. This is a membrane, or disk, of polytetrafluoroethylene (PTFE) fibrils impregnated with small ( $8 \mu\text{m}$ ) particles of adsorbing material such as  $\text{C}_{18}$  silica or poly(styrene–divinylbenzene) (PS–DVB). Flow-rates as fast as 200 ml/min are possible, yet uptake of organic solutes is efficient because of fast kinetics. The fast kinetics are a result of the small particles, close and uniform packing, and elimination of channeling.

SPE disks have been used in the sample preparation steps in a number of methods used for water analysis in environmental laboratories [1–3]. While disks containing  $\text{C}_{18}$  bonded silica sorbents give quantitative recoveries for hydro-

phobic analytes, such as those found in US Environmental Protection Agency (EPA) Method 525.1 [11], low recoveries are often obtained for the more polar, water soluble analytes such as phenols. When extracting a 1-l water sample for the 11 priority pollutants phenols found in EPA Method 625 [12], for example, quantitative results are only obtained for 2,4,6-trichlorophenol and pentachlorophenol. A number of researchers have investigated ways of increasing SPE recoveries for phenol and substituted phenols, such as pH adjustment to neutralize the phenols, salt (NaCl) addition to “salt out” the phenols, alternative sorbents, ion-pairing, larger sorbent beds, or smaller sample volumes [4–8]. This paper explores an alternative SPE sorbent as a way of increasing recoveries for the phenols.

In a classic paper published in 1974, Junk *et al.* [9] showed that porous PS–DVB particles efficiently extract a wide variety of organic compounds, including phenols, present at very low

---

\* Corresponding author.

concentrations in aqueous samples. Werkhoven-Goewie *et al.* [4] claim significantly higher breakthrough volumes on PS–DVB than on  $C_{18}$  silica for dichlorophenols. Sun and Fritz [10] showed that PS–DVB resins give significantly higher recoveries than  $C_{18}$  silica particles for many classes of organic solutes. They also showed that polymeric resins containing a hydrophilic substituent (such as acetyl) often give still higher recoveries than unsubstituted PS–DVB resins.

This paper explores the results obtained when PS–DVB and acetyl-PS–DVB resins are incorporated into SPE membranes and used to extract phenols from water. Also reported is a novel method of packing SPE membranes into standard SPE tubes for the extraction of analytes from smaller volumes of distilled, tap and river water. Good recoveries are obtained for all of the phenols, both from larger volumes (*ca.* 500 ml) through 47-mm disks and from smaller volumes (*ca.* 20 ml) through membrane-packed tubes.

## EXPERIMENTAL

### *Resins and membranes*

Spherical, highly cross-linked PS–DVB resins were obtained from Sarasep (Santa Clara, CA, USA). These had a surface area of approximately 400 m<sup>2</sup>/g and an average particle size of either 5 or 8  $\mu$ m. The acetyl derivative was prepared by reaction with acetyl chloride as described previously [10].

The membranes used in this work were of the general type manufactured by 3M (St. Paul, MN, USA) under the trade name Empore. A typical composition is 90% (w/w) resin and 10% (w/w) PTFE fibrils. The PTFE comprises less than 1% of the total surface area, and the open pore volume is approximately 60% (v/v). The disks used in this work were 47 mm in diameter and 0.5 mm thick. An experimental membrane used in part of this work was approximately 3 mm thick. Smaller circles were cut from these membranes with sharpened metal tubing of the appropriate diameter.

### *Apparatus and equipment*

For SPE experiments a 47-mm membrane was placed in a Millipore filtration apparatus at-

tached to a water aspirator. For elution, a 200  $\times$  25 mm test tube was placed in the side-arm flask. A detailed description of the apparatus has been published [3].

Smaller-scale SPE experiments were carried out with a small column obtained from Alltech (Deerfield, IL, USA). A typical column size was 55  $\times$  7 mm. A membrane circle was cut slightly larger in diameter than the column. It was forced into the column with 20  $\mu$ m polyethylene frits above and below for support. The SPE tube was then connected to a laboratory-made reservoir. Sample solutions were then forced through the membrane at a controlled rate by air pressure applied at the top or by suction from below.

Sample analyses were performed with an HP 5880A gas chromatograph equipped with a flame ionization detector, integrator and auto injector. The column used was a Supelco (Bellefonte, PA, USA) fused-silica capillary SPB-1.

### *Procedures for SPE*

*47-mm Disks.* Standard samples were prepared by adding several phenols to distilled water so that the concentration of each phenol was approximately 100  $\mu$ g/l (0.1 ppm). The pH was adjusted to 2 with hydrochloric acid. In some cases sodium chloride was added to a concentration of 10% (w/v).

The disk was placed in the filtration apparatus and washed with acetone to remove any contaminants from storage, handling or manufacture. It was then conditioned with a small amount of methanol to promote wetting and uniform flow through the hydrophobic PTFE matrix. The aqueous sample was then passed through the membrane without allowing it to go dry at any time. At full aspirator vacuum the flow-rate is approximately 200 ml/min. A typical sample volume was 500 ml. Elution of the retained phenols was carried out with three 3-ml portions of tetrahydrofuran. Each portion was allowed to soak into the disk for about 5 min before pulling it through. The combined aliquots of tetrahydrofuran were made up to exactly 10 ml.

To analyze the extracts, HPLC was used with a 150  $\times$  4.6 mm  $C_{18}$  column and a water–acetonitrile gradient. The water contained 0.1% acetic

acid to suppress ionization of the phenols. A UV detector was used at 272 nm.

*Small disks in SPE column.* The sample solution was prepared by adding a standard methanol solution of phenols (50 ppm each) to 20 ml of water so that the final concentration was approximately 0.4 ppm each. The pH was adjusted to approximately 2 with sulfuric acid to repress the ionization of the more acidic phenols.

Prior to each use a small amount of methanol (ca. 1 ml) was added to wet the disk. Without allowing the column to go dry, the aqueous sample solution was passed through at a flow-rate of 2 ml/min by applying a pressure of 15 p.s.i. (1 p.s.i. = 6894.76 Pa). The column was then washed with 2 ml of distilled water.

The phenols were eluted with 0.75 ml of methanol. The eluate was then collected in a 1.8-ml GC vial, and 0.1 ml of internal standard (500 ppm toluene in methanol) was added. The vial was then capped and a 2- $\mu$ l aliquot was injected onto the gas chromatograph. The percentage recovery was calculated by comparing the peak heights (relative to the internal standard) with those of the original standard methanol solution of the phenols. Internal standard was also added to the methanol solution.

TABLE I

SOLID-PHASE EXTRACTION OF PHENOLS USING 47-mm MEMBRANE DISKS LOADED WITH ACETYL-PS-DVB RESIN

Results are the average of 3 individual results. Elution with 9 ml of tetrahydrofuran.

Analyte	Lot 1				Lot 2			
	Recovery (%)	R.S.D. (%)	10% Salt: recovery (%)	R.S.D. (%)	Recovery (%)	R.S.D. (%)	10% salt: recovery (%)	R.S.D. (%)
Phenol	86	2	90	1	74	1	85	1
4-Nitrophenol	100	1	94	3	100	1	96	2
2,4-Dinitrophenol	98	2	93	2	98	1	96	3
2-Chlorophenol	93	1	87	1	94	2	90	2
2-Nitrophenol	92	2	88	1	95	2	92	2
2,4-Dimethylphenol	90	3	82	4	90	2	83	4
4-Chloro-3-methylphenol	95	2	90	3	97	2	92	4
2-Methyl-4,6-dinitrophenol	95	2	91	3	96	1	93	4
2,4-Dichlorophenol	94	2	88	2	96	1	91	3
2,4,6-Trichlorophenol	94	1	88	3	95	2	90	5
Pentachlorophenol	85	3	77	4	88	2	83	5
Average	93	2	88	2	93	2	90	3

## RESULTS AND DISCUSSION

*SPE with larger disks*

Virtually all of the previous work on resin-loaded membranes for SPE has been with disks 25 mm or 47 mm in diameter. Disks containing PS-DVB particles have been shown to be more efficient for the extraction of polar analytes than those containing C<sub>18</sub> or cyclohexyl-bonded-phase silica particles [3]. However, several phenols gave low recoveries even with membranes loaded with PS-DVB. Somewhat higher recoveries were obtained by adding 10% of salt to the aqueous samples [3].

Membranes containing PS-DVB resins modified by chemical introduction of acetyl groups [10] were evaluated for SPE of phenols from aqueous samples. Two different lots of resin were functionalized separately with acetyl groups and incorporated into membrane disks. The results in Table I show excellent recovery of all eleven phenols with the sole exception of phenol itself with the lot 2 resin. In this particular case addition of salt to the aqueous sample was not necessary. In fact, the recoveries of samples with 10% salt averaged 5% lower than those with no salt.



### SPE with 7 × 3 mm disks

The most common mode of SPE in chemical analysis is with small tubes or cartridges filled with loose polymeric resin or bonded-phase silica particles. Usually a bed height of >1 cm is used to ensure good retention of the desired sample compounds. However, this necessitates a relatively large volume of solvent to elute the adsorbed compounds. By packing a tube with disks 5-7 mm in diameter, cut from resin-loaded membranes, it should be possible to obtain efficient extraction with a very short height of resin membrane. The reason for this is that the resin particles are 5 or 8 μm, closely packed, and evenly dispersed throughout the membrane. Since the particles are immobilized, it should be possible to avoid the channeling that would be likely in a tube containing only a short height of a loose resin bed.

Our first experiments were with a small tube packed with 6 layers of membrane circles cut from a larger membrane. The I.D. of the tube was 4.5 mm and the circles were cut to exactly this diameter. These small circles were packed snugly into the tube with frits above and below for support. The recoveries of several test compounds (*ca.* 5 ppm of each) in aqueous samples were quite good, as shown in Table II. Because of probable channeling, somewhat lower results were obtained in one of the runs, so special care was taken to make the disks fit tightly against the walls of the tube. In other experiments an azo dye (pyridylazonaphthol) was passed through a packed tube. This dye formed a tight, even band on the membrane when the disks were packed carefully but the dye was mostly around the outside edges when the disks were not as tightly packed.

A single thick membrane should be easier to pack into a small column than several layers of a thinner disk. A membrane approximately 3 mm thick containing acetyl-PS-DVB resin particles was cut in a circle 7.5 mm in diameter and forced into a small tube 7.0 mm I.D. Frits were placed above and below the membrane to hold it firmly in place. The membrane fit snugly against the inside of the tube without buckling.

Several sample runs were conducted with this tube. Approximately 1 ml of methanol was added first to prewet the membrane. After

TABLE II

### RECOVERY OF TEST COMPOUNDS USING ACETYL-PS-DVB RESINS IN EMPORE DISKS

Elution with 0.75 ml of ethyl acetate. Results are the average of 4 individual runs.

Compound	Recovery (%)		
	C <sub>18</sub> Silica	Underivatized PS-DVB	Acetyl- PS-DVB
Toluene	43	89	96
Phenol	5	36	91
Indene	43	93	94
<i>p</i> -Cresol	19	76	94
2,4-Dimethylphenol	29	93	96
Naphthalene	57	92	91
<i>p</i> -Propylphenol	34	91	96
<i>sec.</i> -Butylphenol	—	93	96
3-Nitrophenol	—	57	73
Dibutylphthalate	60	89	87
Average, R.S.D. (%)	36, ±52	81, ±23	92, ±8

rinsing with 1-2 ml of water, 20 ml of an aqueous standard was passed through. This standard contained approximately 0.4 ppm each of several phenols and was made up to pH 2 with sulfuric acid to ensure that all phenols were in the molecular form. Three different standard samples were run. One was made up in distilled water, another was in tap water of moderate hardness, and a third was river water to which known amounts of phenols had been added. Two different lots of resin were derivatized separately and tested separately. The results, given in Table III, indicate excellent recoveries for all 16 phenols. The only exception was the somewhat low recovery of 2-methyl-4,6-dinitrophenol from tap water that had been spiked with the test phenols.

### CONCLUSIONS

Phenols in the low ppm concentration range can be effectively concentrated from aqueous samples by SPE with a membrane loaded with acetyl-PS-DVB resin particles. Samples of 500 ml can be passed very rapidly (*ca.* 2.5 min) through a 47 mm membrane disk using conven-

TABLE III

## RECOVERY OF PHENOLS USING THICK MEMBRANES LOADED WITH ACETYL-DERIVATIZED RESIN IN A SMALL TUBE

Elution with 0.75 ml of methanol. Results are the average of 3 individual results.

Analyte	Distilled water		Tap water		River water	
	Recovery (%)	R.S.D. (%)	Recovery (%)	R.S.D. (%)	Recovery (%)	R.S.D. (%)
Phenol	99	2	96	2	97	3
3-Methylphenol	95	1	93	2	92	4
2-Nitrophenol	100	4	102	3	98	1
2,4-Dichlorophenol	98	0	97	3	97	2
4-Chloro-3-methylphenol	98	0	85	2	93	4
2,4,6-Trichlorophenol	102	0.5	98	3	101	0
2-Methyl-4,6-dinitrophenol	94	2	75	4	95	2
Pentachlorophenol	100	2	92	1	100	4
2-Chlorophenol	99	2	106	4	103	2
2-Methylphenol	99	4	100	3	100	1
4-Methylphenol	97	5	98	2	98	4
2,4-Dimethylphenol	97	5	94	2	103	5
2,6-Dichlorophenol	100	5	108	8	104	6
2,4,5-Trichlorophenol	96	5	95	5	107	3
2,3,4,6-Tetrachlorophenol	99	3	95	9	101	0.5
2-sec.-Butyl-4,6-dinitrophenol	101	4	97	4	101	2

tional filtration under reduced pressure. A total of three 3-ml portions of tetrahydrofuran is recommended for subsequent elution of the adsorbed phenols. On a smaller scale, aqueous analytical samples can be effectively preconcentrated by passing through a 3-mm disk packed into a tube 7 mm in diameter. In this case 0.75 ml of methanol are sufficient for elution of the adsorbed phenols. These membrane methods for SPE of phenols are rugged, quick and efficient.

## REFERENCES

- 1 D.F. Hagen, C.G. Markell and G.A. Schmitt, *Anal. Chim. Acta*, 236 (1990) 157.
- 2 C.G. Markell, D.F. Hagen and V.A. Bunnelle, *LC·GC*, 9 (1991) 332.
- 3 C.G. Markell and D.F. Hagen, *Proceedings of the 7th Annual Waste Testing and Quality Assurance Symposium, Washington, DC, July 8-12, 1991*, Vol. II, EPA, Washington, D.C., p. 27.
- 4 C.E. Werkhoven-Goewie, W.M. Boon, A.J.J. Pratt, R.W. Frei, U.A.Th. Brinkman and C.J. Little, *Chromatographia*, 16 (1982) 52.
- 5 M.D. Grieser and D.J. Pietrzyk, *Anal. Chem.*, 45 (1973) 1348.
- 6 F.P. Bigley and R.L. Grob, *J. Chromatogr.*, 350 (1985) 407.
- 7 E. Chaldek and R.S. Marano, *J. Chromatogr. Sci.*, 22 (1984) 313.
- 8 V. Dixit and V.M. Dixit, *Am. Environ. Lab.*, 4 (1992) 313.
- 9 G.A. Junk, J.J. Richard, M.D. Grieser, J.L. Witiak, M.D. Arguello, R. Vick, H.K. Svec, J.S. Fritz and G.V. Calder, *J. Chromatogr.*, 99 (1974) 745.
- 10 J.J. Sun and J.S. Fritz, *J. Chromatogr.*, 590 (1992) 197.
- 11 J.W. Eichelberger, T.D. Behymer and W.L. Budde, *EPA Method 525.1, Determination of organic compounds in drinking water by liquid-solid extraction and capillary column gas chromatography/mass spectrometry*, U.S. Environmental Protection Agency, 1988.
- 12 *EPA method 625, Base/Neutrals and Acids*, U.S. Environmental Protection Agency, 1984.



# Analytical gel filtration of dextran for study of the glomerular barrier function

Lars Hagel\*

R&D Department, Pharmacia LKB Biotechnology AB, S-75182 Uppsala (Sweden)

Anders Hartmann and Kirsten Lund

Department of Medicine, National Hospital, N-0027 Oslo (Norway)

(Received December 23rd, 1992).

---

## ABSTRACT

Analytical gel filtration was used for the study of molecular size distribution of clinical dextran in serum and urine for the purpose of evaluations of changes in the human glomerular barrier function. The column was calibrated in terms of solute size using a simple and accurate technique recently described. Only one sample of a dextran possessing a broad molecular mass distribution was necessary for the calibration procedure and the calculations were performed using an ordinary spreadsheet. The accuracy of the calibration, as evaluated by protein samples, is better than 95%. The simplicity makes the method suitable for use in laboratories not normally specializing in analytical gel filtration. Calibration in terms of size is preferably done with respect to viscosity radius to obtain relevant information about the permeability of dextran into porous membranes.

---

## INTRODUCTION

Characterization of molecular mass distributions of dextran with analytical gel filtration was first described by Granath and Flodin [1] approximately 30 years ago. Granath and Kvist [2] reported some application areas of analytical gel filtration, including the study of the human renal threshold, which they reported to be about 55 000 in mass-average molecular mass of dextran. The technique was soon used for the study of glomerular barrier function both in animals and in humans (see, *e.g.*, refs. 3 and 4). The method is of particular interest in cases of pathological proteinuria due to loss of glomerular sieving function, particularly in diabetic and glomerulonephritic proteinuria. The method evaluates neutral dextran sieving in contrast to

negatively charged proteins in the clinical setting. Negatively charged particles such as proteins are more restricted than neutral dextran of similar size, probably because of the negative charges of fixed barrier proteins. With these limitations dextran clearance is still the most valid and clinically important method for *in vivo* estimation of glomerular sieving function [5–7].

One drawback of the method is the tedious calibration procedure, requiring the use of many samples and involving dedicated software for the calculations [8,9]. Also, the interpretation of the result into solute size will require some precautions, *i.e.*, different substance classes will show different relationships between size and molecular mass, and this may also vary within the substance class [10–12].

Recently, a procedure in which the column was calibrated through the use of a dextran of a broad and known molecular weight distribution was presented [13]. The simplicity of the method

---

\* Corresponding author.

made it very apt for the use in laboratories with limited experience in analytical gel filtration and, furthermore, it requires no sophisticated software for the calibration and evaluations. We here report our experiences of using this procedure for evaluations of molecular size distributions of dextran in serum and urine to study the glomerular barrier function in humans.

#### CALIBRATION PRINCIPLE

Gel filtration, or aqueous size-exclusion chromatography, is frequently used for the determination of size or size distributions of solutes. In the absence of secondary interactions the solutes are eluted strictly according to decreasing size. The column may either be used simply as a separating device and the size of the eluted species determined on- or off-line, *e.g.* by light scattering, or it may be calibrated by the use of reference substance(s) of known size and the size is then related to the elution volume. For the detection of dextran in body fluids, the latter approach combined with a selective chemical assay of dextran content is necessary. Traditionally, the column is calibrated through the use of several standards for which an estimate of the molecular mass distribution, *e.g.*, mass-average molecular mass ( $M_w$ ) or number-average molecular mass ( $M_n$ ), has been determined and the calibration curve is obtained by an iterative procedure to yield the conventionally true values of the estimates [8]. This procedure requires dedicated software for the calculations. Also, in cases where the column is calibrated *versus* the peak values, software is needed for regression of a calibration curve and calculation of size estimates. It may also be noted that the limited number and spread of calibration points used for the regression will of course affect the accuracy of the calibration.

The procedure described by Hagel and Andersson [13] utilizes all the information embedded in the molecular mass distribution curve of a polymer, *i.e.*, the relationship between cumulative mass fraction and molar mass [14]. This relationship may be obtained by traditional methods such as light scattering of fractions after ethanol precipitation, or by using modern detection

principles such as multi-angle laser-light scattering of column effluent. The information may also be obtained from gel filtration analysis using carefully calibrated columns, preferably employing a large number of calibration points.

The column to be used is calibrated over the size range of interest by gel filtering a sample possessing a suitable size distribution, *i.e.*, there is no need for calibration of the entire separation range of the column. The concentration of solute is determined by chemical assay, either of collected fractions or by on-line analysis, or may be monitored by an on-line detector if no interfering substances are co-eluted. The concentration (expressed in units or peak height) at increasing elution volume is noted and the cumulative amount of substance computed. The molecular mass corresponding to the cumulative amount is then calculated from the known molecular mass distribution curve of the sample. Finally, the molecular mass is converted to solute size and, thus, the calibration curve relating solute size to elution volume is established. This procedure may be performed manually or by a personal computer using a simple spreadsheet.

The size-determining factor in gel filtration has yet to be confirmed [12,15–17]. However, the size of globular proteins, expressed either as Stokes radius or as viscosity radius (sometimes called hydrodynamic radius), is closely depicted by the viscosity radius of dextran [15,16]. On the other hand, proteins and dextran do not lie on a common calibration curve when Stokes radius is used as size parameter for dextran [15]. It may from these reports be concluded that in order to study effects based on the size of globular proteins the calibration of the gel filtration column should be made in terms of viscosity radius if dextran is used as test probe. This viscosity radius is calculated from [18]:

$$R_h = 0.271 \cdot M_r^{0.498} \quad (1)$$

and the Stokes radius is given by [7]:

$$R_{St} = 0.33 \cdot M_r^{0.463} \quad (2)$$

As can be seen from these equations, Stokes radius yields values 12–18% lower for solute size

than viscosity radius for solutes in the range 25–70 Å.

## EXPERIMENTAL

### Chromatography

The column, XK 16/100, was packed with Sephacryl S-300 SF to a bed height of 93 cm according to the manufacturer's instructions. The column packing was controlled visually by running a sample of Blue Dextran 2000. The column was connected to a MicroPerpex peristaltic pump (yielding a nominal flow-rate of 0.4 ml/min) and a fraction collector, RediFrac. All equipment was obtained from Pharmacia LKB Biotechnology (Uppsala, Sweden). The eluent was prepared by dissolving 6.9 g of N-tris(hydroxymethyl)methyl 2-aminoethanesulphonic acid, 99% (TES; Sigma), 105 g of sodium chloride (99.5%, Merck), and 3 g of trichlorobutanol (98–99%, Merck) in 2000 ml of distilled water, adding 0.1 ml of mercaptoethanol (98%, Aldrich), adjusting the pH to 7.0 and completing the volume to 3000 ml. A 1-ml aliquot of untreated urine or serum was applied to the column, and up to 35 fractions over the fractionation range of interest were collected and subjected to chemical assay of dextran content. The fraction size, approximately 2 g, was determined by weighing.

### Chemical assay

A detection principle that discriminates between dextran and high-molecular-mass constituents in body fluids was needed for this study, *i.e.* a general detection principle such as refractive index is not applicable. The chemical assay proposed by Scott and Melvin [19] has frequently been used for analysis of dextran. With this method dextran is hydrolysed to glucose and converted to 5-hydroxymethylfurfural when heated with strong acid. Furfural condenses with anthranol to a blue–green chromophore showing an absorption maximum at 625 nm. Thus, all glucose-containing solutes will yield a positive response. It may also be noted that some types of preservatives, *e.g.* sodium azide, are not compatible with the anthrone method. However, for our purpose the anthrone method is very

suitable. The concentration of dextran in the fractions was determined by mixing 1 ml of sample with 2 ml of anthrone reagent (0.5 g of anthrone in 250 ml of sulphuric acid) and immersing the mixture in a boiling water bath for 7 min [19]. The absorbance at 625 nm, using 2 ml of reagent plus 1 ml of buffer treated as above as reference, was taken as the dextran concentration. Fractions displaying an absorbance exceeding 1 were diluted and re-evaluated.

### Calibration

The column was calibrated using a dextran sample possessing a broad molecular mass distribution, *i.e.* with a mass average of 72 300 and a polydispersity,  $M_w/M_n$ , of 2.4, which had been determined by size-exclusion chromatography [20]. This dextran yields an accurate calibration range, corresponding to the 5th and 95th percentiles of the distribution, from 190 000 to 10 000 in molecular mass, which equals 115–27 Å in solute size of dextran [14]. Information from multi-angle laser-light scattering (MALLS) was used to judge the accuracy of the molecular mass distribution of the calibration sample [21]. A 1-ml aliquot of the calibration dextran, containing 3 mg, was applied to the column, and 1- or 2-ml fractions were collected in the range of interest (*i.e.* approximately between 80 and 150 ml). The content of dextran in the fractions was determined by the anthrone method, as described above, and the cumulative area as a function of elution volume was calculated. The calibration curve was obtained by calculation of the molecular mass for which the integral mass coincides with the cumulative area of each fraction [14]. The calibration in molecular mass was then converted to viscosity radius through the use of eqn. 1 or to Stokes radius through the use of eqn. 2. Calculations and reports were performed using a dedicated application of Excel 3.0 (from ref. 22). The accuracy of the calibration was tested by chromatography of two proteins of known size, *i.e.* ferritin and bovine serum albumin. The fractions were in this case analysed for absorbance at 280 nm, and the exact maximum was determined from a third-degree polynomial fit to the five concentrations surrounding the maximum.

### Evaluation of size distributions

The distribution of dextran in urine as compared with that of plasma was studied by applying 1 ml of untreated sample on the column, collecting 2-ml fractions and analysing these for dextran content with the anthrone method. The absorbance values were entered into a spreadsheet (SECSOFT [22]), which calculated elution profiles for the samples and the ratio of the dextran content of urine to that of serum as a function of solute size.

## RESULTS AND DISCUSSION

### Calibration of the column

A typical elution profile of the calibration substance is shown in Fig. 1. The fractionation and subsequent manual analysis yields a variability in the determination of dextran content. Fortunately, this variability does not affect the calibration curve established, since smoothing of the raw data, using a three-point moving average, prior to calculations had no noticeable effect (*i.e.* less than 0.3%) on the final result. The calibration curve obtained from the integral method is shown in Fig. 2. Owing to the large number of data points, *i.e.* fractions, there is no need to apply any curve-fitting procedure to achieve a smooth curve. The figure also illus-

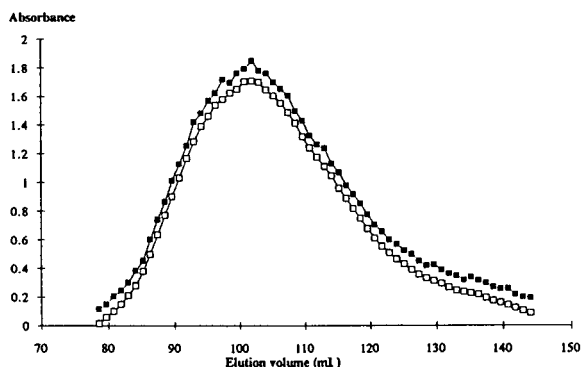


Fig. 1. Typical elution profile of the calibration substance. The sample, dextran with  $M_w = 72\,300$  was chromatographed on Sephacryl S-300 SF. The absorbance, as obtained from the anthrone analysis, is plotted versus the elution volume corresponding to the midpoint of each fraction. The smoothed curve was calculated using a three-point moving average (the curve is displaced  $-0.1$  absorbance units to increase the readability). ■ = Original; □ = smoothed.

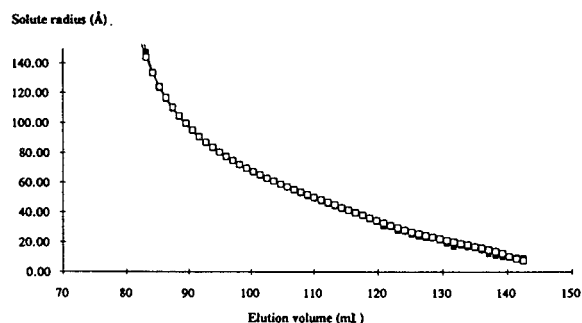


Fig. 2. Calibration curve of dextran on Sephacryl S-300 SF. The solute radius as a function of elution volume was calculated from the elution profile (*e.g.*, see Fig. 1) and the molecular mass distribution of the sample by employing the integral method and converting molecular mass to viscosity radius with the aid of eqn. 1. Calibration curves were calculated using data for molecular mass distribution of the reference sample as obtained by gel filtration (□) and light scattering (■).

trates the reliability of the molecular mass distribution data of the reference sample as determined by gel filtration on a carefully calibrated column set. By using data for the molecular mass distribution of the reference sample, as obtained by an absolute method, *i.e.* on-line MALLS employing a different column set [21], more or less identical calibration curves were obtained. The accuracy of the method, as estimated from the viscosity radii of dextran and proteins, is good, *i.e.* better than 5%, as shown by the data in Table I. Using Stokes radius as size estimate will yield too low an estimate of protein size. Unfortunately, literature data for the viscosity radius of ferritin differ considerably. The reproducibility of the calibration procedure as evaluated by running the sample three times showed a range of roughly 1% in the middle of the calibration area, which increases slightly at the extremes of the calibrated domain (Table II). This is because of variations in the selection of start and end points of sampling, which will influence the cumulative fractions and thus the calculated size. The influence in the centre of the calibration range, *i.e.* 70–30 Å, will be small. However, to obtain an accurate calibration of the entire range it is important that the sampling of fractions is made over the entire separation range of the column! It is also advisable to check

TABLE I  
EVALUATION OF SOLUTE SIZE FROM THE CALIBRATION CURVE

Column	Solute	Calculated size (Å) <sup>a</sup>		Nominal size (Å) <sup>b</sup>		Deviation (%) <sup>c</sup>		Ref.
		R <sub>h</sub>	R <sub>st</sub>	R <sub>h</sub>	R <sub>st</sub>	R <sub>h</sub>	R <sub>st</sub>	
911119	Dextran M <sub>p</sub> 66 700	66.4	54.9	68.4	56.5	-3.0	-3.0	23
911128	Dextran M <sub>p</sub> 66 700	69.6	57.4	68.4	56.5	+1.8	+1.8	23
920123	Bovine serum albumin	35.6	30.8	36	36.1	-1.1	-14.7	12 15
920521	Ferritin	68.0	56.2	65.6 61	67.1 59.3	+3.6 +11.4	-16.2 -5.2	24 12 15
	Bovine serum albumin	37.4	32.2	36	36.1	+3.9	-10.8	12 15
920903	Ferritin	66.6	55.1	65.6 61	67.1 59.3	+1.5 +9.1	-17.9 -7.1	24 12 15
	Bovine serum albumin	34.7	30.0	36	36.1	-3.6	-16.9	12 15

<sup>a</sup> Size calculated from the calibration curve with aid of eqns. 1 and 2.

<sup>b</sup> Nominal size of dextran calculated from nominal molecular mass corresponding to the peak apex, M<sub>p</sub>, (ref. 23), eqns. 1 and 2.

<sup>c</sup> Relative to nominal size.

the calibration curve with a number of samples covering the entire calibrated range.

The data in Table I illustrates that calibration of the column in terms of viscosity radius yields a more accurate estimate of protein size than calibration in terms of Stokes radius, which may yield too low an estimate of approximately 15–25% [15]. Unfortunately in many investigations

dealing with study of barrier function, the molar mass of dextran has been converted to solute size in terms of Stokes radius, which, in view of recent research, turns out to be incorrect for the interpretation of size of globular proteins [15,16].

#### Evaluation of samples

The influence of the glomerular barrier function on the excretion of dextran of various size is illustrated in Fig. 3. The distribution of dextran in urine is displaced towards molecules of lower size owing to the restriction in the glomerular barrier, which increases with size. The peak eluting close to the total liquid volume of the column comes from inulin, a low-molecular-mass polyfructose (M<sub>r</sub> 5200). Inulin clearance provides the measurement of glomerular filtration rate (GFR, ml/min), and is the standard used for measuring ultrafiltration of small solutes and water through the glomeruli. The clearance of a substance, C<sub>x</sub>, is calculated from [25]:

$$C_x = U_x V / P_x \quad (3)$$

TABLE II  
REPEATABILITY OF THE CALIBRATION PROCEDURE

Note that the valid calibration range is from 27 to 115 Å.

Retention volume (ml)	Calculated solute size (Å)			Range (Å)
	Run 1	Run 2	Run 3	
85	135.9	139.2	137.5	3.3
90	102.5	101.0	102.6	1.6
100	70.1	69.4	70.4	1.0
110	51.6	51.3	51.7	0.4
120	35.6	36.0	36.7	1.1
130	22.7	23.5	23.8	1.1



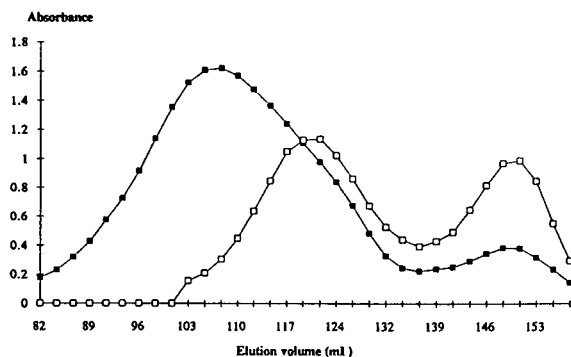


Fig. 3. Typical elution profiles of dextran in serum (■) and urine (□) samples. A 1-ml sample was run on the column, Sephacryl S-300 SF, and the collected fractions analysed with the anthrone method. The first peak represents dextran and the second peak represents inulin. All fractions displaying an absorbancy exceeding 1 were diluted and re-evaluated.

where  $U_x$  is the concentration of a substance (like inulin or dextran) in urine,  $V$  is the urine volume for a given period and  $P_x$  is the concentration of the substance in plasma. The clearance of dextran of different sizes can be calculated by the same formula, using measurements of fractions of concurrent dextran size in urine and blood. The ratio between dextran (dex) and inulin (in) clearance is calculated from:

$$\begin{aligned} C_{\text{dex}}/C_{\text{in}} &= (U_{\text{dex}}V/P_{\text{dex}})/(U_{\text{in}}V/P_{\text{in}}) \\ &= (U_{\text{dex}}/P_{\text{dex}})/(U_{\text{in}}/P_{\text{in}}) \end{aligned} \quad (4)$$

This ratio approaches 1 as the size of the dextrans becomes small and the molecules pass freely through the glomerular barrier like inulin. Greater restriction applies for dextrans of larger size, and the ratio falls towards zero when the dextrans are so large that they no longer appear in the urine. Thus the ratio is a meaningful tool in the evaluation of the relative restriction of large molecules compared with those freely filtered. The calculated clearance of inulin was no different whether inulin was measured in the urine and blood samples in presence or absence of dextran. This is in agreement with experience reported elsewhere [26].

The relative clearance of dextran as a function of solute size, expressed as viscosity radius of dextran, is shown in Fig. 4 (the corresponding plot for Stokes radius is also given, however, as

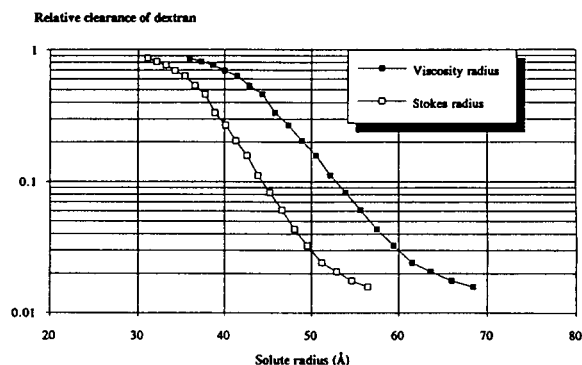


Fig. 4. Relative clearance of dextran,  $C_{\text{dex}}/C_{\text{in}}$ , as a function of solute size. Clearance was calculated from the elution profiles (e.g. see Fig. 3) and eqn. 4. Solute size, expressed as viscosity radius of dextran, was calculated from the calibration curve (Fig. 2). For the purpose of comparison with earlier published results, Stokes radius (eqn. 2) is also given. Please note that Stokes radius will yield too low an estimate of size of globular proteins (see text for explanations).

stated above, we recommend that evaluations are made with respect to viscosity radius to yield an accurate estimation of equivalent size of globular proteins). In some experiments we noticed oscillations of clearance for small solutes. This problem was attributed to the influence of interfering inulin, therefore the data are truncated at a viscosity radius of 30 Å. To obtain data for smaller molecules, another marker of GFR that does not interfere with the anthrone reaction, for example  $^{51}\text{CrEDTA}$ , is more appropriate than inulin. This will also avoid problems with examinations of diabetic patients in whom high blood and urine glucose levels may interfere with the dextran as well as the inulin measurements [27]. In order to check the repeatability of the evaluation step, the complete analysis was repeated five times. The relative error in the determination of dextran clearance is illustrated by Fig. 5. The large uncertainty for solutes of small size, *i.e.* smaller than 45 Å, is evident, however for solutes of primary interest in the evaluation of the glomerular barrier function, *i.e.* larger than 50 Å, the relative error is acceptable (*i.e.* 10–20%). Estimation of the relative dextran clearance also has its limitations for large molecules. The urine concentrations of dextran of sizes exceeding 70 Å in viscosity radius is so low that the extinctions

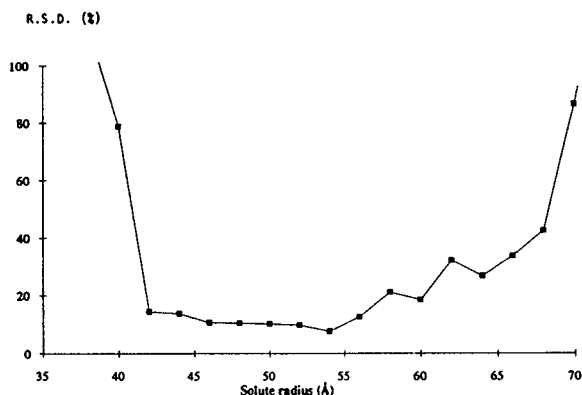


Fig. 5. Precision of the determination of relative clearance as calculated by repeating the entire chromatographic assay five times. The relative standard deviation was calculated for various solute viscosity radii.

with the anthrone method approaches background values, which makes data for clearance unreliable. However, as the clearance approaches zero, the variability is in absolute terms still very small.

One critical issue when it comes to interpretations of the size of dextran into size of proteins is the variability of size of random coils, *i.e.* dextran, as compared with compact charged ellipsoids, *i.e.* proteins, in different solvents. The use of dextran viscosity radius in dilute solutions as representative of protein size in body fluids will of course only be correct as long as the size of the solutes does not vary considerably with ionic strength. The intrinsic viscosity of native dextran was found to increase slightly with ionic strength (*i.e.* by 5% when going from water to 4 M sodium chloride), and the radius of gyration increased by 10% [28]. This was attributed to salt solution being a better solvent for dextran than pure water. The viscosity radius of dextran is rather insensitive to moderate ionic strength (*i.e.* up to at least 0.5 M [29]). The ionic strength of urine does not exceed that of plasma and the plasma sodium ion concentration is about 0.15 mol/l; the chloride ion concentration is about 0.1 mol/l and other anions account for 0.05 mol/l. Therefore, ionic strength probably has a minor impact on dextran size in this setting. For charged molecules, such as proteins, the situation is somewhat different. In solutions of high ionic strength the molecules are less stretched out because of screening of the charged surface.

This is exemplified by the reduced intrinsic viscosity of serum albumin in salt solutions [30]. This illustrates the importance of selecting probes calibrated in the solvent to be studied.

The use of flexible molecules as a model for transport of compact proteins through membranes must also be addressed. The possibility of vermicular motion of flexible molecules may, in theory, enable them to penetrate also small pores, *i.e.* the molecules would then display an apparent smaller size than determined hydrodynamically. However, Davidson and Deen [31] found in a study of transport of flexible molecules through porous membranes that, owing to solvent permeability, random coil molecules appeared physically larger than an impermeable sphere of the same Stokes radius.

These observations support the use of dextran for study of membrane pore dimensions in aqueous solvents of moderate ionic strength and the expression of size of globular proteins in terms of viscosity radii of dextran.

#### ACKNOWLEDGEMENT

MALLS data of the reference sample were kindly provided by Torvald Andersson, Pharmacia LKB Biotechnology.

#### REFERENCES

- 1 K. Granath and P. Flodin, *Macromol. Chem.*, 48 (1961) 160.
- 2 K.A. Granath and B.E. Kvist, *J. Chromatogr.*, 28 (1967) 69.
- 3 R.L.S. Chang, I.F. Ueki, J.I. Troy, W.M. Deen, C.R. Robertson and B.M. Brenner, *Biophys. J.*, 15 (1975) 876.
- 4 B.J. Carrie and B.D. Myers, *Kidney Int.*, 17 (1980) 669.
- 5 T.B. Wiegmann, K.G. Herron, A.M. Chonko, K.L. MacDougall and W.V. Moore, *Diabetes*, 41 (1992) 62.
- 6 N. Loon, O. Shemesh, E. Morelli and B.D. Myers, *Am. J. Physiol.*, 257 (1989) F608.
- 7 A. Remuzzi, E. Peticucci, P. Ruggenti, L. Mosconi, M. Limonta and G. Remuzzi, *Kidney Int.*, 39 (1991) 1267.
- 8 G. Nilsson and K. Nilsson, *J. Chromatogr.*, 101 (1974) 137.
- 9 A.M. Basedow, K.H. Ebert, H. Ederer and H. Hunger, *Makromol. Chem.*, 177 (1976) 1501.

- 10 W.W. Yau and D.D. Bly, in T. Provder (Editor), *Size Exclusion Chromatography (GPC)*, ACS Symposium Series, American Chemical Society, Washington D.C., 1980, pp. 197.
- 11 H. Ellegren and T. Låås, *J. Chromatogr.*, 467 (1989) 217.
- 12 P.L. Dubin and J.M. Prinipi, *Macromolecules*, 22 (1989) 1891.
- 13 L. Hagel and T. Andersson, presented at the *11th International Symposium on HPLC of Proteins, Peptides and Polynucleotides*, Washington D.C., October 20–23, 1991, paper 214.
- 14 L. Hagel, *J. Chromatogr.*, in press.
- 15 R.P. Frigon, J.K. Leypkoldt, S. Uyeil and L.W. Hendersson, *Anal. Chem.*, 55 (1983) 1349.
- 16 M. Potschka, *Anal. Biochem.*, 162 (1987) 47.
- 17 P.L. Dubin, J.L. Kaplan, B.-S. Tian and M. Mehta, *J. Chromatogr.*, 515 (1990) 37.
- 18 L. Hagel, in J.-C. Janson and L. Rydén (Editors), *Protein Purification, Principles, High Resolution Methods and Applications*, VCH, New York, 1989, p. 100.
- 19 T.A. Scott Jr. and E.H. Melvin, *Anal. Chem.*, 25 (1953) 1656.
- 20 K. Nilsson, Kabi-Pharmacia, Uppsala, Sweden, personal communication, 1992.
- 21 T. Andersson, Pharmacia LKB Biotechnology, Uppsala, Sweden, personal communication, 1992.
- 22 L. Hagel, unpublished results, 1992.
- 23 *Pharmacosmos Dextran Standards*, Fairprint, Viby, Denmark.
- 24 C. de Haen, *Anal. Biochem.*, 166 (1987) 235.
- 25 A.S. Levey, M.P. Madaio and R.D. Perrone in B.M. Brenner and F.C. Rector (Editors), *The Kidney*, W.B. Saunders, Philadelphia, 4th ed., 1991, p. 921.
- 26 B.M. Myers, T. Bokarma, S. Friedman, C. Bridges, J. Ross, S. Asseff and W.M. Deen, *J. Clin. Invest.*, 79 (1982) 732.
- 27 G. Norden, S. Björck, G. Granerus and Gudrun Nyberg, *Nephron*, 47 (1987) 36.
- 28 E. Antonioni, L. Bellelli, M.R. Bruzzesi, A. Caputo, E. Chiancone and A. Rossi-Fanelli, *Biopolymers*, 2 (1964) 27.
- 29 K. Granath, Pharmacia, Uppsala, Sweden, personal communication, 1992.
- 30 C. Tanford, *Physical Chemistry of Macromolecules*, Wiley, New York, 1961, p. 517.
- 31 M.C Davidson and W.M. Deen, *J. Membr. Sci.*, 35 (1988) 167.

# Analysis and purification of monomethoxy-polyethylene glycol by vesicle and gel permeation chromatography

Barbara Selisko\*, Cristina Delgado and Derek Fisher

*Molecular Cell Pathology, Royal Free Hospital, School of Medicine, Rowland Hill Street, London NW3 2PF (UK)*

Rudolf Ehwald

*Institute of Plant Physiology and Cell Biology, Department of Biology, Humboldt-University Berlin, Invalidenstrasse 42, 1040 Berlin (Germany)*

(First received December 11th, 1992; revised manuscript received March 18th, 1993)

---

## ABSTRACT

Vesicle chromatography (VC) and gel permeation chromatography (GPC) were used for characterisation and purification of monomethoxy-polyethylene glycol (M-PEG), a reagent for protein modification. Detection of low concentrations of contaminating PEG was facilitated by a very sensitive colourimetric detection method with a detection limit of 1  $\mu\text{g/ml}$ . For analytical purposes GPC on Superose 12 was superior to VC. Molecular masses, polydispersity and percentage of contaminating PEG were estimated. As a comparison  $^1\text{H}$  NMR spectroscopy was carried out. The results were in good accordance with GPC. A two-step preparative purification with VC of M-PEG containing 22.9% PEG reduced the PEG content to 4.4%.

---

## INTRODUCTION

Proteins can be modified by attaching macromolecules. In general, the modification results in an alteration of the physiological properties and/or an increase of the stability of proteins. The main objectives of the modification of proteins are to use them as therapeutic agents or as biocatalysts in biotechnological processes. Polyethylene glycol (PEG) has been applied to various proteins as an agent for modification [1]. Various coupling methods have been developed so far using mainly monomethoxy-polyethylene glycol (M-PEG) as starting material. In this way a PEG molecule is provided which is activated at only one end of the polymeric chain, thus preventing cross-linking of two proteins or the formation of even larger aggregates. However,

M-PEG preparations are often contaminated by PEG with free hydroxyl groups at each end (also called diol-PEG). This contaminant is reported to be formed as a result of simple hydrolysis of some of the ethylene oxide monomers in the starting period of the polymerisation due to the presence of free hydroxyl ions [2]. As a consequence these molecules grow at both ends of the chain and, thus, should have about double the molecular size of M-PEG.

The use of narrow-range M-PEG with a high degree of purity is important to minimise the heterogeneity of the modification products and to prevent the above mentioned formation of aggregates. Thus, the characterisation of the purity and molecular mass distribution of the polymer is necessary. In this study we used gel permeation chromatography (GPC), vesicle chromatography (VC) and  $^1\text{H}$  NMR spectroscopy.

VC is a type of permeation chromatography

---

\* Corresponding author.

using microcapsules made of clusters of extracted higher plant cells from suspension cultures as a separation medium [3–5]. The vesicular packings occur as multicellular complexes of 100–250  $\mu\text{m}$  in diameter. The framework of the primary cell wall remains intact. The cell wall acts as an ultrafiltration membrane which is characterised by a very sharp cut-off or separation limit. Large molecules are excluded and eluted in one fraction with 50% of the bed volume (designated as high-molecular-mass or HMW fraction). Smaller molecules permeate through the thin (less than 1  $\mu\text{m}$ ) vesicle membrane into the stationary liquid phase. The permeable fraction (low-molecular-mass or LMW fraction) leaves the column with the total bed volume. We applied VC to fractionate M-PEG 5000 in analytical and preparative scale.

GPC is widely used for determination of the molecular mass and polydispersity of polymers [6,7]. As a complement to VC it was applied in analytical scale to characterise the original and purified material.

$^1\text{H}$  NMR Spectroscopy was reported to be suitable for characterisation of PEGs [8,9]. Therefore, it was used in this study for determination of molecular mass and purity of the polymer.

## EXPERIMENTAL

### Materials

Preparations of M-PEG 5000 were purchased from Union Carbide (Versoix, Switzerland) ("Carbowax"), Union Carbide (South Charleston, USA) (low-diol "Carbowax") and Aldrich (Milwaukee, WI, USA). M-PEG 2000 was obtained from Aldrich (Gillingham, UK). Trifluoroethanesulphonyl-methoxy-polyethylene glycol (TM-PEG) was prepared using standard M-PEG 5000 according to ref. 10. PEG standards for calibration of the Superose 12 column with molecular masses given by the manufacturer of 4100, 7100 and 8650 were purchased from Polymer Labs. (Church Stretton, UK).

The preparation of the vesicular packing material as well as the estimation of the separation limit was done in the laboratory of Professor Ehwald at the Department of Biology of the

Humboldt-University (Berlin, Germany) as described for  $\text{VP}_1$  (plant cell material with unaltered separation limit) in refs. 11 and 12.

### Methods

*Vesicle chromatography.* Dry vesicular packing material was suspended in 0.05 *M* sodium phosphate buffer, pH 5.5. The packed bed was washed with one volume of the appropriate elution buffer. Samples of given size (about 0.9 to 7.8% of the bed volume) and concentration were eluted with an elution rate of about 0.5 mm/min. The amount of PEG was estimated in all fractions by a colourimetric method according to Childs [13] or by using a Hewlett-Packard refractive index detector 78977A (first preparative fractionation). The preparative separations were carried out under the following conditions: first fractionation —bed volume: 6.5 l (13 cm  $\times$  25.2 cm I.D.), sample: 500 ml of 3% (w/v) M-PEG, elution buffer: 0.01 *M* sodium phosphate, pH 5.5, elution rate: 0.41 mm/min; second fractionation —bed volume: 220 ml (7.8 cm  $\times$  6 cm I.D.), sample: 5 ml of 5% (w/v) M-PEG, elution buffer: 0.05 *M* sodium phosphate, pH 5.5, elution rate: 0.51 mm/min. After preparative purification the HMW fractions (first fractionation: 2700–4100 ml) and LMW fractions (first fractionation: 5400–7400 ml, second fractionation: 180–260 ml) were evaporated under reduced pressure and re-dissolved in ethanol, the insoluble phosphate coming from the elution buffer was removed by filtration. The ethanol was evaporated under reduced pressure and the dried samples were dissolved in acetone and precipitated with *n*-hexane, the solvents were finally removed under vacuum.

*Gel permeation chromatography.* M-PEG samples (1 mg/200  $\mu\text{l}$ ) were analysed on a Pharmacia fast protein liquid chromatography (FPLC) system using a Superose 12 HR 10/30 column previously equilibrated with phosphate-buffered saline (PBS), pH 7.0. The samples were eluted with the same buffer at a flow-rate of 0.3 ml/min (3.8 mm/min); 0.25-ml fractions were collected. The PEG concentrations were estimated colourimetrically in all fractions according to Childs [13]. The column was calibrated using

narrow-range polydisperse PEG standards from Polymer Labs. The estimated linear calibration curve was  $\log M_r = -0.1394 V_e + 5.919$  ( $R = 0.998$ ), where  $V_e$  is the elution volume. The corresponding hydrodynamic diameter ( $d$ ) of the polymer in nm can be calculated using the following equation given by Hagel [14]:  $d$  (nm) =  $0.051 M_r^{0.517}$ . The mass-average molecular mass ( $M_w$ ) and number-average molecular mass ( $M_n$ ) were calculated using the equations  $M_w = \Sigma(w_i M_i)$  and  $M_n = 1/\Sigma(w_i/M_i)$ , where  $w_i$  is the mass fraction and  $M_i$  the molecular mass of fraction  $i$ . The polydispersities of preparations were determined as the ratio  $M_w/M_n$ .

*Detection of PEG using the method of Childs [13].* Fractions of PEG were diluted to the appropriate concentration of 1 to 10  $\mu\text{g/ml}$  to measure absorbances within the linear range. A 200- $\mu\text{l}$  volume of each was pipetted in microtiterplates and mixed with 50  $\mu\text{l}$  of 5%  $\text{BaCl}_2$  in 1 M HCl and 50  $\mu\text{l}$  of 0.05 M iodine solution (12.69 g  $\text{I}_2$  + 20 g K/I). After shaking the plates for 3 to 5 min the absorbance was read at 540 nm against water in a Titertek Multiscan Plus MK II (Flow Labs., Switzerland). Fig. 1 shows the standard curves for M-PEG 5000 (Union Carbide), TM-PEG 5000 and standard PEGs of molecular masses of 4100 and 8650. The detection limit of the method was estimated to be 1.6

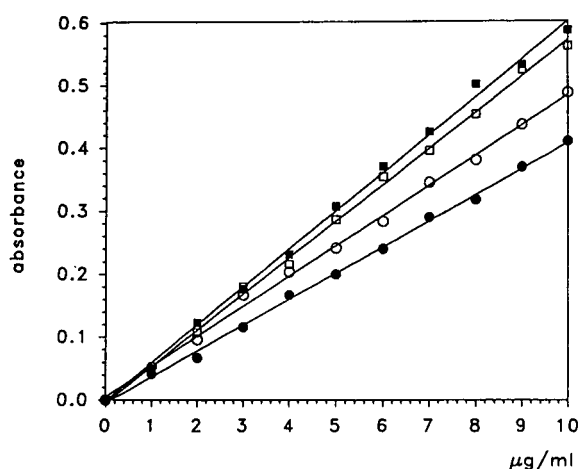


Fig. 1. Standard curves of PEG detection by Childs' method (see Experimental). ■ = PEG 4100; □ = PEG 8650; ○ = M-PEG 5000; ● = TM-PEG 5000.

$\mu\text{g/ml}$  for PEG 4100 and 1.7  $\mu\text{g/ml}$  for PEG 8650.

*NMR Experiments.* Preparations of M-PEG were dissolved in dry [ $^2\text{H}_6$ ]dimethyl sulphoxide ( $\text{DMSO-d}_6$ ) (samples contained 50 to 150  $\text{mg/ml}$ ) and kept overnight over molecular sieve 3A (Aldrich, Gillingham, UK) to remove traces of water. The samples were then injected into standard NMR tubes, previously swept with nitrogen, through the septum cap.  $^1\text{H}$  Fourier transform NMR spectra were recorded within a spectral width of 3760 Hz (15 ppm) on a Bruker spectrometer WM 250 operating at 250 MHz. The reference standard was  $\text{DMSO-d}_6$  itself at 2.5 ppm.

The characteristic signals are as follows: carbon satellite bands of the polymer backbone (due to the natural occurrence of 1.108% of  $^{13}\text{C}$ ): m, 3.22 ppm and 3.78 ppm,  $\text{CH}_3\text{O-}$ : s, 3.25 ppm,  $\text{H}_2\text{O}$ : s, 3.28 ppm,  $\text{CH}_2\text{CH}_2\text{O-}$  polymer backbone: m, 3.40 ppm–3.60 ppm,  $\text{OH-}$ : t, 4.56 ppm.

The percentage of PEG in M-PEG was determined by comparing the integrals of the hydroxyl and methoxy end groups of the polymer. As the first step, the apparent integral of the hydroxyl end groups coming from PEG was calculated as  $n_{\text{OH}} = (\text{OH} - \text{CH}_3\text{O}/3)$ . There the integral of the  $\text{CH}_3\text{O-}$  group divided by three represents the OH groups in M-PEG. The ratio of PEG in M-PEG in mol% is then: % PEG =  $[n_{\text{OH}}/(\text{CH}_3\text{O}/3 + \text{OH})] \times 100$ .

The  $M_n$  value of the polymer was determined on the basis of the average number of  $(\text{CH}_2\text{CH}_2\text{O-})$  units in the polymer backbone. The latter is given by the number of protons in the backbone (the integral for the polymer backbone compared to the integrals of the end group signals which were normalised to a single proton) divided by four:  $n = [(\text{CH}_2\text{CH}_2\text{O-})_n / (\text{CH}_3\text{O-}/3 + \text{OH})/2]/4$ . The integral of the backbone signal was calculated using the carbon satellite signal at 3.78 ppm which represents 0.554% of the backbone protons because they are in the same range of intensity as the end group signals. The  $M_n$  value of the polymer can then be calculated according to  $M_n = 44n + 32 \times$  molar ratio of M-PEG +  $18 \times$  molar ratio of PEG.

## RESULTS

*Chromatographic analysis of M-PEG 5000*

Fig. 2 shows the fractionation of M-PEG by VC and by GPC. VC of M-PEG 5000 (Union Carbide) using vesicular packing material with a separation limit of 5.4 nm results in a profile consisting of two peaks, the HMW fraction and the LMW fraction. The HMW fraction was estimated to be 8.2% (w/w) of the applied sample. The fractionation of M-PEG 5000 by GPC on Superose 12 resulted also in a separation in two peaks corresponding to molecular masses ( $M_r$ ) of 9280 and 5970. In contrast to VC, the HMW fraction represented 22.9% of the total sample. Since there was a discrepancy in the percentage of material eluting with the HMW fraction between GPC and VC, we studied whether the identities of the HMW and

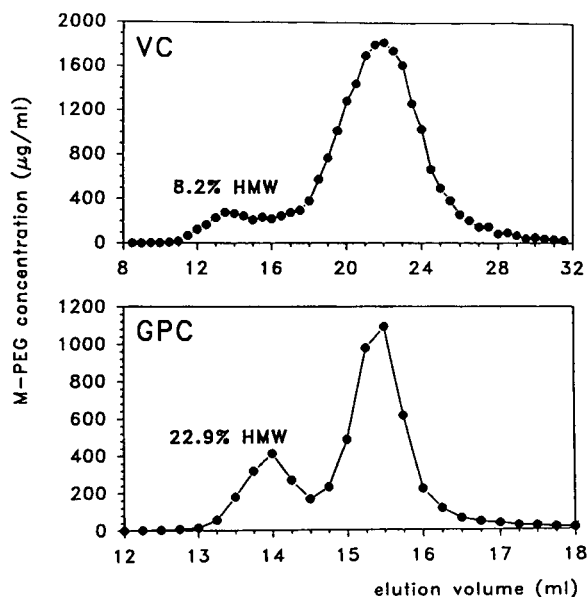


Fig. 2. Vesicle chromatography (VC) and gel permeation chromatography (GPC) of M-PEG 5000. VC: column dimensions 12.4 cm  $\times$  1.5 cm I.D., sample 0.5 ml of 2% (w/v) M-PEG, elution buffer 0.05 M sodium phosphate, pH 5.5, elution rate 0.49 mm/min. GPC: Superose 12 HR 10/30, sample 0.2 ml of 0.5% (w/v) M-PEG, elution buffer: PBS, pH 7.0, elution rate 3.8 mm/min. The M-PEG concentration of all fractions was estimated, the given chromatograms show the part of the profiles where M-PEG was eluted, the ratio of the high-molecular-mass (HMW) fraction is given in percent (w/w).

LMW fractions obtained by both techniques were comparable. The analysis of the HMW fraction from VC by GPC showed a main peak co-eluting with the peak corresponding to a molecular mass of 9280 and some contamination with the LMW component (see below in Fig. 6). Similarly, the LMW fraction from VC showed a main peak which co-eluted with the 5970 peak in the GPC chromatogram of the original M-PEG 5000 and some contamination with the HMW fraction (see below in Fig. 6). Given the identity of the HMW and LMW fractions of GPC and VC, it is clear that GPC outperforms VC regarding the efficiency of the fractionation of the two components.

As a pre-step of the preparative purification the influence of sample concentration on the resolution of the fractionation of M-PEG on Superose 12 was studied. Increasing the sample concentration tenfold causes a strong right-shift, which is accompanied by an almost complete loss of resolution (Fig. 3). In Fig. 4 the influence of sample concentration on VC of M-PEG 5000 and tresylated M-PEG (trifluoroethanesulphonyl-methoxy-polyethylene glycol or TM-PEG) is shown. Despite an increase in the sample concentration from 0.2 to 6%, the HMW and LMW fractions appear in the same place, there is no

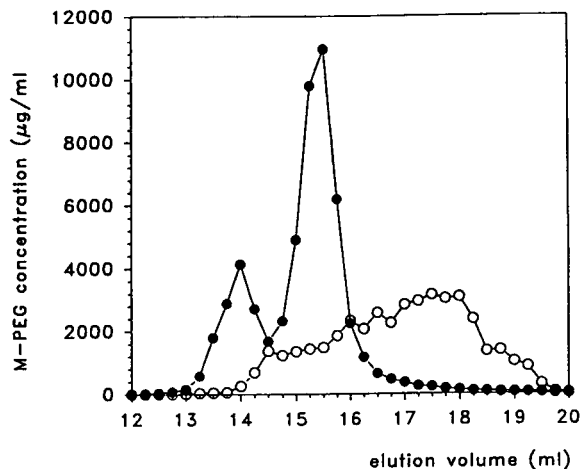


Fig. 3. Influence of sample concentration on GPC of M-PEG 5000. Column: Superose 12 HR 10/30; sample 0.2 ml; sample concentration in % (w/v): (●) 0.5, (○) 5; elution rate: 0.3 ml/min. FPLC profile of M-PEG with a sample concentration of 0.5% was upscaled by factor 10.

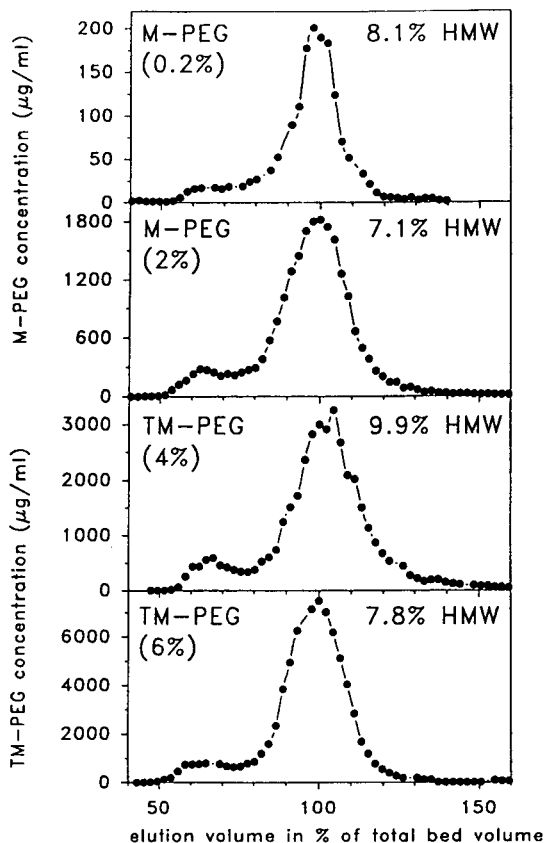


Fig. 4. Influence of sample concentration on VC of M-PEG and TM-PEG 5000. Column dimensions 12.4 cm × 1.5 cm I.D., sample volume 0.5 ml, sample concentrations in % (w/v) are given in parentheses, elution buffer 0.05 M sodium phosphate, pH 5.5 (M-PEG 0.2%) or 0.08 M PBS, pH 7.0. % HMW gives the percentage (w/w) of the high-molecular-mass fraction.

right-shifting. Furthermore, the resolution of the separation remains almost unchanged with only slight decreases in the percentage of the HMW fraction (up to 2.1) despite increases in the sample concentration applied of up to tenfold (Fig. 4).

In view of the possibility to apply higher sample concentrations VC was selected for a large-scale preparative fractionation. Fig. 5 gives the chromatogram of the first preparative fractionation of M-PEG 5000 (Union Carbide) by VC. The scale-up from around 25 to 6500 ml bed volume causes an obvious loss in resolution. The indicated fractions from 2700 to 4100 ml (HMW) and 5400 to 7400 (LMW) were collected and

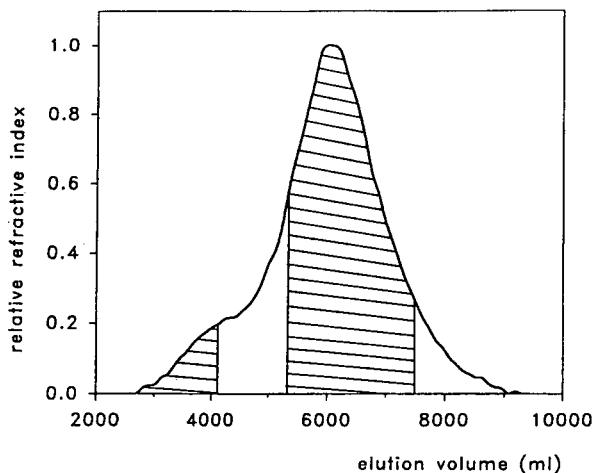


Fig. 5. Preparative fractionation of M-PEG 5000 by VC. Column dimensions 13.0 cm × 25.2 cm I.D., sample 500 ml of 3% (w/v) M-PEG, elution buffer 0.01 M sodium phosphate, pH 5.5, elution rate 0.41 mm/min. Indicated fractions were collected and prepared to give purified HMW and LMW preparations.

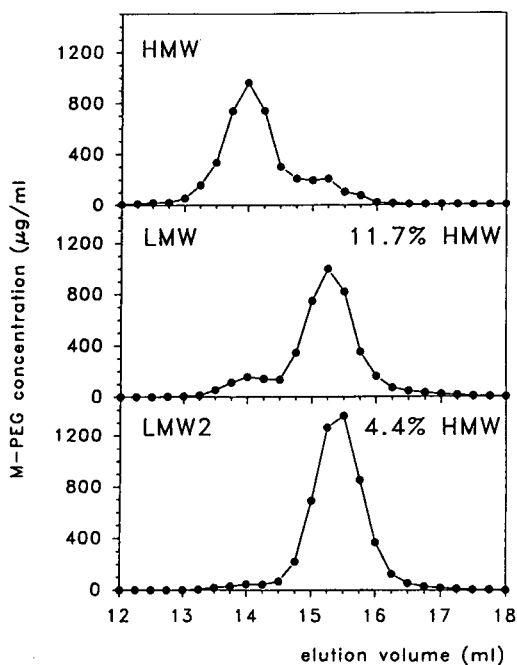


Fig. 6. GPC of low-molecular-mass (LMW) and high-molecular-mass (HMW) fractions coming from preparative VC of M-PEG 5000. Sample: 1 mg of M-PEG in 200 µl PBS, pH 7.0, column: Superose 12 HR 10/30, elution rate: 3.8 mm/min. LMW2 = Purified M-PEG obtained by a second preparative VC of LMW, the ratio of HMW in LMW and LMW2 is given top right in percent (w/w).



treated as described in Experimental. To characterise the purified preparations GPC was carried out (Fig. 6). The LMW preparation was still contaminated with 11.7% of HMW component and therefore further purification was required. A second preparative fractionation with VC provides a LMW fraction (LMW2) which contains only 4.4% HMW component as analysed by GPC (Fig. 6).

To further characterise the M-PEG preparations (original M-PEG 5000, LMW preparation from first purification step and LMW2 from second purification), their molecular masses and polydispersities were estimated. In order to do this the GPC column was calibrated with narrow-range polydisperse PEG standards of known molecular masses. Table I summarises the results. With each preparative purification step carried out using VC the average molecular mass as well as the polydispersity is reduced as expected after the removal of the high-molecular-mass contamination.

#### Estimation of purity and molecular mass of M-PEGs by NMR

As a reference method the  $^1\text{H}$  NMR spectra of the different preparations were recorded. Fig. 7 shows the NMR spectrum of the original M-PEG 5000 in  $\text{DMSO-d}_6$ . The  $\text{CH}_3$  signal at 3.25 ppm was overlapped by one of the  $^{13}\text{C}$  carbon satellite signals, each of which equals 0.554% of the backbone signal (according to the natural occurrence of  $^{13}\text{C}$  of 1.108%). Thus, for quantitative

TABLE I

MOLECULAR MASS AND POLYDISPERSITY OF ORIGINAL M-PEG 5000 (UNION CARBIDE) AND PURIFIED PREPARATIONS ESTIMATED BY GPC

Sample: 1 mg of M-PEG in 200  $\mu\text{l}$  PBS, pH 7.0, column: Superose 12 HR 10/30, elution rate: 0.3 ml/min, for calculation see Experimental.

PEG-preparation	$M_w$	$M_n$	Polydispersity $M_w/M_n$
M-PEG 5000 original	6550	6059	1.081
M-PEG LMW	6500	6230	1.043
M-PEG LMW2	5970	5820	1.026

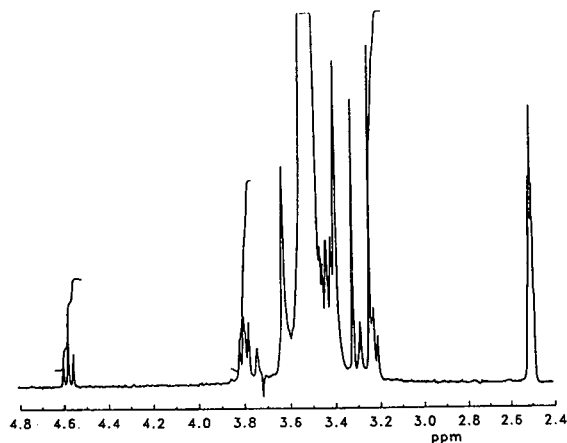


Fig. 7. 250 MHz  $^1\text{H}$  NMR spectrum of M-PEG 5000 (containing 23.9% PEG). Peaks: 50 mg/ml in  $\text{DMSO-d}_6$ , 2.5 ppm: DMSO; 3.22 and 3.78 ppm: carbon satellite bands; 3.25 ppm:  $\text{CH}_3\text{O-}$ ; 3.28 ppm:  $\text{H}_2\text{O}$ ; 3.29, 3.42, 3.64 and 3.74 ppm: spinning side bands of the backbone signal; 3.40–3.60 ppm:  $\text{CH}_2\text{CH}_2\text{O-}$  (polymer backbone); 4.56 ppm:  $\text{OH-}$ .

calculations the integral of the  $\text{CH}_3\text{O-}$  signal was corrected by subtracting from it the integral of the carbon satellite at 3.87 ppm, which was free of contributions from other signals. Based on the intensities of the signals of the polymer backbone and the methoxy and hydroxyl groups the molecular mass of the polymer and the percen-

TABLE II

MOLECULAR MASS AND PEG CONTENT OF VARIOUS M-PEG PREPARATIONS ESTIMATED BY  $^1\text{H}$  NMR SPECTROSCOPY

250 MHz, 50–150 mg/ml in  $\text{DMSO-d}_6$ , calculation of  $M_n$  and % PEG see *Methods*.

Sample	$M_n^a$	% PEG <sup>a</sup>
M-PEG 5000 (Union Carbide)	6040 (12.9%, 6)	23.9 (2.8%, 6)
LMW	6372	11.1
	6084	5.1
LMW2	5195	0
M-PEG 5000 low-diol (Union Carbide)	5390 (9.9%, 3)	0.6

<sup>a</sup> Standard deviation (M-PEG 5000 from Union Carbide) in percent of the mean value and number of independent measurements are given in brackets, otherwise single estimations or duplicates (LMW).

tage of PEG were estimated as described in Experimental. Table II shows the results of the calculations. The percentage of PEG in the LMW preparation was reduced compared to the original M-PEG. However,  $^1\text{H}$  NMR spectroscopy failed to show any PEG content in the LMW2 preparation which according to GPC contained 4.4%. In order to test this apparent discrepancy we subjected a commercial low-diol M-PEG 5000 from Union Carbide to the same analysis.  $^1\text{H}$  NMR spectroscopy showed a content of 0.6% PEG while GPC combined with the applied detection method indicated a PEG contamination of 2.15%.

## DISCUSSION

The fractionation of M-PEG by VC and GPC results in a profile showing two fractions. For original M-PEG 5000 (Union Carbide) the  $M_r$  values of the HMW and the LMW fraction were estimated to be 9280 and 5970, respectively. The percentage of the HMW fraction was 8.2 and 22.9%, estimated by VC and GPC, respectively. The reason for this discrepancy lies in the separation limit of 5.4 nm of the vesicular packing material used. It allows part of the HMW fraction, the molecules which are smaller than 5.4 nm, to permeate through the cell wall. These molecules are eluted with the LMW fraction. Figs. 2 and 6 show that the trough between the two peaks in the GPC elution profile corresponds to an elution volume of 14.7 ml. The corresponding molecular size of PEG is 5.1 nm. The efficiency of the separation by VC could therefore be increased by using a vesicle packing material with this separation limit. For that purpose plant cell material with smaller natural pore size has to be found.

Experiments concerning the influence of sample concentration on the resolution showed right shifting and a severe loss in resolution for M-PEG on Superose 12 at a sample concentration of 5% (w/v). In contrast, sample concentrations up to 6% (w/v) had little influence on the resolution of VC. Mori [15,16] reported a concentration effect when fractionating 0.1 to 0.4% polystyrene on porous glass packing materials due to a decrease in the hydrodynamic

volume of the polymer with increasing polymer concentration. They found a slight right shifting and increase in the slope of the calibration curve resulting in reduced separation efficiency. A decrease in the hydrodynamic volume of the polymer could be the reason for the slight decrease in the percentage of the HMW component in VC we have observed when increasing the concentration of M-PEG and TM-PEG in the sample. However, a reduction in the hydrodynamic volume cannot explain the magnitude of the observed loss of resolution and right shifting of M-PEG on Superose 12. As possible explanations we consider an overload effect [17,18] which might be more likely to occur in the gel structure of Superose 12 than in the vesicular structure of the packing material for VC, and the occurrence of phase separation on the surface of the agarose gel. The latter is worth being taken into account because the phenomenon of phase separation has been reported for a wide variety of polysaccharides [19], in addition to the well-studied phase system of dextran and polyethylene glycol [20–22].

For the detection of PEG we used a very sensitive colourimetric method developed by Childs [13]. So far, this method has been used to measure PEG concentrations in solutions of proteins precipitated by the polymer. Although more laborious than standard methods such as refractive index and direct UV detection, it is superior in its detection limit, which was estimated to be 1.6  $\mu\text{g}/\text{ml}$  for PEG 4100 and 1.7  $\mu\text{g}/\text{ml}$  for PEG 8650, *i.e.* 0.4 and 0.2 nmol/ml, respectively. In contrast, detection limits of other methods are reported to be in the submilligram range for refractive index detection or to be in the range of 5 to 10 nmol/ml, which would equal 25  $\mu\text{g}/\text{ml}$  for PEG 5000, for UV detection of derivatised PEG (dibenzoates) at 254 nm [23]. For the direct UV detection of PEG 200 at 185 nm a molar extinction coefficient  $\epsilon$  of 148  $\text{l mol}^{-1} \text{cm}^{-1}$  has been estimated [24], whereas  $\epsilon$  of PEG 4100 using Childs' method is  $4.4 \cdot 10^5 \text{ l mol}^{-1} \text{cm}^{-1}$ . The limit of detection of an indirect UV detection method at 210 nm for GPC of oligomers of ethylene glycol is given as 0.6 nmol/ml [25]. It was found that the detection method of Childs is influenced by the molecular mass of

the sample (Fig. 1). Therefore, for quantitative measurements it is advisable to use standard curves of PEGs with similar molecular mass.

The results of  $^1\text{H}$  NMR spectroscopy showed that the removal of the HMW fraction by VC is accompanied by a decrease in the amount of diol-PEG in the preparation. Thus,  $^1\text{H}$  NMR spectroscopy confirmed the fact that the HMW fraction contains largely diol-PEG. The resolution of the OH signal was very much dependent on the pH of the solution from which the sample was freeze dried prior to dissolving it in  $\text{DMSO-d}_6$ . Adjusting the pH of the solutions from a pH of around 5.5 to a pH of 6.0 improved the appearance of the OH peak dramatically. The calculated percentages of PEG determined by  $^1\text{H}$  NMR spectroscopy correspond very well to the GPC results for the original preparation and the LMW fraction from the first purification. However, the standard deviation of the data are relatively high. In the case of the low-diol M-PEG from the second purification step (LMW2) the percentage of PEG was zero in contrast to the 4.4% detected by GPC. The analysis of a commercial low-diol M-PEG 5000 from Union Carbide showed a similar discrepancy between  $^1\text{H}$  NMR spectroscopy and GPC. Thus, a contamination of less than 4.4% PEG in M-PEG 5000 cannot be detected by  $^1\text{H}$  NMR spectroscopy. The molecular masses of the original M-PEG, the LMW fractions (LMW and LMW2) and low-diol M-PEG 5000 from Union Carbide are in good accordance to the GPC data. The relatively high standard deviations were not unexpected as similar findings had been reported by Dust *et al.* [9] for PEG samples with molecular masses around 5000. For the HMW fraction (with a molecular mass of *ca.* 10 000 as estimated by GPC)  $^1\text{H}$  NMR spectroscopy could not be used to estimate the molecular mass and the PEG content because the signals for the end groups were marginal in comparison to the backbone signal as well as to the  $^{13}\text{C}$  carbon satellite signal. Especially the signal for the hydroxyl end groups was negligible although the pH was adjusted to 6.0 as for the other samples. The basis for this observation still remains unclear.

## CONCLUSIONS

GPC on Superose 12 in combination with the detection method of Childs is a good method to analyse the purity and molecular mass distribution of M-PEG preparations. In its accuracy and reliability it is superior to  $^1\text{H}$  NMR spectroscopy especially in the high-molecular-mass range above 5000. Vesicle chromatography is very useful for preparative fractionation applying high sample concentrations, *e.g.* for the removal of an excess of polymer from the reaction mixture of a protein modification process. However, a material with the appropriate separation limit for every particular fractionation problem has to be selected. It was already shown that the cut-off limit of vesicular packing material can be increased by depolymerisation of the polysaccharides in the cell wall [11]. The degree of enlargement is determined by the specific conditions of treatment (pH, temperature, time), as a result a variety of material with different separation limit ( $\geq 5.4$  nm) is available. For smaller separation limits other types of plant cell material have to be found.

## ACKNOWLEDGEMENTS

We thank Mrs Jane Hawkes and Mr Jonathan Cobb of ULIRS, Kings College, London, UK for providing the  $^1\text{H}$  NMR spectra and for their advice. B.S. is supported by the German Academic Exchange Service.

## REFERENCES

- 1 C. Delgado, G.E. Francis and D. Fisher, in S. D. Bruck (Editor), *Critical Reviews in Therapeutic Drug Carrier Systems*, 9 (3.4), CRC Press, Boca Raton, FL, 1992, pp. 249–304.
- 2 J.M. Harris and M. Yalpani, in H. Walter, D.E. Brooks and D. Fisher (Editors), *Partitioning in Aqueous Two-Phase Systems*, Academic Press, Orlando, FL, 1985, Ch. 16, p. 593.
- 3 R. Ehwald, G. Fuhr, M. Olbrich, H. Göring, R. Knösche and R. Kleine, *Chromatographia*, 28 (1989) 561–564.
- 4 A. Jäschke, D. Cech and R. Ehwald, *J. Chromatogr.*, 585 (1991) 57–65.
- 5 R. Kleine, H. Woehlecke and R. Ehwald, *Acta Biotechnol.*, 12 (1992) 87–98.

- 6 A.R. Cooper, in J.V. Dawkins (Editor), *Developments in Polymer Characterisation* —5, Elsevier, London, 1986, Ch. 4, pp. 131–173,
- 7 C.Y. Kuo and T. Provder, in T. Provder (Editor), *Detection and Data Analysis in Size Exclusion Chromatography* (ACS Symposium Series, No. 352), American Chemical Society, Washington, DC, 1987, Ch. 1, pp. 2–28.
- 8 R. de Vos and E.J. Goethals, *Polymer Bull.*, 15 (1986) 547–549.
- 9 J.M. Dust, Z. Fang and J.M. Harris, *Macromolecules*, 23 (1990) 3742–3746.
- 10 C. Delgado, J.N. Patel, G.E. Francis and D. Fisher, *Biotechnol. Appl. Biochem.*, 12 (1990) 119–128.
- 11 R. Ehwald, H. Woehlecke and C. Titel, *Phytochemistry*, 31 (1992) 3033–3038.
- 12 R. Ehwald, P. Heese and U. Klein, *J. Chromatogr.*, 542 (1991) 239–245.
- 13 C.E. Childs, *Microchem. J.*, 20 (1975) 190–192.
- 14 L. Hagel, in P.L. Dubin (Editor), *Aqueous Size Exclusion Chromatography* (Journal of Chromatography Library, Vol. 40), Elsevier, Amsterdam, 1988, Ch. 5, p. 141.
- 15 S. Mori, *J. Appl. Polym. Sci.*, 21 (1977) 1921–1932.
- 16 S. Mori, in P.L. Dubin (Editor), *Aqueous Size Exclusion Chromatography* (Journal of Chromatography Library, Vol. 40), Elsevier, Amsterdam, 1988, Ch. 7, p. 183.
- 17 J.C. Moore, *Sep. Sci.*, 5 (1970) 723–730.
- 18 A.C. Ouano, *J. Polym. Sci. A-1*, 9 (1971) 2179–2192.
- 19 F. Tjerneld and G. Johansson, *Bioseparation*, 1 (1990) 255–263.
- 20 A.G. Ogston and P. Silpananta, *Biochem. J.*, 116 (1970) 171–175.
- 21 P.-A. Albertsson, *Partition of Cell Particles and Macromolecules*, Wiley, Chichester, 1986.
- 22 H. Walter, D.E. Brooks and D. Fisher, *Partitioning in Aqueous Two-phase Systems*, Academic Press, Orlando, FL, 1985.
- 23 R. Murphy, A.C. Selden, M. Fisher, E.A. Fagan and V.S. Chadwick, *J. Chromatogr.*, 211 (1981) 160–165.
- 24 S. van der Wal and L.R. Snyder, *J. Chromatogr.*, 255 (1983) 463–474.
- 25 T. Takeushi and D. Ishii, *J. Chromatogr.*, 403 (1987) 324–330.



# Phytoecdysteroid analysis by high-performance liquid chromatography–thermospray mass spectrometry

Maria-Pilar Marco, Francisco J. Sánchez-Baeza\*, Francisco Camps and José Coll

*Department of Biological Organic Chemistry CID-CSIC, J. Girona Salgado 18–26, Barcelona 08034 (Spain)*

(First received December 1st, 1992; revised manuscript received March 3rd, 1993)

---

## ABSTRACT

The potential of high-performance liquid chromatography–mass spectrometry with thermospray interface to identify and analyse ecdysteroids has been investigated. The response of eight different ecdysteroids and their acetonide derivatives is studied by positive- and negative-ion detection as well as with single-ion monitoring and scan mass detection modes. The usefulness of this technique for ecdysteroid identification and quantitation is discussed and, finally, the identification of a new phytoecdysteroid isolated from *Polypodium vulgare* is presented as an application of this technology. A fast and easy procedure for the extraction and purification of phytoecdysteroids is also described.

---

## INTRODUCTION

Ecdysteroids are a family of compounds structurally related to the insect moulting hormones, ecdysone and 20-hydroxyecdysone. Briefly, they are highly hydroxylated  $5\beta$  steroids with a 7-en-6-one group and are widely distributed in plants, insects and other Arthropod families as well as in other invertebrates [1]. In insects, they act as a signal to start the moulting process at the cellular level, but the whole regulation system, biosynthesis and transport are not well defined. More than 100 different ecdysteroids also have been isolated from plants (phytoecdysteroids) [2–4]. Although it is supposed that phytoecdysteroids could be a part of an integrated plant defence against insects, it is not clear if this is their only role [5]. On the other hand, it has been shown that ecdysteroids are able to participate in mammal biological processes [6] with a very low

toxicity rate, which make these compounds interesting targets in the medical research field.

For several years, our group has been working with plant natural products, and recently we focused our attention on ecdysteroids. We are interested in compounds with anti-ecdysone activity in insects as well as in increasing ecdysteroid production in modified plants [7]. One of the main problems in ecdysteroid research is related to analysis owing to their presence in low amount in biological materials, their chromatographic behaviour (low number of theoretical plates per m of column) and their similar physical and chemical properties [8]. In order to resolve this problem we enhanced HPLC performance using 2-propanol–water as eluent at a temperature of 40–55°C [9], and later our objective was to improve the ecdysteroid identification techniques.

An ideal analytical method should be easy to implement, fast and sensitive. Mass spectrometry can approach that goal, especially when coupled with chromatographic methods. GC–MS is a well-known and easy technique, but previous reports in this field discouraged its use [10]. An

---

\* Corresponding author.

easy and attractive idea is the combination TLC–fast atom bombardment MS [11], but TLC lacks the necessary resolution. On the other hand, we considered that HPLC–MS could combine the resolution and the specificity of these two techniques. For this purpose we have used a thermospray interface, which is one of the most widely known, because of its high sensitivity and good results in fragmentation of steroids [12] and other polar compounds. In this paper, we describe the application of HPLC–thermospray (TSP) MS to the identification and quantification of ecdysteroids.

## MATERIALS AND METHODS

### HPLC

A Waters (Milford, MA, USA) system with two 510 pumps, a 680 gradient controller, a Rheodyne 7125 injector (Cotati, CA, USA) and a lambda 530 UV detector was used. The HPLC column, Spheri-5-RP-18, 25 × 0.47 cm I.D., 5 μm particle size, was purchased from Brown-Lee Labs. (Sunnyvale, CA, USA).

### MS system

A Model 5988A mass spectrometer with a thermospray probe and a Model 35741B data acquisition and treatment from Hewlett-Packard (Palo Alto, CA, USA) was used.

### Chemicals and solvents

In all cases HPLC-grade solvents were used. Ammonium acetate and formate were obtained from Carlo Erba (Milan, Italy). All other reagents were obtained from usual vendors and used without further purification.

### Phytoecdysteroid isolation

Samples, usually 50 mg, of lyophilized vegetable material were homogenized in a Braun Potter S homogenizer (Melsungen, Germany) for 1 min at 1100 rpm with 2 × 5 ml of methanol and 2 × 5 ml of methanol–water (7:3). The combined extracts were washed with hexane, 2 × 10 ml, centrifuged and the methanol phase was evaporated under vacuum. The residue was redissolved in 3 ml of methanol–water (1:9) and poured into a preconditioned C<sub>18</sub> Sep-Pak car-

tridge (Millipore, Milford, MA, USA). The pure ecdysteroid fraction was obtained after washing the cartridge with 10 ml of methanol–water (1:4) and eluting them with 10 ml of methanol–water (7:3).

### Acetonide preparation

*Standard ecdysteroids.* Pure ecdysteroids (10 mg) were dissolved in 1 ml of 2,2-dimethoxypropane containing 0.5 mg of anhydrous *p*-toluenesulphonic acid. After 10 min, 1 ml of 5% aqueous sodium hydrogencarbonate was added and the mixture extracted with chloroform (3 × 1 ml). The combined organic extracts were washed with water (2 × 1 ml), evaporated with nitrogen and dried under vacuum. The acetonides were stored at –20°C in a dry box filled with argon and dissolved immediately before their use. All acetonides were fully characterized by spectroscopic techniques.

*Phytoecdysteroids.* A 2-ml volume of the above methanol–water (7:3) eluate was evaporated to dryness (content in ecdysteroids between 100 and 5 μg depending on the plant source) and treated as above.

### HPLC–TSP–MS conditions

The optimum temperature conditions were as follows: ion source 280°C, vapour 250°C, tip 190°C and steam 108°C. In all cases “filament on” ionization mode (ionization by an electron beam) was selected. The ecdysteroid acetonides were eluted with acetonitrile–buffer (7:3) at 1.4 ml/min with a mass scan range of 300–700 u and free ecdysteroids with 2-propanol–buffer (11:89) at 1 ml/min with 200–600 u scanning. The buffer was 0.2 M in ammonium acetate or formate.

## RESULTS AND DISCUSSION

To test the usefulness of HPLC–TSP–MS in ecdysteroids analyses we used a set of eight common ecdysteroids (see Fig. 1 for structures) previously isolated and fully characterized (IR, NMR, MS) in our laboratory. HPLC conditions were those we reported previously [9], with the exception that the chromatography was carried

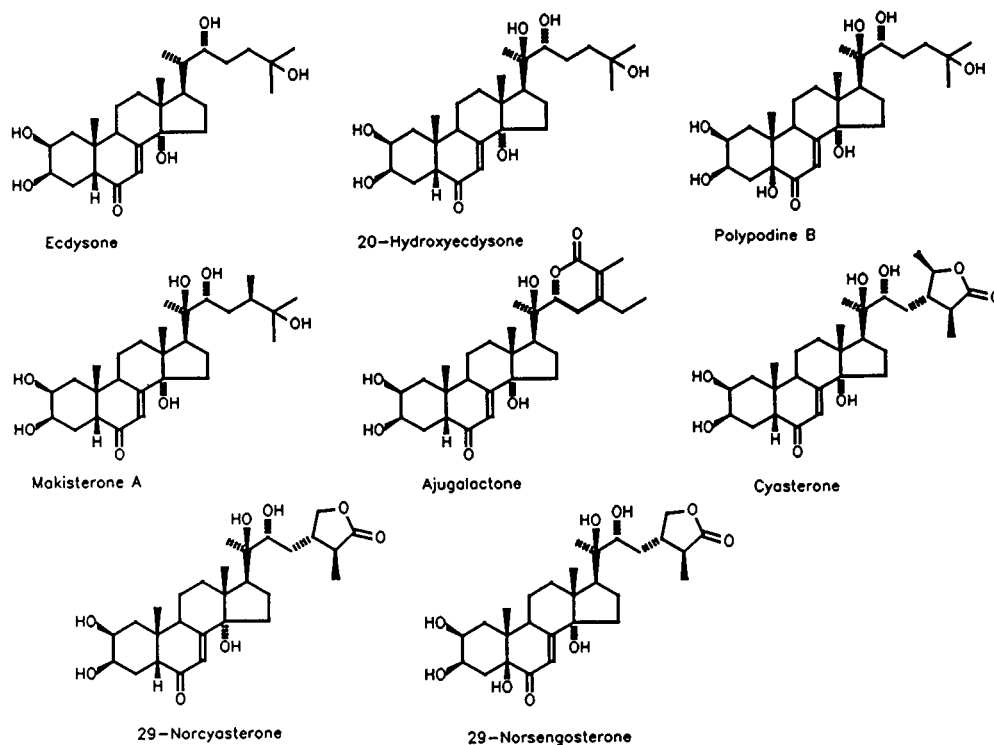


Fig. 1. Structures of the eight standard ecdysteroids used in this work: ecdysone (E), 20-hydroxyecdysone (20E), polypodine B (PB), makisterone (MK), ajugalactone (AJ), cyasterone (C), norcysterone (NC) and norsengosterone (NS).

out at room temperature, and with buffer added to the eluent. The electrolyte presence causes only a slight decrease in the column efficiency (about 5%) when compared with our previous conditions.

The main fragmentation of ecdysteroids in HPLC-TSP-MS conforms to a common pattern

(giving the most important fragments) with a secondary one derived from each peculiar structure (see Fig. 2 and Table I). MS spectra obtained resemble chemical ionization (CI) spectra, giving high intensity of high-mass fragments, especially those derived from electrolyte adduct  $[M+H]^+$  and its dehydration ions (only in

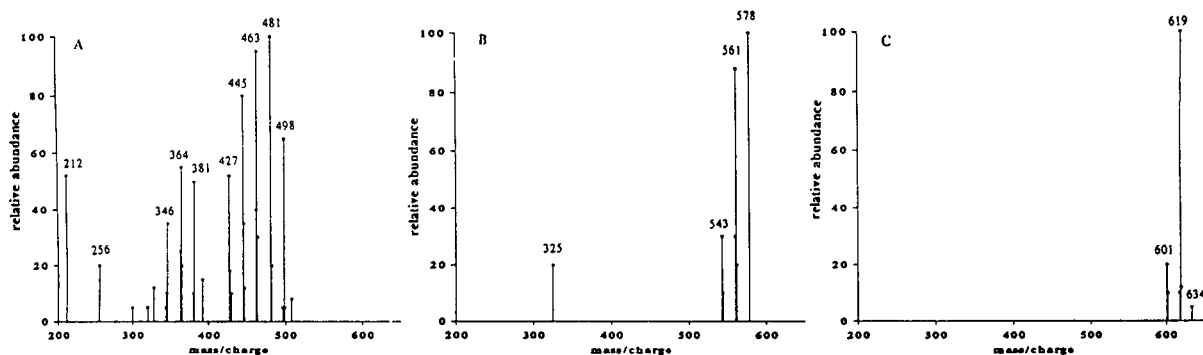


Fig. 2. Fragmentation patterns, in direct flow injection for (A) 25  $\mu$ g of 20E, positive-ion detection mode, eluent 2-propanol-buffer (11:89), 1 ml/min; (B) 50 ng of 20E diacetone, positive-ion detection, eluent acetonitrile-buffer (70:30), 1.3 ml/min and (C) 50 ng of 20E diacetone, negative-ion detection, the same eluent as B. Buffer ammonium acetate 0.2 M.



TABLE I

MAIN COMMON FRAGMENTATION PATTERNS OF ECDYSTEROIDS AS A FUNCTION OF THE DETECTION MODE AND THE ECDYSTEROID FORM

Ecdysteroid	Fragment list
Free ecdysteroid, positive ions	$[M + NH_4]^+$ , $[M + H]^+$ , $[M + H - H_2O]^+$ , $[M + H - 2H_2O]^+$ , $[M + H - 3H_2O]^+$ , $[M + H - [C20 - C22]]^+$ (side chain, SC, cleavage between C-20 and C-22), $[M + 2H - SC - H_2O]^+$ , $[M + H - SC - 2H_2O]^+$
Acetonides, positive ions	$[M + NH_4]^+$ , $[M + H]^+$ , $[M + H - H_2O]^+$
Acetonides, negative ions	$[M + HCOO]^-$ or $CH_3COO^-$ (electrolyte anion)

positive ion detection). In this work we also establish the sensitivity level of detection of ecdysteroids with this methodology and test it with pure ecdysteroid mixtures and with vegetable samples.

Using this technique, free ecdysteroids exhibit complex fragmentation patterns, which are advantageous for identification purposes, however this implies a reduction in the sensitivity with concomitant problems for quantification. To overcome this problem we decided to protect the glycol groups in the form of acetonides because the silyl ethers or acetate esters used as classical derivatives in GC-MS analysis are not stable enough under HPLC-TSP-MS conditions. We slightly modified one well-known acetonization procedure using anhydrous media and 2,2-dimethoxypropane as solvent. These changes led us to a very easy, fast and quantitative derivatization procedure that was highly efficient in all assayed cases. Likewise, to apply this procedure to real samples we optimized an easy and reproducible method for ecdysteroid extraction and purification that requires very little vegetable material. This method had been successfully used for quantitative ecdysteroid analysis of different tissue culture samples of *Polypodium vulgare*. The recovery is better than 94% for ecdysone (calculated from three replicates of the whole procedure with samples containing radio-labelled ecdysone). Subsequent to the isolation procedure, a Sep-Pak prepurification [13] was performed and, when it was needed, the acetonide derivatization was carried out as before.

For acetonide derivatives we could not find any appropriate chromatographic conditions to resolve completely the eight-ecdysteroid mixture, as we had accomplished for the free ecdysteroids [9]. With solvent mixtures containing methanol or isopropanol, the acetonides co-eluted in groups, according to the number of glycol groups in the molecule and the presence or absence of a hydroxyl group at carbon 5 (see Fig. 3). However, this characteristic and constant behaviour was also useful for us because, as we will explain below, it gave some structural information when we tried to identify a new ecdysteroid. The best performance was obtained with acetonitrile as organic modifier and, in this case, the electrolyte addition only decreased the capacity factor by only a small amount. It is important to note that chromatographic efficiency for separation of acetonides is much better than that of free ecdysteroids, thus considerably improving the sensitivity. This effect could be attributed to the change in the column efficiency  $N$  (theoretical plates per m), which, in the case of 20-hydroxyecdysone and its diacetonide, had the value of 15 200 and 27 600, respectively, very close to the average value of  $N$  in the set ecdysteroids or ecdysteroid acetonides studied (13 900 and 27 100).

The acetonide fragmentation in HPLC-TSP-MS was very low but gave enough structural information (working with positive ions, see Table I) to allow positive identification of known ecdysteroids with a sensitivity similar to classical UV, which could be increased working in single-ion monitoring (SIM) mode with detection of

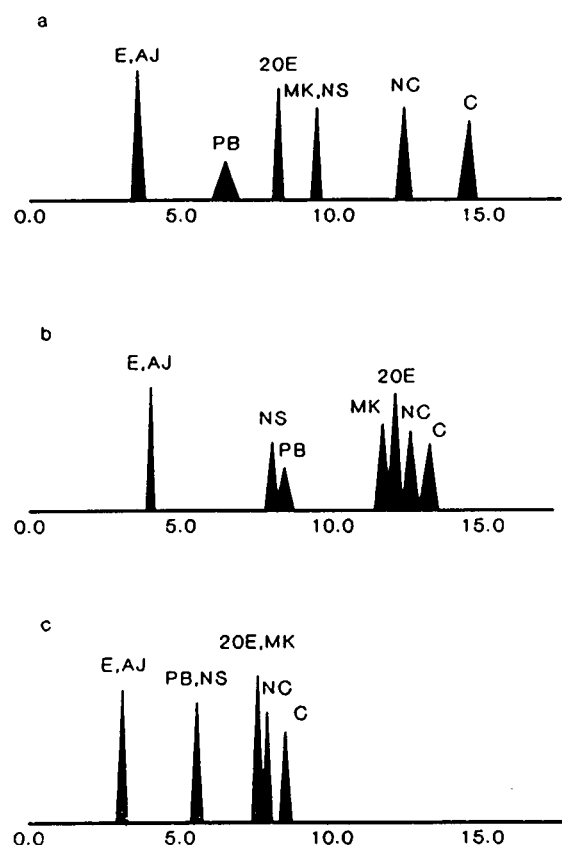


Fig. 3. HPLC elution profiles of ecdysteroid acetonides under several eluting systems. (a) acetonitrile–buffer (70:30), 1.3 ml/min; (b) methanol–buffer (75:25), 1.3 ml/min; and (c) 2-propanol–buffer (11:89), 1.0 ml/min. Buffer ammonium acetate 0.2 M; column RP-18, 25 × 0.47 cm I.D.

negative ions (see Table II). Previous reports using supercritical fluid chromatography–MS showed a sensitivity similar to that obtained by us with free ecdysteroids [14].

The second step in our work was to test the system performance when injecting a test mixture containing different amounts of the eight standard ecdysteroids working at different conditions (see Fig. 4). We obtained similar relative responses as when single pure ecdysteroid acetonides were injected. This was the first evidence that HPLC–TSP–MS could be a good ecdysteroid analytical method for quantification and identification.

Finally, we used HPLC–TSP–MS to analyse the ecdysteroid content (see Fig. 5) of the fern *Polypodium vulgare*. Since we began working with this fern, the existence of other ecdysteroids in this plant, in addition to those previously described (ecdysone, 20-hydroxyecdysone and polypodine B), was supported by the appearance of other small peaks during quantitative analysis by HPLC–UV of the isolated ecdysteroid fraction. Finally, with the optimization of this analytical technique we found that, for one of these minor compounds, the fragmentation pattern in positive- and negative-ion mode was similar to the behaviour of the standard ecdysteroid acetonides. The main fragments for this compound (617 and 634 in positive and 661 in negative), as well as its chromatographic

TABLE II

EXPERIMENTAL HPLC–TSP–MS SENSITIVITY OF THE EIGHT STANDARD ECDYSTEROIDS EXPRESSED AS AMOUNT OF COMPOUND NEEDED FOR A SIGNAL-TO-NOISE RATIO OF 5:1 AS A FUNCTION OF ECDYSTEROID FORM AND ION MONITORING MODE

PI = Positive-ion mode; NI = negative-ion mode

Ecdysteroid	Free scan, PI (μg)	Acetonide scan, PI (ng)	Acetonide scan, NI (ng)	Acetonide SIM, NI (ng)
E	7	50	25	3
20E	5	20	8	1
PB	18	100	50	6
MK	6	50	30	3
AJ	7	50	20	2
C	12	80	30	4
NC	8	70	30	3

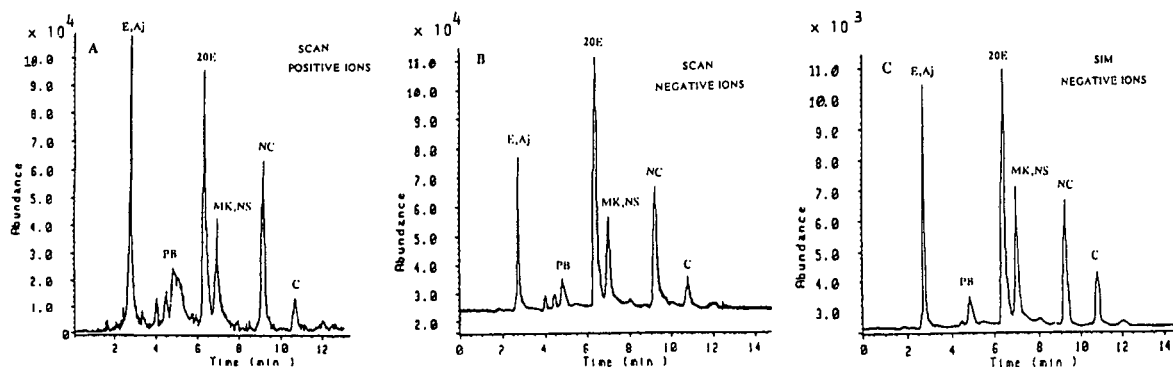


Fig. 4. HPLC–TSP–MS chromatogram of a mixture of standard ecdysteroid acetonides in acetonitrile–ammonium formate 0.2 M buffer (70:30), 1.8 ml/min (AJ 0.2  $\mu$ g, E 0.2  $\mu$ g, PB 0.1  $\mu$ g, 20E 0.3  $\mu$ g, MK 0.1  $\mu$ g, NS 0.1  $\mu$ g, NC 0.3  $\mu$ g and C 0.1  $\mu$ g; in SIM mode ten-fold less) in scan mode monitoring: (A) positive and (B) negative ions; and (C) SIM mode monitoring simultaneously the following negative ions ( $m/z$  549, 601, 605, 619, 621, 631, 645, 647 u).

behaviour (long retention time), indicates a structure such as the triacetonide of the 20,26-dihydroxyecdysone (see Fig. 5). Prior to derivatization this compound exhibited higher polarity than the other ecdysteroids in the mixture. Later, by isolating larger amounts of this compound, its structure was completely confirmed by spectroscopic techniques (IR,  $^1\text{H-NMR}$  and  $^{13}\text{C-NMR}$ ).

## CONCLUSIONS

The results of this work show that HPLC–TSP–MS is a useful analytical tool in the

ecdysteroid field. Working with free ecdysteroids it is possible to obtain enough structural information, but the sensitivity is very low compared with UV detection. When acetonide derivatives were used the sensitivity increased, with the additional advantage of giving complementary structural information, especially when positive- and negative-ion detection are used sequentially. For quantitation, the method requires internal standard calibration (preferably another ecdysteroid) because of the large response variations of the HPLC–TSP–MS system and negative-ion detection. This technique could be the first choice in the research of new ecdysteroids of plant or insect origin.

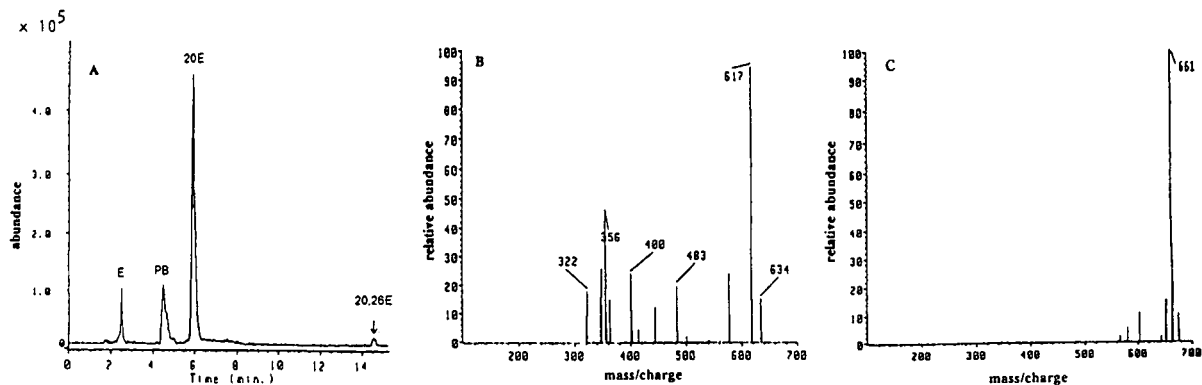


Fig. 5. HPLC–TSP–MS of a sample of *Polydodium vulgare*, one-fifth fraction of purified extract from 50 mg of starting plant, derivatized and diluted to 100  $\mu$ l. (A) Total ion current of 25  $\mu$ l of the above sample eluted with acetonitrile–ammonium formate 0.2 M buffer (70:30), 1.8 ml/min in positive scan mode. (B and C) Fragmentograms obtained in positive- and negative-ion detection modes for the peak at 16.2 min, assigned as 20,26-dihydroxyecdysone.

## REFERENCES

- 1 J.A. Hoffman, *Insect. Biochem.*, 16 (1986) 1.
- 2 F. Camps, in J.B. Harborne and F.A. Tomas Barberán (Editors), *Ecological Chemistry and Biochemistry of Plant Terpenoids*, Clarendon Press, Oxford, 1991, p. 331.
- 3 D.H.S. Horn and R. Bergamasco, in G.A. Kerkut and L.I. Gilbert (Editors), *Comprehensive Insect Physiology, Biochemistry and Pharmacology*, Vol. 7, Pergamon Press, Oxford, 1985, Ch. 2, p. 186.
- 4 R. Bergamasco and D.H.S. Horn, in R.G.H. Downer and H. Laufer (Editors), *Insect Endocrinology*, Alan R. Liss, Inc. New York, 1983, p. 627.
- 5 R. Lafont and D.H.S. Horn, in J.A. Koolman (Editor), *Ecdysone*, Georg Thieme, Stuttgart, 1989, p. 39.
- 6 V.N. Syrov, *Farmakol. Toksikol.*, 49 (1986) 100.
- 7 F. Camps, E. Claveria, J. Coll, M.-P. Marco, J. Messeguer and E. Mele, *Phytochemistry*, 29 (1990) 3819.
- 8 E.D. Morgan and M.P. Marco, *Invertebr. Reprod. Dev.*, 18 (1990) 55.
- 9 F. Camps, J. Coll, M.P. Marco and J. Tomas, *J. Chromatogr.*, 514 (1990) 199.
- 10 R.P. Evershed, J.G. Mercer and H.H. Rees, *J. Chromatogr.*, 390 (1987) 357.
- 11 I.D. Wilson, R. Lafont and P. Wall, *J. Planar Chromatogr.*, 1 (1988) 357.
- 12 D.J. Liberato, A.L. Yergey, N.V. Esteban, C.E. Gomez-Sanchez and C.H.L. Shackleton, *J. Steroid Biochem.*, 27 (1987) 61.
- 13 M. Cleator, C.J. Delves, R.E. Howells and H.H. Rees, *Mol. Biochem. Parasitol.*, 25 (1987) 93.
- 14 M.W. Raynor, J.P. Kithinji, K.D. Bartle, D.E. Games, I.C. Mylchreest, R. Lafont, E.D. Morgan and I.D. Wilson, *J. Chromatogr.*, 467 (1989) 292.



# Trace determination of weathered atrazine and terbuthylazine and their degradation products in soil by high-performance liquid chromatography–diode-array detection

R. Schewes\*, F.X. Maidl and G. Fischbeck

*Lehrstuhl für Pflanzenbau und -züchtung, W-8050 Freising-Weihenstephan (Germany)*

J. Lepschy von Gleissenthall and A. Süss

*Bayerische Landesanstalt für Bodenkultur und Pflanzenbau, W-8050 Freising (Germany)*

(First received August 14th, 1992; revised manuscript received March 10th, 1993)

---

## ABSTRACT

It is important to optimize extraction, clean-up and determination of weathered pesticide residues in order to predict their fate in the unsaturated soil zone. A method including hot extraction with acetone, clean-up with solid-phase extraction (cation exchanger) and HPLC–diode-array detection for atrazine and terbuthylazine and their chlorinated and hydroxylated metabolites at relatively low levels, less than 5 µg per kg of soil, is presented.

---

## INTRODUCTION

Application of the pesticide atrazine (2-chloro-4-ethylamino - 6 - isopropylamino - 1,3,5-triazine) can cause pollution of drinking water by the compound in its unmetabolized form or its breakdown product, exceeding the EEC limit of 0.1 µg/l per substance and resulting eventually in an undesirable accumulation of phytotoxic residues in soil. The same potentially applies to terbuthylazine (2-chloro-4-ethylamino-6-butylamino-1,3,5-triazine), an atrazine substitute. It is important to optimize the extraction and clean-up of weathered pesticide residues in order to predict their fate in the environment, especially if one seeks to explain their movement in the unsaturated soil zone. A review of solvent ex-

traction systems for weathered herbicide residues has been reported [1]. The soil extracts are usually subjected to a liquid–liquid partition step before they are cleaned up further by gel permeation chromatography (GPC). The liquid–liquid partition step often results in the formation of emulsions, which render phase separation difficult and cause losses of substance. Frequently, components of soil extracts interfere with compound identification. The application of solid-phase extraction (SPE) offers advantages such as reduced solvent consumption and fewer interferences compared with clean-up with GPC [2].

Gas chromatography (GC) is a common method for the determination of atrazine and its non-polar degradation products with high sensitivity and good separation efficiency. A disadvantage of GC is that it is limited to volatile chlorotriazines. The hydroxy derivatives cannot

---

\* Corresponding author.

be analysed without derivatization. However, in order to determine total atrazine residues in soil, the polar degradation products have to be included. High-performance liquid chromatography (HPLC) is directly applicable to *s*-triazines and their degradation products.

This paper will describe a method for the extraction, clean-up and determination of atrazine and terbuthylazine and their chlorinated and hydroxylated metabolites at relatively low levels, less than 5  $\mu\text{g}$  per kg of soil.

## EXPERIMENTAL

### *Soil sampling*

Aiming for representative soil samples, 25 single cores per sampling site were mixed. Characteristic soil parameters of the sampled site were 19% clay, 1.2% organic carbon and pH 6.0. In order to obtain weathered residues, sampling was conducted 1 year after spraying. A hydraulically driven, tractor-mounted drilling device (Fritzmeyer, Grosshelfendorf, Germany) was used for time-efficient and easy sampling down to a depth of 90 cm.

### *Sample preparation*

The complete samples, each around 4 kg of soil, were sieved in the field with a 1-cm screen and transported to the laboratory in aluminium trays. The samples were air dried, homogenized with a mixer and ground with a rotor-disc mill.

### *Reagents*

Atrazine, terbuthylazine and their metabolites were obtained from Ehrenstorfer (Augsburg, Germany). All organic solvents used were of HPLC grade (Labskan, Dublin, Ireland) and used as received.

### *Extraction*

Subsamples of 50 g were extracted with 250 ml of acetone, methanol and a mixture of methanol–water (8:2) in a hot extractor for 2 h, then the volume of the soil extracts was reduced with a Turbovap evaporation workstation (Zymark, Hopkinton, MA, USA) at 40°C water bath temperature. The evaporation was stopped at a volume of around 2 ml.

### *Clean-up with solid-phase extraction (SPE)*

A 0.1-ml aliquot of 10  $\mu\text{g}/\text{ml}$  propazine was used as internal standard and acetone was added to a final volume of 5 ml. The clean-up was performed by a sulphonic acid-type silica gel-based cation exchanger (SCX) from Supelco (Bellefonte, PA, USA). The solutions were passed through the 3-ml tubes by using a vacuum manifold (Analytichem, Harbor City, CA, USA). Four samples were cleaned up simultaneously. Before use, the mini-columns were activated with 4 ml of 0.12 *M* hydrochloric acid in methanol at a flow-rate of 0.8 ml/min, followed by 3 ml of methanol and 3 ml of acetone. A 3-ml volume of soil extract was added. Unwanted, weakly retained material was removed by washing the packing with 2 ml of acetone. Atrazine, terbuthylazine and metabolites were eluted with 2.5 ml of potassium chloride-saturated methanol. A 200- $\mu\text{l}$  aliquot of methanolic solution of ammonia (0.1 mol/l) was added to this solution to neutralize the acidity. Methanol was removed with a vacuum rotary evaporator (Heidolph, Kelheim, Germany) at 40°C and the residue was reconstituted with 1 ml of mobile phase acetonitrile–water (1:9) for RP-HPLC.

### *Clean-up with gel permeation chromatography (GPC)*

The soil extract was evaporated to 0.1 ml and ethyl acetate–cyclohexane (1:1) was added to a final volume of 5 ml. Eluent delivery (ethyl acetate–cyclohexane, 1:1) at 4 ml/min was provided by a Model FR-30 high-pressure pump (Knauer, Homburg, Germany). Sample volumes of 3 ml were injected via a 5-ml sample loop of a Rheodyne valve (Cotati, CA, USA). A glass column (450 mm  $\times$  30 mm), packed with Bio-Beads SX-3, mesh size 200–400 (Bio-Rad Labs., Richmond, CA, USA), was used.

### *HPLC apparatus*

A Gynkotek (Germering, Germany) M 480 gradient pump, fitted with a Gilson-Abimed (Langenfeld, Germany) Model 231 sample injector, injection volume 100  $\mu\text{l}$ , and a Hewlett-Packard (Palo Alto, CA, USA) diode-array detector, 1040 M 50 Series II, detection wavelength 220 nm, was employed. A Hypersil ODS

column (250 × 4 mm I.D., 5 μm) together with a precolumn from Grom (Herrenberg, Germany) was used. The gradient programme was from 10 to 60% acetonitrile in 50 min; water was buffered with ammonium acetate at pH 6.8 and column temperature was kept at 40°C with a column oven (Gynkotek).

## RESULTS AND DISCUSSION

### Extraction

The search for a standard extraction method for weathered pesticide residues in soil has been continuous. There is growing evidence that time-dependent non-equilibrium sorption processes can render some analytes more resistant to extraction [3,4]. Therefore recovery values from weathered field samples could be lower than those predicted on the basis of a freshly added spike.

Numerous authors [1,4–6] have compared the efficiency and simplicity of various methods, which are typically shaking, refluxing or sonicating at various temperatures with methanol, acetonitrile, dichloromethane or Soxhlet extractions for 2–24 h. Cotterill [5] reported that shaking with methanol with a water content of 20% is more efficient for the extraction of simazine than other solvent systems based on acetonitrile or chloroform. Mattson *et al.* [4] obtained similar recoveries of triazine herbicides

from soil either by using an aqueous methanol (10% water) Soxhlet extraction for 24 h or by refluxing with aqueous acetonitrile (10% water) for 1 h. He concluded that water as one of the components of the extracting system appears to be essential. Huang and Pignatello [6] obtained maximum yields of weathered atrazine soil samples by batch extraction at 75°C for 2–16 h with methanol–water (8:2).

Experiments in our laboratory showed, contrary to the results described above, that hot extraction with methanol–water (8:2) provides the lowest efficiency and the highest coefficient of variation, whereas acetone or methanol yields higher and more reproducible values. With the exception of soil II and the comparison of acetone and methanol, the *t*-test indicated statistically significant differences between the three extraction solvents (Table I). When acetone is used as extraction and clean-up solvent, there is no need to evaporate the soil extract to dryness and therefore one means of losing the analyte is obviated.

### Clean-up

We aimed to find a clean-up procedure that results in high recovery values not only for the chlorotriazines but also for the hydroxy derivatives, which are supposed to be important metabolites in soil.

We applied GPC to soil extracts and standards

TABLE I

EFFICIENCY OF HOT EXTRACTION WITH ACETONE, METHANOL AND METHANOL–WATER (8:2)

Values are atrazine concentration (μg/kg) extracted with the indicated extraction solvent and temperature. A = Acetone; M = methanol; M/W = methanol–water.

	Soil I			Soil II			Soil III		
	A, 55°C	M, 63°C	M/W, 66°C	A, 55°C	M, 63°C	M/W, 66°C	A, 55°C	M, 63°C	M/W, 66°C
Extraction 1	12	7	3	68	55	41	148	143	124
Extraction 2	12	5	4	61	64	48	148	147	98
Extraction 3	12	5	4	63	61	28	149	145	138
Mean	12	6	4	64	60	40	148	145	120
S.D.	0.3	1.1	0.6	3.1	3.9	8.6	1.0	3.2	17.1
R.S.D. (%)	3	19	16	5	7	22	1	2	14.3



containing triazines, but this resulted in a complete loss of hydroxy derivatives. We attributed this loss to solubility problems of the hydroxy derivatives in the mobile phase (cyclohexane-ethyl acetate) and/or to a low elution strength of the mobile phase.

Gordon [7] stated that, under strictly anhydrous conditions, very weakly basic compounds are adsorbed on a strong acid exchanger via salt formation. Battista *et al.* [8] reported the successful use of SPE for the isolation of eight triazines from soil extracts. We aimed to use the same type of column, but for the parent compounds and their degradation products. Our experiments confirmed that only 1% water in acetone resulted in a considerable loss of triazines (Table II). Recovery experiments with standard solutions and the use of the internal standard propazine assure the necessary quality of acetone. The analytical recovery of the complete method (extraction with acetone and SPE) was assessed by extracting freshly spiked soil samples (Table III); the hydroxy derivatives in particular showed high recovery values.

#### Detection

Because of their wide  $k'$  range, triazine-containing samples cannot be easily handled by isocratic HPLC methods. Early-eluting peaks are poorly resolved, later peaks are very wide and exhibit tailing and the separation time is exces-

TABLE II

PERCENTAGE LOSS OF A 1 mg/l STANDARD OF DESETHYLATRAZINE (DEA), ATRAZINE (ATR) AND TERBUTHYLAZINE (TERB) DURING SPE, DEPENDING ON THE WATER CONTENT OF ACETONE

The values give the range of results of triplicate determinations at each level of water content.

Water content (%)	DEA (%)	ATR (%)	TERB (%)
<0.03	0	0	0
0.5	0	0–1	0–1
1	0–9	2–12	4–12
2	37–60	47–67	56–72
3	58–79	65–83	68–85

TABLE III

MEAN RECOVERIES OF TRIAZINES IN SPIKED (30  $\mu\text{g}/\text{kg}$ ) SOIL SAMPLES

Triazine	Recovery (%) <sup>a</sup>	R.S.D. (%)
Atrazine	86	4
Hydroxyatrazine	92	4
Desethylatrazine	87	5
Desisopropylatrazine	78	7
Terbuthylazine	88	4
Hydroxyterbuthylazine	90	4
Desethylterbuthylazine	85	6

<sup>a</sup> Mean values obtained from triplicate determinations.

sive. The  $k'$  values and therefore the separation of the *s*-triazines depend on the organic solvent content and pH and ionic strength of the mobile phase [9]. Acetonitrile–water was used instead of a methanol–water mobile phase because acetonitrile has advantages over methanol: lower operating pressure and applicability for detection in the very low UV range [10]. A major problem is the separation of desethylatrazine and hydroxyatrazine. *s*-Triazines are weak bases whose  $\text{p}K_a$  values range from 1.6 for chlorotriazines to about 5 for hydroxy derivatives [9,11]. The chlorotriazines are not protonated at pH values between 3 and 7, and thus their retention time is pH independent. The retention times of hydroxy derivatives increase with increasing pH, the change being largest within the  $\text{p}K_a$  region. In acidic mobile phases the peaks exhibit tailing, owing to *s*-triazine protonation [9]. A water phase containing 2 mmol/l ammonium acetate, pH 6.8, was selected as optimal as the peak separation is satisfying and does not vary over time. Furthermore, the use of a neutral mobile phase improves the peak symmetry. Vermeulen *et al.* [11] used a neutral but more concentrated (50 mmol/l) ammonium acetate mobile phase.

Fig. 1A shows a triazine standard of 30  $\mu\text{g}/\text{l}$ , which corresponds to 1  $\mu\text{g}/\text{kg}$  in soil. Usually the peak identification is done by comparing the absolute or relative retention times of the peaks in the sample with those in a standard solution. The diode-array detector records a predetermined spectral range during the analysis, and facilitates positive peak identification and peak

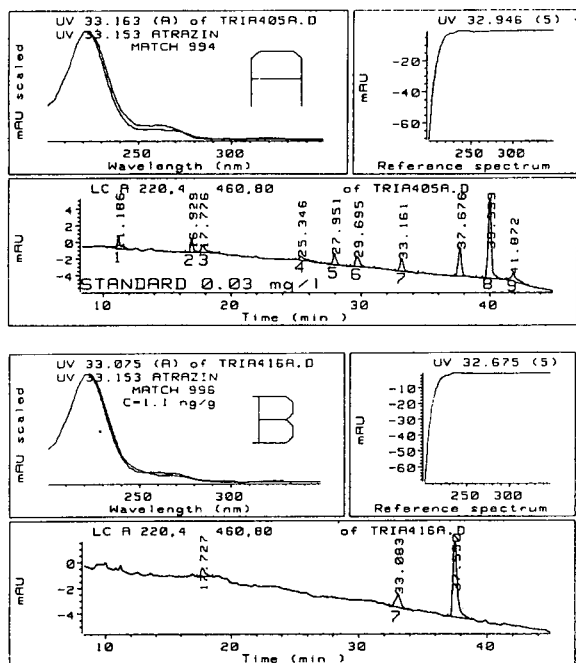


Fig. 1. HPLC chromatograms of (A) a triazine standard corresponding to 30  $\mu\text{g/l}$ , (B) a soil sample with an atrazine concentration of 1.1  $\mu\text{g/kg}$ . 1 = Desisopropylatrazine; 2 = desethylatrazine; 3 = hydroxyatrazine; 4 = hydroxyterbutylazine; 5 = desethylterbutylazine; 6 = atratone; 7 = atrazine; 8 = propazine; 9 = terbutylazine.

purity analysis. The spectra obtained are compared with those stored in a library. The chromatogram of a soil extract after clean-up with an

SCX column is shown in Fig. 1B. The atrazine peak corresponds to 1.1  $\mu\text{g}$  per kg of soil.

#### ACKNOWLEDGEMENT

We would like to thank the Volkswagen-Foundation, Hannover, Germany, for the financial support of this research project.

#### REFERENCES

- 1 A.E. Smith, *Int. J. Environ. Anal. Chem.*, 46 (1992) 111.
- 2 R. Brennecke, *Fresenius' J. Anal. Chem.*, 339 (1991) 399.
- 3 J.J. Pignatello, in B.L. Sawhney and K. Brown (Editors), *Reactions and Movement of Organic Chemicals in Soils (Special Publication, No. 22)*, Soil Science Society of America, Madison, 1989, Ch. 3, p. 345.
- 4 P.M. Mattson, R.A. Kahrs and R.T. Murphy, in F.A. Gunther and J.D. Gunther (Editors), *Residue Reviews*, Springer, New York, 1970, 371.
- 5 E.G. Cotterill, *Pestic. Sci.*, 11 (1980) 23.
- 6 L.Q. Huang and J.J. Pignatello, *J. Assoc. Off. Anal. Chem.*, 73 (1990) 443.
- 7 J.E. Gordon, *J. Chromatogr.*, 18 (1965) 542.
- 8 M. Battista, A. Di Corcia and M. Marchetti, *J. Chromatogr.*, 454 (1988) 233.
- 9 V. Pacakova, K. Stulik and M. Prihoda, *J. Chromatogr.*, 442 (1988) 147.
- 10 L.R. Snyder, J.G. Glajch and J.J. Kirkland, *Practical HPLC Method Development*, Wiley, New York, 1988.
- 11 N.M.J. Vermeulen, Z. Apostolides and D.J.J. Potgieter, *J. Chromatogr.*, 240 (1982) 247.



# Isolation and determination of AAL phytotoxins from corn cultures of the fungus *Alternaria alternata* f. sp. *lycopersici*

G.S. Shephard\*, P.G. Thiel, W.F.O. Marasas and E.W. Sydenham

Programme on Mycotoxins and Experimental Carcinogenesis, South African Medical Research Council, P.O. Box 19070, Tygerberg 7505 (South Africa)

R. Vleggaar

Department of Chemistry, University of Pretoria, Pretoria 0002 (South Africa)

(First received September 1st, 1992; revised manuscript received February 10th, 1993)

---

## ABSTRACT

The fungus *Alternaria alternata* f. sp. *lycopersici* produces a group of four related host-specific phytotoxins (AAL toxins) which can be divided into two groups (TA and TB), each of which exists as an equilibrium mixture of two structural isomers. The AAL toxins were isolated from corn cultures by aqueous extraction, followed by purification on Amberlite XAD-2 resin, separation of TA from TB on silica gel and final purification on a semi-preparative high-performance liquid chromatographic (HPLC) system. A rapid, sensitive and reproducible method was developed to determine these toxins in culture material in order to monitor toxin production on corn cultures. The method consisted of aqueous extraction, C<sub>18</sub> solid-phase extraction clean-up, precolumn derivatization with *o*-phthalaldehyde and reversed-phase HPLC with fluorescence detection. An isocratic HPLC system was developed that separated the structural isomers of TA and TB within a chromatographic analysis time of 24 min.

---

## INTRODUCTION

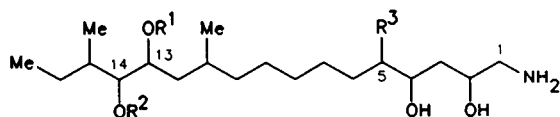
The fungus *Alternaria alternata* (Fr.) Keissler f. sp. *lycopersici* causes a stem canker disease in certain susceptible tomato cultivars [1]. The fungal growth occurs on the stem, where it produces dark brown to black cankers. Although the pathogen occurs only on the stem, it also causes interveinal necrosis of the leaves by the translocation of fungal toxins. The cause of the disease has been traced to the production of host-specific phytotoxins (AAL toxins) [2–4]. Cell-free culture filtrates yielded two ninhydrin-

positive fractions, TA and TB, each consisting of a mixture of two structural isomers [5]. Each fraction reproduced the disease symptoms on susceptible cultivars [2,3,6]. In addition, these same toxins have been extracted from necrotic leaves of tomato plants infected with *A. alternata* f. sp. *lycopersici* [2]. A recent report, utilizing a bioassay technique, presented evidence that these toxins can also be produced in very low yield by an isolate of *A. alternata* obtained from ripe tomatoes and previously considered to be non-pathogenic [7].

The AAL toxins have been shown to be esters of propane-1,2,3-tricarboxylic acid with either 1 - amino - 2,4,5,13,14 - pentahydroxy - 11,15 - dimethylheptadecane or the C-5 deoxy analogue [5] (Fig. 1). Their structural similarity to the

---

\* Corresponding author.



TA<sub>1</sub>:R<sup>1</sup> = CO-CH<sub>2</sub>-CH(CO<sub>2</sub>H)-CH<sub>2</sub>-CO<sub>2</sub>H,R<sup>2</sup> = H,R<sup>3</sup> = OH

TA<sub>2</sub>:R<sup>1</sup> = H,R<sup>2</sup> = CO-CH<sub>2</sub>-CH(CO<sub>2</sub>H)-CH<sub>2</sub>-CO<sub>2</sub>H,R<sup>3</sup> = OH

TB<sub>1</sub>:R<sup>1</sup> = CO-CH<sub>2</sub>-CH(CO<sub>2</sub>H)-CH<sub>2</sub>-CO<sub>2</sub>H,R<sup>2</sup> = H,R<sup>3</sup> = H

TB<sub>2</sub>:R<sup>1</sup> = H,R<sup>2</sup> = CO-CH<sub>2</sub>-CH(CO<sub>2</sub>H)-CH<sub>2</sub>-CO<sub>2</sub>H,R<sup>3</sup> = H

Fig. 1. Structures of the isomers of the AAL toxins.

recently described fumonisin mycotoxins [8] has renewed interest in these compounds. Both fumonisin B<sub>1</sub> and TA have similar phytotoxic properties [9,10]. In addition, fumonisins B<sub>1</sub> and B<sub>2</sub> and TA have recently been shown to be toxic to certain cultured mammalian cell lines [11].

Previously, the AAL toxins have been isolated from culture filtrates either by barium acetate precipitation, butanol extraction, gel filtration and semi-preparative thin-layer chromatography (TLC) [12] or by direct absorption and partitioning on C<sub>18</sub> reversed-phase columns and clean-up by gel filtration [13]. The toxins were analysed by high-performance liquid chromatography (HPLC) of their maleyl derivatives. Although these derivatives of TA and TB could be separated by isocratic HPLC, a binary gradient (60-min analysis time) was required for partial separation of the individual structural isomers of the toxins [12].

This paper reports the isolation of the AAL phytotoxins from corn cultures of *A. alternata* f. sp. *lycopersici* using aqueous extraction and purification on Amberlite XAD-2 resin and silica gel, followed by reversed-phase semi-preparative HPLC. In order to monitor toxin production in culture, a rapid, sensitive and reproducible HPLC method, similar to that used for the structurally similar fumonisins [14], was developed using precolumn *o*-phthalaldehyde (OPA) derivatization and fluorescence detection. Separation of all structural isomers was achieved in 24 min using isocratic conditions on a reversed-phase column.

## EXPERIMENTAL

### Materials

Amberlite XAD-2 and silica gel 60 (Kieselgel 60, 0.063–0.200 mm) were purchased from Merck (Darmstadt, Germany). Bond-Elut C<sub>18</sub> cartridges (3-ml capacity containing 500 mg of sorbent) were obtained from Analytichem International (Harbor City, CA, USA). A reversed-phase C<sub>18</sub> column packing used for desalting was prepared from silica gel 60 (0.063–0.200 mm) according to the method of Kingston and Gerhart [15]. All other reagents and solvents were of analytical-reagent grade from Merck.

### Fungal cultures

Lyophilized cultures of *A. alternata* f. sp. *lycopersici* MRC 6231 (As27-3p2), supplied by Professor D.G. Gilchrist (University of California, Davis, CA, USA), were used to inoculate autoclaved, ground, moistened yellow corn. The corn cultures were incubated in the dark at 25°C for 16 days, after which the material was dried (45°C, 24 h) and ground in a laboratory mill.

### Isolation of fungal toxins

A 500-g sample of culture material was extracted by blending with 1000 ml of chloroform-methanol (10:3, v/v). The mixture was filtered, washed with 300 ml of extraction solvent and dried under vacuum on the filter. Subsamples (30 g) of this dried culture material were further extracted three times in centrifuge bottles with 110 ml of water using a Polytron homogenizer (Kinematica, Lucerne, Switzerland). After each extraction, the homogenate was centrifuged (4000 g, 10 min, 4°C) and supernatants from all extractions were pooled, acidified to pH 2.7 with 2 M hydrochloric acid and then recentrifuged. The clear supernatant was applied to a column packed with Amberlite XAD-2 resin (35 × 3.0 cm I.D.) that had previously been washed with 500 ml of methanol and 500 ml of water. After application of the sample, the resin was washed with 100 ml of water and 400 ml of methanol-water (1:3, v/v) and the toxins were eluted with 400 ml of methanol, which was removed under vacuum on a rotary evaporator at 40°C.

The residue was dissolved in 20 ml of ethyl acetate–acetic acid–water (12:6:1, v/v/v) and applied to a column packed with silica gel 60 (50 × 3.0 cm I.D.). The column was eluted with the same solvent and 20-ml fractions were collected. The fractions were tested for the presence of TA or TB by TLC using precoated silica gel 60 plates (Merck) developed with ethyl acetate–acetic acid–water (6:3:1, v/v/v). An authentic standard of TA and TB (donated by Professor D.G. Gilchrist) was used to identify the AAL toxins. The toxins were revealed as purple spots by spraying with *p*-anisaldehyde reagent [8]. Fractions containing TA or TB were separately pooled and dried under vacuum at 40°C.

Both pooled fractions were separately dissolved in 12 ml of methanol–water (1:1, v/v) and individually purified in a semi-preparative isocratic HPLC system at room temperature using a Phenomenex (Rancho Palos Verdes, CA, USA) analytical column (250 × 4.6 mm I.D.) packed with Ultracarb 7- $\mu$ m ODS 30 reversed-phase (C<sub>18</sub>) material incorporated in an automated system consisting of a Waters (Milford, MA, USA) WISP autoinjector, Waters Model 590 programmable pump, Waters automated switching valve and Waters Lambda-Max variable-wavelength ultraviolet detector set at 215 nm. The mobile phase for the purification of TA was methanol–0.05 M sodium dihydrogenphosphate (47:53, v/v) adjusted with orthophosphoric acid to pH 3.4 and pumped at a flow-rate of 1.5 ml min<sup>-1</sup>. For purification of TB, the mobile phase was methanol–0.05 M sodium dihydrogenphosphate (53:47, v/v), also at pH 3.4. The autoinjector was programmed for repeated injections (100  $\mu$ l) of aliquots of the semi-purified toxin solution and the eluate fraction containing the AAL toxin was collected using the automated switching valve. Most of the methanol was removed on a rotary evaporator and the toxins were then recovered by passing the concentrate down a short column containing C<sub>18</sub> packing material (20 g). After washing the salt from the column with 150 ml of water, the toxin was eluted with 200 ml of methanol.

The NMR spectra were recorded for solutions

in [<sup>2</sup>H<sub>6</sub>]dimethyl sulphoxide on a Bruker AC-300 spectrometer operating at 7.0 T.

#### *Determination of TA and TB in corn culture*

A 5-g sample of culture material was blended with 50 ml of water using a Polytron homogenizer and then centrifuged at 2000 g for 10 min at 4°C. The supernatant was filtered, acidified to pH 2.9 with 2 M hydrochloric acid and then recentrifuged at 3000 g. A 2-ml aliquot of this supernatant was applied to a Bond-Elut C<sub>18</sub> solid-phase extraction cartridge that had been preconditioned by washing with 5 ml of methanol and 5 ml of water. The cartridge was washed with 8 ml of water, drained under vacuum and then eluted with 10 ml of methanol. The eluate was evaporated to dryness at 60°C in a stream of nitrogen and the residue dissolved in 2 ml of methanol, prior to derivatization and HPLC analysis.

#### *Chromatographic analysis*

The AAL toxins in the sample residue were determined by reversed-phase HPLC of preformed OPA derivatives. The OPA reagent was prepared by dissolving 40 mg of OPA in 1 ml of methanol followed by addition of 5 ml of 0.1 M sodium borate and 50  $\mu$ l of 2-mercaptoethanol. The reagent was stored in the dark for up to 1 week without deterioration. Derivatives were prepared by mixing a 50- $\mu$ l aliquot of purified sample extract with 200  $\mu$ l of OPA reagent.

The analytical HPLC system consisted of a Waters M-45 pump and U6K injector. The fluorimetric detector was a Perkin-Elmer (Norwalk, CT, USA) Model 650S with an 18- $\mu$ l flow cell. The excitation and emission wavelengths were 335 and 440 nm, respectively. Quantification was achieved by peak-area measurement using a Waters Model 745 data module. Chromatographic separation was achieved using either of two systems. One system, which separated the derivatives of TA and TB but not their structural isomers, consisted of a Phenomenex Ultracarb 7- $\mu$ m ODS 30 analytical column and a mobile phase of methanol–0.1 M sodium dihydrogenphosphate (75:25, v/v) with the pH adjusted to 3.4 with orthophosphoric acid and

pumped at a flow-rate of  $1 \text{ ml min}^{-1}$ . The other system, which separated the structural isomers, consisted of a Phenomenex Ultracarb  $5\text{-}\mu\text{m}$  ODS 30 column ( $250 \times 4.6 \text{ mm I.D.}$ ) eluted with methanol– $0.1 \text{ M}$  sodium dihydrogenphosphate (70:30, v/v) at a flow-rate of  $1 \text{ ml min}^{-1}$ . The pH was measured at 6.1 and was not adjusted.

## RESULTS AND DISCUSSION

The method for the determination of the AAL toxins in corn culture material was developed to monitor toxin production by various *A. alternata* f. sp. *lycopersici* strains and to select suitable batches for isolation purposes. The HPLC systems developed were also used to monitor the elution of the toxins from preparative columns during isolation. The first HPLC system developed was based on an analytical column packed with Ultracarb  $7\text{-}\mu\text{m}$  ODS 30 packing and separated TA and TB. Elution under conditions that suppress the ionization of the carboxylic acid groups (pH 3.4) failed to separate the individual isomers of each AAL toxin. The use of a mobile phase of similar composition but at pH 6.1 achieved a partial separation of these isomers. In the second HPLC system, an improved separation of the structural isomers was achieved using a column of higher efficiency packed with Ultracarb  $5\text{-}\mu\text{m}$  ODS 30 packing. Fig. 2a shows such a separation of the isolated AAL toxins and Fig. 2b shows the separation of the AAL toxins in a cleaned-up culture sample. Confirmation of the identity of the TA and TB peaks is shown in Fig. 2c, where the same culture sample was spiked with authentic toxin. These separations were achieved by isocratic HPLC within 24 min as opposed to the previously published method, which required a binary gradient over a 60-min period [12].

The assay was validated with respect to precision and accuracy. Six replicate determinations of TA and TB in a corn culture sample of *A. alternata* f. sp. *lycopersici* MRC 6231 containing  $0.34 \text{ mg g}^{-1}$  of TA and  $0.05 \text{ mg g}^{-1}$  of TB gave a precision of 1.4% [relative standard deviation (R.S.D.)] for TA and 2.2% for TB. The accuracy of the method was assessed by spiking an extract of a corn culture of *A. alternata* strain

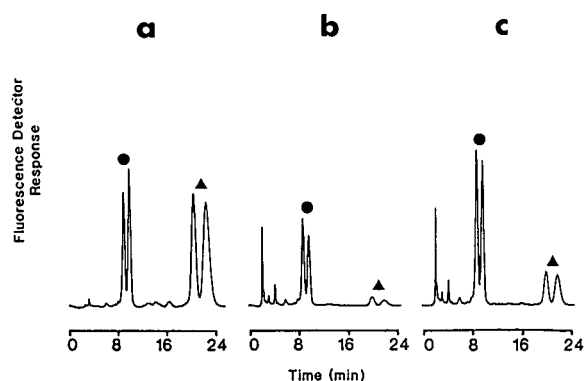


Fig. 2. Chromatograms of OPA-derivatized (●) TA and (▲) TB. In this chromatographic system,  $\text{TA}_2$  elutes before  $\text{TA}_1$  and  $\text{TB}_2$  before  $\text{TB}_1$ . (a) Sample of isolated toxins (200 ng of TA, 280 ng of TB); (b) purified corn culture extract (130 ng of TA, 20 ng of TB); (c) the same purified corn extract spiked with authentic TA and TB.

MRC 5494, which did not contain AAL toxins, with the equivalent of  $0.18 \text{ mg g}^{-1}$  of TA and  $0.28 \text{ mg g}^{-1}$  of TB. The recoveries for six replicates were found to be  $94.2\% \pm 5.4\%$  R.S.D. and  $99.8\% \pm 6.1\%$  R.S.D. for TA and TB, respectively.

The detection limit of the method was found to be of the order of 2 ng of injected toxin with a signal-to-noise ratio of 3:1. The absence of interfering peaks was shown by the analysis of a corn culture of *A. alternata* MRC 5494 which did not produce the AAL toxins. The OPA derivatization procedure is rapid, but the resulting derivatives are unstable and must be injected at a reproducible time within 2 min of preparation. The detector response was found to be linear over the range tested (5–130 ng of injected toxin). The method was applied to assess culture conditions for optimum toxin production and hence to select suitable cultures for toxin isolation.

Initial studies indicated that water or methanol–water (1:3, v/v) achieved similar extraction efficiencies for these toxins from corn cultures. The use of methanol–water extraction solvents with methanol proportions of 50%, 75% and 100% resulted in extracted toxin levels of 90%, 65% and 30%, respectively, of the levels achieved with aqueous extraction. The use of water as extraction solvent facilitated the adsorp-

tion, after acidification, of these toxins on Amberlite XAD-2 resin, as no change in solvent composition was required. Chromatography on silica achieved a separation of TA and TB. The separately pooled toxin fractions were further purified without derivatization on an automated semi-preparative isocratic HPLC system. Fractions collected from the semi-preparative system were analysed for the individual structural isomers, TA<sub>1</sub>, TA<sub>2</sub>, TB<sub>1</sub>, and TB<sub>2</sub>, on the second analytical HPLC system described above. It was shown that the semi-preparative system separated the non-derivatized TA and TB toxins into their respective individual isomers TA<sub>1</sub> and TA<sub>2</sub>, and TB<sub>1</sub> and TB<sub>2</sub>, which differ in that either the C-13 (TA<sub>1</sub> and TB<sub>1</sub>) or the C-14 (TA<sub>2</sub> and TB<sub>2</sub>) hydroxy group is involved in the ester linkage with the terminal carboxy group of the tricarballylic acid moiety (Fig. 1). The location of the ester group in the toxins was deduced from the <sup>1</sup>H chemical shift values in the respective NMR spectra and from the proton–proton connectivity pattern established in a COSY-45 NMR experiment [16]. Thus the signals at  $\delta$  3.227dd (*J* 6.9 and 4.5 Hz) and 4.904m ppm in the <sup>1</sup>H NMR spectrum of TA<sub>1</sub> were assigned to the C-14 and C-13 protons, respectively, and establish that in TA<sub>1</sub> it is the C-13 hydroxy group that is involved in the ester linkage. In contrast in TA<sub>2</sub>, it is the C-14 hydroxy group that is involved in the ester linkage: the signals of the C-14 and C-13 protons in the <sup>1</sup>H NMR spectrum appear at  $\delta$  4.583dd (*J* 6.4 and 5.0 Hz) and  $\delta$  3.558m ppm, respectively. The ester linkage in the TB<sub>1</sub> and TB<sub>2</sub> toxins was established in a similar manner.

The structural isomers undergo a slow isomerization via an intramolecular transesterification mechanism to form an equilibrium mixture of the C-13 and C-14 esters. This process is analogous to the well characterized isomerization of the mono-esters of glycerol in which the acid moiety is transferred by an intramolecular mechanism to a vicinal hydroxy group [17]. The formation of an equilibrium mixture of the isomers of TA and TB was also evident in each instance from the signals in the <sup>1</sup>H and <sup>13</sup>C NMR spectra of these toxins. Two sets of signals were discernible in each instance and for both TA and TB an equilibrium ratio of 55:45 in favour of ester

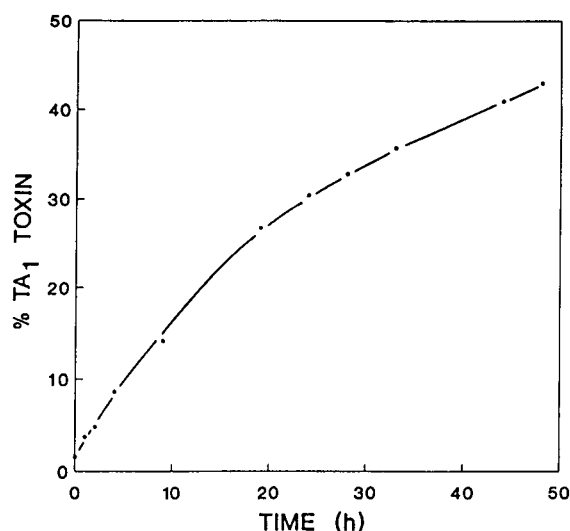


Fig. 3. Formation of TA<sub>1</sub> by isomerization during incubation of TA<sub>2</sub> in the HPLC mobile phase (methanol–0.05 M sodium dihydrogenphosphate, 47:53, v/v, pH 3.4) at 45°C.

formation with the C-13 hydroxy group is established. Fig. 3 illustrates the rate of the isomerization reaction in which TA<sub>2</sub>, collected from the semi-preparative HPLC system, was incubated at 45°C in the HPLC mobile phase. The formation of TA<sub>1</sub> was monitored by HPLC over a period of 2 days, during which time its concentration in the sample increased from 1% in the starting material to over 40% after 48 h.

After elution from the semi-preparative HPLC system, the samples were desalted on a reversed-phase column. Based on HPLC analysis, the isolated TA and TB were *ca.* 95% pure. The identity of the isolated compounds was confirmed both by HPLC after spiking a sample with authentic toxin donated by Professor D.G. Gilchrist and observing its co-elution with the isolated compound and also by comparison of the <sup>1</sup>H and <sup>13</sup>C NMR spectra with published data [5].

## CONCLUSIONS

A convenient procedure has been developed for the isolation of the AAL phytotoxins from corn cultures of *A. alternata* f. sp. *lycopersici*. The determination of these toxins in culture material by the proposed HPLC procedure is



sensitive, reproducible and accurate. The individual structural isomers of TA and TB can be separated as OPA derivatives on a reversed-phase isocratic HPLC system. The isolation of sufficient amounts of these toxins will enable their biological activities to be compared with those of the structurally similar fumonisins.

#### ACKNOWLEDGEMENTS

The authors thank Professor D.G. Gilchrist for the donation of a toxin producing *A. alternata* f. sp. *lycopersici* culture and for authentic samples of TA and TB, M. Schlechter for technical assistance in the production of culture material and the South African Medical Research Council for financial support (to R.V.).

#### REFERENCES

- 1 R.G. Grogan, K.A. Kimble and I. Misaghi, *Phytopathology*, 65 (1975) 880.
- 2 D.J. Siler and D.G. Gilchrist, *Physiol. Plant Pathol.*, 23 (1983) 265.
- 3 D.G. Gilchrist, S.D. Clouse, B.L. McFarland and A.N. Martensen, *Molecular Genetics of Filamentous Fungi*, Alan R. Liss, New York, 1985, p. 405.
- 4 S. Nishimura and K. Kohmoto, *Annu. Rev. Phytopathol.*, 21 (1983) 87.
- 5 A.T. Bottini, J.R. Bowen and D.G. Gilchrist, *Tetrahedron Lett.*, 22 (1981) 2723.
- 6 D.G. Gilchrist and R.G. Grogan, *Phytopathology*, 66 (1976) 165.
- 7 D.G. Gilchrist, B. Ward, V. Moussato and C.J. Mirocha, *Mycopathologia*, 117 (1992) 57.
- 8 M.E. Cawood, W.C.A. Gelderblom, R. Vleggaar, Y. Behrend, P.G. Thiel and W.F.O. Marasas, *J. Agric. Food Chem.*, 39 (1991) 1958.
- 9 C.J. Mirocha, D.G. Gilchrist, A. Martensen, H.K. Abbas, J. Plasencia and R.F. Vesonder, *Phytopathology*, 80 (1990) 1004 (abstract).
- 10 S.C. Lamprecht, W.F.O. Marasas, J.F. Alberts, M.E. Cawood, W.C.A. Gelderblom, G.S. Shephard and P.G. Thiel, *Phytophylactica*, 24 (1992) 112 (abstract).
- 11 W.T. Shier, H.K. Abbas and C.J. Mirocha, *Mycopathologia*, 116 (1991) 97.
- 12 D.J. Siler and D.G. Gilchrist, *J. Chromatogr.*, 238 (1982) 167.
- 13 S.D. Clouse, A.N. Martensen and D.G. Gilchrist, *J. Chromatogr.*, 350 (1985) 255.
- 14 G.S. Shephard, E.W. Sydenham, P.G. Thiel and W.C.A. Gelderblom, *J. Liq. Chromatogr.*, 13 (1990) 2077.
- 15 G.I. Kingston and B.B. Gerhart, *J. Chromatogr.*, 116 (1976) 182.
- 16 A.E. Derome, *Modern NMR Techniques for Chemistry Research*, Pergamon Press, Oxford, 1987.
- 17 I.L. Finar, *Organic Chemistry*, Vol. 1, Longmans, London, 5th ed., 1967, p. 290.

# Chromatographic behaviour of some platinum(II) complexes on octadecylsilica dynamically modified with a mixture of a cationic and an anionic amphiphilic modifier

M. Macka\* and J. Borák

Lachema, Research Institute of Fine Chemicals, Karásek 28, 62133 Brno (Czech Republic)

(First received October 15th, 1992; revised manuscript received January 18th, 1993)

---

## ABSTRACT

A method for the separation of anionic, uncharged and cationic platinum(II) complexes in one run was developed. The separation is based on an octadecylsilica sorbent dynamically modified with a mixture of an anionic (octanesulphonate, OS) and a cationic (tetrabutylammonium, TBA) amphiphilic modifier dissolved in aqueous mobile phase. Unless a tenfold excess of TBA is used, a sorbent with prevailing cation-exchange properties is generated. The retentions of the anionic complexes are, however, greater than retentions that would result from a pure ion-exclusion mechanism on a cation-exchange column and enable the anionic complexes to be separated also. Effects of the mobile phase composition parameters (concentration of the amphiphilic modifiers, phosphate and pH) on the separation were studied. Applications to the purity determination of cisplatin and to the reactions of the platinum(II) complexes in solutions are presented.

---

## INTRODUCTION

Cisplatin [*cis*-diamminedichloroplatinum(II), CDDP] and carboplatin [*cis*-diammine-1,1-cyclobutanedicarboxylateplatinum(II), Pt-CBDCA] (Fig. 1) are widely used cytostatic agents [1]. Regarding the synthesis and stability of cisplatin and carboplatin, several other platinum(II) complexes (starting compounds, intermediates, side-products and products of ligand-exchange reactions in solutions) should be considered (Fig. 1).

Owing to the kinetic stability of platinum complexes [2], separation methods such as liquid chromatography can be applied. Most HPLC methods utilize reversed-phase sorbents dynam-

ically modified with a cationic [3–9] or an anionic [6,10–17] amphiphilic modifier dissolved in the mobile phase. However, solutes having the same charge as the amphiphilic modifier generally elute with negligible retentions that do not allow the separation and quantification of these complexes. The charges of the platinum(II) complexes I–XI (Fig. 1) vary from –2 to +2 and therefore their simultaneous determination has not been possible using a reversed-phase sorbent modified with either a cationic or an anionic amphiphilic modifier.

Regarding the simultaneous separation of anionic and cationic platinum(II) complexes, tetrachloroplatinate and the positively charged aquation products of cisplatin (X and XI) have been previously separated by TLC on silica, however, the complexes X and XI were retained at the start [18].

In principle, a cation-exchange column plus an

---

\* Corresponding author. Present address: Analytical Department WAQ-1, LONZA AG, CH-3930 Visp, Switzerland.

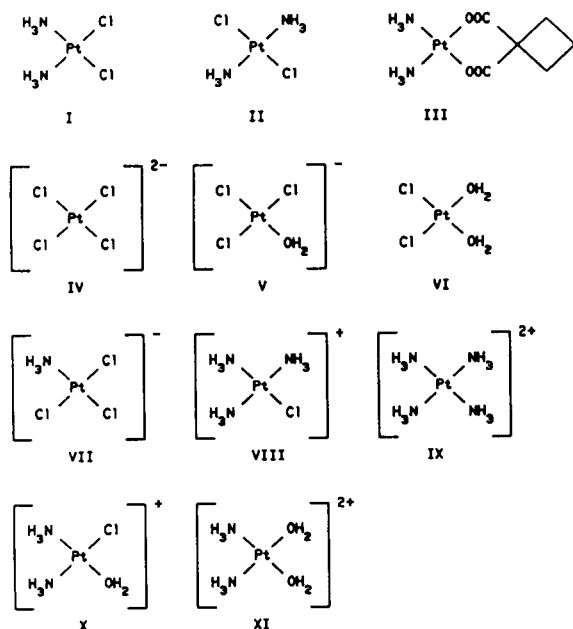


Fig. 1. Structures of platinum (II) complexes, their charges and symbols used in graphs if not specified: I = *cis*-diamminedichloroplatinum(II) CDDP, 0 (○); II = *trans*-diamminedichloroplatinum(II) (transplatin, TDDP) 0 (●); III = *cis*-diammine-1,1-cyclobutanedicarboxylateplatinum(II) (carboplatin, Pt-CBDCA), 0 (□); IV = tetrachloroplatinum(II), -2 (□); V = aquatrichloroplatinum(II), -1 (△); VI = *cis*-diaquachloroplatinum(II), 0 (+); VII = amminetrichloroplatinum(II), -1 (▲); VIII = triamminechloroplatinum(II), +1 (◇); IX = tetraammineplatinum(II), +2 (◆); X = *cis*-diammineaquachloroplatinum(II), +1 (∇); XI = *cis*-diamminediaquaplatinum(II), +2 (▼).

anion-exchange column connected in series could be used to achieve sufficient retentions of both positively and negatively charged complexes. This arrangement was previously used in the separation of cisplatin and its aquation products X and XI [19]. In this case, however, the anion-exchange column was obviously needed to increase the retention of cisplatin ascribed to ion-dipole interactions of the quaternary ammonium groups and the uncharged but polar molecule (dipole moment 5.3 D) of cisplatin [3].

A mixture of both cationic (ammonium type) and anionic amphiphilic modifiers dissolved in a mobile phase was used to dynamically modify a silica sorbent [20–22]. This was based on the primary sorption of the long-chain alkylam-

monium amphiphilic modifier on the silica caused by the affinity to the silanol groups and secondary sorption of the anionic amphiphilic modifier due to hydrophobic interactions with the sorbed cationic modifier. On changing the ratio of the concentrations of the oppositely charged amphiphilic modifiers, the character of the sorbent changed from an anion exchanger to a cation exchanger and *vice versa*, making possible the generation of sorbents with a variety of selectivities.

Applications of mobile phases containing both anionic and cationic amphiphilic modifiers to chromatography on reversed-phase sorbents are limited to additions of triethylamine or tetramethylammonium to a mobile phase containing an anionic amphiphilic modifier, obviously to prevent peak tailing when chromatographing bases [23,24]. Another interesting application of a mobile phase containing both an anionic and a cationic amphiphilic modifier is to speed up the transition between two rotamers of the dipeptide enalapril, thus making possible the chromatography of the analyte at ambient temperature [25]. In this case the mobile phase, however, contained a high percentage (60–70%) of methanol, which usually shifts the sorption equilibria of surfactants on reversed-phase sorbents in favour of the mobile phase.

The aim of this work was to study a chromatographic system using an octadecylsilica sorbent dynamically modified with a mixture of a cationic and an anionic amphiphilic modifier dissolved in the mobile phase that could be used to achieve sufficient retentions of both the positively and negatively charged platinum(II) complexes. Such a separation system will presumably differ substantially from a mixed-bed ion exchanger or a pair of columns filled with cation exchanger and anion exchanger as the charges of the oppositely charged amphiphilic modifiers in the stationary phase will probably be considerably compensated for owing to the formation of ion pairs. However, the idea was that the retentions of the ions that under normal conditions would be excluded could be increased owing to mixed interactions with the dynamically generated polar stationary phase.

## EXPERIMENTAL

*Materials*

Sodium octanesulphonate (NaOS), tetrabutylammonium hydrogensulphate (TBAHSO<sub>4</sub>), sodium dihydrogenphosphate, potassium chloride and fructose were of analytical-reagent grade (Merck). Dextran T 2000 (standard for size-exclusion chromatography,  $M_r = 2 \times 10^6$ ) was obtained from Pharmacia, (Uppsala, Sweden).

Potassium tetrachloroplatinate(II) (IV, Fig. 1) was purchased from Aldrich, (Milwaukee, WI, USA), assay >99.99%. It was used as a 1 mg/ml solution in 0.15 M potassium chloride. The assay in the solution was 87% (HPLC, internal normalization 210 nm); the remainder was the aquation product V.

Aquatrichloroplatinate(II) (V, Fig. 1) complex was prepared by aquation of a 1 mg/ml potassium tetrachloroplatinate(II) solution in water at 25°C. The solution was used after 3 days. The assay was 75%, the remainder was IV (15%) and VI (8%) (HPLC, internal normalization 210 nm).

*cis*-Diaquadichloroplatinum(II) (VI, Fig. 1) was prepared according to ref. 26 in alkaline medium. A 1 mg/ml solution of potassium tetrachloroplatinate(II) in 0.01 M sodium hydroxide was used after ageing for 1 day. The assay was 70% (HPLC, internal normalization 210 nm); the remainder was V (17%), an unknown compound (ca. 10%) and IV (ca. 3%). The solution was unstable and after several days solid Pt<sup>0</sup> was formed. The solution could not be acidified in order to improve the stability of the solution as the equilibrium was then shifted back to V.

Cisplatin (I, Fig. 1) and carboplatin (III, Fig. 1) were obtained from Lachema (Brno, Czech Republic). The assay was >99.5% (HPLC).

*trans*-Diamminedichloroplatinum(II) (II, Fig. 1) complex was prepared according to ref. 27. It contained <0.1% of CDDP and the assay was >99% (HPLC, internal normalization 210 nm).

*cis*-Diamminediaquaplatinum(II) (XI, Fig. 1) complex was prepared by a modified procedure according to Dhara [28]. To a CDDP solution (concentration 1 mg/ml), solid silver sulphate

was added at a CDDP:Ag molar ratio of 1:2.2. The mixture was shaken and allowed to stand overnight. After centrifugation the supernatant was acidified with sulphuric acid to pH 2 and stored in a dark bottle. The chromatogram showed one major peak and less than 1% CDDP and *cis*-diammineaquachloroplatinum(II). The advantage of using silver sulphate over nitrate (which had been used previously [17] and partly also in this work) is that the reference sample does not contain a highly absorbing anion such as nitrate.

*cis*-Diammineaquachloroplatinum(II) (X, Fig. 1) complex was prepared by modifying the above procedure so that silver sulphate was added to CDDP in molar ratio of only 1:1.1. The chromatogram showed one major peak, 21% of *cis*-diamminediaquaplatinum(II) and 16% of CDDP.

Amminetrichloroplatinum(II) (VII, Fig. 1) was prepared as the potassium salt according to ref. 27. The assay was 99% (HPLC, internal normalization 210 nm).

Triamminechloroplatinum(II) (VIII, Fig. 1) was prepared by partial ammination of CDDP (concentration 1 mg/ml) in 3.3 mM ammonium chloride at 90°C. Small portions of 0.2 M ammonia solution were used, so that the pH did not exceed 7.5. The reaction was stopped when the amount of side-product, tetraammineplatinum(II), formed was about the same as that of unreacted CDDP. The product was purified three times by fractional precipitation from a water–2-propanol mixture. The assay of triamminechloroplatinum(II) was 55% (HPLC, internal normalization 210 nm); the remainder was CDDP (13%, HPLC, external standard), TDDP (9%, HPLC, external standard) and tetraammineplatinum(II) (26%, HPLC, external standard).

Tetraammineplatinum(II) (IX, Fig. 1) was prepared according to ref. 27. The assay was >99% (HPLC, internal normalization 210 nm).

As potentially all platinum(II) complexes are light sensitive [29] and some are even extremely sensitive [30], all solutions were prepared in vials of dark-brown glass. Also, the use of ultrasound to facilitate the dissolution of the platinum(II)

complexes was avoided, as at least in some instances decomposition by ultrasound is evident [30]. Unless specified, all solutions of platinum(II) complexes were prepared and stored at ambient temperature.

The HPLC method described here was used to characterize the reference samples of the platinum complexes I, II and IV–VII. The HPLC method reported recently [17] was used to characterize the reference samples of the platinum(II) complexes III and VIII–XI.

#### *Apparatus and chromatographic conditions*

The system used was a Hewlett-Packard Model 1090 chromatograph consisting of an HP 79880A diode-array detector, a DR5 binary pumping system, an HP 79846A variable-volume injector equipped with a 25- $\mu$ l syringe and an HP 79847A autosampler; if not specified otherwise, volumes of 10  $\mu$ l were injected. For system control and data evaluation an HP 79994A Workstation based on an HP 310 computer was used.

A stainless-steel column (250  $\times$  4 mm I.D.) packed with Silasorb SPH C<sub>18</sub> (surface area ca. 300 m<sup>2</sup>/g, particle diameter 7.5  $\mu$ m) (Lachema) was used. The column temperature was maintained at 30°C.

The mobile phases contained 0–4 mM octanesulphonate, 0–6 mM tetrabutylammonium and 5–200 mM dihydrogenphosphate. The pH of the mobile phase was adjusted with sodium hydroxide to the desired value. The composition of the final mobile phase for the analysis of impurities in cisplatin was as follows: (A) 4 mM sodium octanesulphonate, 6 mM tetrabutylammonium (pH 5.9) and (B) the same as A plus 0.20 M dihydrogenphosphate (pH 5.9).

Analyses were run under isocratic conditions (90% A–10% B) or with an ionic strength gradient as follows [17]:

gradient programme I:

time (min)	0	3	7	8	8.1
B (%)	5	5	100	100	5

gradient programme II:

time (min)	0	4	8	9	9.1
B (%)	10	10	100	100	10

The stationary phase was generated by pumping the mobile phase through the column until

the retention times were constant (usually 1–2 h). If not specified otherwise, the flow-rate was 1.0 ml/min, resulting in a column inlet pressure of ca. 90 bar.

#### *Determination of the limit of detection*

Limits of detection (LODs) of the complexes were calculated for a signal equal to ten times the standard deviation of the baseline noise. The baseline noise was evaluated from the raw data by a program using statistics as described previously [22].

#### *Determination of the void volume of the column*

Fructose (10  $\mu$ l of a 1% solution in the mobile phase) was injected and detected at 210 nm; the elution volume was 2.00  $\pm$  0.02 ml. Further, dextran T 2000 (10  $\mu$ l of a 1% solution in the mobile phase) was injected and detected at 190 nm or with an SP 6040 refractometric detector (Spectra-Physics, Darmstadt, Germany) connected to the workstation via an HP 35900 dual-channel interface. As detection both at 190 nm and with the refractometer gave the same values, only photometric detection was subsequently used. With all mobile phases the elution volume of dextran T 2000 was 1.50  $\pm$  0.02 ml.

The thermodynamic definition of the capacity factor leads to negative capacity factors for excluded ions. However, if the elution volume of fructose were to be used as the value of the void volume, the capacity factors of the excluded anions would be  $k' < 0$  and could not be used for log  $k'$  graphs. For this reason the elution volume of dextran T 2000 was used to calculate the capacity factor  $k'$  of all the solutes and is used throughout this paper to express retentions. Knowing the elution volumes of fructose and dextran T 2000 the capacity factors can be recalculated if needed.

#### *Determination of the amounts of sorbed amphiphilic modifiers*

The column was flushed with 20 ml of water and then the sorbed surfactants were eluted with 50 ml of methanol and the eluate was evaporated to dryness. The residue was analysed for nitro-

gen (Dumas) and sulphur (Schöniger). From the percentage of N and S and the mass of the eluted amphiphilic modifiers, the corresponding amounts of the sorbed OS and TBA were calculated. The completeness of the elution of TBA was checked by further elution (50 ml) with 0.1 g/l lithium perchlorate solution in methanol and evaporation to dryness. The residue was analysed for nitrogen (Kjeldahl). Its content was lower than *ca.* 5% relative to the amount of TBA determined in the first step.

After all the experiments had been completed the column was flushed with water and methanol and the sorbent was pressed out of the column and dried to constant mass at 110°C. The column contained 2.04 g of the sorbent.

## RESULTS AND DISCUSSION

### *Choice of the modifiers*

Preliminary studies on chromatographic systems using octadecylsilica and buffered mobile phases containing one anionic amphiphilic modifier (octanesulphonate or dodecyl sulphate) and one cationic amphiphilic modifier (tetrabutylammonium, dodecyltrimethylammonium or hexadecyltrimethylammonium) showed two major sources of problems:

(i) the precipitation of the oppositely charged long-chain ( $n_c \geq 12$ ) amphiphilic modifiers (surfactants) in aqueous media limits their application either to extremely low concentrations or to micellar liquid chromatography with mobile phases containing both anionic and cationic surfactants but one (*e.g.*, sodium dodecyl sulphate) being in excess over the other (*e.g.*, HTMABr) and thus solubilizing the formally uncharged very lipophile ion pairs [22];

(ii) the lipophilicity of the two oppositely charged amphiphilic modifiers must be balanced, so that both amphiphilic modifiers can be sorbed on the reversed phase and influence the resulting sorbent ion-exchange properties. We preferred a column that would behave generally as a cation exchanger, because of the complexes to be separated the majority are cationic. Octanesulphonate and tetrabutylammonium were a suitable combination adopted in further work.

### *Effect of molar fraction of TBA on the amounts of sorbed TBA and OS*

The amounts of the sorbed amphiphilic modifiers are plotted as a function of  $x_{TBA}$  are plotted in Fig. 2a. A pronounced synergistic effect on the sorption of the two oppositely charged amphiphilic modifiers is observed, which can be ascribed to the formation of formally uncharged ion pairs in the stationary phase. In the range  $0.25 < x_{TBA} < 0.75$  the concentration of both amphiphilic modifiers in the stationary phase decreases with increasing  $x_{TBA}$ , suggesting that the sorption of OS is probably primary and TBA acts more as a counter ion. However, with increasing  $x_{TBA} > 0.9$ , TBA is likely also to be sorbed directly on the octadecylsilica.

The sorbed OS and TBA as calculated from the elemental analysis and further their difference as the approximate capacity of the column (charge compensation of the oppositely charged modifiers in the stationary phase) are shown in Fig. 2b. A sorbent with a significantly lower capacity is generated when a mixture of OS and TBA is used instead of only one of them.

### *Effect of molar fraction of TBA on the retention and selectivity*

The influence of  $x_{TBA}$  as the molar fraction of the TBA in the total (TBA + OS) amphiphilic modifier concentration of 4 mM is illustrated for the cationic complexes and carboplatin in Fig. 3a and for the anionic and the remainder of the neutral complexes in Fig. 3b. As was expected, as a result of the presumable charge compensation of the oppositely charged amphiphilic modifiers in the stationary phase, it is possible to achieve significant retentions either of cationic ( $x_{TBA} \rightarrow 0$ ) or anionic solutes ( $x_{TBA} \rightarrow 1$ ). At  $x_{TBA} < 0.8$  the column behaves generally as a cation exchanger, then it reverses its ion-exchange properties and at  $x_{TBA} > 0.9$  the column behaves as an anion exchanger.

The curve for cisplatin in Fig. 3b shows slight "anion-like" behaviour. Such a behaviour of the formally uncharged molecule VI (Fig. 3b) is caused by the dissociation of the H<sub>2</sub>O ligand, resulting in a negative charge of the molecule. The  $pK_a$  is reported to be 6.5 at 35°C [31]. With I, however, ion-dipole interactions are consid-

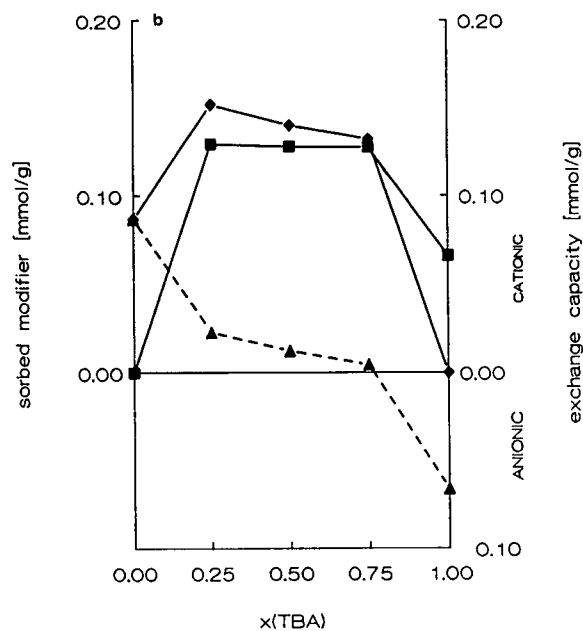
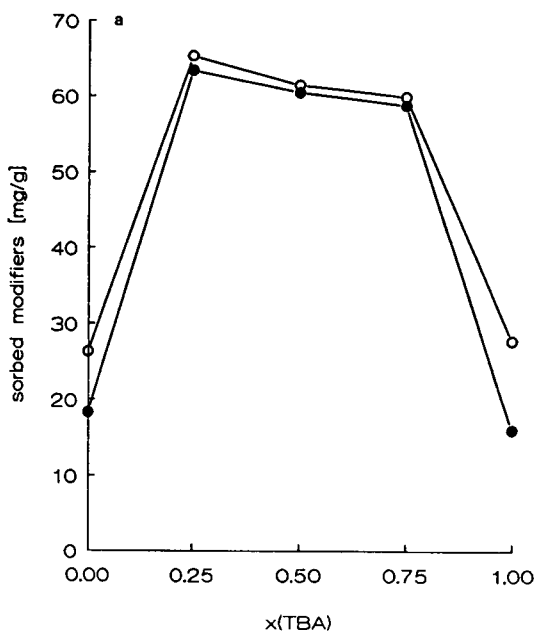


Fig. 2. (a) Amounts of sorbed modifiers versus  $x_{\text{TBA}}$ : (O) = mass of residue including potassium and phosphate as counter ions; (●) = summed amounts of OS + TBA as calculated from the elemental analysis. Chromatographic conditions: eluent, OS and TBA in 0.02 M phosphate, pH adjusted to 5.9. (b) Amount of sorbed OS and TBA and the column capacity versus  $x_{\text{TBA}}$ : the amount of sorbed surfactant as calculated from the elemental analysis for (◆) OS and (■) TBA; ▲ = ion-exchange capacity of the sorbent. Chromatographic conditions as in (a).

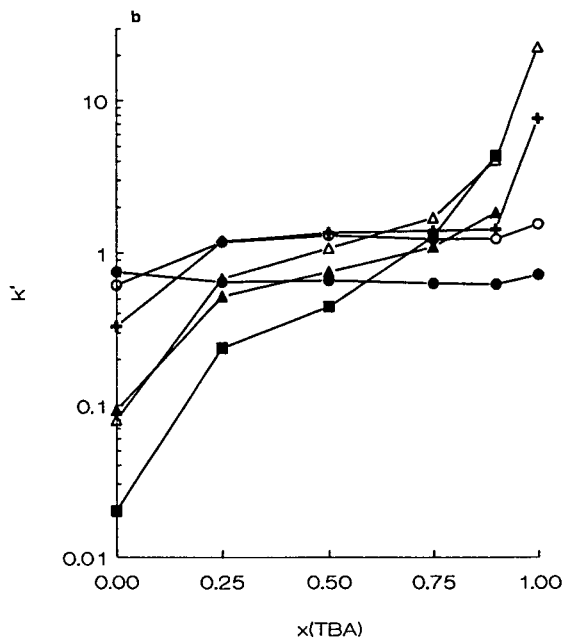
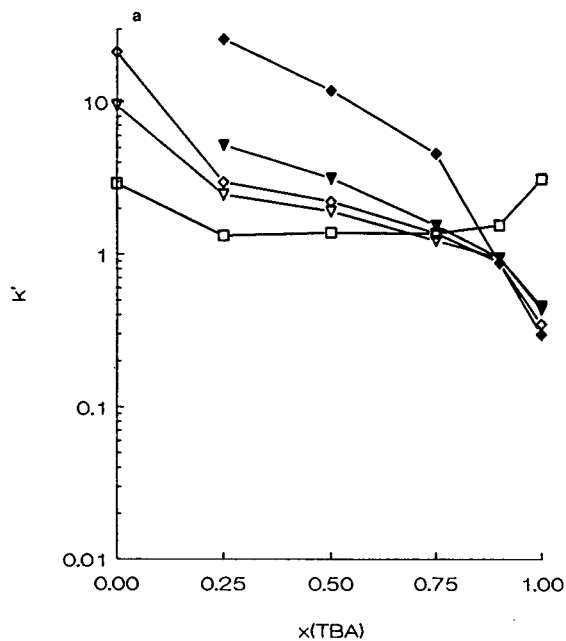


Fig. 3. (a) Retentions ( $k'$ ) of the cationic platinum(II) complexes (VIII–XI) and the uncharged III versus  $x_{\text{TBA}}$  as the fraction of TBA in the total (TBA + OS) amphiphilic modifier concentration (4 mM). (b) Retentions ( $k'$  values) of the anionic platinum(II) complexes (IV, V and VII) and the uncharged I, II and VI versus  $x_{\text{TBA}}$ . Symbols as in Fig. 1. Chromatographic conditions as in Fig. 2.

ered to be the cause of the behaviour [3]. In agreement with this, columns with anion-exchange properties (mostly reversed-phase sorbents dynamically modified with a cationic amphiphilic modifier) allowing sufficient retention of **I** to be achieved are generally used.

For a mixture of both cationic and anionic platinum(II) complexes a clearly better separation is achieved when using a mixture of both OS and TBA in the mobile phase instead of only OS or TBA. The separation of anions, expressed as the resolution of several pairs of anionic analytes (Fig. 4) has an optimum and then deteriorates again as the region  $0.8 < x_{\text{TBA}} < 0.9$  is approached where the elution order changes. On the other hand, for the cationic complexes illustrated with the examples of **VIII** and **IX** it is not surprising that the highest resolution is achieved at  $x_{\text{TBA}} \rightarrow 0$  as their retentions are maximum there. The resolution of the pair **VIII–IX** in the whole range  $x_{\text{TBA}} < 0.8$  is, however, sufficient and hence the optimum range for the separation of both anionic and cationic solutes is  $x_{\text{TBA}} \approx 0.25–0.65$ .

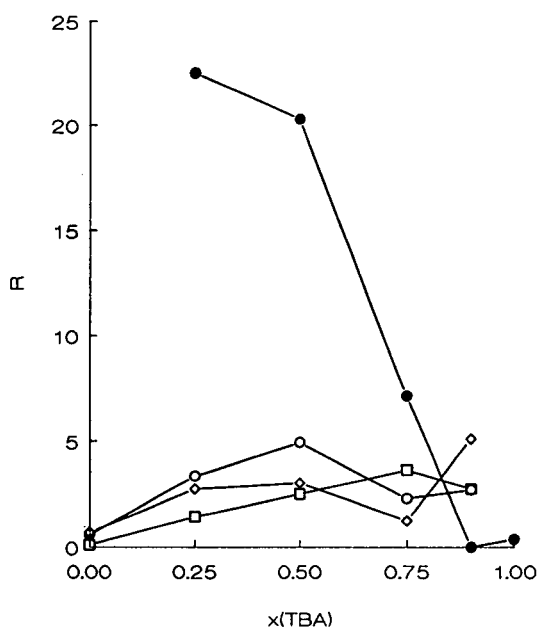


Fig. 4. Resolution ( $R$  value) of pairs of complexes versus  $x_{\text{TBA}}$ :  $\circ = R(\text{IV-V})$ ;  $\diamond = R(\text{IV-VII})$ ;  $\square = R(\text{V-VII})$ ;  $\bullet = R(\text{VIII-IX})$ . Chromatographic conditions as in Fig. 2.

#### Effect of phosphate and TBA concentration at constant OS concentration

From the  $\log k' - \log c(\text{PO}_4)$  dependence (Fig. 5) for the cationic analytes it can be concluded that their predominant retention mechanism is ion exchange. As expected, the slopes of the curves for the +1 (**VIII** and **X**) and the +2 (**IX** and **XI**) charged complexes clearly differ.

Concerning the retentions of anions (**IV**, **V** and **VII**) under these conditions, their capacity factors rapidly increase with addition of TBA (Fig. 6). From the character of the curves (**IV**, **V** and **VII**) at low TBA concentration ( $c_{\text{TBA}} \leq 1$ ) and from the negative rather than positive slopes of their  $\log k' - \log c(\text{PO}_4)$  dependence (Fig. 5), ion exclusion can be concluded to be the predominant retention mechanism. This is also supported by the fact that their capacity factors at low TBA concentration are less than 0.3, which is the capacity factor of the unretained low-molecular-mass solute fructose (high-molecular-mass dextran T 2000 is used as a void volume marker). However, for  $c_{\text{TBA}} > 1$  the anions are sorbed on the stationary phase, also. It can be concluded

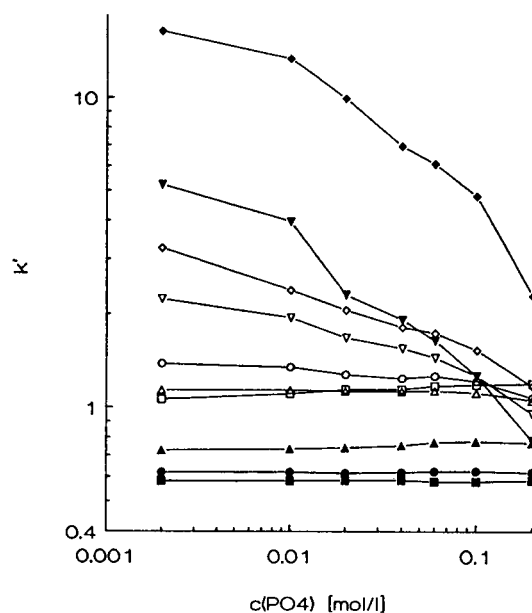


Fig. 5. Retentions ( $k'$ ) of the platinum(II) complexes versus phosphate concentration. Symbols as in Fig. 1. Chromatographic conditions: eluent, 0.002–0.2 M phosphate in 4 mM OS and 6 mM TBA, pH adjusted to 5.9.



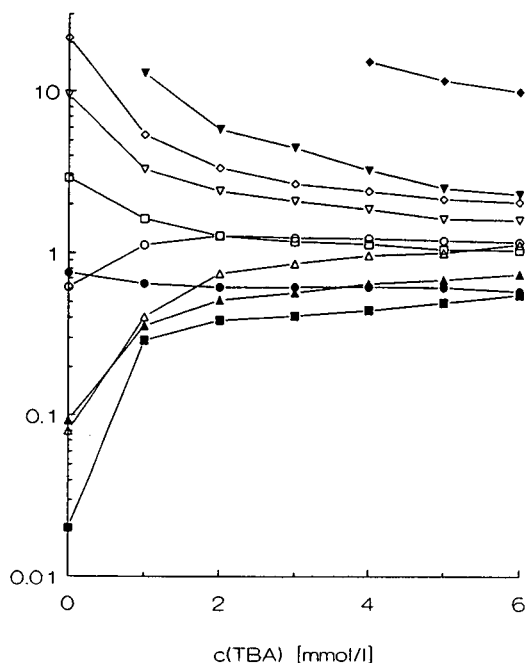


Fig. 6. Retentions ( $k'$ ) of the platinum(II) complexes versus concentration of TBA. Symbols as in Fig. 1. Chromatographic conditions: eluent, 0 and 6 mM TBA in 4 mM OS–0.02 M phosphate, pH adjusted to 5.9.

that the retention mechanism of anions under the conditions of prevailing cation-exchange character of the stationary phase is complex, involving ion exclusion, ion exchange and partitioning, probably based on ion–dipole interactions with the polar layer of amphiphilic modifiers covering the octadecylsilica.

The retention of the uncharged molecule of **II** possessing no dipole moment is low and almost uninfluenced by any parameter of the mobile phase composition.

The slightly negative slope of the  $\log k' - \log c(\text{PO}_4)$  graph of the complex **III** (Fig. 5) can be explained by the salting-out effect due to the hydrophobic interactions of the cyclobutane-dicarboxylate ligand. The molecule also shows a “cation-like” behaviour (Figs. 2a and 6). As a result of the decrease in retention after addition of TBA to the mobile phase the separation of carboplatin from cisplatin begins to be a problem, and therefore for the separation of cisplatin and carboplatin we preferred mobile phases with low TBA content or only with OS [17].

### Effect of pH

The retentions of the complexes containing at least one water molecule as ligand (**V**, **VI**, **X** and **XI**) are pH dependent (Fig. 7), which is not the case with the remaining solutes. The reason is the deprotonation reaction on the water ligand that causes a change in the effective charge of the molecule. As the charge of the molecule becomes more negative with increasing pH of the mobile phase, their retentions decrease. For **XI**,  $pK_{a1}$  is reported to be 5.56 and  $pK_{a2}$  7.32 at 20°C [32]. The effect of pH was advantageously applied to achieve the separation of **VIII** from **X** and of **IX** from **XI**, which originally failed at pH 3.2. A pH of 5.9 was found to be optimum for the separation of **I**, **X** and **VIII** (see Fig. 9).

The unknown peak **UI** in the chromatogram of a 16-month-old solution of **IV** in 1 mM hydrochloric acid (Fig. 8) obviously also corresponds to an aqua complex, because its retention is pH dependent (Fig. 7). It may be the *trans*-diaquadi-chloroplatinum(II) which is formed, as opposed to the *cis*-complex, much more slowly [25]. Note

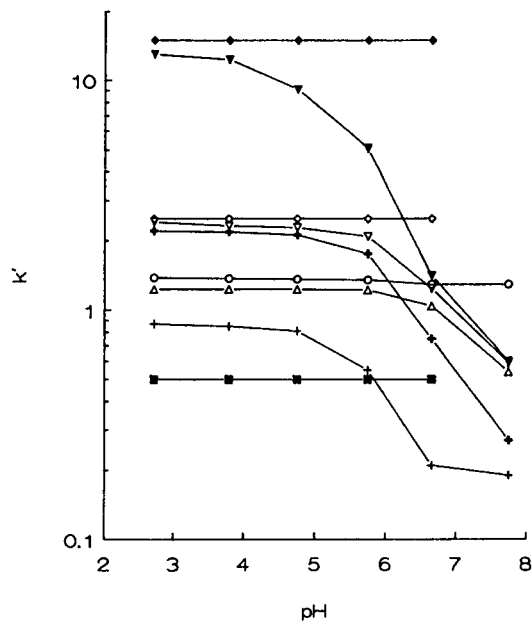


Fig. 7. Retentions ( $k'$ ) of the platinum(II) complexes versus pH of the mobile phase. + = Presumably *trans*-diaquadi-chloroplatinum(II); other symbols as in Fig. 1. Chromatographic conditions: eluent, 4 mM OS and 6 mM TBA in 0.02 M sodium dihydrogenphosphate, pH adjusted to desired value.

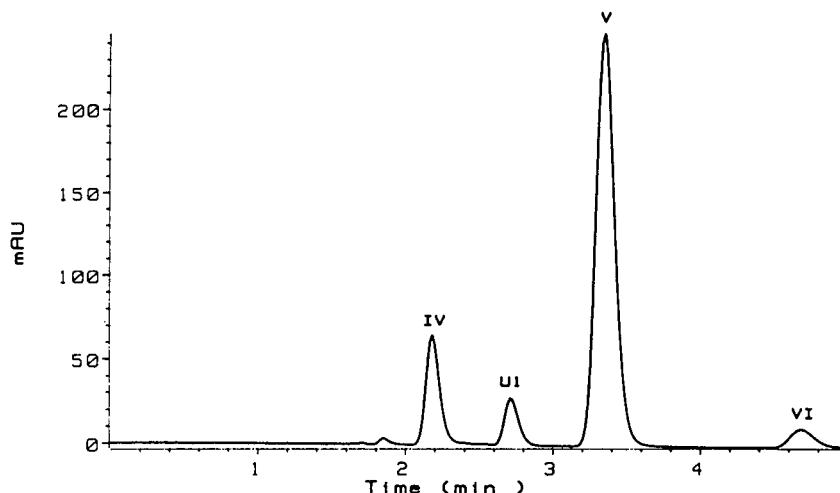


Fig. 8. Chromatogram of tetrachloroplatinate (1 mg/ml solution in 1 mM HCl, ambient temperature, 16 months). For peak identification, see Fig. 1. Chromatographic conditions as in Fig. 10, except pH = 4.8.

that here at pH 4.8 the complex VI is eluted later than at pH 5.9 (see Fig. 11).

#### Applications

The separation of a model mixture of the complexes I, II, IV, V and VII–XI shown in Fig. 9 illustrates the separation potential of the method.

*Purity of cisplatin.* According to the USP XXII [33], the impurities II and VII are determined in I using two different chromatographic systems.

This method makes it possible to determine both II and VII in I in one run (Fig. 10). The limit of detection expressed relative to I is 0.005% for both II and VII. The method that has been used in our laboratory for more than 1 year offered reproducible selectivities and retentions from column to column. The application of the method to the study of the decomposition of cisplatin in aqueous solutions containing chlorides by ultrasonic energy and light will be reported separately [30].

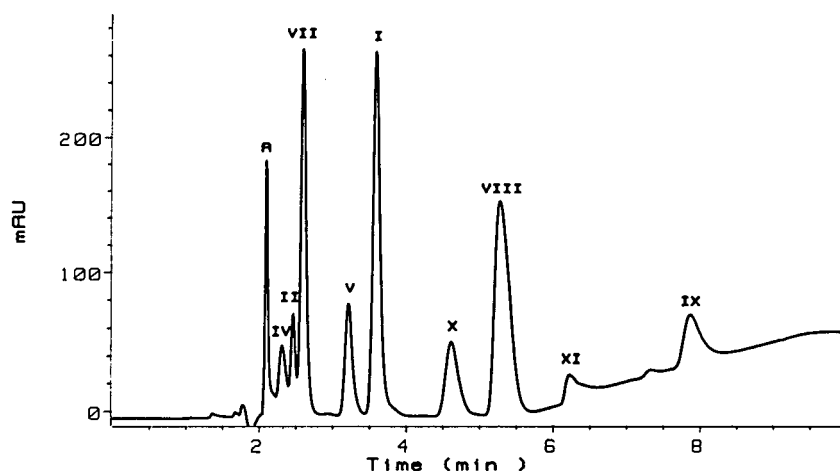


Fig. 9. Chromatogram of a model mixture of complexes I, II, IV, V and VII–XI. For peak identification, see Fig. 1; A = nitrate as impurity. Chromatographic conditions: injection, 20  $\mu$ l; eluent, 4 mM OS and 6 mM TBA, pH adjusted to 5.9; ionic strength gradient I. For other conditions, see Experimental.

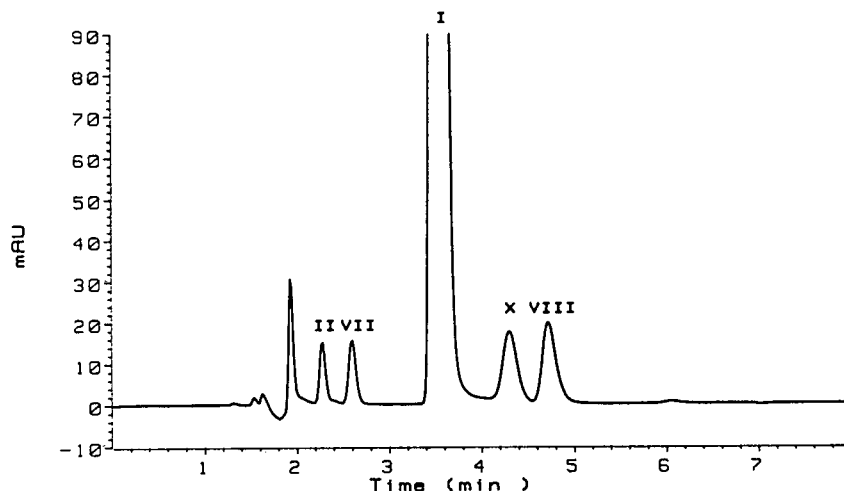


Fig. 10. Chromatogram of cisplatin drug substance, 1 mg/ml solution in 0.15 M KCl, with 0.5% of each impurity **II**, **VII** and **VIII** added. **X** is present as a result of aquation of **I**. For peak identification, see Fig. 1. Chromatographic conditions: injection, 20  $\mu$ l; eluent, 4 mM OS and 6 mM TBA in 0.02 M phosphate, pH adjusted to 5.9. For other conditions, see Experimental.

*Aquation of tetrachloroplatinate.* The conversion of **IV** into **V** and **VI** in aqueous media [26] may be followed by the separation system described here. In Fig. 11a, b and c the chromatograms of tetrachloroplatinate **IV** in 0.15 M KCl, water and 0.01 M NaOH, respectively, are shown.

*Amination of tetrachloroplatinate (Fig. 12) and cisplatin (Fig. 13).* Here **VII**, **I**, **VIII** and **IX** are formed consecutively from **IV**; **II** is the

product of isomerization of **I** and/or the product of deamination of **VIII** [2]. The method has been used to study amination reactions of **IV** in aqueous–organic solutions under various conditions [34].

#### *Kinetic stability of the complexes*

To obtain a true view of the analysed solution, it is important that during the chromatographic separation the extent of the ligand-exchange

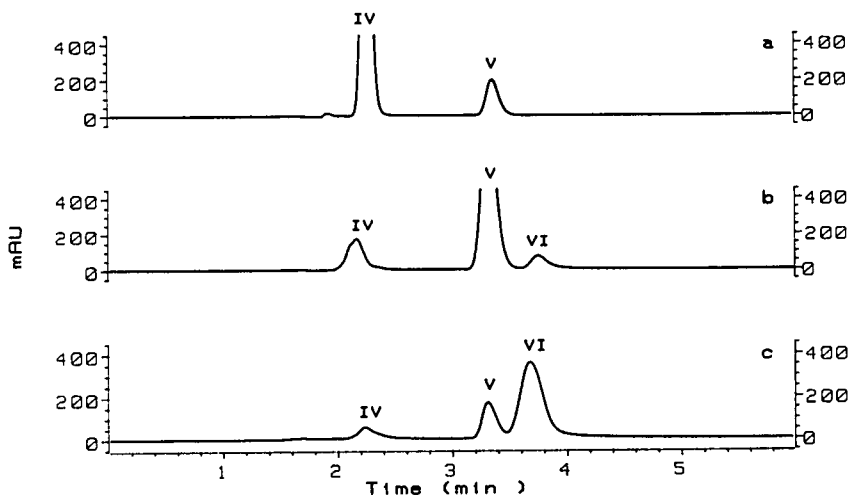


Fig. 11. Chromatograms of tetrachloroplatinate undergoing aquation in various solutions. For peak identification, see Fig. 1. Chromatographic conditions as in Fig. 10. For other conditions, see Experimental. (a) 1 mg/ml solution of **IV** in 0.15 M KCl, ambient temperature, 21 h; (b) 1 mg/ml solution of **IV** in water, ambient temperature, 14 days; (c) 1 mg/ml solution of **IV** in 0.01 M NaOH, ambient temperature, 21 h.

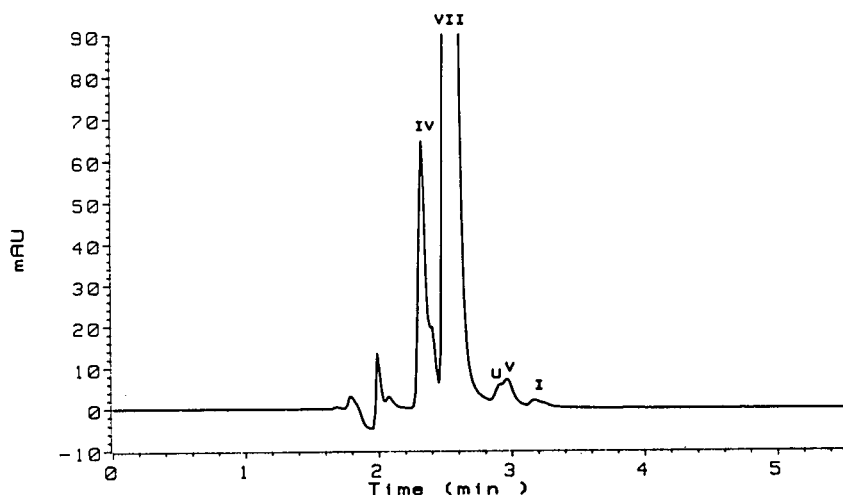


Fig. 12. Chromatogram of a crude preparation of **VII** prepared by amination of tetrachloroplatinate (1 mg/ml solution of the sample in 0.15 M KCl). For peak identification, see Fig. 1. Chromatographic conditions as in Fig. 10, except 5.0 mM TBA and pH = 6.5.

reactions is negligible. Therefore, the aqua complexes with the least thermodynamically stable aquo ligands compared with the other ligands [29] should be checked for stability under the given conditions.

For practical purposes, the stability of the complexes in a mobile phase in the time range of *ca.* 10 min would be sufficient. Using the final mobile phase (pH 5.9) we examined the stability of **X** and **XI** in this medium by mixing 10  $\mu$ l of

the reference sample in the loop of the auto-sampler with the mobile phase. After waiting for 10 min the samples were injected. The peak area decreased to 99.7% and 95.4% of the original concentration for **X** and **XI**, respectively. Therefore, it can be concluded that the stability of **X** and **XI** in the final mobile phase during the analysis is acceptable.

If the reference solutions of the aqua complexes **X** and **XI** were mixed 1:1 (v/v) with the

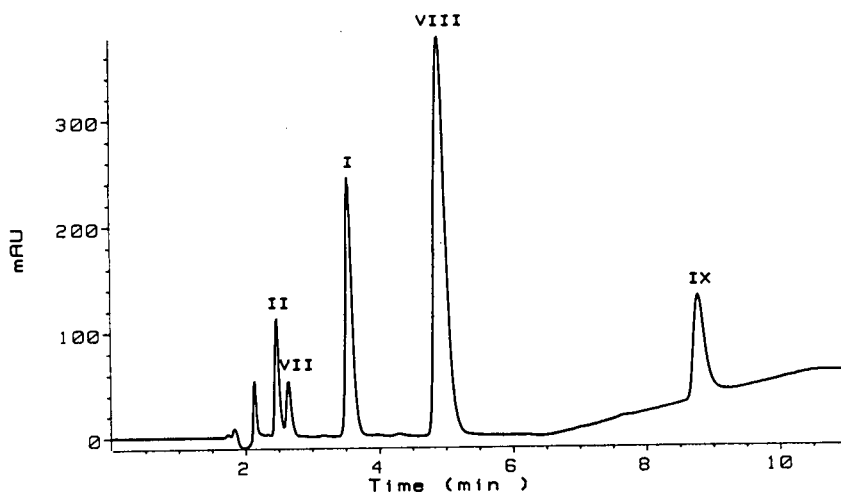


Fig. 13. Chromatogram of raw **VIII** prepared by amination of cisplatin (1 mg/ml solution of the sample in 0.15 M KCl). For peak identification, see Fig. 1. Chromatographic conditions as in Fig. 9, except ionic strength gradient II. For other conditions, see Experimental.

mobile phase (0.020 M phosphate, pH 3.2) and stored for 1 h at ambient temperature, two unknown peaks appeared (one major at  $k' = 1.7$  and one minor at  $k' = 2.4$ ) and the amounts of **X** and **XI** in the solutions decreased to 62% and 50% of the original concentrations, respectively. As the spectrum of the major unknown peak is very similar to that of **XI** itself, the major unknown may be a complex with an oxo ligand, e.g., phosphate, in place of the aquo ligand.

#### Electron absorption spectra

The absorption spectra of the platinum(II) complexes in the ultraviolet and visible region consist of an intense ( $\epsilon \approx 10^4$ ) charge-transfer band near 200 nm and several d–d bands of low intensity shifted to the long-wavelength region [29]. The first band is used to achieve sensitive detection and the later bands are very useful for identification. Characteristic absorption maxima of the spectra for the complexes **I–XI** measured from the eluted peaks are given in Table I.

The measured maxima agree with those given in the literature [2,26,35–37]. The maxima follow the rule of shifting towards higher energy on replacing a Cl ligand with H<sub>2</sub>O and then with NH<sub>3</sub> [29]. In the case of the aqua complexes (**V**, **VI**, **X** and **XI**) the weak d–d maxima shifted with increasing pH slightly to the short-wavelength region owing to the deprotonization of the water

ligands, the largest shift being in the case of **XI**, the maxima of which at pH 3.2 were 252 and ca. 330 nm. Consequently, for identification of aqua complexes it is important to use reference spectra registered at the same pH.

#### CONCLUSIONS

The use of a reversed-phase sorbent and two oppositely charged ionic amphiphilic modifiers in the mobile phase makes it possible for sufficient retentions for both anionic and cationic solutes to be achieved, although in such a system cation- or anion-exchange properties may prevail.

Using this approach, dynamically generated sorbents with controlled cation- or anion-exchange character and controlled capacity may be prepared. Owing to the charge compensation of the oppositely charged modifiers such systems have a considerably lower capacity than sorbents modified with a cationic or an anionic amphiphilic modifier only. Such sorbents, especially the low-capacity ones, may find applications in ion chromatography. Also, the mobile phase concentration of a certain modifier needed to generate a sorbent of a certain capacity is considerably higher when using it in a mixture with an oppositely charged modifier. This may result in a shorter time being needed to generate the sorbent until the retentions are constant.

TABLE I  
WAVELENGTHS OF ABSORPTION MAXIMA OF PLATINUM(II) COMPLEXES

pH = 5.9; for other conditions, see Experimental.

Complex	Formula	Maxima (nm)
<b>I</b>	<i>cis</i> -[Pt(NH <sub>3</sub> ) <sub>2</sub> Cl <sub>2</sub> ] <sup>0</sup>	ca. 275, 301.0, 365.5
<b>II</b>	<i>trans</i> -[Pt(NH <sub>3</sub> ) <sub>2</sub> Cl <sub>2</sub> ] <sup>0</sup>	270.5, 312.5
<b>III</b>	[Pt(NH <sub>3</sub> ) <sub>2</sub> (C <sub>6</sub> H <sub>6</sub> O <sub>4</sub> )] <sup>0</sup>	ca. 230, 316
<b>IV</b>	[PtCl] <sub>4</sub> <sup>2-</sup>	330.5, 391.0, ca. 480
<b>V</b>	[Pt(H <sub>2</sub> O)Cl <sub>3</sub> ] <sup>-</sup>	318, ca. 380
<b>VI</b>	<i>cis</i> -[Pt(H <sub>2</sub> O) <sub>2</sub> Cl <sub>2</sub> ] <sup>0</sup>	306.5
<b>VII</b>	[Pt(NH <sub>3</sub> )Cl <sub>3</sub> ] <sup>-</sup>	300.0, 344.5
<b>VIII</b>	[Pt(NH <sub>3</sub> ) <sub>3</sub> Cl] <sup>+</sup>	254.5, ca. 320
<b>IX</b>	[Pt(NH <sub>3</sub> ) <sub>4</sub> ] <sup>2+</sup>	286.5
<b>X</b>	<i>cis</i> -[Pt(NH <sub>3</sub> ) <sub>2</sub> (H <sub>2</sub> O)Cl] <sup>+</sup>	266.0, ca. 346
<b>XI</b>	<i>cis</i> -[Pt(NH <sub>3</sub> ) <sub>2</sub> (H <sub>2</sub> O) <sub>2</sub> ] <sup>2+</sup>	247.5, ca. 322
<b>UI</b>	( <i>trans</i> -[Pt(H <sub>2</sub> O) <sub>2</sub> Cl <sub>2</sub> ] <sup>0</sup> ) <sup>a</sup>	305.5, ca. 355

<sup>a</sup> Presumed.

## ACKNOWLEDGMENTS

We thank Dr. K. Šlais for the valuable discussions on the manuscript, Dr. I. Závodná and Dr. F. Kiss for the preparation of the complexes II and VI–IX and Mrs. A. Doubravová and Mrs. M. Weisslampelová for their assistance.

## REFERENCES

- M. Nicolini (Editor), *Platinum and Other Metal Coordination Compounds in Cancer Chemotherapy, Proceedings of XV ISPCG '87, Padua*, Martinus Nijhoff, Boston, 1988.
- F.R. Hartley, *The Chemistry of Platinum and Palladium*, Applied Science, Barking, 1973.
- C.M. Riley, L.A. Sternson and A.J. Repta, *J. Chromatogr.*, 217 (1981) 405–420.
- C.M. Riley, L.A. Sternson, A.J. Repta and R.W. Siegler, *J. Chromatogr.*, 229 (1982) 373–386.
- S.J. Bannister, L.A. Sternson and A.J. Repta, *J. Chromatogr.*, 273 (1983) 301–318.
- C.M. Riley, L.A. Sternson, A.J. Repta and S.A. Slyter, *Anal. Biochem.*, 130 (1983) 203–214.
- C.M. Riley, L.A. Sternson and A.J. Repta, *J. Pharm. Sci.*, 72 (1983) 351–355.
- C. Gooijer, A.C. Veltkamp, R.A. Bauman, N.H. Veltorst, R.W. Frei and W.J.F. van der Vijgh, *J. Chromatogr.*, 312 (1984) 337–344.
- K.C. Marsh, L.A. Sternson and A.J. Repta, *Anal. Chem.*, 56 (1984) 491–497.
- P.T. Daley-Yates and D.C.H. McBrien, *Biochem. Pharmacol.*, 32 (1983) 181–184.
- P.T. Daley-Yates and D.C.H. McBrien, *Biochem. Pharmacol.*, 33 (1984) 3063–3070.
- P.J. Parsons and A.F. LeRoy, *J. Chromatogr.*, 378 (1986) 395–408.
- P.J. Parsons, P.F. Morrison and A.F. LeRoy, *J. Chromatogr.*, 385 (1987) 323–335.
- W.A.J. de Waal, F.J.M.J. Maessen and J.C. Kraak, *J. Chromatogr.*, 407 (1987) 253–272.
- G.S. Baldew, K.J. Volkers, J.J.M. de Goeij and N.P.E. Vermeulen, *J. Chromatogr.*, 491 (1989) 163–174.
- R. Kizu, M. Kaneda and M. Miyazaki, *Anal. Sci.*, 8 (1992) 145–150.
- M. Macka, J. Borák and F. Kiss, *J. Chromatogr.*, 586 (1991) 291–295.
- B. de Spiegeleer, G. Slegers, W. van den Bossche and P. de Moerloose, *J. Chromatogr.*, 315 (1984) 481–487.
- A.A. Hincal, D.F. Long and A.J. Repta, *J. Parent. Drug Assoc.*, 33 (1979) 107–116.
- B.A. Persson, S.O. Jansson, M.L. Johansson and P.O. Lagerstrom, *J. Chromatogr.*, 316 (1984) 291–300.
- P. Helboe, S.H. Hansen and M. Thomsen, *Adv. Chromatogr.*, 28 (1989) 195–265.
- M. Macka, J. Borák, L. Seménková, M. Popl and V. Mikeš, *J. Liq. Chromatogr.*, in press.
- W.R. Sisco, C.T. Rittenhouse, L.A. Everhart and A.M. McLaughlin, *J. Chromatogr.*, 354 (1986) 355–366.
- S.L. Richeimer and T.M. Amer, *J. Pharm. Sci.*, 72 (1983) 1349–1351.
- J. Šalamoun and K. Šlais, *J. Chromatogr.*, 537 (1991) 247–257.
- L.I. Elding, *Dissertation*, Carl Blooms Botryckerei, Lund, 1970.
- I.I. Chernyaev, A.V. Babaeva, V.A. Golovnya, O.E. Zvyagintsev, L.A. Nazarova and I.A. Fedorov (Editors), *Sintez Kompleksnykh Soedinenii Metallov Platinovoi Gruppy (Spravochnik)*, Nauka, Moscow, 1964.
- S.C. Dhara, *Indian. J. Chem.*, 8 (1970) 193.
- A.J. Thomson, R.J.P. Williams and S. Reslova, *Struct. Bonding (Berlin)*, 11 (1972) 28–29, and references cited therein.
- M. Macka, J. Borák and L. Seménková, in preparation.
- N.M. Nikolaeva, B.V. Ptitsyn and I.I. Gorbacheva, *Zhur. Neorg. Khim.*, 10 (1965) 1051.
- K.A. Jensen, *Z. Anorg. Chem.*, 242 (1939) 87.
- The United States Pharmacopeia, XXII Revision*, Mack, Easton, PA, 1989.
- F. Kiss, *Dissertation*, Research Institute of Fine Chemicals, Lachema Brno, 1990.
- A.V. Babaeva and R.I. Rudyi, *Zhur. Neorg. Khim.*, 1 (1956) 921.
- J. Chatt, G.A. Gamlen and L.E. Orgel, *J. Chem. Soc.*, (1958) 486.
- H. Ito, J. Fujita and K. Saito, *Bull. Chem. Soc. Jpn.*, 42 (1969) 2863.



CHROM. 25 000

# Systematic analysis of naturally occurring linear and branched polyamines by gas chromatography and gas chromatography–mass spectrometry

Masaru Niitsu\* and Keijiro Samejima

*Faculty of Pharmaceutical Sciences, Josai University, 1-1 Keyakidai, Sakado, Saitama 350-02 (Japan)*

Shigeru Matsuzaki

*Department of Biochemistry, Dokkyo University School of Medicine, 880 Kitakobayashi, Mibu, Tochigi 321-02 (Japan)*

Koei Hamana

*College of Medical Care and Technology, Gunma University, 3-39-15 Showa, Maebashi, Gunma 371 (Japan)*

(First received November 13th, 1992; revised manuscript received February 22nd, 1993)

---

## ABSTRACT

Using heptafluorobutyl derivatives of a series of 27 linear di-, tri-, tetra-, penta- and hexamines containing various sets of isomers, and a series of four tertiary tetraamines and five quaternary pentaamines, mostly with three or four methylene chain units, their gas chromatographic (GC) and gas chromatographic–mass spectrometric (GC–MS) properties were compared and examined in detail. Several results useful for their systematic analysis were found: assured baseline separation of one methylene difference in linear di- and polyamines and tertiary tetraamines by GC; distinct pyrolytic decomposition patterns of quaternary pentaamines by GC; distinct cleavage patterns of three or four methylene chain units by GC–MS; and distinct mass spectra of linear polyamines and tertiary tetraamines by GC–MS.

---

## INTRODUCTION

Putrescine, spermidine and spermine are the most common di- and polyamines in living organisms, and are usually the target molecules in the field of polyamine research [1]. In the last decade, however, “unusual” aliphatic polyamines, including those possessing tertiary amine or quaternary ammonium groups, have been discovered successively from a variety of natural

sources. Most of them are shown with their chemical structures in Tables I and II [2–13]. These findings necessitated an improved and systematic method for their identification, and convincing proof of the major polyamines, spermidine and spermine, in natural sources.

During the course of the discovery of some unusual polyamines having linear or branched structures with three or four methylene chain units, we have extensively applied HPLC, GC and GC–MS to identify them, and found GC and GC–MS to be very useful in polyamine analysis [10–15, and references cited therein on methods for polyamine analysis]. This paper

---

\* Corresponding author.



TABLE I  
LINEAR DIAMINES AND POLYAMINES

Diamines	$H_2N(CH_2)_aNH_2$	Triamines	$H_2N(CH_2)_aNH(CH_2)_bNH_2$
	<i>a</i>		<i>a-b</i>
Diaminopropane	3	Norspermidine	3-3
Putrescine	4	Spermidine	3-4
Cadaverine	5	Homospermidine	4-4
		Aminopropylcadaverine	3-5
Tetraamines		$H_2N(CH_2)_aNH(CH_2)_bNH(CH_2)_cNH_2$	
		<i>a-b-c</i>	
Norspermine		3-3-3	
Thermospermine		3-3-4	
Spermine		3-4-3	
Aminopropylhomospermidine		3-4-4	
Canavalmine		4-3-4	
Homospermine		4-4-4	
Aminopentylhomospermidine		3-3-5	
N,N'-Bis(3-aminopropyl)cadaverine		3-5-3	
Pentaamines		$H_2N(CH_2)_aNH(CH_2)_bNH(CH_2)_cNH(CH_2)_dNH_2$	
		<i>a-b-c-d</i>	
Caldopentamine		3-3-3-3	
Homocaldopentamine		3-3-3-4	
Thermopentamine		3-3-4-3	
Aminopropylcanavalmine		3-4-3-4	
Aminobutylcanavalmine		4-3-4-4	
Homopentamine		4-4-4-4	
		3-3-4-4 <sup>a</sup>	
		3-4-4-3 <sup>a</sup>	
		4-3-3-4 <sup>a</sup>	
		3-4-4-4 <sup>a</sup>	
Hexaamines		$H_2N(CH_2)_aNH(CH_2)_bNH(CH_2)_cNH(CH_2)_dNH(CH_2)_eNH_2$	
		<i>a-b-c-d-e</i>	
Caldohexamine		3-3-3-3-3	
Homocaldohexamine		3-3-3-3-4	

<sup>a</sup> So far not discovered from natural sources.

deals with the simultaneous GC analysis of various polyamines, including those not previously discovered from natural sources, the characteristic degradation behaviour of branched

quaternary polyamines by GC and several characteristic mass fragment ions by GC-MS, all these being useful for differentiating and identifying structurally similar polyamines.

TABLE II  
BRANCHED POLYAMINES

Tertiary tetraamines	$\text{H}_2\text{N}(\text{CH}_2)_a\text{N} \begin{cases} (\text{CH}_2)_c\text{NH}_2 \\ (\text{CH}_2)_b\text{NH}_2 \end{cases}$
	<i>a(b)c</i>
N <sup>4</sup> -Aminopropylnor-spermidine	3(3)3
N <sup>4</sup> -Aminopropyl-spermidine	3(3)4 3(4)4 <sup>a</sup> 4(4)4 <sup>a</sup>
Quaternary pentaamines	$\text{H}_2\text{N}(\text{CH}_2)_a\text{N}^+ \begin{cases} (\text{CH}_2)_c\text{NH}_2 \\ (\text{CH}_2)_d\text{NH}_2 \\ (\text{CH}_2)_b\text{NH}_2 \end{cases}$
	<i>a(b)(c)d</i>
N <sup>4</sup> -Bis(aminopropyl)-norspermidine	3(3)(3)3
N <sup>4</sup> -Bis(aminopropyl)-spermidine	3(3)(3)4 3(3)(4)4 <sup>a</sup> 3(4)(4)4 <sup>a</sup> 4(4)(4)4 <sup>a</sup>

<sup>a</sup> So far not discovered from natural sources.

## EXPERIMENTAL

### Chemicals

All the polyamines listed in Tables I and II were obtained as hydrochloride salts. The following commercially available amines were used after recrystallization: diaminopropane and putrescine from Tokyo Kasei Kogyo (Tokyo, Japan), cadaverine from Wako (Osaka, Japan) and spermidine and spermine from Sigma (St. Louis, MO, USA). The other polyamines were synthesized in our laboratory [16,17]. Heptafluorobutyric anhydride (HFBA) was purchased from Wako.

### Preparation of HFB derivatives of polyamines

In the presence of 0.2 ml each of acetonitrile and HFBA, 200–300 nmol of dry residue of each polyamine hydrochloride were heated in a sealed tube at 100°C for 30 min. After cooling, the reaction mixture was evaporated with a stream

of nitrogen and the residue was dissolved in 0.5 ml of diethyl ether. The ether solution was washed with 0.5 ml of 0.5 M Na<sub>2</sub>CO<sub>3</sub> and centrifuged. The ether phase was displaced into a sample tube and an aliquot of the solution was injected into the GC or GC–MS system.

### Instruments

A GC-9A gas chromatograph (Shimadzu, Kyoto, Japan) equipped with a flame ionization detector was employed. A Pyrex glass column (2.1 m × 3 mm I.D.) was packed with 3% SE-30 on 100–120 mesh Chromosorb W HP (Gasukuro Kogyo, Tokyo, Japan). Helium was used as the carrier gas at a flow-rate of 40 ml/min. The temperatures of the injector and the detector were 300°C and the column oven temperature was programmed from 180 to 280°C at 8°C/min or from 100 to 280°C at 16°C/min.

A JMS-DX 300 mass spectrometer (JEOL, Tokyo, Japan) was employed for GC–MS and operated in the electron impact mode at an ionization energy of 70 eV. The GC conditions were almost the same as above.

## RESULTS AND DISCUSSION

In the GC analysis of polyamines, their pentafluoropropionyl (PFP) derivatives have often been used [3,9,18–20]. We also tried PFP derivatives in the initial stage of this work, but often encountered unknown decomposition peaks appearing behind each PFP polyamine peak on the gas chromatograms when PFP derivatives stored at –20°C were injected one day after derivatization. As instability seemed to be inevitable for PFP polyamines and made it difficult to analyse simultaneously as many polyamines as possible, we tested heptafluorobutyryl (HFB) derivatives of polyamines, and confirmed them to be very stable, *e.g.*, for at least one month at –20°C in diethyl ether extracts, as has also been reported by Fujihara *et al.* [21]. Subsequent studies were carried out with HFB derivatives of polyamines.

### Separation of HFB derivatives of diamines, linear polyamines and tertiary tetraamines by GC

A typical gas chromatogram of HFB derivatives of diamines and linear polyamines with

three, four, or five methylene chain units is shown in Fig. 1, in which the compounds listed in Table I are shown with their abbreviated forms expressing the numbers of methylene chain units. As can be seen, their retention times increased with the increasing number of amino groups, except for 4-4-4-4 and 3-3-3-3-3. Moreover, one methylene difference in a series of di-, tri-, tetra-, penta- or hexaamines was sufficient to obtain a baseline separation under the conditions described. Among the five pairs of tetraamines with identical molecular mass in each pair, *i.e.*, 3-3-4 and 3-4-3, 4-3-4 and 3-4-4, 3-3-5 and 3-5-3, 4-3-4 and 3-3-5, and 3-4-4 and 3-5-3, each isomer of the first three pairs was recognized as a separated peak, whereas those of the last two pairs were not separated. A difficulty in separation was also observed with a triamine pair, 4-4 and 3-5. With pentaamines, there are three sets of isomers, *i.e.*, 3-3-3-4 and 3-3-4-3; 4-3-4-4 and 3-4-4-4; and 4-3-3-4, 3-3-4-4, 3-4-3-4 and 3-4-4-3. Each isomer of the first two pairs was recognized as a separated peak, and the last four isomers gave three

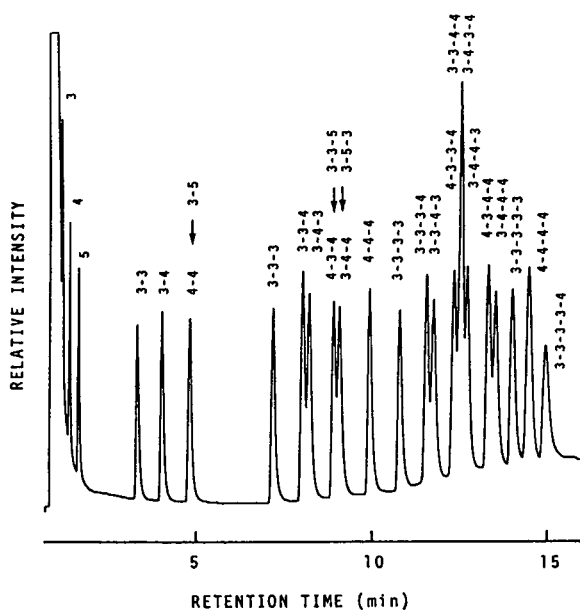


Fig. 1. Gas chromatogram of HFB derivatives of diamines and linear polyamines. The amount of each amine injected was *ca.* 1 nmol. For peak abbreviations, see Table I. GC column temperature increased from 180 to 280°C at 8°C/min.

adjoining peaks with an overlapped centre peak of 3-3-4-4 and 3-4-3-4. These results showed that an isomer having an aminobutyl group at its terminal portion eluted faster than the other isomer having an aminopropyl group.

A gas chromatogram of tris-HFB derivatives of a series of four tertiary tetraamines listed in Table II is shown in Fig. 2, with the indication of the elution positions of tetrakis-HFB derivatives of the corresponding linear tetraamines. Again, one methylene group difference among the tertiary tetraamines resulted in a baseline separation. Each tertiary tetraamine eluted faster than the corresponding linear tetraamine with the same molecular mass, and the retention times of 3(3)4 and 3(4)4 were almost the same as those of 3-3-3 and 3-3-4, respectively. This tendency might be simply explained by the difference in molecular mass of corresponding HFB derivatives, *e.g.*, tris-HFB 3(3)3 and tetrakis-HFB 3-3-3, but it should be noted that tertiary tetraamines modified by HFB still retain basic properties.

#### Gas chromatography of HFB derivatives of quaternary pentaamines

GC analysis of quaternary ammonium compounds has usually been performed with the

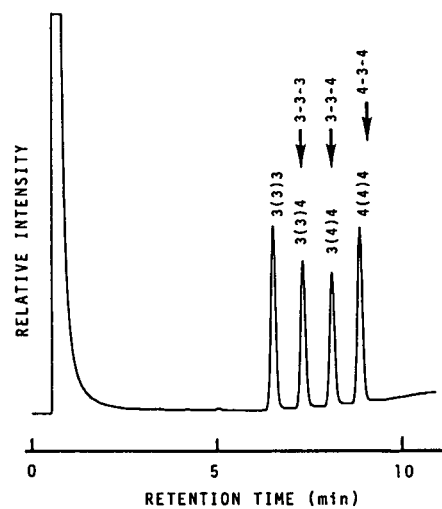


Fig. 2. Gas chromatogram of HFB derivatives of tertiary tetraamines. For peak abbreviations, see Table II. GC column temperature increased from 180 to 280°C at 8°C/min.

detection of pyrolytic decomposition products derived from the ammonium compound [22–25]. Gas chromatograms of tetrakis-HFB derivatives of a series of five quaternary pentaamines listed in Table II are shown in Fig. 3. Each HFB derivative was decomposed under the conditions described to reveal corresponding tertiary tetraamine(s) and HFB monoamine, *i.e.*, HFB allylamine derived from an eliminated aminopropyl group or HFB pyrrolidine derived from an eliminated aminobutyl group, which was identified by GC–MS, the latter being further

confirmed using an authentic pyrrolidine. Three quaternary pentaamines, 3(3)(3)4, 3(3)(4)4 and 3(4)(4)4, were expected to show two kinds of tertiary tetraamines, 3(3)3 and 3(3)4, 3(3)4 and 3(4)4, and 3(4)4 and 4(4)4, respectively. However, 3(4)(4)4 showed a single tertiary tetraamine corresponding to 3(4)4. Moreover, the major tertiary amine from 3(3)(3)4 was 3(3)3, its peak area being about five times greater than that of 3(3)4, and the major one from 3(3)(4)4 was 3(3)4, its peak area being about 20 times greater than that of 3(4)4. These results clearly

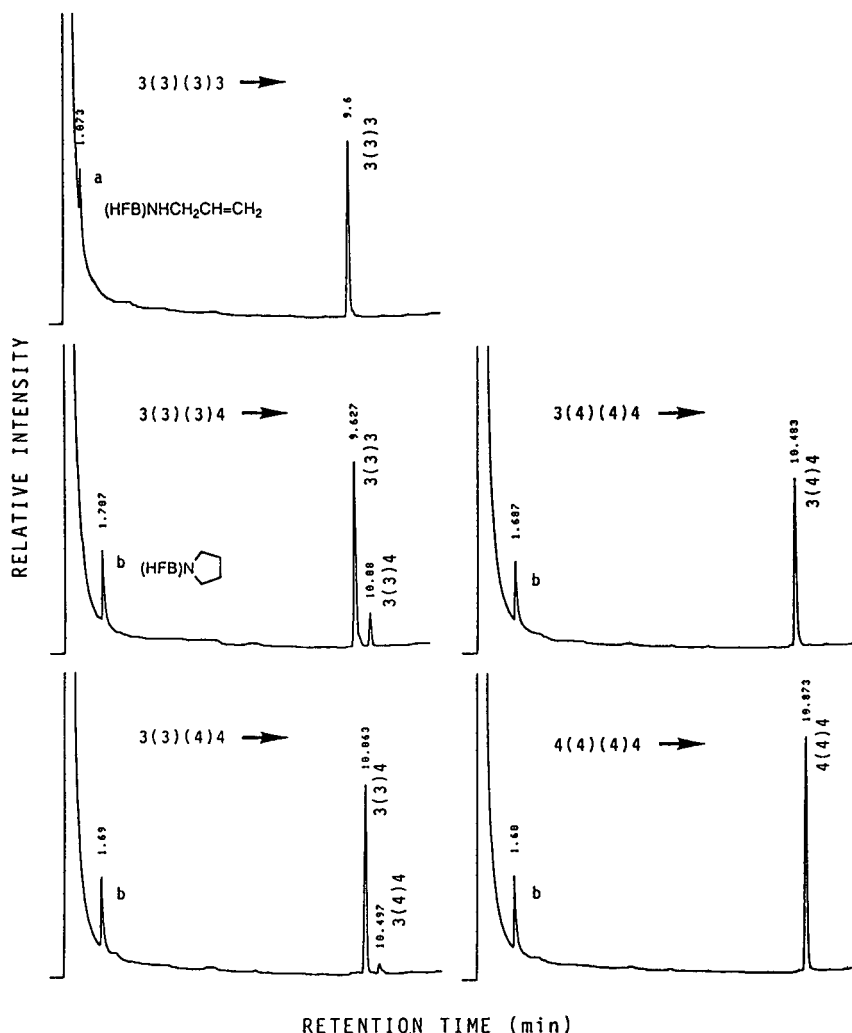


Fig. 3. Gas chromatograms of HFB derivatives of quaternary pentaamines. For peak abbreviations, see Table II. GC column temperature increased from 100 to 280°C at 16°C/min.

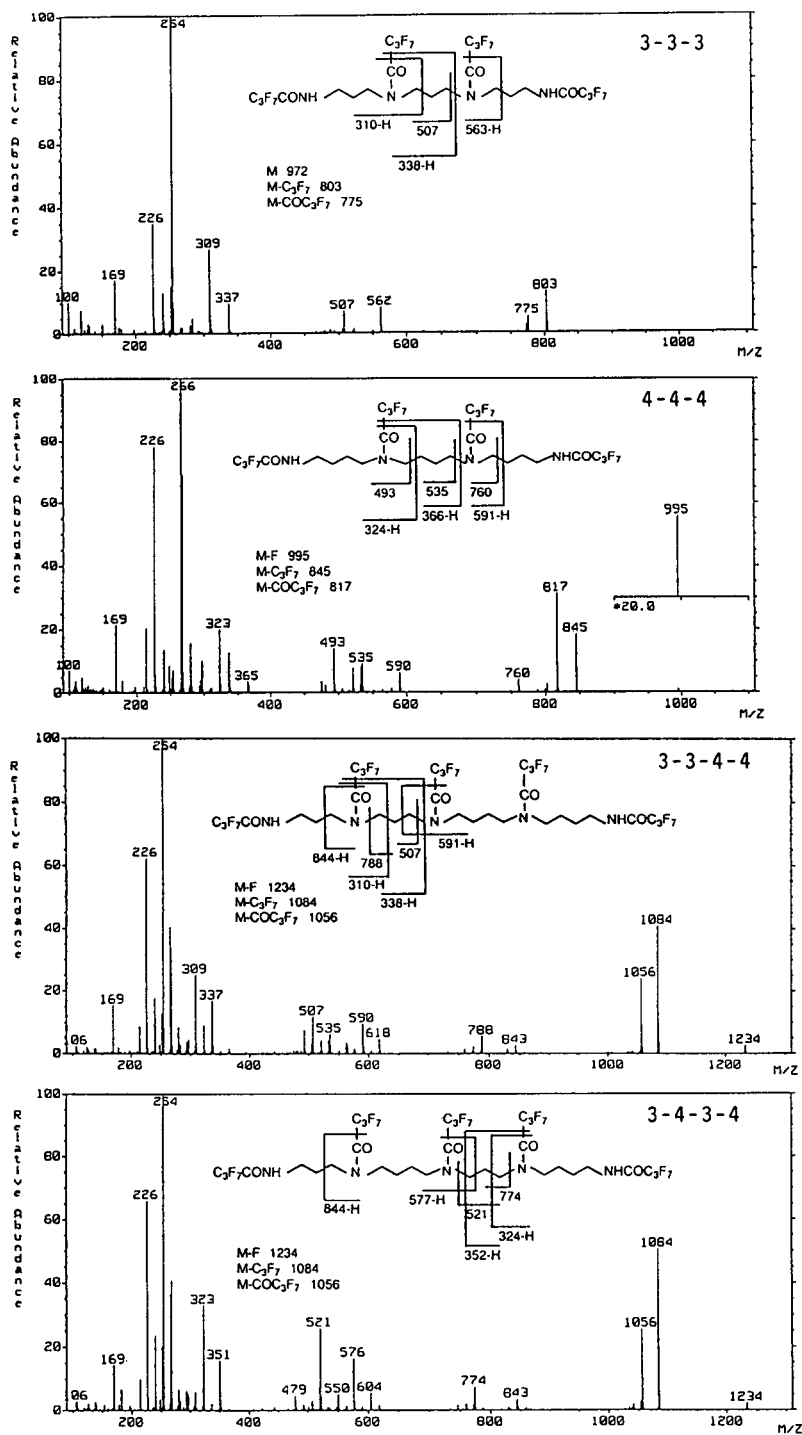


Fig. 4. Mass spectra of HFB derivatives of two comparable tetraamines and pentaamines.

show that elimination of the aminobutyl group occurred much more rapidly than elimination of the aminopropyl group in the quaternary pentaamines. The significant difference in the elimination rates of the two groups might be referred to two distinct mechanisms of elimination as were indicated by the two elimination products, HFB allylamine probably formed by Hofmann elimination [26] and HFB pyrrolidine by a cyclization reaction. These GC properties indicate that the presence of quaternary pentaamines must be tested by HPLC whenever a tertiary tetraamine is detected from unknown samples.

#### GC-MS of HFB derivatives of polyamines

GC-MS was very useful in identifying HFB derivatives of various polyamines, particularly when two compounds gave overlapping GC peaks, such as 3-3-4-4 and 3-4-3-4. Some useful information is presented below.

In a series of HFB derivatives of the diamines and the linear polyamines, molecular ions ( $M^+$ ) were detected at a relative intensity of 10–20% for the diamines and less than 2% for the triamines. Detection of  $M^+$  was difficult for the tetraamines, pentaamines and hexaamines. In these higher polyamines, instead, a pair of  $[M - C_3F_7]^+$  and  $[M - COC_3F_7]^+$  ions with relatively high intensity were useful for the determination of  $M^+$ .  $[M - F]^+$  ions observed with most of the polyamines were also useful, although their intensities were low in general.

Mass spectra of two simple tetraamines, 3-3-3 and 4-4-4, which were suitable for assigning fragment ions, are shown in Fig. 4 together with cleavage sites on their chemical structures. Cleavage sites of the C-C bond or N-C bond of the polyamine skeleton were similar in the two tetraamines, but there were some ions in the 4-4-4 spectrum that had no counterpart in the 3-3-3 spectrum (e.g.,  $m/z$  493 and 760). The mass spectra of the two pentaamines, 3-3-4-4 and 3-4-3-4, are also shown in Fig. 4. Fragment ions were assigned with reference to the information obtained from the 3-3-3 and 4-4-4 spectra. The two pentaamines were well distinguished by the comparison of fragment ions observed in the following four ranges of  $m/z$  values: 309–351, 479–521, 576–618 and 774–788. The fragment

ions observed in these ranges were found to be derived as the results of preferred cleavages of a three methylene chain unit to a four methylene chain unit. That is, the ions at  $m/z$  309 and 337 in the mass spectrum of 3-3-4-4 are assigned to  $C_3F_7CONH(CH_2)_3N(CO)CH_2 - H$  and  $C_3F_7CONH(CH_2)_3N(CO)(CH_2)_3 - H$ , respectively, and those at  $m/z$  323 and 351 in that of 3-4-3-4 to  $C_3F_7CONH(CH_2)_4N(CO)CH_2 - H$  and  $C_3F_7CONH(CH_2)_4N(CO)(CH_2)_3 - H$ , respectively, showing a difference of 14 mass unit between their corresponding mass fragment ions derived from the cleavage at similar sites on the inside three methylene chain unit.

The characteristic cleavage sites on the three or four methylene chain unit of the linear polyamines are summarized in Fig. 5 after confirmation for all polyamines listed in Table I. Cleavages of methylene chains between primary and secondary amines occurred at the C-C bond situated  $\alpha, \beta$  to the primary amine and at the C-N bond connected to the secondary amine. The mass fragment ion at  $m/z$  254 corresponding to the terminal aminopropyl moiety usually appeared as a base peak in the mass spectra of such

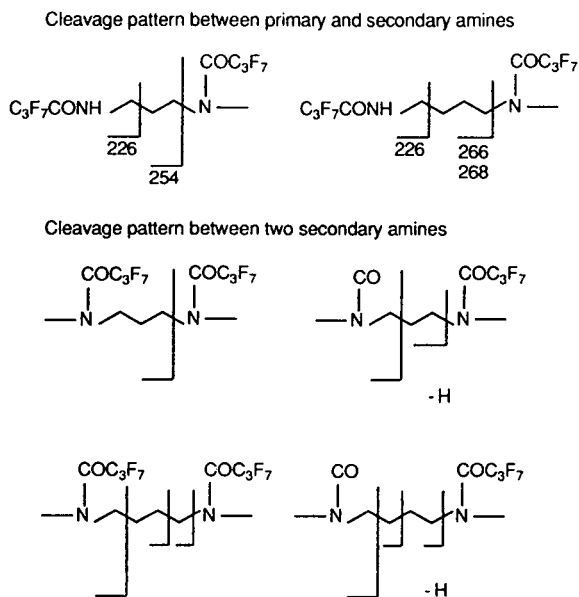


Fig. 5. Characteristic cleavage sites of the three and four methylene chain unit of the linear polyamines.

polyamines. Similarly, the mass fragment ions at  $m/z$  266 and 268 corresponding to the terminal aminobutyl moiety appeared with high relative abundance, e.g., 100 and 70%, respectively, for 4–4–4, 75 and 70% for 4–3–4, 75 and 80% for 4–3–3–4 and 100 and 75% for 4–4–4–4. Cleavages of methylene chains between two secondary amines, on the other hand, were more complicated, as shown in Fig. 5. They were classified into two groups: those which retain two entire HFB groups and those which lose  $C_3F_7$  from one of the HFB groups. In the former, cleavages occurred at C–N bonds for the three methylene unit and at C–C bonds situated  $\alpha,\beta$  to secondary amines in addition to C–N bonds for the four methylene unit. In the latter, with all fragment ions showing  $m/z$  values reduced by one mass unit, cleavages occurred at the C–N bond (nitrogen keeping HFB) and at the C–C bond situated  $\alpha,\beta$  to another nitrogen losing  $C_3F_7$  of HFB for the three methylene unit, and at the C–N bond (nitrogen keeping HFB) and the C–C bond situated  $\alpha,\beta$  or  $\beta,\gamma$  to another nitrogen losing

$C_3F_7$  of HFB for the four methylene unit. The decrease of one mass unit in these fragment ions can be explained by the loss of a hydrogen in the process of unstable dicationic ions generated on cleavage of two sites turning into stable monocationic ions. A mechanism specifying the hydrogen, however, is still open to question.

The mass spectra of two tertiary tetraamines, 3(3)4 and 3(4)4, are shown in Fig. 6. Significant fragment ions were observed at  $m/z$  536 and 550 for 3(3)4 and at  $m/z$  550 and 564 for 3(4)4. As the result of cleavage at the C–C bond situated  $\alpha,\beta$  to the tertiary amine, the former ions for 3(3)4 and 3(4)4 were assigned as  $M^+ - C_3F_7CONH(CH_2)_3$  and the latter as  $M^+ - C_3F_7CONH(CH_2)_2$ . It is a matter of course that a single significant ion was observed at  $m/z$  536 for 3(3)3 and at  $m/z$  564 for 4(4)4. These characteristic fragment ions often appeared as the base peak. It was easy from these results to distinguish linear tetraamines and tertiary tetraamines if they were overlapped, as in the case of 3–3–3 and 3(3)4 or 3–3–4 and 3(4)4 in Fig. 2.

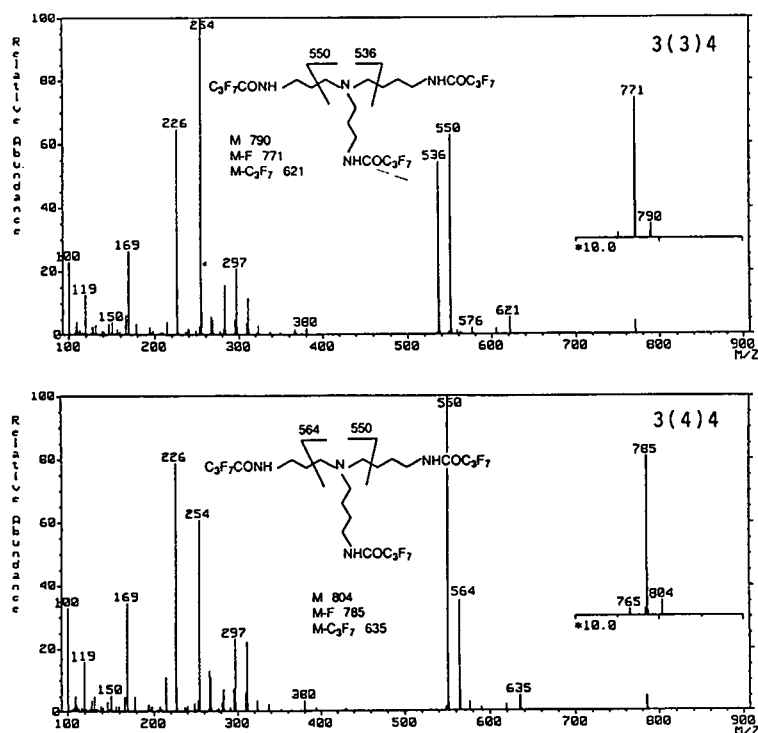


Fig. 6. Mass spectra of HFB derivatives of tertiary tetraamines containing both aminopropyl and aminobutyl groups.

## REFERENCES

- 1 A.E. Pegg, *Biochem. J.*, 234 (1986) 249.
- 2 T. Oshima, *J. Biol. Chem.*, 257 (1982) 9913.
- 3 S. Fujihara, T. Nakashima and Y. Kurogochi, *Biochem. Biophys. Res. Commun.*, 107 (1982) 403.
- 4 T. Oshima and S. Kawahata, *J. Biochem.*, 93 (1983) 1455.
- 5 T. Oshima and M. Senshu, in K. Imahori, F. Suzuki, O. Suzuki and U. Bachrach (Editors), *Polyamines: Basic and Clinical Aspects*, VNU Science Press, Utrecht, 1985, p. 113.
- 6 T. Oshima, N. Hamasaki, M. Senshu, K. Kakinuma and I. Kuwajima, *J. Biol. Chem.*, 262 (1987) 11979.
- 7 T. Oshima, N. Hamasaki and T. Uzawa, in V. Zappia and A.E. Pegg (Editors), *Progress in Polyamine Research*, Plenum Press, London, 1988, p. 633.
- 8 K. Hamana, M. Niitsu, K. Samejima and S. Matsuzaki, *FEMS Microbiol. Lett.*, 50 (1988) 79.
- 9 S. Fujihara and Y. Harada, *Biochem. Biophys. Res. Commun.*, 165 (1989) 659.
- 10 K. Hamana, M. Niitsu, K. Samejima and S. Matsuzaki, *FEMS Microbiol. Lett.*, 68 (1990) 27.
- 11 S. Matsuzaki, K. Hamana, M. Okada, M. Niitsu and K. Samejima, *Phytochemistry*, 29 (1990) 1311.
- 12 K. Hamana, M. Niitsu, K. Samejima and S. Matsuzaki, *J. Biochem. (Tokyo)*, 109 (1991) 444.
- 13 K. Hamana, M. Niitsu, K. Samejima and S. Matsuzaki, *Phytochemistry*, 30 (1991) 3319.
- 14 K. Hamana, M. Niitsu, S. Matsuzaki, K. Samejima, Y. Igarashi and T. Kodama, *Biochem. J.*, 284 (1992) 741.
- 15 K. Hamana, M. Niitsu, K. Samejima and S. Matsuzaki, *Phytochemistry*, 31 (1992) 1410.
- 16 M. Niitsu and K. Samejima, *Chem. Pharm. Bull.*, 34 (1986) 1032.
- 17 M. Niitsu, H. Sano and K. Samejima, *Chem. Pharm. Bull.*, 40 (1992) 2958.
- 18 T. Ohki, A. Saito and K. Ohta, *J. Chromatogr.*, 233 (1982) 1.
- 19 S. Fujihara and Y. Harada, *Soil Biol. Biochem.*, 21 (1989) 449.
- 20 K. Samejima, M. Furukawa and M. Haneda, *Anal. Biochem.*, 147 (1985) 1.
- 21 S. Fujihara, T. Nakashima and Y. Kurogochi, *J. Chromatogr.*, 277 (1983) 53.
- 22 K. Chan, N.E. Williams, J.D. Baty and T.N. Calvey, *J. Chromatogr.*, 120 (1976) 349.
- 23 F. Mikeš, G. Boshart, K. Wüthrich and P.G. Waser, *Anal. Chem.*, 52 (1980) 1001.
- 24 T. Lukaszewski, *J. Anal. Toxicol.*, 9 (1985) 101.
- 25 H. Tsuchihashi, M. Tatsuno and M. Nishikawa, *Eisei Kagaku*, 36 (1990) 28.
- 26 F. Leuzinger, M. Hesse and H. Schmid, *Helv. Chim. Acta*, 51 (1968) 1641.





# Quantitative analysis of polyethoxylated octylphenol by capillary supercritical fluid chromatography

Zhendi Wang\* and Merv Fingas

*Emergencies Science Division, River Road Environmental Technology Centre, Environment Canada, 3439 River Road, Ottawa K1A 0H3 (Canada)*

(First received October 30th, 1992; revised manuscript received March 8th, 1993)

---

## ABSTRACT

The rapid separation and quantitative determination of oligomers of polyethoxylated octylphenol surfactants was achieved using capillary supercritical fluid CO<sub>2</sub> chromatography. The oligomer distribution of all surfactants studied was graphically depicted, and the average ethylene oxide number of each individual surfactant was calculated. Temperature programming was investigated in combination with linear pressure programming to enhance long-chain surfactant analysis. The effect of the variable chromatographic parameters, including temperature, pressure programming ramp rate, and solvents used to prepare surfactant solutions, on the separation of polyethoxylated octylphenols are discussed. The capillary supercritical fluid chromatographic analysis results were validated by comparing them to the values obtained from C1 reversed-phase HPLC analyses.

---

## INTRODUCTION

Non-ionic surfactant polyethoxylated alkylphenols are used in a wide variety of applications, including liquid laundry detergents, wetting agents, emulsifiers, agricultural agents, biochemical research, and in institutional and industrial cleaners [1,2]. These surfactants are manufactured by the polymerization of ethylene oxide (EO) to alkylphenols. Consequently, these surfactants are complex mixtures in which the oligomer index, namely the number of EO units in each individual oligomer, varies over a considerable range.

The analysis of such complex samples is not trivial, and much research has been carried out in this area. It is possible to separate and identify oligomers of the Triton family of surfactants for which the EO units are relatively small (less than 5 units) by gas chromatographic (GC) analysis [3], although the prior formation of volatile

derivatives of such surfactants is usually required [3–5]. High-temperature GC (oven temperature of about 400–430°C) has been shown to be applicable for the analysis of Triton X-100, a higher-average-molecular-mass member of that family [6,7]. Alternatively, Stephanou [8,9] reported the identification and determination of polyethoxylated alkylphenols and linear alcohols in untreated municipal wastewaters by GC–mass spectrometry (MS) using chemical ionization.

Normal-phase high-performance liquid chromatography (HPLC) coupled with UV detection and fluorescence has been used for the separation and measurement of ethoxy oligomers in polyethoxylated alkylphenols [10–16]. For example, Macomini and co-workers [17,18] and Ahel and co-workers [19,20] recently reported on reversed-phase HPLC methods for simultaneous quantitation of linear alkyl benzenesulfonates (LAS) and polyethoxylated alkylphenols (PEAP) in wastewater and other environmental samples. In their methods, all oligomers of PEAP eluted out as one or two peaks and the determination of individual oligomers required

---

\* Corresponding author.

additional information from normal-phase HPLC. Allen and Rice [21] described a HPLC method for the separation of alkylphenol ethoxylate adducts of up to 9 or 10 EO units. Very recently, we reported on a rapid and simple approach for the separation and identification of polyethoxylated octylphenol surfactants that allows for the quantitative determination of the relative distribution of each oligomer using a C1 TMS (trimethylsilyl) column reversed-phase HPLC [22]. Polyethoxylated octylphenol oligomers up to 40 EO units (molecular mass up to approximately 2000) were satisfactorily separated and identified.

Parallel to the developments in high-temperature capillary GC, considerable progress has been achieved in supercritical fluid chromatography (SFC). The introduction of high-quality syringe pumps, narrow-bore capillary columns with immobilised stationary phase, density and pressure programming have made capillary SFC accessible for everyday chromatography. The high solvating power of supercritical fluid allows for the elution of high-molecular-mass components at much lower temperatures than in high-temperature GC. Capillary SFC was shown to be an effective means for the separation of ethoxylate adducts in polyethoxylated alcohol [23–25]. Knowles *et al.* [26] and colleagues recently published a review of polymer analysis by capillary supercritical fluid chromatography.

We are now reporting on a relatively simple, rapid and reproducible capillary SFC method for the separation and identification of polyethoxylated octylphenol surfactants, and on the determination of the ethylene oxide adduct distribution in each individual sample. The SFC analysis results are validated by comparing them to the values obtained from C1 reversed-phase HPLC analyses [22]. Work on the separation and the identification of polyethoxylated nonylphenols, by both capillary SFC and HPLC, will be presented elsewhere.

## EXPERIMENTAL

### Materials

All solvents were chromatographic grade and were used without further purification. The poly-

ethoxylated octylphenol surfactant samples (Triton is a trade name for many of these surfactants) were purchased from Sigma (St. Louis, MO, USA) and Rohm & Haas (Philadelphia, PA, USA), and were used as is. The surfactant samples were dissolved in dichloromethane and methanol at concentrations ranging from 1.0 mg/ml to 10.0 mg/ml, depending on the average EO numbers and average molecular masses of the samples. A solution of *tert.*-octyl phenol was used as standard for the capillary SFC analyses.

### Instrumentation

The capillary supercritical fluid chromatograph was made up of a Brownlee microgradient fluid delivery system (Brownlee Labs., Santa Clara, CA, USA), and a Hewlett-Packard Model 5890 gas chromatograph (Hewlett-Packard, Avondale, PA, USA) equipped with a flame ionization detector operated at 350°C. SFC-grade carbon dioxide (99.99%) with helium backpressure in the tank (Matheson Gas Products, East Rutherford, NJ, USA) was used as the mobile fluid. The pump cylinder was filled with liquid carbon dioxide at a starting pressure of 2000 p.s.i. (1 p.s.i. = 6894.76 Pa).

A Model 7520 Rheodyne microinjector equipped with a 0.5- $\mu$ l sample loop (Rheodyne, Cotati, CA, USA) was mounted above the oven of the gas chromatograph with the outlet stator flow-passage facing downward into the oven. The data were collected by a Hewlett-Packard integrator Model 3396.

The separation of surfactant oligomers was achieved using an isothermal linear pressure program for most of the samples investigated. A simultaneous linear pressure and temperature program was used for long-chain surfactant analysis to improve resolution, and especially to completely elute high-molecular-mass oligomers.

### Column and restrictor

A 5 m  $\times$  50  $\mu$ m SB-Biphenyl-30 (30% biphenyl, 70% methylpolysiloxane) with 0.25  $\mu$ m film thickness (Lee Scientific, Salt Lake City, UT, USA), equipped with an integrated on-column frit restrictor, was used. This type of restrictor resists plugging, allowing for fine tuning of the flow-rate. The outlet of the capillary

column was positioned into the flame ionization detector liner such that the restrictor end was even with the detector jet tip.

The capillary column was connected to the microinjector by means of a splitter. A 70 cm  $\times$  15  $\mu$ m fused-silica tubing was used as split restrictor to obtain an approximately 1:10 split ratio. The ratio can be modified by adjusting the length and the internal diameter of the split restriction tubing.

## RESULTS AND DISCUSSION

### Supercritical fluid chromatography separation

The solvating power of carbon dioxide is a function of its density, which in turn is dependent upon pressure. The elution of the various oligomers, for which volatility decreases as molecular mass increases, is accomplished by means of pressure programming. Non-ionic surfactant samples containing oligomers with EO units varying from 0 to 25 were investigated. Figs. 1 and 2 show SFC chromatograms of Triton X-102 and Triton X-100, respectively, using a linear

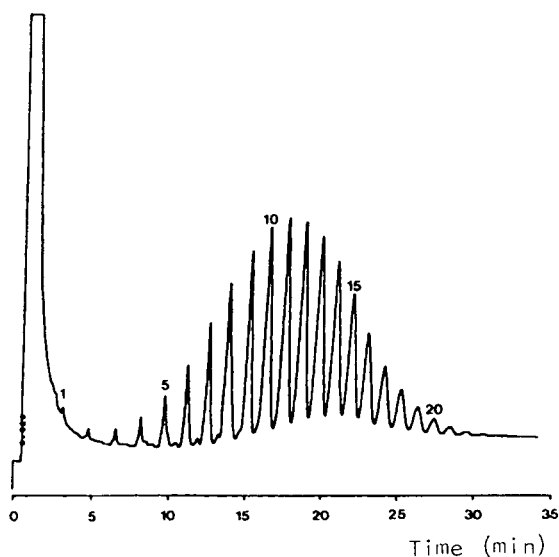


Fig. 1. Capillary SFC chromatogram of Triton X-102 (10.0 mg/ml) using a linear pressure program. Conditions: 5 m  $\times$  50  $\mu$ m SB-Biphenyl-30 column; linear pressure program from 2000 p.s.i. with 2-min initial hold to 5500 p.s.i. in 33 min; CO<sub>2</sub> mobile phase at 100°C; FID at 350°C; integrator attenuation at 2. The number assigned to the individual peaks represent the number of EO units in the oligomers.

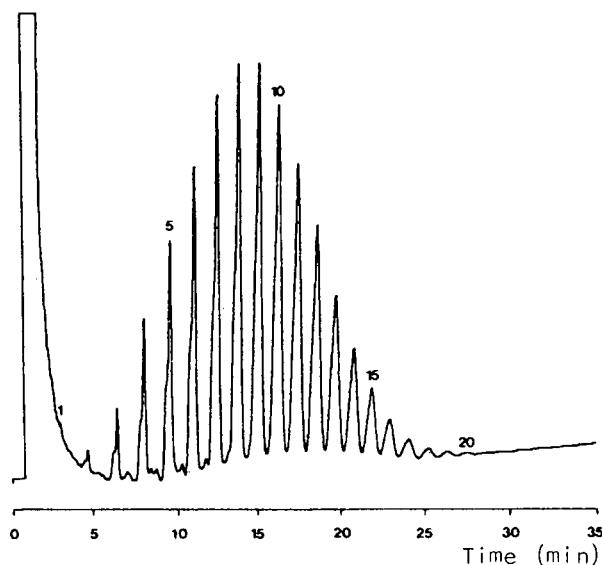


Fig. 2. Capillary SFC chromatogram of Triton X-100 (5.0 mg/ml) using a linear pressure program. Conditions are the same as those given in Fig. 1.

pressure program (starting from 2000 psi with 2 min hold, and then 2000 to 5500 p.s.i. in 33 min). Twenty-three peaks and twenty peaks can be discerned for Triton X-102 and Triton X-100, respectively. The numbers assigned to the individual peaks in Figs. 1 and 2 represent the number of EO units for each oligomer. The retention times can be correlated to the molecular masses and to the boiling points of the oligomers in the samples, the shorter-chain-length oligomers being eluted first. The peaks representing oligomers with increasing EO units, are nearly equally spaced throughout the chromatograms. The EO (23) octylphenol and the EO (20) octylphenol eluted at approximately 30.7 and 27.4 min are the last peaks visible in the chromatograms 1 and 2, respectively.

Because of the lack of single-EO-number octylphenol standards, the identification of these peaks was based on comparison of retention times with that of reference materials octylphenol (EO = 0) and Triton X-15 [its major component is EO (1) octylphenol], and on the assumption that they differ from each other by one EO unit; the rationale for this well-accepted assumption was presented elsewhere [16,22].

Figs. 1 and 2 show that there is a very slight

baseline drift as the pressure increases. The small shoulder eluted prior to the first oligomer peak (EO = 1) in Fig. 1 is the parent octylphenol remaining unconverted. The smaller intermediate peaks are thought to arise from alkyl groups of differing lengths but the same number of EO units as the main adjacent peak.

In capillary SFC, solute retention and its reproducibility is governed by a number of parameters such as the nature of the stationary and mobile phase, the pressure and/or density programming, the temperature, the injection technique and the mode of interfacing the capillary column to the valve. Under the chosen conditions (constant temperature and fixed fluid pressure program), the valve was manually actuated and good reproducibility for retention times and peak areas was achieved. Table I lists the average values of retention times and peak area percentages from typical 5 injections for the

analysis of Triton X-100. Table I shows that the reproducibility is quite satisfactory with the relative standard deviations (R.S.D.) for the retention times of less than 0.5% and for peak area percentages below 4.0%. The work reported by Richter *et al.* [27] showed that the injection valve actuated by air or helium may give better precision and reproducibility.

#### *Oligomer distribution and its comparison with HPLC results*

In order for the method to be able to produce quantitative distributions, the flame ionization detection (FID) response factors for each individual oligomer should be known, in addition to acceptable separation of the components and the identity of the various ethoxylate peaks. Some authors have discussed FID response factors for quantitative analyses [28–32]. Single-EO-number octylphenols were not available to

TABLE I  
REPRODUCIBILITY OF RETENTION TIME AND PEAK AREA PERCENTAGE OF TRITON X-100

Peak	Retention time <sup>a</sup>			Peak area		
	Average (min)	S.D. (min)	R.S.D. (%)	Average (%)	S.D. (%)	R.S.D. (%)
1	3.18	0.018	0.56	0.114	0.004	3.58
2	4.79	0.014	0.28	0.420	0.015	3.48
3	6.577	0.030	0.46	1.411	0.049	3.45
4	8.233	0.035	0.43	3.311	0.043	1.29
5	9.794	0.037	0.38	5.354	0.056	1.04
6	11.254	0.042	0.37	7.206	0.044	0.62
7	12.635	0.045	0.36	9.425	0.076	0.80
8	13.938	0.048	0.34	11.396	0.079	0.69
9	15.193	0.047	0.31	12.433	0.052	0.42
10	16.383	0.061	0.37	12.184	0.029	0.24
11	17.538	0.046	0.26	10.788	0.064	0.59
12	18.659	0.057	0.31	8.761	0.072	0.82
13	19.724	0.058	0.30	6.532	0.050	0.76
14	20.788	0.080	0.39	4.496	0.034	0.75
15	21.839	0.056	0.26	2.851	0.025	0.88
16	22.912	0.085	0.37	1.669	0.035	2.10
17	23.977	0.085	0.36	0.901	0.027	2.95
18	25.08	0.083	0.33	0.451	0.013	2.90
19	26.23	0.082	0.31	0.204	0.008	3.87
20	27.43	0.082	0.30	0.082	0.003	3.68
Average of total area (counts)	2 851 164 (S.D.: 117 768; R.S.D.: 4.13%)					
Average EO number ( $\bar{n}$ )	9.51					

<sup>a</sup> S.D. = Standard deviation; R.S.D. = relative standard deviation (5 injections).

us, hence, the area percentage method was used to calculate the oligomer distribution and the sample molecular mass (see ref. 22 about the detailed discussion for the mathematical quantitation of the average EO number and average molecular mass). The accuracy of this method was evaluated by comparing the calculated results with the values obtained from the HPLC analysis of the same samples. It has been demonstrated that the octylphenol oligomers have nearly equal molar absorptivities at the selected UV wavelengths, and therefore the molar response factor for all oligomers can be taken as equal [16,22] in HPLC measurements.

Once each sample had been run and each peak representing a different oligomer had been identified, the peak areas were tabulated. Table II lists the peak area percentages for Triton X-102

oligomers from four repeated analyses. The average area percentage for each peak, standard deviations and relative standard deviations are also given in Table II. The average EO number for Triton X-102 was determined to be 11.67. As comparison, the corresponding value obtained from HPLC analysis was 11.61 [22]. Fig. 3 shows the oligomer distribution curves of Triton X-102 by SFC and HPLC analysis.

Table III lists the peak area percentages, standard deviations, relative standard deviations, and the average EO number for Triton X-15, Triton X-35 and Triton X-45. Their EO units range from 1 to 11. Similarly, Table IV gives the data for two other longer-chain polyethoxylated octylphenol samples (Triton X-114 and Triton X-165) with EO units ranging from 1 to 25. All statistical data given in Tables III and IV are

TABLE II  
REPRODUCIBILITY OF PEAK AREA PERCENTAGE FOR THE ANALYSIS OF TRITON X-102

Peak	Peak area (%)				Average (%)	S.D. (%)	R.S.D. (%)
	Run 1	Run 2	Run 3	Run 4			
1	0.148	0.174	0.158	0.160	0.160	0.011	6.69
2	0.214	0.251	0.229	0.231	0.231	0.015	6.69
3	0.352	0.402	0.367	0.355	0.369	0.023	6.22
4	0.821	0.702	0.690	0.728	0.735	0.059	8.07
5	1.469	1.463	1.409	1.464	1.451	0.028	1.95
6	2.332	2.303	2.301	2.314	2.313	0.014	0.61
7	3.670	3.649	3.826	3.606	3.688	0.096	2.60
8	5.751	5.666	5.654	5.669	5.685	0.044	0.78
9	7.817	7.727	7.687	7.658	7.722	0.069	0.90
10	9.552	9.543	9.438	9.409	9.486	0.073	0.77
11	10.803	10.840	10.673	10.668	10.746	0.089	0.82
12	11.117	11.215	11.117	10.994	11.111	0.091	0.81
13	10.707	10.801	10.745	10.725	10.745	0.041	0.38
14	9.547	9.631	9.618	9.552	9.587	0.044	0.46
15	7.862	7.931	7.940	7.950	7.921	0.040	0.50
16	6.055	6.110	6.236	6.285	6.172	0.107	1.74
17	4.344	4.382	4.454	4.469	4.412	0.059	1.34
18	3.050	2.949	3.128	3.113	3.060	0.081	2.66
19	1.899	1.881	1.917	2.046	1.936	0.075	3.87
20	1.206	1.172	1.186	1.281	1.211	0.049	4.01
21	0.733	0.690	0.701	0.755	0.720	0.030	4.13
22	0.366	0.340	0.351	0.377	0.359	0.016	4.55
23	0.182	0.173	0.175	0.189	0.180	0.007	4.05
Total area (counts)	4 835 871	4 809 275	5 241 771	4 558 626	4 861 386	282 679	5.81
Average EO number (n)	11.67						

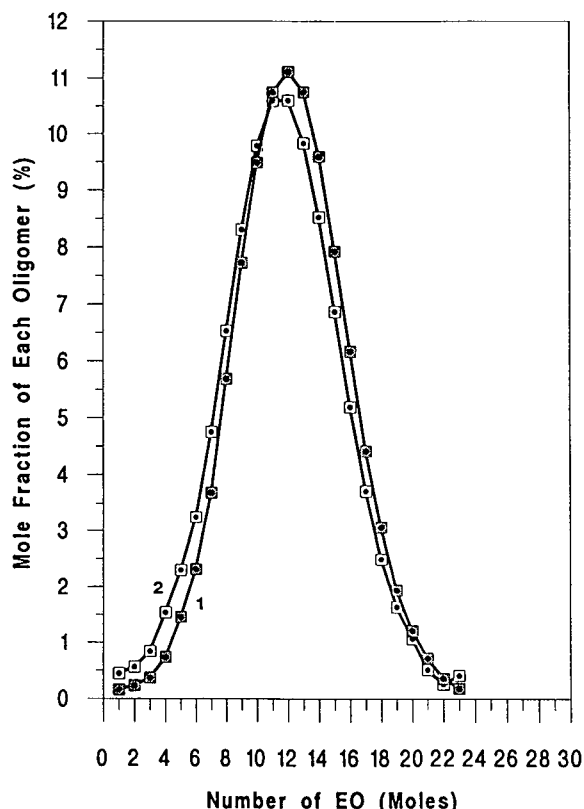


Fig. 3. Oligomer distribution curves for Triton X-102. (1) by capillary SFC; (2) by C1 reversed-phase HPLC.

obtained from four analyses for each sample. The average EO number for these six surfactants are determined to be 1.25, 3.23, 4.50, 7.63, 9.51 and 15.19, respectively. The corresponding values by HPLC measurement are 1.21, 2.99, 4.32, 7.43, 9.42 and 14.70.

Figs. 4 and 5 depict graphically the oligomer distribution as determined for samples given in Tables III and IV, respectively. For comparison purposes, Figs. 4 and 5 also present the oligomer distribution curves for Triton X-15, Triton X-35 and Triton X-45, and for Triton X-114, Triton X-100 and Triton X-165 from HPLC analyses. The Poisson distribution for samples having lower molecular masses and the Gaussian distribution for samples having higher molecular masses are obvious.

From Figs. 3 through 5, it is evident that the EO distributions obtained from SFC and from HPLC analyses are basically identical.

#### *Effect of temperature on separation of oligomers*

The influence of temperature on the separation of oligomers is illustrated in Fig. 6 and in Table V. In Fig. 6, chromatograms of Triton X-35 at four different temperatures (100, 110, 130 and 150°C) are shown. The pressure pro-

TABLE III

AREA PERCENTAGE AND AVERAGE EO NUMBER OF TRITON X-15, X-35 AND X-45

Peak	Triton X-15			Triton X-35			Triton X-45		
	Aver. area (%)	S.D. (%)	R.S.D. (%)	Aver. area (%)	S.D. (%)	R.S.D. (%)	Aver. area (%)	S.D. (%)	R.S.D. (%)
1	76.659	0.759	0.99	5.304	0.103	1.94	0.901	0.012	1.33
2	21.501	0.659	3.06	28.921	0.537	1.86	11.367	0.139	1.22
3	1.84	0.17	9.24	30.089	0.595	1.98	21.501	0.300	1.40
4				19.299	0.220	1.14	22.590	0.200	0.89
5				9.298	0.464	4.99	17.262	0.205	1.19
6				4.483	0.273	6.09	11.897	0.182	1.53
7				1.681	0.200	11.90	7.192	0.094	1.31
8				0.636	0.080	12.58	4.134	0.105	2.54
9				0.289	0.025	8.65	1.927	0.071	3.68
10							0.876	0.031	3.54
11							0.354	0.021	5.93
Total (%)	100			100			100		
Average EO number		1.25			3.23			4.50	

TABLE IV  
AREA PERCENTAGE AND AVERAGE EO NUMBER OF TRITON X-114 AND X-165

Peak	Triton X-114			Triton X-165		
	Aver. area (%)	S.D. (%)	R.S.D. (%)	Aver. area (%)	S.D. (%)	R.S.D. (%)
1	0.220	0.008	3.73	0.242	0.014	5.79
2	1.100	0.040	3.64	0.252	0.010	3.97
3	4.352	0.052	1.19	0.224	0.010	4.46
4	8.281	0.058	0.70	0.255	0.011	4.31
5	11.157	0.059	0.53	0.358	0.019	5.31
6	12.375	0.030	0.24	0.493	0.011	2.23
7	13.254	0.268	2.02	0.783	0.032	4.09
8	12.956	0.063	0.49	1.479	0.058	3.92
9	11.223	0.056	0.50	2.552	0.044	1.72
10	8.858	0.058	0.65	3.956	0.026	0.66
11	6.406	0.026	0.41	5.607	0.021	0.37
12	4.283	0.016	0.37	7.351	0.041	0.56
13	2.670	0.033	1.24	8.866	0.032	0.36
14	1.548	0.037	2.39	10.128	0.087	0.86
15	0.880	0.021	2.39	10.680	0.037	0.35
16	0.439	0.010	2.28	10.074	0.015	0.15
17				9.102	0.038	0.42
18				7.973	0.042	0.53
19				6.134	0.077	1.26
20				4.797	0.034	0.71
21				3.320	0.060	1.81
22				2.261	0.054	2.39
23				1.678	0.046	2.74
24				0.919	0.020	2.18
25				0.518	0.012	2.32
Total (%)	100			100		
Average EO number		7.63			15.19	

gram was the same for all cases: 2 min at 2000 p.s.i., then a linear pressure ramp up to 5000 p.s.i. in 28 min, and then 5 min with pressure downward to 2000 p.s.i. The last peak was EO (9) octylphenol and eluted at 14.6, 15.2, 16.4 and 17.0 min for the four different temperatures, respectively.

Some peak splitting was observed in Fig. 6. The lower the temperature, the more pronounced the peak splitting. When temperature was increased to 150°C, no peak splitting was observed for those relatively low-molecular-mass ethoxy adducts.

Table V lists the retention times for the solvent and nine oligomers at four different temperatures. Table V shows that at lower temperature, a longer time was needed for the elution of the

first oligomer and a shorter time, however, was needed for complete elution of all components.

Work has been reported on the theoretical aspects involved with temperature effects on the separation of compounds [33]. A combination of factors is responsible for the poor performance at relatively low temperature. First, a better separation of the lower-molecular-mass components can be achieved with GC-like conditions. This means that at the same pressure and at a higher temperature, the density of the mobile phase is lower and that the chromatographic conditions are more like those of GC, which leads to a more rapid diffusion and a higher efficiency. Secondly, lower temperature is unfavourable to mass transfer, as discussed by Novotny *et al.* [34] in a paper about the tempera-



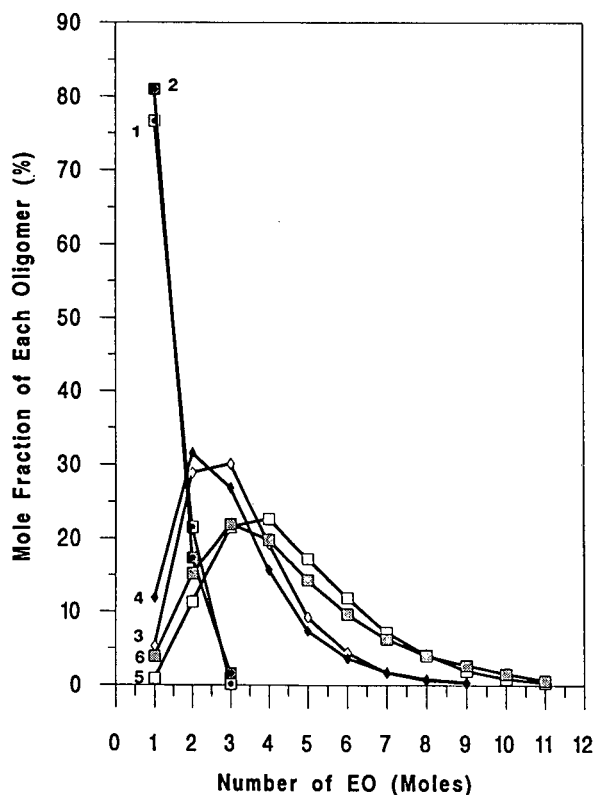


Fig. 4. Oligomer distribution curves for Triton X-15, Triton X-35 and Triton X-45. Triton X-15: (1) by capillary SFC; (2) by C1 reversed-phase HPLC. Triton X-35: (3) by capillary SFC; (4) by C1 reversed-phase HPLC. Triton X-45: (5) by capillary SFC; (6) by C1 reversed-phase HPLC.

ture effect in SFC and by Schwartz *et al.* [35] in work on simulated distillation of high-boiling petroleum fractions by capillary SFC. Finally, a lower temperature results in a decrease in solubility for the non-volatile surfactant oligomers. Chromatographically, this brings about a decrease in peak heights and areas. Consequently, better resolution and higher sensitivity can be obtained at higher temperature (*e.g.* 150°C for Triton X-35). However, it must be noted that the optimum temperature for different samples is not the same. For the Triton family of surfactants, a lower temperature is preferred for samples containing relatively high-molecular-mass oligomers. Studies showed that 150°C was the optimal temperature for the separation of Triton X-15, Triton X-35, and Triton X-45, whereas

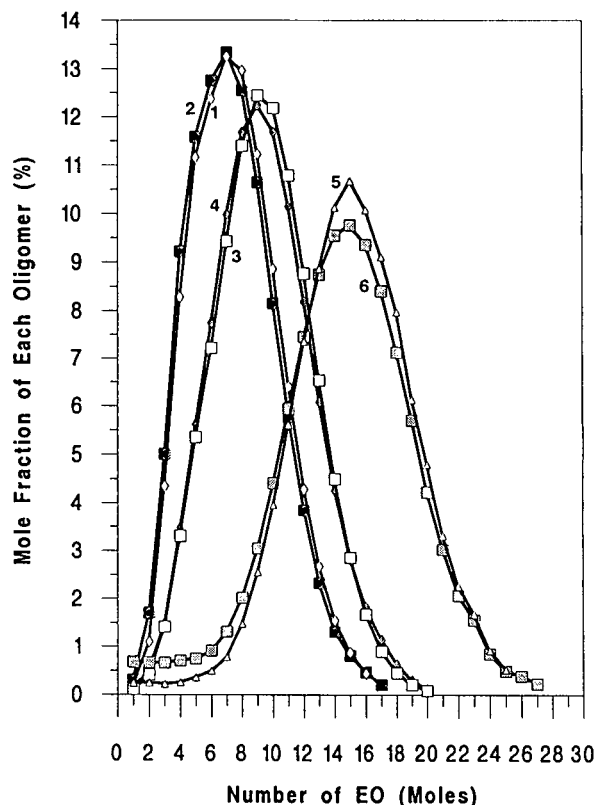


Fig. 5. Oligomer distribution curve for Triton X-114, Triton X-100 and Triton X-165. Triton X-114: (1) by capillary SFC; (2) by C1 reversed-phase HPLC. Triton X-100: (3) by capillary SFC; (4) by C1 reversed-phase HPLC. Triton X-165: (5) by capillary SFC; (6) by C1 reversed-phase HPLC.

100°C was optimum for Triton X-114, Triton X-100, Triton X-102, and Triton X-165.

Temperature programming was investigated in combination with pressure programming in order to enhance the performance of longer-chain surfactant analysis. Fig. 7 shows the chromatogram of Triton X-165 using a simultaneous temperature-decreasing programming (5 min initial hold at 100°C, then to 88°C in 30 min at  $-0.4^{\circ}\text{C}/\text{min}$ , and then 10 min for 88°C hold time) and pressure-increasing programming. Improved peak shape, better resolution and shorter analysis time for complete elution is achieved, compared with the chromatograms using varying simultaneous temperature-increasing and pres-

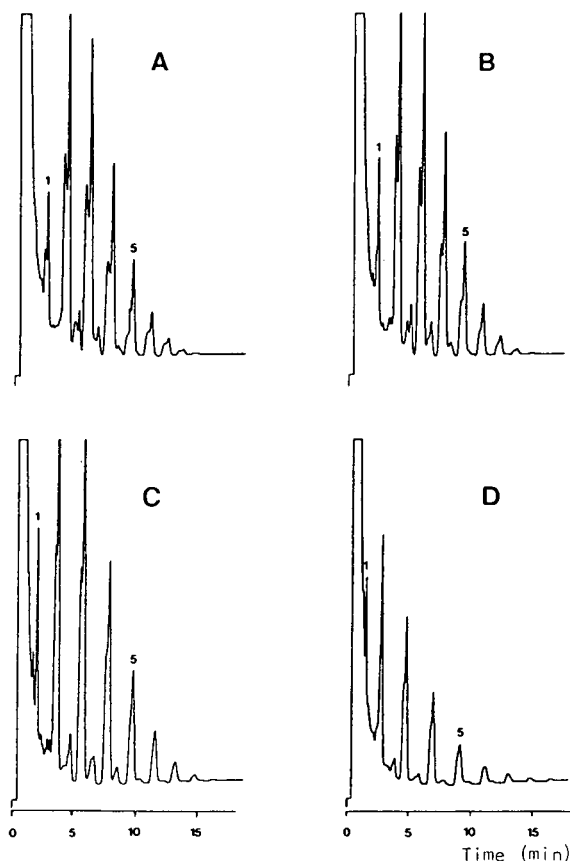


Fig. 6. Effect of temperature on the SFC separation of Triton X-35 oligomers. A, B, and C: isothermally at 100°, 110° and 130°C, respectively, and concentration of Triton X-35, 2.5 mg/ml. D: isothermally at 150°C; 1.0 mg/ml. Other conditions same as in Fig. 1.

sure-increasing programmings. This may be mainly because simultaneous temperature decrease and pressure increase lead to greater increase in fluid density and solvating power, resulting in an increased solubility of higher-molecular-mass components of Triton X-165 in the supercritical fluid.

It has been noticed that the data obtained from studying the influence of temperature on the separation of Triton surfactant oligomers are contrary to data already published by Later *et al.* [36] and Knowles *et al.* [26]. Their data show that enhanced resolution for some other polymers was obtained using a combination of positive temperature and pressure or density pro-

TABLE V

EFFECT OF TEMPERATURE ON THE SEPARATION OF TRITON X-35 OLIGOMERS

Peak No.	Retention time (min)			
	100°C	110°C	130°C	150°C
Solvent	0.558	0.545	0.525	0.510
1	2.41	2.27		
	2.66	2.44	1.99	1.61
2	3.98	3.89	3.46	2.98
	4.38	4.21	3.69	
3	5.74	5.80	5.54	
	6.19	6.17	5.81	5.02
4	7.51	7.60		
	7.96	7.95	7.88	7.27
5	9.25	9.31		
	9.63	9.61	9.85	9.53
6	10.82			
	11.16	11.14	11.66	11.56
7	12.24			
	12.57	12.58	13.39	13.50
8	13.52	13.94	14.94	15.30
9	14.62	15.24	16.44	17.00

gramming. More studies need to be done to find out the reasons for the discrepancies between these data.

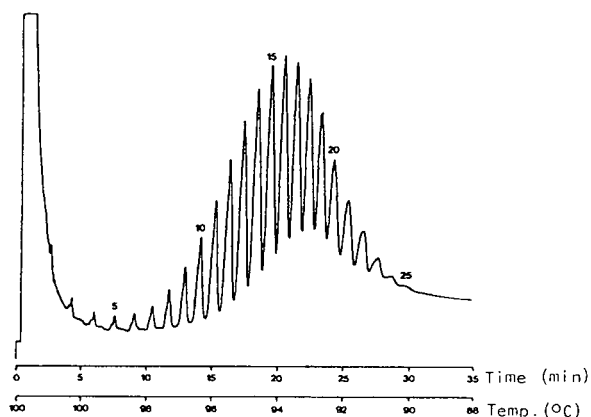


Fig. 7. Capillary SFC chromatogram of Triton X-165 (10.0 mg/ml) using a simultaneous linear pressure/temperature program. Linear pressure program from 2000 p.s.i. (2 min initial hold) to 5500 p.s.i. in 33 min; linear temperature programmed simultaneously from 100°C (5 min initial hold) to 88°C at  $-0.4^{\circ}\text{C}/\text{min}$ . Other conditions are the same as in Fig. 1.

### Effect of solvent on separation of oligomers

Two solvents —methanol and dichloromethane— were used to prepare solutions of polyethoxylated octylphenol samples. All samples tested can readily be dissolved in these two solvents. It is interesting to note that the chromatograms obtained from solutions which were made from the same surfactant at the same concentration, but with different solvents, are quite different. Fig. 8 shows the typical chromatograms of Triton X-114 under identical SFC conditions.

There are three differences between Fig. 8A and B: (1) the baseline of Triton X-114 in methanol is much better, and all components are completely resolved to the baseline. (2) The peak profiles in Fig. 8A are much better, the peak width is smaller and the sensitivity is higher. (3) The elution time is different. For the methanol solution, it ranges between 3.89 to 21.96 min, whereas it ranges from 4.60 to 22.57 min for dichloromethane solution.

The non-aqueous surfactant solution is a very complex system [37]. The microstructure of surfactant micelle may be different in different solvents with different physical and chemical properties (for example, the boiling point and the Hildebrand solubility parameter of methanol are 64°C and 14.4, and 40°C and 9.7 for dichloromethane, respectively), which could result in different chromatographic behaviour. Another possible reason for such phenomena may be that the diffusion of the analyte varies with the solvents used. Prior to injection, all components are equally dissolved in solvents. However, right after injection, a much faster evaporation of the dichloromethane at the top of capillary column, combined to a constant transfer rate onto the column, lead to an analyte concentration gradient, resulting in wider peaks and incomplete resolution of the oligomers.

### Effect of pressure programming ramp rate

In order to optimize the SFC condition, the analyst must use conditions which maximize diffusion of analytes into the mobile phase. The most important parameters which affect analyte diffusion are temperature and pressure. When

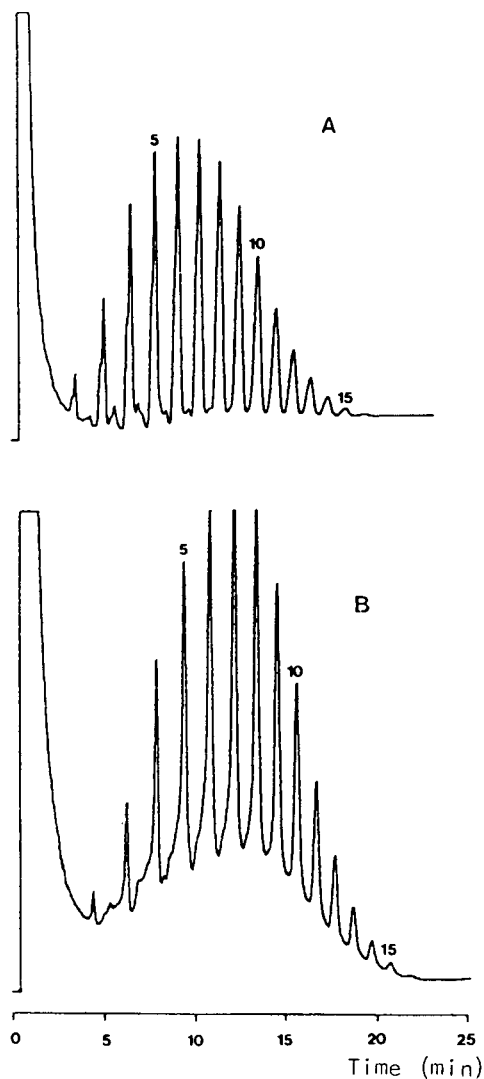


Fig. 8. Effect of solvent on the SFC separation of Triton X-114 (5.0 mg/ml) oligomers under identical SFC conditions as Fig. 1. The upper trace, chromatogram of Triton X-114 methanol solution, integrator attenuation at 2; the lower trace, chromatogram of Triton X-114 dichloromethane solution, integrator attenuation at 1.

the analysis is performed isothermally at 100°C, the retention and resolution will strongly depend on the pressure programs used. Fig. 9 shows the chromatogram of Triton X-102 in 0–35 min using the chromatographic conditions identical to those used in Fig. 1 except for using a low-pressure programming ramp rate —starting from

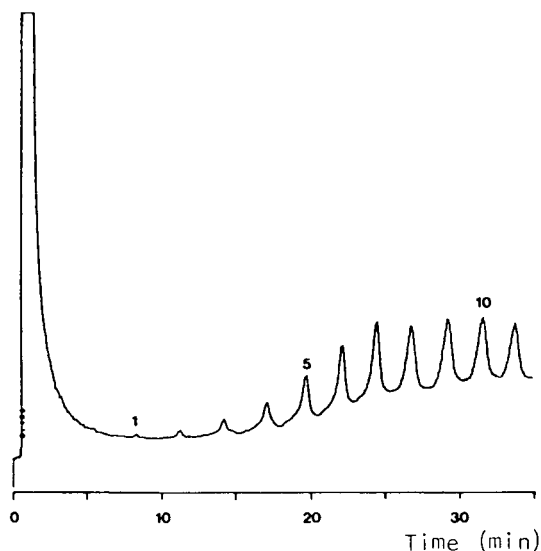


Fig. 9. Capillary SFC chromatogram of Triton X-102 using identical conditions as Fig. 1 but approximately half that of the pressure program ramp used in Fig. 1 (pressure ramp rate starting from 2000 p.s.i. and 2 min initial hold, and then linear pressure ramp to 5000 p.s.i. in 58 min, instead of 33 min).

2000 p.s.i. pressure with 2 min hold, then applying a linear pressure ramp to 5000 p.s.i. in 58 min, approximately one-half of the pressure ramp rate used for data presented in Fig. 1.

The most striking difference observed between Figs. 1 and 9 is that using the low-pressure ramp rate programming, the highest oligomer eluted in 35 min was the one with EO number = 11, and in contrast, the highest oligomer using the high-pressure ramp rate programming was the one with EO number = 23. In addition, the peaks were largely broadened, the sensitivity was much decreased, and the first two oligomers in the early part of the chromatogram were barely distinguished from the baseline, which can be clearly seen from Fig. 9. In general, if optimal resolution is achieved, the higher pressure programming rate would be preferred so as to shorten the analysis time and to increase the analysis sensitivity.

## CONCLUSIONS

In this paper, a method for the analysis of

non-ionic surfactant polyethoxylated octylphenols using capillary supercritical fluid chromatography has been described. The validity of the capillary SFC methods was examined and demonstrated by comparing the SFC results with corresponding data obtained from HPLC analysis. The advantage of the HPLC method is its simplicity because all oligomers of polyethoxylated alkylphenols have nearly equal molar absorptivities, and therefore the response factor of all oligomers can be considered equal. However, its applicability is limited to the compounds containing UV-absorbing chromophores. Compared with GC, the capillary SFC-FID system operates at a relatively low temperature. It provides another effective, convenient and economic means for the analysis of non-ionic surfactants. It is expected that reasonable results may be obtained for the analysis of more complex and higher molecular-mass surfactant oligomers and components using supercritical fluid chromatography coupled with a universal detection method such as FID.

## REFERENCES

- 1 P.L. Layman, *Chem. Eng. News*, January (1984) 17.
- 2 P.L. Layman, *Chem. Eng. News*, January (1986) 21.
- 3 H.G. Nadeau, D.M. Oaks, Jr., W.A. Nichols and L.P. Carr, *Anal. Chem.*, 36 (1964) 1914.
- 4 F.J. Ludwig, Sr., *Anal. Chem.*, 40 (1968) 1620.
- 5 L. Gildenberg, and J.R. Trowbridge, *J. Am. Oil Chem. Soc.*, 42 (1965) 69.
- 6 S.R. Lipsky and M. L. Duffy, *LC·GC*, 4 (1986) 898.
- 7 P. Sandra, F. David, F. Munari, G. Mapelli and S. Trestianu, in R.M. Smith (Editor), *Supercritical Fluid Chromatography*, The Royal Society of Chemistry, London, 1988, p. 153.
- 8 E. Stephanou, *Chemosphere*, 13 (1984) 43.
- 9 E. Stephanou, *Int. J. Environ. Anal. Chem.*, 27 (1985) 41.
- 10 P. Rudewicz and B. Munson, *Anal. Chem.*, 58 (1986) 674.
- 11 F.P.B. Van der Maeden, M.E.F. Biemond and P.C.G.M. Janssen, *J. Chromatogr.*, 149 (1978) 539.
- 12 M.S. Holt, E.H. McKerrell, J. Perry and R.J. Watkinson, *J. Chromatogr.*, 362 (1986) 419.
- 13 J.A. Pilc and P.A. Sermon, *J. Chromatogr.*, 398 (1987) 375.
- 14 *Separating Homologs and Polymers by HPLC*, HPLC Bulletin 796D, Supelco, Bellefonte, PA, 1988.
- 15 M.C. Allen and D.E. Linder, *J. Am. Oil Chem. Soc.*, 58 (1981) 950.

- 16 J.F.K. Huber, F.F.M. Kolder and J.M. Miller, *Anal. Chem.*, 44 (1972) 105.
- 17 A. Marcomini and W. Giger, *Anal. Chem.*, 59 (1987) 1709.
- 18 A. Marcomini, S. Capri and W. Giger, *J. Chromatogr.*, 403 (1987) 243.
- 19 M. Ahel and W. Giger, *Anal. Chem.*, 57 (1985) 1577.
- 20 M. Ahel and W. Giger, *Anal. Chem.*, 57 (1985) 2584.
- 21 C.F. Allen and L.I. Rice, *J. Chromatogr.*, 110 (1975) 151.
- 22 Z. Wang and M. Fingas, *J. Chromatogr.*, 637 (1993) 145.
- 23 P.R. Geissler, *J. Am. Oil Chem. Soc.*, 66 (1989) 685.
- 24 A.E. Johnson, Jr., P.R. Geissler and L.D. Tally, *J. Am. Oil Chem. Soc.*, 67 (1990) 123.
- 25 *SFC Columns & Accessories*, Lee Scientific, 1991.
- 26 D.E. Knowles, L. Nixon, E.R. Campbell, D.W. Later and B.E. Richter, *Fresenius' Z. Anal. Chem.*, 330 (1988) 225.
- 27 B.E. Richter, D.E. Knowles, M.R. Andersen, N.L. Porter, E.R. Campbell and D.W. Later, *J. High Resolut. Chromatogr. Chromatogr. Commun.*, 11 (1988) 29.
- 28 A.H. Silver and H.T. Kalinoski, *J. Am. Oil Chem. Soc.*, 69 (1992) 599.
- 29 J.T. Scanlon and D.E. Willis, *J. Chromatogr. Sci.*, 23 (1985) 333.
- 30 R.G. Ackman, *J. Gas Chromatogr.*, 6 (1968) 497.
- 31 R.G. Ackman, *J. Gas Chromatogr.*, 2 (1964) 173.
- 32 J.C. Sternberg, W.S. Gallaway and D.T.L. Jones, in N. Brenner, J.E. Callen and M.D. Weiss (Editors), *Gas Chromatography*, Academic Press, New York, 1962, Ch. XVIII.
- 33 D. Leyendecker, in R.M. Smith (Editor), *Supercritical Fluid Chromatography*, The Royal Society of Chemistry, London, 1988, Ch. 3.
- 34 M. Novotny, W. Bertsch and A. Zlatkis, *J. Chromatogr.*, 61 (1971) 17.
- 35 H.E. Schwartz, R.G. Brownlee, M.M. Boduszynski and Fu Su, *Anal. Chem.*, 59 (1987) 1393.
- 36 D.W. Later, E.R. Campbell and B.E. Richter, *J. High Resolut. Chromatogr. Chromatogr. Commun.*, 11 (1988) 65.
- 37 K.L. Mittal (Editor), *Solution Chemistry of Surfactants*, Vols. 1 and 2, Plenum Press, New York, 1979.

CHROM. 25 017

## Specific effects of modifiers in subcritical fluid chromatography of carotenoid pigments

E. Lesellier\*

LETIAM, IUT d'Orsay, Le Plateau Moulon, B.P. 127, 91403 Orsay Cedex (France)

A.M. Krstulović

Synthelabo Recherche (LERS), 23–25 Avenue Morane Saulnier, 92360 Meudon-la-Forêt (France)

A. Tchaplà

LETIAM, IUT d'Orsay, Le Plateau Moulon, B.P. 127, 91403 Orsay Cedex (France)

(First received November 5th, 1992; revised manuscript received February 12th, 1993)

---

### ABSTRACT

The use of subcritical fluid chromatography with filled columns for the analysis of carotenoid pigments affords a threefold reduction in analysis times with respect to HPLC. The addition of modifiers to CO<sub>2</sub> increases the solubility of pigments in the mobile phase. This paper reports the influence of modifiers on the separation of carotenoids in terms of specific interactions, such as hydrogen bonding and  $\pi$ - $\pi$  interactions between the solvent and the solute. The understanding of these interactions allowed the optimization of the separation of seven carotenoids and some of their *cis* isomers; this separation required less than 20 min.

---

### INTRODUCTION

Carotenoid pigments are important for human health. Although the provitamin A activity of certain carotenoids is well documented, their potential anticarcinogenic activity is still the subject of intensive research. Further, these compounds are used in foodstuffs as colouring agents ( $\beta$ -carotene, cathaxanthin), and some of their derivatives, such as acitretin, are used for the treatment of skin diseases [1].

Carotenoids are not synthesized *in vivo*; they are introduced into the organism through food intake and are transported by the blood. The main carotenoids that can be detected in blood

[2–4] are lutein, zeaxanthin, lycopene,  $\beta$ -cryptoxanthin and  $\alpha$ -,  $\beta$ , and  $\gamma$ -carotene.

Some of these compounds contain a hydroxyl or a ketone function on the terminal ring, arising from cyclization or double-bond conformation. These structural properties are of interest, as each compound will not have an identical behaviour in a given chromatographic system. Hence it is important to know these parameters and their possible effects in order to optimize a given separation. These interactions involve both the stationary and the mobile phase. The retention of carotenes in normal-phase chromatography on a polar stationary phase (silica) decreases with increasing number of double bonds and increases with cyclized lateral chains [5]. The trend is the opposite in reversed-phase chromatography with octadecyl-bonded phases. In the

---

\* Corresponding author.

latter instance, other workers have confirmed the influence of the degree of end-capping of residual silanols on the separation of xanthophylls [6,7]. The effect of polymeric phases on the separation of *trans/cis* isomers of different provitamin A activities has also been reported [8–10]. Zakaria *et al.* [11] and Nelis and De Leenheer [12] pointed out improved solubilities of these hydrophobic compounds in non-aqueous reversed-phase (NARP) chromatography. Other researchers have shown the relationship between the retention of xanthophylls and the methanol content of the eluent [6,7].

The simultaneous separation of these compounds, which has been the subject of several studies [13,14], poses two main problems. The first concerns the separation of luteine and zeaxanthine, which both bear a hydroxyl group and which are the least retained among the carotenes. Thus the elution strength of the mobile phase should not be elevated for the separation of these two compounds, which in turn results in excessive retention of other carotenes. The second problem stems from the difficulty in simultaneously separating the *trans* and *cis* isomers. The choice of both the mobile and the stationary phase is of great importance in achieving this separation.

We have already reported on the separation of carotenes by supercritical fluid chromatography (SFC) using filled columns [15]. This method offers the advantage of speed of analysis and efficiency of separation. In addition, it allows one to modulate the solvent strength by means of an appropriate modifier. We have therefore undertaken a systematic study of the influence of modifiers on the separation of carotenes in SubFC, resulting in an optimized separation method.

## EXPERIMENTAL

### Chemicals

The solvents used were of HPLC grade and were purchased from Prolabo (Paris, France), SDS (Vitry sur Seine, France), Carlo Erba (Milan, Italy) and Merck (Darmstadt, Germany).

Pigment extracts were kindly provided by

Hoffmann La Roche (Basle, Switzerland), lycopene,  $\gamma$ -carotene, lutein, zeaxanthin,  $\beta$ -cryptoxanthin and 15-*cis*- $\beta$ -carotene except for all-*trans*- $\alpha$ - and - $\beta$ -carotene which were purchased from Sigma (St. Louis, MO, USA).

Carbon dioxide (N45 grade, containing less than 7 ppm of water) was purchased from Alphagaz (Bois d'Arcy, France).

### Apparatus

Chromatographic separations were carried out using equipment manufactured by Jasco (Tokyo, Japan). The two pumps (Model 880-PU) were connected to a Sédéré pulse damper (Touzart et Matignon, Vitry sur Seine, France). The head of the pump used for carbon dioxide was cooled to  $-2^{\circ}\text{C}$  by an F 10c cryostat (Julabo, Seelbach, Germany). The pulse damper was connected to a Model 7125 injection valve fitted with a 20- $\mu\text{l}$  loop (Rheodyne, Cotati, CA, USA).

The chromatographic column was octadecylsilica-based, 5- $\mu\text{m}$  Ultrabase UB 225 (250  $\times$  4.6 mm I.D.) from SFCC-Shandon (Eragny, France). The column was placed in a Crocosil thermostatically controlled oven (Cluzeau, Ste. Foy-la-Grande, France) maintained at  $25^{\circ}\text{C}$ .

Detection was carried out by a UV-Vis detector (Hewlett-Packard Model 1050) with a high-pressure-resistant cell. The detection wavelength was 450 nm. Chromatograms were recorded using a Model CR 6A electronic integrator (Shimadzu, Kyoto, Japan).

## RESULTS AND DISCUSSION

### Carotenes

The first part of the study was conducted using lycopene and  $\gamma$ -,  $\alpha$ - and  $\beta$ -carotenes (all-*trans* and *cis* isomers), the structures of which are shown in Fig. 1. Their elution order in SubFC was found to be the same as in NARP LC [16]. The results concerning the selectivity factors for all-*trans*- $\alpha$ - and - $\beta$ -carotenes and their isomers has already been discussed [17].

The influence of the type and percentage composition of modifiers in  $\text{CO}_2$  under subcritical conditions on the selectivity of pairs of compounds whose separation is difficult, such as

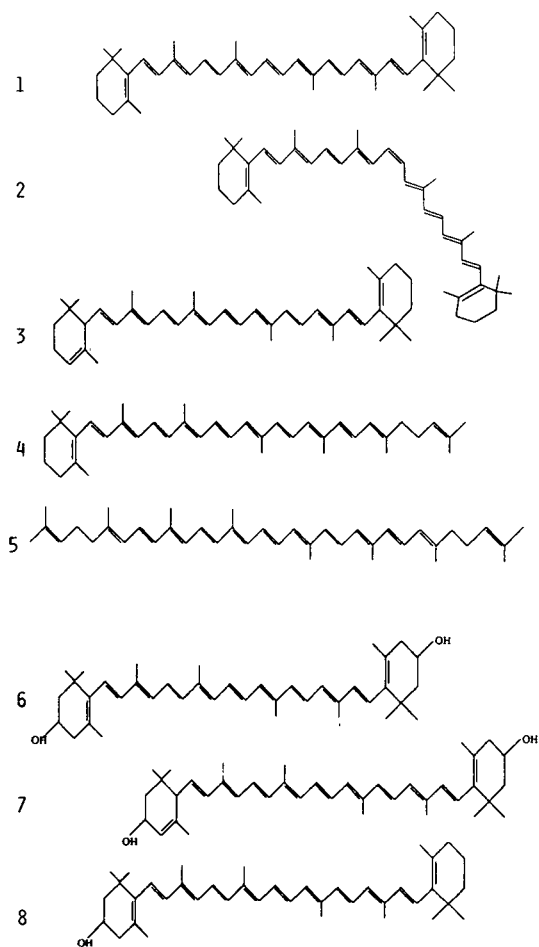


Fig. 1. Structures of carotenoids. 1 = All-*trans*- $\beta$ -carotene; 2 = 15-*cis*- $\beta$ -carotene; 3 = all-*trans*- $\alpha$ -carotene; 4 =  $\gamma$ -carotene; 5 = lycopene; 6 = zeaxanthin; 7 = lutein; 8 =  $\beta$ -cryptoxanthin.

lycopene and  $\alpha$ -carotene or  $\gamma$ -carotene and  $\alpha$ -carotene, was studied.

Fig. 2a shows the variation of selectivity between lycopene and  $\alpha$ -carotene as a function of the percentage of modifier used. The selectivity increases with increasing modifier concentration for most of the compounds studied. This increase is observed for solvents whose effects on the retention of carotenes are not necessarily identical. We have already shown that an increase in the concentration of tetrahydrofuran (THF), acetone or methylene chloride leads to decreased retention of carotenes, whereas with methanol, acetonitrile and nitromethane an initial decrease

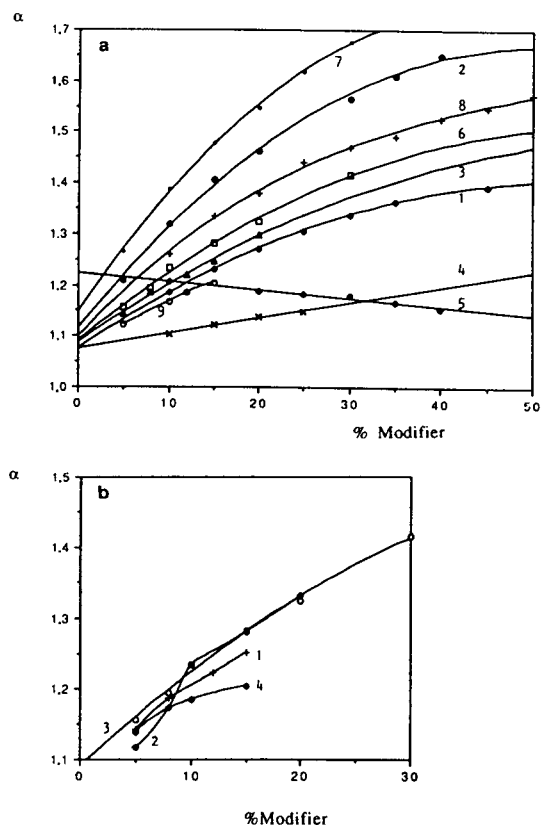


Fig. 2. (a) Variation of the lycopene- $\alpha$ -carotene selectivity as a function of the percentage of the modifier in subcritical fluid chromatography. Flow-rate, 3.0 ml/min; temperature, 25°C; output pressure, 15 MPa. 1 = Acetone; 2 = acetonitrile; 3 = dioxane; 4 = hexane; 5 = methanol; 6 = methylene chloride; 7 = nitromethane; 8 = propionitrile; 9 = tetrahydrofuran. (b) Variation of the lycopene- $\alpha$ -carotene selectivity as a function of the percentage of the chlorinated modifier in subcritical fluid chromatography. Analytical conditions as in (a). 1 = Chloroform; 2 = 1,2-dichloroethane; 3 = methylene chloride; 4 = tetrachloroethylene.

followed by an increase in retention was observed [17]. The selectivity observed therefore does not depend on the factors that govern retention, such as interfacial tension between the stationary and the mobile phases. On the basis of Hildebrand partial solubility parameters [18] (Table I), the solvents that lead to the largest increase in selectivity between lycopene and  $\alpha$ -carotene are those which possess the highest dipole moment ( $\delta_0$ ), *i.e.*, nitromethane ( $\delta_0 = 8$ ), acetonitrile ( $\delta_0 = 7$ ) and methylene chloride ( $\delta_0 = 5.5$ ), followed by a group of solvents whose



TABLE I

## PHYSICAL AND CHEMICAL CONSTANTS OF SOME SOLVENTS USED AS MODIFIERS IN SUBCRITICAL FLUID CHROMATOGRAPHY

$\epsilon$  = Dielectric constant;  $\gamma$  = surface tension;  $\delta$  = Hildebrand solubility parameters:  $\delta_p$  = dispersion parameter;  $\delta_0$  = dipole–dipole parameter;  $\delta_a$  = proton acceptor parameter;  $\delta_d$  = proton donor parameter.

Solvent	$\epsilon$	$\gamma$	$\delta$	$\delta_p$	$\delta_0$	$\delta_a$	$\delta_d$
Methanol	32.7	22.5	12.9	6.2	5	7.5	7.5
Acetonitrile	37.5	29.1	11.8	6.5	8	2.5	0
Nitromethane	36	37	11.0	7.3	8	1	0
Ethanol	24.6	22.3	11.2	6.8	4	5	5
Propionitrile	27.2	27.2	10.8	7.5	7	2.7	0
Acetone	21.4	23.3	9.4	6.8	5	2.5	0
1-Propanol	20.1	23.7	10.2	7.2	2.5	4	4
Heptane	1.92	20.8	7.4	7.4	0	0	0
Dioxane	2.2	34.4	9.8	7.8	4	3	0
Tetrahydrofuran	7.6	27.6	9.1	7.6	4	3	0
Methylene chloride	8.9	28.1	9.6	6.4	5.5	0.5	0
Chloroform	4.80	26.5	9.1	8.1	3	0.5	0
1,2-Dichloroethane	10.36	32.2	9.7	8.2	4	0	0
Tetrachloroethylene	2.3	31.2	9.3	9.3	0	0	0

partial solubility parameter is between 4 and 5 (dioxane, acetone and THF). As the main structural difference between these compounds stems from the presence or absence of terminal cyclization of the polyethylene side-chain and the presence of two double bonds in lycopene, one can postulate the existence of dipole–dipole ( $\pi$ – $\pi$ ) interactions between these solvents and the pigments.

The extent of these interactions therefore depends on two factors: the number of double bonds in the molecule and the dipole moment of the solvent. The higher the dipole moment, the higher is the solubility of lycopene.

The difference in relative retention (measured by selectivity) between these compounds will increase with increasing concentration of the solvent in the mobile phase. It should be noted, nevertheless, that an increase in heptane concentration leads to the same effect, although it does not have a permanent dipole moment. One can therefore postulate the effect of the London-type dispersion forces, which could explain why nitromethane causes a larger increase in selectivity

than acetonitrile, although their dipole moments expressed in terms of the Hildebrand partial solubility parameters are the same.

Fig. 2b also illustrates the variation in selectivity for chlorinated modifiers, for which it is easier to explain the small fluctuations in behaviour in terms of their inherent properties. The comparison of pairs of solvents confirms the previously evoked hypothesis. Thus, chloroform and 1,2-dichloromethane have similar dispersion forces (8.1 for chloroform and 8.2 for 1,2-dichloromethane), whereas the latter solvent has a larger dipole moment.

The variation of selectivity is larger for 1,2-dichloroethane. The influence of this solvent is comparable to that of methylene chloride, in spite of its lower dipole moment. Here again, the larger dispersion forces in 1,2-dichloroethane could counterbalance this difference. These interactions could also explain why the variation observed with tetrachloroethylene is almost identical with that of chloroform, in spite of the zero dipole moment. In contrast, the addition of methanol to the mobile phase entails a decrease

in selectivity, which diminishes the difference between these compounds needed for the separation.

Fig. 3 shows the behaviour of other solvents with a hydroxyl group. Solvents such as ethanol, 1-propanol, 1-butanol and 1-pentanol have only a limited influence on selectivity compared with other solvents; the selectivity varies only from 1.14 to 1.21. Conversely, one observes an initial increase followed by a decrease for alcohol concentrations close to 20%. It is possible that the proton donor character of these solvents is responsible for the observed decrease in selectivity.

This effect, which should be operative regardless of the methanol concentration owing to its large proton donor character ( $\delta_d$ ), would be operative for other solvents at higher concentrations. This decrease is nevertheless critical for the separation of the pigments under study.

We also studied the evolution of selectivity between  $\gamma$ - and  $\alpha$ -carotene (Fig. 4). These two pigments differ only in the additional cyclization at one extreme of the  $\alpha$ -carotene molecule. Both compounds have provitamin A activity and their separation is of interest. The selectivity factors between  $\gamma$ - and  $\alpha$ -carotene are lower than those between lycopene and  $\alpha$ -carotene, as  $\gamma$ -carotene is eluted between them.

The change in selectivity is comparable to the

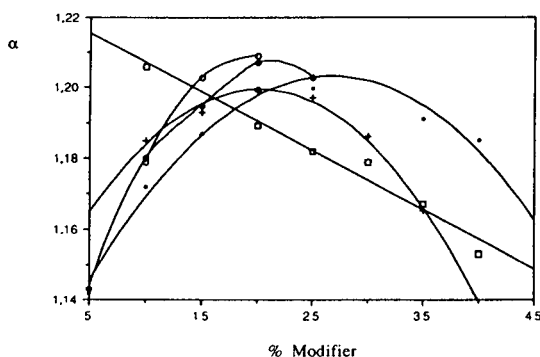


Fig. 3. Variation of the lycopene- $\alpha$ -carotene selectivity as a function of the percentage of the alcoholic modifier in subcritical fluid chromatography. Analytical conditions as in Fig. 2a.  $\blacklozenge$  = 1-Butanol;  $\bullet$  = ethanol;  $\square$  = methanol;  $\circ$  = 1-pentanol;  $+$  = 1-propanol.

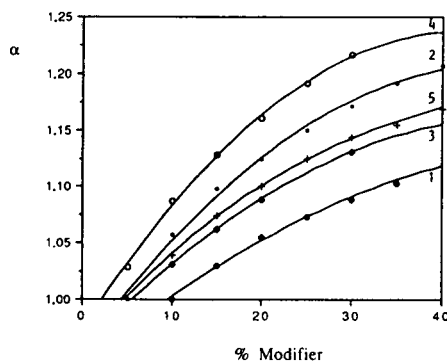


Fig. 4. Variation of the  $\gamma$ -carotene- $\alpha$ -carotene selectivity as a function of the percentage of the modifier in subcritical fluid chromatography. Analytical conditions as in Fig. 2a. 1 = Acetone; 2 = acetonitrile; 3 = methylene chloride; 4 = nitromethane; 5 = propionitrile.

previous one, and can be explained in the same manner, *i.e.*, by the  $\pi$ - $\pi$  interactions between the double bonds and the solvents, and they are especially operative with solutes bearing an additional double bond. The sequence of solvents in terms of this effect is nitromethane, acetonitrile, propionitrile, methylene chloride and acetone. However, it is not possible to separate these two solutes with the alcohols (methanol, ethanol). The use of these solvents is therefore not advantageous for the separation of complex mixtures of carotenes.

The influence of these solvents is nevertheless very important for the separation of the *cis-trans* compounds. Similarly to the behaviour of the *cis-trans* isomers of  $\alpha$ - and  $\beta$ -carotene discussed above, the *cis* isomer of  $\gamma$ -carotene is eluted after the *trans* compound. According to this hypothesis, it seems evident for the all-*trans*-carotenes and, in particular,  $\gamma$ - and  $\alpha$ -carotene which have similar chromatographic behaviours, that the larger the extent of this separation, the smaller is the extent of co-elution of the *cis* and *trans* isomers of a given carotene.

By comparing the percentages of solvents needed to obtain identical selectivities, one can see that, for example, 15% nitromethane, 22% acetonitrile, 27% propionitrile, 30% methylene chloride and 45% acetone are required. It is known that for the last three solvents, the

selectivity between the *cis* and *trans* isomers diminishes with increasing percentage of these solvents in the mobile phase.

Two solvents appear to be particularly interesting for these analyses: nitromethane and acetonitrile. Fig. 5 shows the separation of these compounds with a mobile phase containing 15% of nitromethane, which is judged to be the best solvent. Nevertheless, the use of this solvent with a UV absorbance detector is difficult owing to the pronounced baseline noise. Identical behaviour is observed with propionitrile. However, this type of detection is of interest for the analysis of *cis* isomers or retinols.

The use of acetonitrile can also be envisaged, even though a decrease in selectivity is observed for *cis-trans* isomers at higher modifier percentages [17]. Nevertheless, the resolution between the isomers does not diminish as much as one would expect, as the retention of carotenes increases again at acetonitrile concentrations above 20%. In this instance, according to the resolution equation, the increase in the capacity factor  $k'$  entails a slight increase in resolution,

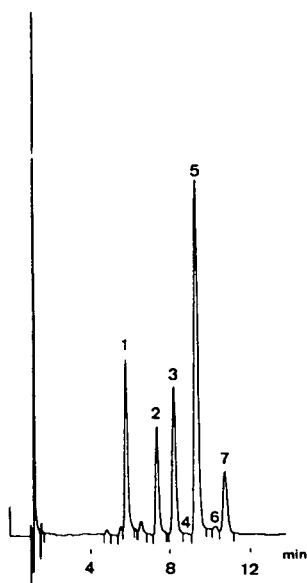


Fig. 5. Subcritical fluid chromatogram of a mixture of carotenes. Peaks; 1 = lycopene; 2 =  $\gamma$ -carotene; 3 = all-*trans*- $\alpha$ -carotene; 4 = *cis*- $\alpha$ -carotene; 5 = all-*trans*- $\beta$ -carotene; 6 = 9- and/or 13-*cis*- $\beta$ -carotene; 7 = 15-*cis*- $\beta$ -carotene. Analytical conditions as in Fig. 2a; mobile phase, nitromethane-CO<sub>2</sub> (15:85, v/v).

which partially counteracts the decrease in selectivity.

### Xanthophylls

We also studied the influence of these solvents on the retention and selectivity of lutein and zeaxanthin. These compounds are difficult to elute without an alcohol. Nevertheless, in LC they were separated without the use of alcohols [19,20]. It is possible that the retention of hydroxylated carotenoids is related to the presence of surface silanols. This is confirmed by studies that have shown that end-capping [7] or addition of triethylamine [21] diminished the retention of xanthophylls. In spite of that, these compounds were separated on a non-end-capped column [22]. The addition of alcohol to the mobile phase leads to blocking of residual silanols and thus decreases the interactions between xanthophylls and silanols [6].

An increase in the percentage of an alcohol decreases the extent of retention in SubFC. The selectivity also decreases from 1.2 for 5% methanol to 1.1 for 15% methanol (Fig. 6a). This effect is similar for the five solvents with alcohol functionalities, although it is observed that, for an identical alcohol content, the selectivity between lutein and zeaxanthin increases with increasing length of the solvent alkyl chain. In the presence of an alcohol lutein is eluted before zeaxanthin, which is followed by lycopene, the first carotene eluted. The variation in selectivity between zeaxanthin and lycopene as a function of the nature and percentage of the alcohol modifier is illustrated in Fig. 6a.

These results illustrate that as the retention of xanthophylls decreases rapidly with increasing alcohol content, the selectivity between zeaxanthin and lycopene increases in a pronounced manner. In contrast, the increase in selectivity is inversely proportional to the alkyl chain length of the alcohol, which is in contrast with the selectivity between lutein and zeaxanthin. This is probably due to the relative importance of the hydroxyl group in the case of a homologue with a low mass. Hence a smaller amount of methanol is needed to cover the silanols compared with 1-pentanol. In addition, the solubility of these solutes must be favoured in the same manner,

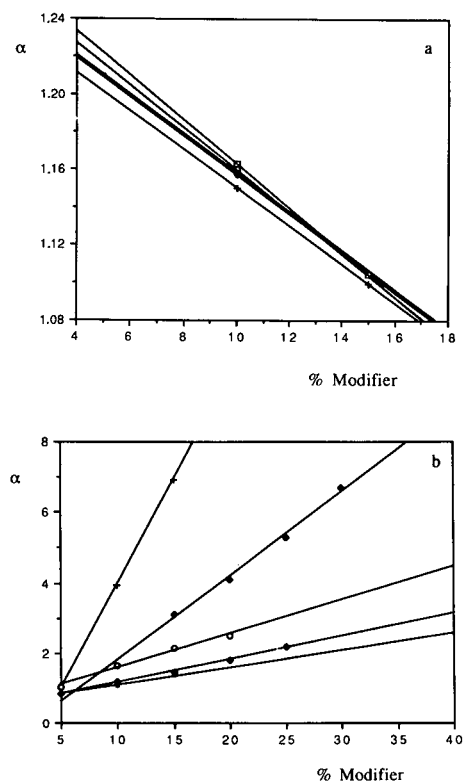


Fig. 6. (a) Variation of the zeaxanthin–lutein selectivity as a function of the percentage of alcohol modifier in subcritical fluid chromatography. Analytical conditions as in Fig. 2a.  $\diamond$  = 1-Butanol;  $\bullet$  = ethanol; + = methanol;  $\square$  = 1-pentanol;  $\circ$  = 1-propanol. (b) Variation of the lycopene–zeaxanthine selectivity as a function of the percentage of alcoholic modifier in subcritical fluid chromatography. Analytical conditions as in Fig. 2a.  $\diamond$  = 1-Butanol;  $\blacklozenge$  = ethanol; + = methanol;  $\bullet$  = 1-pentanol;  $\circ$  = 1-propanol.

therefore leading to faster elution in the presence of these solvents.

In conclusion, it can be said that whereas the presence of an alcohol is needed to elute xanthophylls, an increase in alcohol content is unfavorable for the separation of lutein and zeaxanthin and of  $\gamma$ -carotene and  $\alpha$ -carotene. Hence the amount of alcohol should be optimized in order to achieve the best separation.

#### Simultaneous separation of seven carotenoids

The analyses were carried out by using a mixture of two modifiers [acetonitrile–methanol (95:5, v/v)] and by varying the percentage of the

modifier in the mobile phase. Methanol was chosen as it affords high selectivity between lycopene and zeaxanthin.

Fig. 7a shows the variation of the  $\log k'$  value for the seven carotenoids under consideration. The variation is non-linear and differs depending on the type of compound. This behaviour is typical of solvents with a high dielectric constant [17]. This phenomenon is identical for the four carotenes, while the minimum retention of xanthophylls is displaced towards higher solvent contents. Xanthophylls have higher solubility parameters than carotenes [23], which favours their solubility in the mobile phase. The mini-

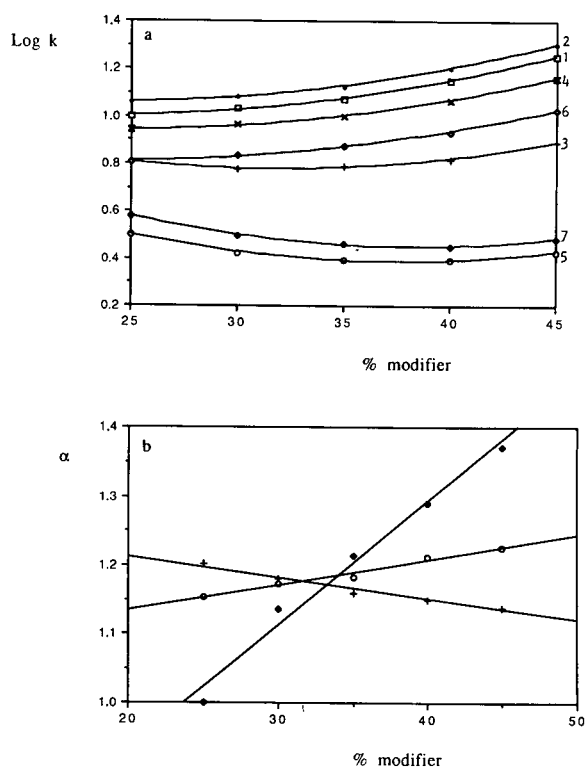


Fig. 7. (a) Variation of the capacity factor of standard carotenoids as a function of percentage of a binary modifier in subcritical chromatography. Analytical conditions as in Fig. 2a. Modifier: acetonitrile–methanol (95:5, v/v). 1 =  $\alpha$ -Carotene; 2 =  $\beta$ -carotene; 3 =  $\beta$ -cryptoxanthin; 4 =  $\gamma$ -carotene; 5 = lutein; 6 = lycopene; 7 = zeaxanthin. (b) Variation of the selectivity of some pairs of pigments as a function of the percentage of binary modifier in subcritical fluid chromatography. Analytical conditions as in Fig. 2a. + = Zeaxanthin–lutein;  $\blacklozenge$  = lycopene– $\beta$ -cryptoxanthin;  $\circ$  =  $\alpha$ - $\gamma$ -carotene.

imum retention depends on the number of hydroxyl groups in the molecules:  $\beta$ -cryptoxanthin, which has a hydroxyl group, exhibits minimum retention between those of carotenes and lutein.

When the effects of the dielectric constant of polarity of the solvent become too large for a given compound, the resistance to surface tension or solubilization in the eluent becomes more difficult. Fig. 7a also shows that  $\beta$ -cryptoxanthin is eluted just after lycopene.

Fig. 7b shows the evolution of selectivity of the pairs of compounds whose separation is often difficult with these solvents, *i.e.*, lutein–zeaxanthin, lycopene– $\beta$ -cryptoxanthin and  $\alpha$ -carotene– $\gamma$ -carotene. These variations are in agreement with those predicted by the preceding study. An increase in the modifier content in the mobile phase entails an increase in selectivity between  $\alpha$ - and  $\gamma$ -carotene, related to the overall increase of acetonitrile content, and a decrease in selectivity between lutein and zeaxanthin as the methanol content also increases.

The selectivity between lycopene and  $\beta$ -cryptoxanthin also increases with increasing modifier content, probably owing to favoured elution of a pigment with a hydroxyl group with increasing alcohol concentration. The optimum separation can be achieved with 30–35% modifier. Nevertheless, the chromatograms obtained show that it is preferable to favour the

separation between  $\alpha$ - and  $\gamma$ -carotene in order to improve the separation of *cis*- $\gamma$ -carotene and all-*trans*- $\alpha$ -carotene. Hence the best compromise is obtained at 35% (Fig. 8).

## CONCLUSIONS

Subcritical fluid chromatography with conventional columns affords both faster analyses and better utilization of the properties of modifiers than LC. The separation of seven carotenoid pigments and their isomers is obtained in 15 min. This study has demonstrated the particular roles of the solvents examined, which are related to their specific character. The influence of these solvents is comparable to that observed in NARP LC. A better knowledge of the effects exerted by these modifiers permits an easier choice for the separation of the pigments studied. These effects can improve the separation of certain solutes, but also render more difficult the separation of others present in the mixtures of pigments under consideration. Hence a fine adjustment of the percentage of modifier is needed to optimize a complex separation.

For carotenes, nitromethane enables one to obtain a better separation, whereas for the xanthophylls, long-chain alcohols afford a better separation than methanol of lutein and zeaxanthin. The presence of a solvent with a high dipole moment is indispensable for the separation of compounds with different numbers of double bonds; although the presence of an alcohol is needed to elute xanthophylls rapidly, its content should be reduced to a minimum in order to obtain a satisfactory separation of these pigments.

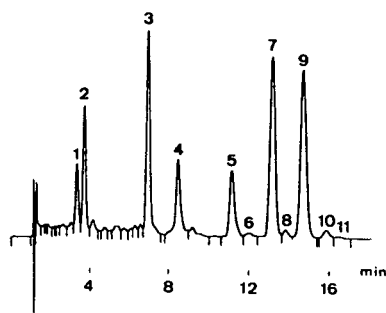


Fig. 8. Subcritical fluid chromatogram of a mixture of carotenoids. Peaks: 1 = lutein; 2 = zeaxanthin; 3 =  $\beta$ -cryptoxanthin; 4 = lycopene; 5 = all-*trans*- $\gamma$ -carotene; 6 = *cis*- $\gamma$ -carotene; 7 = all-*trans*- $\alpha$ -carotene; 8 = *cis*- $\alpha$ -carotene; 9 = all-*trans*- $\beta$ -carotene; 10 = 9- and/or 13-*cis*-carotene; 11 = 15-*cis*- $\beta$ -carotene. Flow-rate, 3.0 ml/min; temperature, 25°C; output pressure, 15 MPa; mobile phase, acetonitrile–methanol- $\text{CO}_2$  (33.25:1.75:65, v/v/v).

## REFERENCES

- 1 E. Meyer, W.E. Lambert and A.P. De Leenheer, *J. Chromatogr.*, 570 (1991) 149.
- 2 J.G. Bieri, E.D. Brown and J.C. Smith, Jr., *J. Liq. Chromatogr.*, 8 (1985) 473.
- 3 F. Khachik, G.R. Beecher and M.B. Goli, *Pure Appl. Chem.*, 63 (1991) 71.
- 4 T. van Vliet, F. van Schaik, J. van Schoonhoven and J. Schrijver, *J. Chromatogr.*, 553 (1991) 179.

- 5 S.H. Rhodes, A.G. Netting and B.V. Milborrow, *J. Chromatogr.*, 442 (1988) 412.
- 6 D.R. Lauren and D.E. McNaughton, *J. Liq. Chromatogr.*, 9 (1986) 2013.
- 7 Z. Matus and R. Ohmacht, *Chromatographia*, 30 (1990) 318.
- 8 R.J. Bushway, *J. Liq. Chromatogr.*, 8 (1985) 1527.
- 9 F.W. Quackenbush, *J. Liq. Chromatogr.*, 10 (1987) 643.
- 10 E. Lesellier, C. Marty, C. Berset and A. Tchaplá, *J. High Resolut. Chromatogr.*, 12 (1989) 447.
- 11 M. Zakaria, K. Simpson, P.R. Brown and A. Krstulović, *J. Chromatogr.*, 176 (1979) 109.
- 12 H.J.C.F. Nelis and A.P. De Leenheer, *Anal. Chem.*, 55 (1983) 270.
- 13 B. Olmedilla, F. Granado, E. Rojas-Hidalgo and I. Blanco, *J. Liq. Chromatogr.*, 13 (1990) 1455.
- 14 F. Granado, B. Olmedilla, I. Blanco and E. Rojas-Hidalgo, *J. Liq. Chromatogr.*, 14 (1991) 2457.
- 15 M.-C. Aubert, C.R. Lee, A.M. Krstulović, E. Lesellier, M.R. Péchard and A. Tchaplá, *J. Chromatogr.*, 557 (1991) 47.
- 16 A. Tchaplá, S. Heron and E. Lesellier, *Spectra 2000*, 158 (1991) 42.
- 17 E. Lesellier, A.M. Krstulović and A. Tchaplá, *Chromatographia*, 36 (1993) 275.
- 18 J.H. Hildebrand and R.L. Scott, *The Solubility of Non-Electrolytes*, Dover, New York, 1964.
- 19 R.K. Juhler and R.P. Cox, *J. Chromatogr.*, 508 (1990) 232.
- 20 C.A. Bailey and B.H. Chen, *J. Food Sci.*, 54 (1989) 584.
- 21 H.J.C.F. Nelis, M.M.Z. Van Steenberge, M.F. Lefevère and A.P. De Leenheer, *J. Chromatogr.*, 353 (1986) 295.
- 22 A.M. Gilmore and H.Y. Yamamoto, *J. Chromatogr.*, 543 (1991) 137.
- 23 F. Favati, J.W. King, J.P. Friedrich and K. Eskins, *J. Food Sci.*, 53 (1988) 1532.



# Inter-company cross-validation exercise on capillary electrophoresis

## I. Chiral analysis of clenbuterol

K.D. Altria\*

*Pharmaceutical Analysis, Analytical Evaluation Group, Glaxo Group Research, Park Road, Ware, Herts. SG12 0DP (UK)*

R.C. Harden

*Lilly Research Centre Ltd., Windlesham (UK)*

M. Hart

*Rhone-Poulenc-Rorer Ltd., Dagenham (UK)*

J. Hevizi

*SmithKline Beecham, Welwyn Garden City (UK)*

P.A. Hailey

*Pfizer Central Research, Sandwich (UK)*

J.V. Makwana

*Boots Company, Nottingham (UK)*

M.J. Portsmouth

*Fisons Pharmaceuticals, Loughborough (UK)*

(First received January 19th, 1993; revised manuscript received March 16th, 1993)

---

### ABSTRACT

In order to assess the repeatability of capillary electrophoresis (CE) and to demonstrate the successful transfer of CE methods between independent laboratories a working party comprising seven pharmaceutical companies was established. Three cross-validation exercises are scheduled. The first is the chiral analysis of clenbuterol. This paper gives the results from this initial study. The method was successfully transferred between all the participating companies. In each case baseline separation or better of the enantiomers was obtained. Good performance in terms of precision for both peak area and migration time, linearity and accuracy was obtained. This exercise clearly demonstrates that the CE method investigated is capable of generating accurate and precise data.

---

\* Corresponding author.



## INTRODUCTION

Capillary electrophoresis (CE) is rapidly becoming established as an alternative and complementary analytical technique to HPLC for the quantitative analysis of pharmaceuticals. CE has been employed for the determination of the active ingredients in formulations [1–3], and for the determination of drug-related impurities [4–6]. Several groups have also demonstrated the use of CE for chiral analysis of pharmaceuticals [7–9]. Good cross-correlation of CE data with those generated by chromatographic methods has been shown [1,2,5,6]. However, as with all developing techniques performance is rightfully being questioned. Several reports [1–6] have shown CE to be capable of generating high-quality data with good performance in terms of precision, accuracy and linearity. However, repeatability and the transfer of methods has yet to be reported.

Given the increased use of CE for pharmaceutical analysis a working group of seven pharmaceutical companies was established with the objective of assessing the ability of CE methods to be transferred successfully between independent laboratories. The working group was established through their involvement in the UK Pharmaceutical Analysis Science Group, an organisation of research based pharmaceutical companies established to mutually develop areas of common interest in the field of pharmaceutical analysis.

It was agreed that selected CE methods would be validated by each of the participating companies using a common validation protocol. Given the principal application areas of CE, three studies were considered: (1) separation of the enantiomers of a chiral drug substance, (2) determination of the active ingredients in a formulation, and (3) quantitative analysis of drug-related impurities.

This paper is the first in a series of 3 and details the inter-company cross-validation of a CE method for the separation of the enantiomers of a chiral drug substance.

A CE method for the separation of the enantiomers of the bronchodilator, clenbuterol has been published [9]. These reported operating

conditions were modified in terms of the selection of electrolyte and cyclodextrin. Previously a citrate–phosphate electrolyte with  $\beta$ -cyclodextrin had been employed for the separation of clenbuterol enantiomers with a run-time of 33 min. In this study a borate–phosphate electrolyte was employed incorporating hydroxypropyl- $\beta$ -cyclodextrin which has a higher enantioselectivity for clenbuterol. This increase in selectivity permitted a typical reduction in analysis time to *ca.* 12 min. In both instances chiral selectivity was achieved through incorporation of a cyclodextrin into a low-pH carrier electrolyte. This is the most common mode of chiral analysis in CE and has been successfully applied to a number of basic compounds [10].

Future papers will cover the quantitative assay of the active ingredients in a formulation and the determination of drug related impurities.

## EXPERIMENTAL

The compounds and reagents selected for this exercise are commercially available.

CE instrumentation from three suppliers, Applied Biosystems (San Jose, CA, USA), Beckman (Palo Alto, CA, USA) and Spectra-Physics (Freemont, CA, USA) was employed. Standard capillary lengths and bores were adopted. Sampling times for the various instruments were set to produce an injection volume of 8 nl. Hydroxypropyl- $\beta$ -cyclodextrin was purchased from Aldrich (Gillingham, UK). The method details are as follows:

Rinse 1	0.1 M NaOH 1 min
Rinse 2	Electrolyte 2 min
Injection	8 nl
Detection	UV absorbance at 214 nm
Voltage	+30 kV
Temperature	Ambient
Capillary	Fused silica 57 cm $\times$ 50 $\mu$ m
Sample	0.15 mg/ml in water

Electrolyte: 30 mM hydroxypropyl- $\beta$ -cyclodextrin (typically 0.83 g per 20 ml) in 50 mM disodium tetraborate (typically 1.91 g  $\text{Na}_2\text{B}_4\text{O}_7 \cdot 10\text{H}_2\text{O}$  per 100 ml), pH adjusted to 2.2 with concentrated orthophosphoric acid.

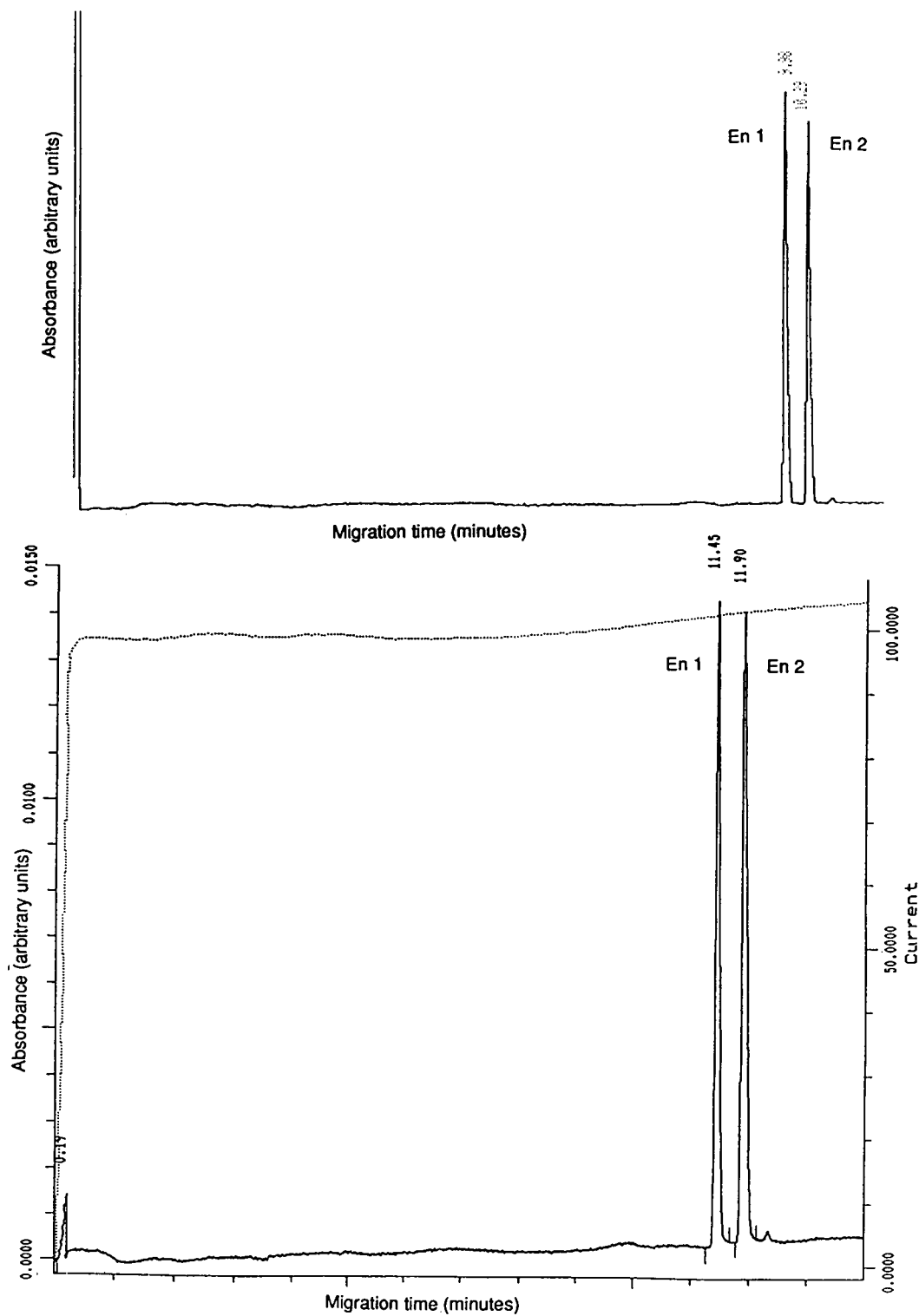


Fig. 1.

(Continued on p. 150)

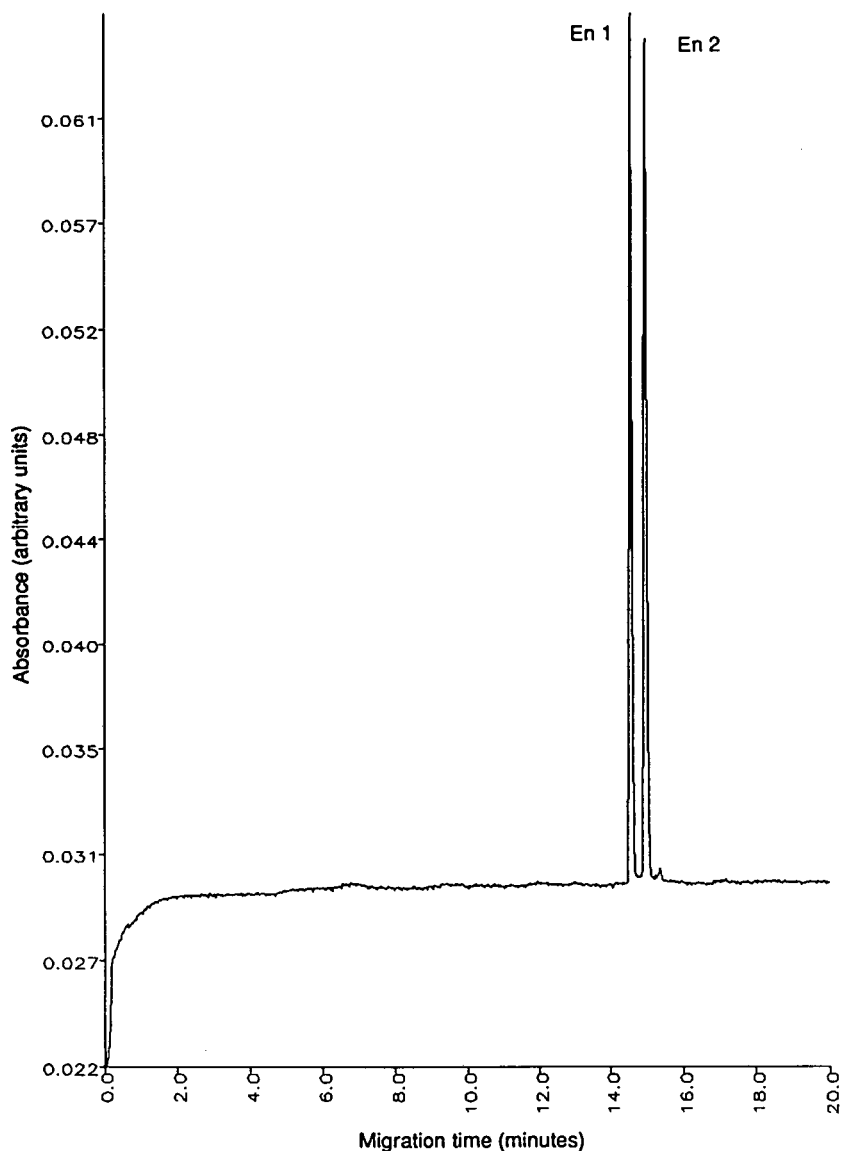


Fig. 1. Chiral CE separations of clenbuterol. Separation conditions as given in Experimental. Current measured in  $\mu\text{A}$ .

A clenbuterol sample was purchased from Sigma (Poole, UK) and subsamples were dispatched to each of the companies for testing.

The following experiments were performed:

(i) Repeated injections of a clenbuterol sample solution (target concentration 0.15 mg/ml) were used to measure precision.

(ii) Detector linearity over a range of 10–150% of clenbuterol target concentration was measured. Two samples were prepared and serially diluted to give appropriate standards of

10, 25, 50, 75, 100 and 150% of target concentration.

#### RESULTS AND DISCUSSION

The following measures of method performance were assessed: (i) selectivity, (ii) migration time precision, (iii) peak area and peak height precision, (iv) detector response linearity with sample concentration, and (v) %area/area accuracy in comparison with theoretical value.

### Selectivity

Using the separation conditions given in the Experimental section all companies were able to achieve baseline separation or greater of the clenbuterol enantiomers. Fig. 1 shows three representative electropherograms. An impurity was present in the clenbuterol sample which consistently migrated after the second enantiomer in all separations. Variations in actual migration times were mainly due to differences in the distances along the capillary to the detector in the various instruments employed, and to variations in operating temperature.

### Migration time precision

Table I shows the average relative standard deviation (R.S.D.) for the precision of migration time for the first migrating enantiomer to be under 1%. In all cases precision of less than 0.05% R.S.D. was obtained for the relative migration time (RMT) of enantiomer 1, relative to enantiomer 2. These data indicate that excellent consistency of selectivity was obtained during the injection sequences.

### Linearity data

The linearity of detector response for peak area over a range of 10–150% of clenbuterol target concentration was measured. Acceptable linearity data (Table II) were obtained by all companies with an average correlation coefficient of 0.995. The average % intercept was +1.2% of detector response for target clenbuterol concentration.

TABLE I  
MIGRATION TIME PRECISION (ENANTIOMER 1)

Company	Instrument supplier	Migration time (%R.S.D.) (n = 10)	RMT	RMT En1 (%R.S.D.) (n = 10)
1	Beckman	1.3	0.98	<0.05
2	Beckman	0.3	0.94	<0.05
3	Beckman	0.8	0.96	<0.05
4	Spectra-Physics	0.4	0.96	<0.05
5	ABI	0.6	0.97	<0.05
6	Beckman	0.5	0.96	<0.05
7	ABI	0.2	0.97	<0.05

TABLE II  
PEAK AREA LINEARITY DATA (CORRELATION COEFFICIENT)

Company	En1	
	Linearity	Intercept
1	0.999	0.98
2	0.997	0.31
3	0.999	-0.33
4	0.992	5.10
5	0.996	0.33
6	0.990	-1.34
7	0.994	3.53

### Peak area precision

Peak area precision improves in CE with increased sample concentration [11]. When employing high sample concentrations [1,2,12,13] typical CE peak area precision in the order of 1–2% R.S.D. can be obtained. This is in contrast to precision of 5% R.S.D. which has been reported for low-concentration test mixtures [14,15].

In CE, peak areas are related to both sample concentration and migration time. Later migrating peaks pass more slowly through the detector giving a higher apparent peak area response. This effect can be compensated for by the division of the area of each peak by its corresponding migration time [16]. The impact of not normalising areas upon %area/area impurity data and chiral separations has been reported [17].

TABLE III  
PEAK AREA PRECISION

Company	Precision (R.S.D.) of peak area En1		Precision (R.S.D.) of peak area En2		Peak area ratio En1/En2 (PAR)	
	Actual	Normalised	Actual	Normalised	PAR	R.S.D. (n = 10)
1	1.2	0.8	1.4	0.8	0.974	0.2
2	2.6	2.5	1.9	1.8	1.004	0.5
3	0.6	1.0	0.4	1.1	0.993	0.4
4	1.3	1.2	1.7	1.6	0.992	0.9
5	2.2	2.1	2.2	2.0	0.998	0.3
6	2.5	1.1	2.9	1.8	1.000	0.6
7	1.7	1.7	1.5	1.5	1.000	0.9

Peak area precision was measured (Table III) for the repeated injections of the clenbuterol sample. Table III shows that normalisation can improve peak area precision, the improvement was more pronounced when a higher variation in migration times was observed.

Peak area ratios were calculated using the ratio of enantiomer 2 (En2) unnormalised peak area divided by the un-normalised peak area of enantiomer 1 (En1). The precision was clearly improved with all R.S.D. values below 1% (Table III), as variations in sample injection volumes and migration times are internally compensated for. Use of internal standards has been suggested to improve quantitative analysis in CE [18].

#### Peak height precision

The precision for peak height was measured by several companies and R.S.D. values of 1–2% were obtained (Table IV) indicating re-

TABLE IV  
PEAK HEIGHT PRECISION

Company	Peak height En1 (%R.S.D.) (n = 10)
1	1.0
2	2.3
3	2.1
4	Not recorded
5	1.7
6	1.4
7	1.7

producible data could be obtained employing these measurements. However, non-linear increases in peak height with increased sample loadings, at higher sample concentrations, have been observed [19].

#### % Peak area data

Clenbuterol is a racemic compound and should therefore give a %area/area result of 50:50 for the two enantiomers. Table V shows the average %area/area to be 50:50 with an acceptable precision of 0.6% R.S.D. for the seven results.

#### CONCLUSIONS

This first inter-company cross-validation exercise has confirmed that a CE method was able to be transferred between seven companies. Instruments from three manufacturers were employed

TABLE V  
% NORMALISED PEAK AREA DATA (n = 10)

Company	% Peak area		
	En1	En2	
1	49.4	50.6	
2	50.2	49.8	
3	49.6	50.4	
4	49.6	50.4	
5	49.9	50.1	
6	50.0	50.0	
7	50.0	50.0	
Mean	49.8	50.2	R.S.D. = 0.6%

in this study. In all instances baseline resolution or greater of the two enantiomers was achieved. Acceptable measures of linearity and precision of both migration time and peak area were obtained. The %area/area results clearly indicate that this chiral CE method is capable of generating precise data.

## REFERENCES

- 1 M.T. Ackermans, J.L. Beckers, F.M. Everaerts and I.G.J.A. Seelen, *J. Chromatogr.*, 590 (1992) 341.
- 2 E.W. Tsai, M.M. Singh, H.H. Lu, D.P. Ip and M.A. Brooks, *J. Chromatogr.*, 626 (1992) 24.
- 3 R. Weinberger and M. Albin, *J. Liq. Chromatogr.*, 14 (1991) 953.
- 4 M. Swartz, *J. Liq. Chromatogr.*, 14 (1991) 923.
- 5 K.D. Altria, *J. Chromatogr.*, 634 (1993) 323.
- 6 A. Pluym, W. Van Ael and M. De Smet, *Trends Anal. Chem.*, 11 (1992) 27.
- 7 S. Fanali, *J. Chromatogr.*, 545 (1991) 437.
- 8 M.J. Sepaniak, R.O. Cole and B.K. Clark, *J. Liq. Chromatogr.*, 15 (1992) 1023.
- 9 K.D. Altria, D.M. Goodall and M.M. Rogan, *Chromatographia*, 34 (1992) 19.
- 10 R. Kuhn and S. Hoffstetter-Kuhn, *Chromatographia*, 34 (1992) 505.
- 11 H. Wätzig and C. Dette, *J. Chromatogr.*, 636 (1993) 31.
- 12 G.M. McLaughlin, J.A. Nolan, J.L. Lindahl, J.A. Morrison and T.J. Bronzert, *J. Liq. Chromatogr.*, 15 (1992) 961.
- 13 S.E. Moring, J.C. Colburn, P.D. Grossman and H.H. Lauer, *LC·GC Int.*, 3 (1990) 46.
- 14 Q. Dang, L. Yan, Z. Sun and D. Ling, *J. Chromatogr.*, 630 (1993) 363.
- 15 T. Nagawaka, Y. Oda, A. Shibukawa, H. Fukuda and H. Tanaka, *Chem. Pharm. Bull.*, 37 (1989) 707.
- 16 M.W.F. Nielen, *J. Chromatogr.*, 588 (1991) 321.
- 17 K.D. Altria, *Chromatographia*, 35 (1993) 177.
- 18 E.V. Dose and G.A. Guiochon, *Anal. Chem.*, 63 (1991) 1154.
- 19 D.M. Goodall, S.J. Williams and D.K. Lloyd, *Trends Anal. Chem.*, 10 (1991) 272.



# Automated isotachophoretic analyte focusing for capillary zone electrophoresis in a single capillary using hydrodynamic back-pressure programming

N.J. Reinhoud, U.R. Tjaden\* and J. van der Greef

*Division of Analytical Chemistry, Leiden/Amsterdam Center for Drug Research, Leiden University, P.O. Box 9502, 2300 RA Leiden (Netherlands)*

(First received December 3rd, 1992; revised manuscript received January 25th, 1993)

---

## ABSTRACT

An automated isotachophoretic (ITP) analyte focusing procedure prior to capillary zone electrophoresis (CZE) is described. The ITP focusing step is carried out in the same capillary as the CZE. Hydrodynamic back-pressure programming resulted in a reduction in the effects of the electroosmotic flow-rate during the ITP step and allowed the removal of terminating buffer before the CZE run was started. The characteristics of this on-line focusing procedure were studied for several anionic test compounds.

---

## INTRODUCTION

Capillary electrophoresis (CE) has become an important separation technique complementary to high-performance liquid chromatography (HPLC). Several reviews have described the role of capillary electrophoretic separation methods in analytical chemistry [1–3]. Improvements in detection techniques resulted in the detection of extremely small amounts of analyte. Nevertheless, owing to the small dimensions of the separation system and the small injection volumes, the corresponding concentration detection limits are relatively high.

Different on- and off-line methods to improve the concentration detection limits in CE have been described. Off-line sample pretreatment and preconcentration, such as concentrating liquid–liquid or solid-phase extraction, offer flexibility in the choice of buffers and the amount of sample to be pretreated. These procedures are

laborious and time consuming. On-line sample pretreatment offers the possibility of automation but has some restrictions with respect to the following step in the analytical method. Examples of on-line sample pretreatment and/or preconcentration are the combination of LC and CE [4–6] and of isotachophoresis (ITP) and capillary zone electrophoresis (CZE) [7–10].

An elegant way of lowering the determination limits that is typical for zone electrophoretic separations is the application field-amplified on-capillary sample concentration or stacking. This can be done in several ways, by using low-conductivity sample buffers, by using sample self-stacking, by addition of an electrolyte to the sample, allowing a transient isotachophoretic preconcentration, or by combining some of these methods [11–16].

In this paper we describe a procedure for the automated coupling of ITP with CZE using a single open capillary in a commercially available electrophoresis system without modification of the system. By using hydrodynamic back-pressure programming during the focusing step the

---

\* Corresponding author.



terminating buffer could be removed before the CZE step, resulting in highly efficient separations.

## EXPERIMENTAL

Untreated fused-silica (100  $\mu\text{m}$  I.D.) (SGE, Ringwood, Victoria, Australia) and UV-transparent (75  $\mu\text{m}$  I.D.) (Polymicro Technologies, Phoenix, AZ, USA) capillaries were used. A programmable injection system for CE (PRINCE; Lauerlabs, Emmen, Netherlands) equipped with a reversible polarity power supply and the possibility of pressurized and/or electrokinetic injection was used for the analyte-focusing process.

On-capillary laser-induced fluorescence (LIF) detection took place using a water-cooled argon ion laser (Model 2025-03; Spectra-Physics, Mountain View, CA, USA) lasing at multiple wavelengths of 351.1 and 363.8 nm at 20 mW for excitation. The excitation wavelengths were filtered through a 350-nm band pass filter (10-nm band width). Fluorescence light was transported to the photomultiplier tube (PMT) through a liquid light guide (1000  $\times$  5.0 mm I.D.) (Model 77556; Oriol, Stratford, CT, USA) equipped with a plano-convex fused-silica lens ( $D = 11$  mm, focal length = 19 mm) (Model 41210; Oriol) at each end. The fluorescence light was directed on to a 450-nm band pass interference filter (10-nm band width, Type 53830; Oriol) for *o*-phthaldialdehyde derivatives or on to a 525-nm interference filter (10-nm band width) for fluorescein and analogues. The PMT (Model 9635B; Thorn EMI, Ruislip, Middlesex, UK) was operated at 800 V (Model 244 power supply; Keithley Instruments, Cleveland, OH, USA).

The signal was amplified by a current amplifier (Model 427; Keithley Instruments) and registered on a chart recorder (Kipp and Zonen, Delft, Netherlands) or digitized using a laboratory-made 12-bit A/D converter operating at a frequency of 20 Hz. The A/D converter was connected to a computer (Mega ST4; Atari, Sunnyvale, CA, USA) controlling the sampling frequency of the converter and the data handling.

## Chemicals

Phosphoric acid, barium hydroxide, glutamic acid (Glu), aspartic acid (Asp) and bromophenol blue were obtained from Merck (Darmstadt, Germany). Sodium cacodylate and fluorescein (F) were purchased from Janssen Chimica (Beerse, Belgium). Hydroxypropylmethylcellulose (HPMC) was supplied by Sigma (St. Louis, MO, USA). The viscosity of a 2% aqueous HPMC solution is 4000 cP. Fluorescein isothiocyanate isomer I (FITC), *o*-phthaldialdehyde (OPA) and mercaptoethanol (ME) were obtained from Aldrich Chemie (Steinheim, Germany). In all experiments deionized water was used, obtained with a Milli-Q system (Millipore, Bedford, MA, USA).

OPA derivatives of amino acids were prepared by adding 1 ml of amino acid dissolved in leading buffer to an OPA solution of 1 mg/ml in leading buffer containing 0.1% ME. Unless mentioned otherwise, the OPA derivatives were analysed after 5 min. Sample solutions of fluoresceins were prepared in leading buffer unless mentioned otherwise.

## RESULTS AND DISCUSSION

### *Analyte focusing after hydrodynamic sample introduction*

A discontinuous buffer system was used to permit ITP sample preconcentration (Fig. 1). The capillary and ITP anode vial (which is also the CZE cathode vial) are filled with leading buffer consisting of 10 mmol/l sodium phosphate (pH 9.4). To the leading buffer 0.05% (w/v) of HPMC was added. The HPMC only reduced the electroosmotic flow in the fused-silica capillary to such an extent that acceptable preconcentration runs could be made. The leading buffer was also used as the CZE buffer.

*Step 1.* Injections were made hydrodynamically at a pressure of 10–600 mbar. After injection, a terminating buffer vial containing 10 mmol/l sodium cacodylate buffer (pH 8.2) with 0.05% (w/v) HPMC was placed at the capillary inlet. For the analysis of OPA derivatives the pH was raised to 9.4 using  $\text{Ba}(\text{OH})_2$ .

*Step 2.* The analyte focusing started by applying a voltage of  $-25$  kV in conjunction with a

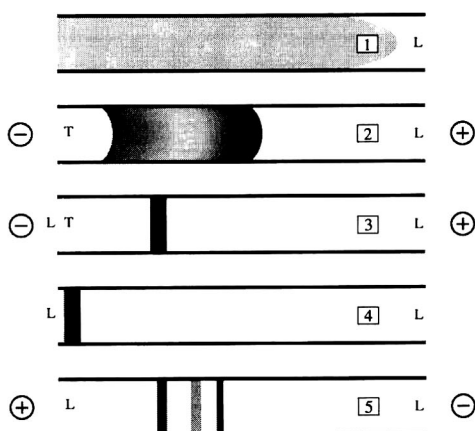


Fig. 1. Schematic representation of ITP-CZE in a single capillary. The leading buffer (L) is also used as electrophoresis buffer in the CZE step. The terminator buffer (T) is removed from the capillary in step 3. See text for further details.

hydrodynamic back-pressure of 40 mbar. This negative voltage resulted in an electroosmotic flow in the direction of the capillary inlet. To prevent the analyte from migrating out of the capillary a hydrodynamic back-pressure was applied. Because of the self-correcting properties of the ITP zones, the hydrodynamic back-pressure did not result in peak broadening. This is in contrast to field-amplified injection techniques where electroosmotic convections are a major source of peak broadening of large injection plugs [11].

**Step 3.** After 5–20 min of focusing, depending on the volume injected, the cacodylate buffer vial was replaced with the CZE buffer vial. A voltage of  $-20$  kV was applied without a hydrodynamic back-pressure. As the capillary still contained cacodylate buffer, this step was carried out under real isotachophoretic conditions, although a vial containing phosphate buffer was placed at the terminator end. The sample zones were sandwiched between the anodic leading buffer and the terminating buffer plug, which is in the capillary. The electroosmotic flow-rate was higher than the mobility of the phosphate ions in the vial at the terminator end, thus preventing these ions from entering the capillary. Simultaneously the plug of terminating buffer was removed from the capillary. It is important for the

next step that the CZE buffer vial is already in position.

**Steps 4 and 5.** At the time that the sample zone was approaching the capillary inlet the voltage was reversed and the CZE run was started at a positive voltage of 30 kV. The correct timing of the voltage switching is important. If the ITP process is continued for too long, the sample zones will migrate out of the capillary into the inlet buffer vial. If the voltage is switched too early a plug of terminating buffer is still in the capillary and will disturb the homogeneity of the electric field necessary for CZE, resulting in peak broadening. Initially bromophenol blue was used as a visible marker. When reproducible ITP run times were measured, automated programming was applied and the marker could be omitted. When the use of a visible marker is inconvenient because of hardware incompatibility, timing can be done by monitoring the current. Applying a constant voltage, the current increases as long as the terminating ions leave the capillary.

In principle, all terminating ions and sample ions with mobilities below that of the analyte ion can be removed by the described procedure. This is an important difference from transient-like isotachophoretic preconcentration [12,15]. Another advantage of focusing under isotachophoretic conditions using a hydrodynamic back-pressure is that the time needed for focusing can in principle be as long as necessary for a given analysis without peak broadening or loss of analyte. An optimum can be found between the determination limit of an analyte for a given injection volume and the time needed for focusing.

The analyte focusing was studied for OPA derivatives of Glu and Asp derivatized before injection. The derivatives have an excitation maximum at 340 nm fitting with the 351.1/363.8 nm lasing wavelengths of the argon ion laser. The laser beam was filtered with a 350-nm band pass filter before focusing on to the capillary. This reduced considerably the background at 450 nm, the emission maximum of the OPA derivatives. Because OPA derivatives are not stable with time [17], some characteristics of the system were investigated with F and FITC. These com-

pounds have native fluorescence with an excitation maximum around 490 nm. Although this excitation maximum fits perfectly with the 488-nm lasing wavelength of the argon ion laser, a good signal was obtained using the 351.1/363.8 nm lasing wavelengths for excitation. For convenience the laser optics were not changed and all experiments were done using the same laser system, except for the emission wavelength, which was 525 nm for the fluoresceins. The effect of analyte focusing was compared with CZE runs without focusing.

#### Loadability and linearity for OPA derivatives

When analyte focusing was carried out for injection volumes similar to those in CZE runs, the improvement in detectability was limited (Fig. 2A and B). An explanation for this effect is that in CZE the analytes migrate through a background electrolyte whereas in ITP the analytes are sandwiched as distinct zones between leading and terminating electrolytes. In ITP-CZE, when the focusing procedure has been completed and the CZE is started, mixing of the analyte zones with the background electrolyte occurs. This results in some band broadening and dilution. In Fig. 2B the ITP preconcentration of analyte is levelled by this mixing process, resulting in comparable peak

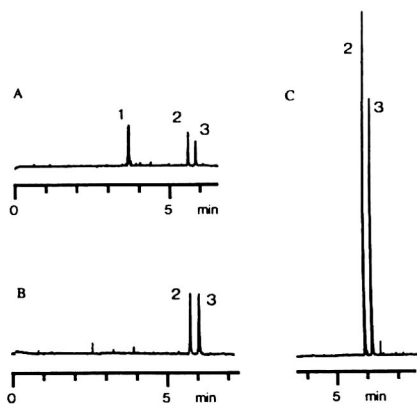


Fig. 2. Electropherograms of a mixture of 200 ng/ml OPA derivatives of (1) Phe, (2) Glu and (3) Asp. Injection volume of (A) 70 nl using CZE compared with (B) 70 nl and (C) 350 nl using ITP-CZE. A  $700 \times 0.1$  mm I.D. fused-silica capillary was used. The derivative of Phe had a lower mobility as the terminator and was removed from the capillary in ITP-CZE.

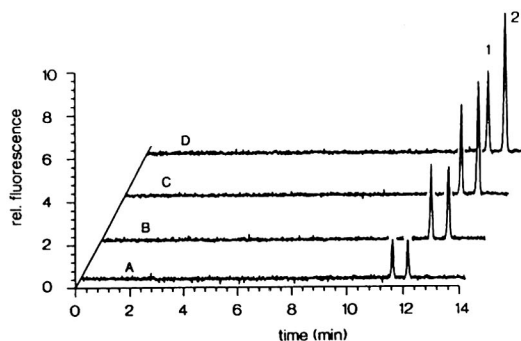


Fig. 3. Effect of injection volume on the analysis of a derivatization mixture of  $1 \mu\text{g/ml}$  of (1) Glu and (2) Asp with OPA. Injection volume: (A) 0.2; (B) 0.7; (C) 1.4; (D)  $2.4 \mu\text{l}$ . A  $700 \times 0.1$  mm I.D. fused-silica capillary was used.

heights. Fig. 2C shows that increasing the injection volume by a factor of 5 results in an increase in the signal by a factor of 5.

Figs. 3 and 4 show that the capillary can be filled to 50% ( $2.4 \mu\text{l}$ ) without band broadening. For the OPA derivative of Glu there is an optimum in the loadability with respect to peak height, whereas the peak height of the Asp derivative does not increase linearly with the injection volume. At larger injection volumes longer focusing times were necessary, resulting in degradation of the unstable derivatives. The focusing time increased from 4 min for a  $0.2\text{-}\mu\text{l}$  to 20 min for a  $2.4\text{-}\mu\text{l}$  injection volume. To eliminate these effects we studied the loadability, linearity and reproducibility with F and FITC.

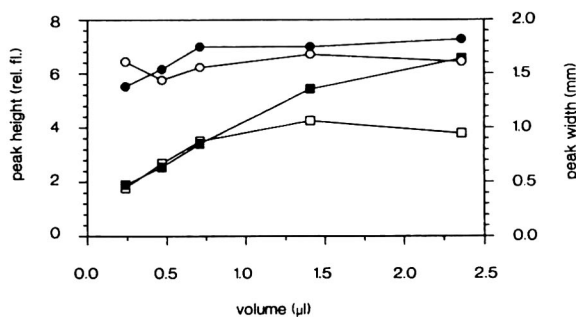


Fig. 4. The peak height of (■) Asp increases whereas the peak widths of (●) Asp and (○) Glu remain the same with increasing injection volume. The peak height of (□) Glu shows an optimum. The peak width is given as half of the peak height measured at 60% of the peak height. The corresponding electropherograms are shown in Fig. 3.

### Loadability, linearity and reproducibility for fluoresceins

F and FITC are more stable than OPA derivatives under alkaline conditions. FITC is a well known fluorescent probe for the derivatization of amines. The reaction products are usually anionic because of the charges on FITC. It is therefore expected that the reaction products can be analysed in a similar way using ITP-CZE.

As can be seen from Fig. 5, the increase in detectability of F corresponds to the increase in injection volume. The total analysis time for the CZE run was 10 min, whereas the ITP-CZE run took 20–24 min. This included a flush of 1 min with 10 mmol/l KOH, 1 min with leading buffer and an ITP focusing step of 10 min. The flushing was necessary to obtain reproducible migration times.

Loading of the capillary with large sample plugs changes the condition of the capillary wall, especially when a dynamic coating of HPMC is used. For relatively clean samples and constant injection volumes, this resulted in a small shift in the migration time. However, when the injection volumes are increased the effects on the capillary wall are more severe. In Fig. 5 the migration times in the CZE step increased by *ca.* 65% for both analytes. In the study of fluoresceins a buffer of pH 8.1 was used, implying that at longer focusing times the pH in the capillary decreases. As a result, the electroosmotic flow in the CZE decreased, resulting in increased migration times. This shift did not occur with the OPA

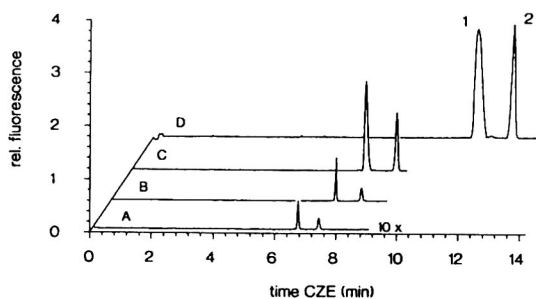


Fig. 5. Loadability in ITP-CZE of a mixture of (1) FITC and (2) F at a concentration of 500 ng/ml in leading buffer. Injection volume: (A) 14; (B) 140; (C) 750; (D) 1500 nl. The peak height of F and the peak area of F and FITC showed a linear increase with increasing injection volume. A  $700 \times 0.075$  mm I.D. fused-silica capillary was used.

derivatives (Fig. 3). For the OPA derivatives a terminator buffer at the same pH as the leading buffer (pH 9.4) was used. The use of a buffering counter ion (*e.g.*  $\text{Tris}^+$ ) is therefore advisable. However, for our test compounds the CZE performance was better with sodium phosphate buffer.

In Fig. 6 the effect of the focusing time on the performance in ITP-CZE is demonstrated. A focusing time of less than 5 min results in a decrease in signal because of incomplete focusing. However, increasing the focusing time from 10 to 34 min did not result in a change in resolution or efficiency. This is an important observation because it demonstrates that band broadening is independent of time in the focusing procedure, although a hydrodynamic back-pressure is used. Everaerts *et al.* [18] used a counterflow of electrolyte in ITP to increase the effective length of the separation system. They measured a considerable disturbance when a counterflow higher than 30% of the mobility of the sample zones was applied. They concluded that the optimum counterflow depended on, amongst other things, the capillary diameter, the viscosity and the temperature in the capillary. In our ITP-CZE system no peak broadening was seen at a back-pressure which is 100% of the analyte mobility. In principle this means that the effective length of our ITP system has been increased to infinity. However, the analysis time increases similarly. Therefore, an optimum has

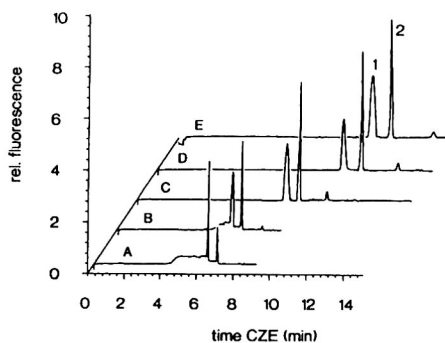


Fig. 6. Effect of focusing time on the performance in ITP-CZE of a mixture of 50 ng/ml of (1) FITC and (2) F. Injection volume,  $1.5 \mu\text{l}$ . A  $700 \times 0.075$  mm I.D. fused-silica capillary was used. Focusing time: (A) 1.8; (B) 4.5; (C) 10; (D) 18; (E) 34 min.

to be found between the injection volume, the complexity of the sample, the determination limit and the time needed for focusing of large injection plugs.

A study of the reproducibility in CZE and ITP–CZE of a mixture of FITC with F is shown in Fig. 7. Peak areas gave better results than peak heights. In ITP the zone length varies with the concentration. As a result, it is expected in ITP–CZE that the peak area will give a better correlation than peak height with analyte concentration. The relative standard deviations (R.S.D.s) of peak areas for CZE were 3.5% and 5.3% for F and FITC, respectively (Fig. 7A), and those of peak heights were 8.4% and 8.6%, respectively. For ITP–CZE R.S.D.s of peak areas of 6.5% and 5.3% were measured for F and FITC, respectively (Fig. 7B); the corre-

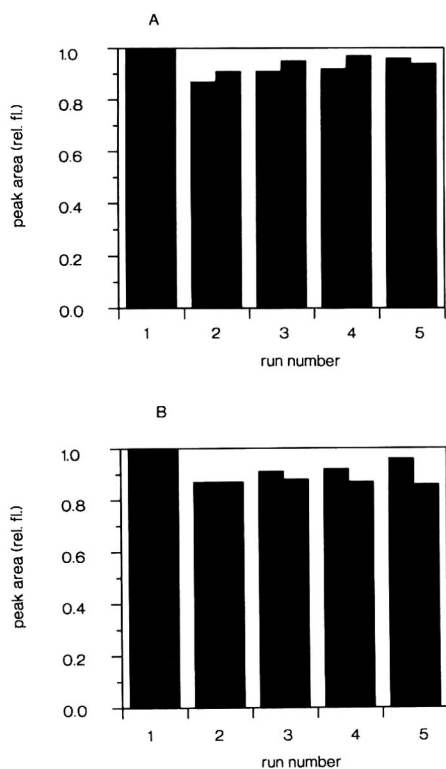


Fig. 7. (A) Reproducibility of peak areas of five CZE runs of a mixture of 1 µg/ml of F (grey bars) and 0.5 µg/ml of FITC (black bars) at an injection volume of 30 nl. (B) Reproducibility of peak areas of five ITP–CZE runs of a mixture of 10 ng/ml of F (grey bars) and 5 ng/ml of FITC (black bars) at an injection volume of 1.7 µl.

sponding values were 9.8% and 18% for peak heights. When the ratio of peak areas was used R.S.D.s of 4.6% in CZE and 4.8% in ITP–CZE were found. The improvement in the R.S.D.s for peak-area ratios demonstrates the necessity to use an internal standard in quantitative analysis with ITP–CZE.

The linearity of the method was studied at a concentration level just above the detection limit. Calibration graphs were constructed for FITC between 0.2 and 18 ng/ml. F was used as internal standard at a concentration of 25 ng/ml. The peak-area ratios were used for linear regression. Table I gives the regression data calculated for linear regression as described by Miller [19].

#### Practical considerations

Several practical aspects are of importance for the applicability of the method to analyses in complex matrices such as urine or plasma samples.

First, a separation window exists in the ITP step within which the analyte of interest is focused. This separation window is an important tool in sample clean-up and can be tuned by the choice of the leading and terminating buffer. In the literature numerous ITP systems have been described [18].

The anions that are faster than the leading buffer ions migrate into the separation capillary already during the ITP step. Ions with lower mobilities than the terminator ions, including neutral species and cations, are removed from

TABLE I  
REGRESSION DATA FOR ITP–CZE OF FITC USING F AS AN INTERNAL STANDARD

A 700 × 0.075 mm I.D. fused-silica capillary was used with an injection volume of 1.7 µl. Weighting factors were not necessary because calibration was carried out with five different concentrations with constant concentration intervals of 0.4 ng/ml for the low concentration range and 4.0 ng/ml for the higher concentration range.

Range (ng/ml)	Slope	S.D.	Intercept	S.D.	Correlation coefficient
0.2–1.8	0.137	0.010	–0.012	0.01	0.985
2.0–18.0	0.142	0.015	0.02	0.15	0.965

the capillary in the ITP step, resulting in a considerable sample clean-up. It is therefore important to choose a favourable set of buffers, *i.e.*, a leading buffer with a high mobility to reduce the number of matrix anions with a higher mobility. The electrophoretic mobility of the terminator buffer should be as close to that of the analyte as possible. The pH of the buffers is often an important parameter for fine tuning the mobilities of the analytes and the buffer ions.

Second, the separation order of anions in ITP is reversed with respect to CZE. Anions with a high electrophoretic mobility migrate, after focusing and reversal of the voltage, through the analyte zones with a lower electrophoretic mobility. In the analysis of, *e.g.*, urine samples, the possibility exists that a zone of matrix ions migrates as a spacer between two analyte zones. Depending on the zone length of the matrix ions, the migration times in CZE may change. With clean samples as described above, no difference in migration times in ITP–CZE with respect to CZE has been observed. Because a low concentration of analyte (*i.e.*, nanomolar range) is concentrated in the ITP step to approximately that of the leading buffer ions (*i.e.* millimolar range), the starting zone length will be reduced from decimetres to micrometres. A mixing of zones occurs as soon as the ITP has ended and the CZE has started, which is caused by diffusion, convection and dilution with background electrolyte. As a result, although strongly concentrated, the analyte ions start in the CZE process more or less as one mixed zone. In biological samples, however, a number of ions are present at a much higher concentration. Depending on their mobilities and of the separation window, these matrix ions may act as spacers for analyte ions. After switching from the ITP to the CZE mode, the analytes start the CZE run at different positions in the capillary, resulting in different migration lengths. In these cases a sample pretreatment might be necessary to obtain reproducible results. On the other hand, an excess of spacer ions can be added deliberately to the sample to improve the resolution in ITP–CZE separations.

Finally, in the ITP step a hydrodynamic back-pressure is levelling the electroosmotic flow-rate.

It is obvious that fluctuations in either of them would result in decreased reproducibility. It is therefore of crucial importance that the pressure can be monitored and controlled accurately during the process, which is the case with the described system. Further, the electroosmotic flow should not change from run to run. A constant pH is important with respect to the electroosmotic flow-rate and it is therefore advisable to use a buffering counter ion. Injection of large sample plugs of a different pH may cause local changes in the electroosmotic flow. In these cases the samples should be pH adjusted or pretreated. The same applies to samples with large differences in salt concentration. As a consequence, the method will be suitable especially for the analysis of compounds in a constant matrix with respect to pH and salt concentration, such as plasma.

#### CONCLUSIONS

An automated procedure has been developed for the isotachophoretic preconcentration of low concentrations of analyte using ITP–CZE in a single capillary in combination with hydrodynamic back-pressure programming. The described method is reproducible and linear at low concentrations. An improvement in the determination limit of more than 100 with respect to CZE has been demonstrated. The increase in loadability is only limited by the capillary volume. An optimum has to be found between the injection volume, the determination limit and the time needed for focusing of large injection plugs.

#### REFERENCES

- 1 W.G. Kuhr, *Anal. Chem.*, 62 (1990) 403R.
- 2 W.G. Kuhr and C.A. Monnig, *Anal. Chem.*, 64 (1992) 389R.
- 3 R.A. Wallingford and A.G. Ewing, *Adv. Chromatogr.*, 29 (1989) 1.
- 4 N.A. Guzman, M.A. Trebilcock and H.P. Advis, *J. Liq. Chromatogr.*, 14 (1991) 997.
- 5 M.M. Bushey and J.W. Jorgenson, *Anal. Chem.*, 62 (1990) 978.
- 6 J. Cai and Z. Elrassi, *J. Liq. Chromatogr.*, 15 (1992) 1179.

- 7 F. Foret, V. Sustacek and P. Bocek, *J. Microcol. Sep.*, 2 (1990) 229.
- 8 D.S. Stegehuis, H. Irth, U.R. Tjaden and J. van der Greef, *J. Chromatogr.*, 538 (1991) 393.
- 9 D. Kaniansky and J. Marak, *J. Chromatogr.*, 498 (1990) 191.
- 10 V. Dolnik, K.A. Cobb and M. Novotny, *J. Microcol. Sep.*, 2 (1990) 127.
- 11 R.L. Chien and D.S. Burgi, *Anal. Chem.*, 64 (1992) A489.
- 12 F. Foret, E. Szoko and B.L. Karger, *J. Chromatogr.*, 608 (1992) 3.
- 13 R.L. Chien and D.S. Burgi, *Anal. Chem.*, 64 (1992) 1046.
- 14 D.S. Burgi and R.L. Chien, *Anal. Chem.*, 63 (1991) 2042.
- 15 C. Schwer and F. Lottspeich, *J. Chromatogr.*, 623 (1992) 345.
- 16 F.E.P. Mikkers, F.M. Everaerts and T.P.E.M. Verheggen, *J. Chromatogr.*, 169 (1979) 11.
- 17 J.F. Stobaugh, A.J. Repta, L.A. Sternson and K.W. Garren, *Anal. Biochem.*, 135 (1983) 495.
- 18 F.M. Everaerts, J.L. Beckers and T.P.E.M. Verheggen, *Isotachopheresis: Theory, Instrumentation and Practice*, Elsevier, Amsterdam, 1976.
- 19 J.N. Miller, *Analyst*, 116 (1991) 3.

CHROM. 25 010

# Optimizing dynamic range for the analysis of small ions by capillary zone electrophoresis

G.W. Tindall\*, D.R. Wilder and R.L. Perry

*Research Laboratories, Eastman Chemical Company, Eastman Kodak Company, P.O. Box 1972, Kingsport, TN 37662 (USA)*

(First received November 16th, 1992; revised manuscript received February 23rd, 1993)

---

## ABSTRACT

Many applications of capillary zone electrophoresis (CZE) are for the determination of UV transparent ions. Indirect UV detection can be used for these analyses, but one problem with indirect detection is a limited dynamic range for analysis. A strategy for optimizing dynamic range for CZE analyses with indirect detection is described. Optimization involves chromophore-electrolyte selection, concentration and wavelength optimization and tuning the electrolyte mobility through complexation. The strategy is illustrated for the analysis of aliphatic acids. We found that 2,6-naphthalenedicarboxylate is an ideal chromophore-electrolyte for aliphatic acid analysis. Through complexation with  $\beta$ -cyclodextrin its mobility can be tuned to match the mobility of aliphatic acids. By optimizing detection wavelength and electrolyte concentration and mobility as little as 0.025 mg/l of aliphatic acids can be detected and up to 1000 mg/l can be quantitated. Under optimized conditions CZE can be used for trace analyses.

---

## INTRODUCTION

Capillary zone electrophoresis (CZE) has been proposed for the determination of anions such as inorganic anions, aliphatic acids, aromatic acids and anionic surfactants [1–7]. CZE can have advantages over ion chromatography for these determinations. CZE separations have very high resolution, they are typically fast, sample size is small and consumables costs (especially columns) are nearly insignificant. Neutral species are usually well separated from anions so large concentrations of neutrals, for example solvents, generally do not interfere with anion analyses by CZE. This is often not the case in ion chromatography. These advantages have been demonstrated in the cited references.

Many applications of CZE are for the determination of UV transparent ions. Indirect UV

detection can be used for these analyses. A problem with indirect detection is a limited dynamic range for analysis [8,9]. The low concentration end of this range is the limit of quantitation, often defined as three times the detection limit. Photometric factors that determine detection limit for indirect detection have been investigated [9,10–15]. These authors conclude that detection limits are lowest when the indirect chromophore has a large molar absorptivity at the detection wavelength and the concentration is adjusted for optimum photometric sensitivity. For the circular cell geometry of on column detection, the background absorbance should not exceed about 0.1 AU [9]. Wang and Hartwick [15] have found, however, that fluctuations in electrolyte concentration could be the limiting factor in detection limit. They concluded there could, in theory, be situations where only the concentration of the electrolyte affected limit of detection and other situations where only the molar absorptivity of the electrolyte affected the

---

\* Corresponding author.



limit of detection. Poppe [16] calculated that one-to-one displacement of analyte for indirect chromophore only occurs when the mobilities of these ions are equal. Therefore, mobility of the indirect chromophore also has an effect on detection limit and limit of quantitation.

The utility of CZE lies in its ability to effect high-resolution separations. For typical separations, the high end of the dynamic range for analysis is most often limited by loss of resolution due to concentration overload (electromigration dispersion) rather than photometric signal saturation [16]. This limitation can be overlooked in investigations of dynamic range that only consider a single component. The severe dispersion encountered at high analyte concentrations results from a mismatch between analyte and electrolyte mobility [16,17]. Since the driving force for separation by CZE is differences in analyte mobility, there will never be a mobility match for more than one component. Hence, the upper end of the dynamic range for a separation is generally limited by dispersion rather than photometric factors. Dispersion is negligible when there is a large difference between the concentration of electrolyte and analyte, but it broadens the analyte peaks when the analyte concentration becomes a significant fraction of the electrolyte concentration. In the limit, this dispersion destroys peak separation and establishes the effective upper limit for quantitation.

Concentration overload can be minimized, and dynamic range extended, by increasing the electrolyte concentration and optimizing the mobility of the electrolyte. Limit of quantitation can be lowered by increasing the molar absorptivity of the electrolyte, lowering its concentration to keep the background absorbance less than about 0.1 and optimizing the electrolyte mobility for the separation. The conflict of these goals is obvious.

This paper presents a strategy for optimizing dynamic range for CZE analyses with indirect detection. Optimization involves chromophore–electrolyte selection, concentration and wavelength optimization and a new concept, mobility tuning. The strategy is illustrated for the analysis of aliphatic acids. By using this strategy, as little

as 0.025 mg/l of aliphatic acids can be detected and up to 1000 mg/l can be quantitated.

## EXPERIMENTAL

### *Materials*

Acetic, propionic and butyric acids and 2,6-naphthalenedicarboxylic acid were purchased from Aldrich (Milwaukee, WI, USA).  $\beta$ -Cyclodextrin was purchased from Advanced Separation Technologies (Whippany, NJ, USA). Water was obtained from a Millipore ultrafiltration system (Bedford, MA, USA). Adjustment of electrolytes pH was performed using sodium hydroxide purchased from Mallinckrodt (Paris, KY, USA).

### *Instrumentation*

Analyses were performed on an ABI (Foster City, CA, USA) 270A-HT capillary electrophoresis system. The separation was performed on a 72 cm  $\times$  50  $\mu$ m I.D. (injector to detector length equals 50 cm) Polymicro Technologies (Phoenix, AZ, USA) fused-silica column with an applied potential of 30 kV positive. Column chamber temperature was 30°C. Detection was by indirect UV at 240 nm or 283 nm. Sample injection was by vacuum for 5 s.

## DISCUSSION

A strategy for optimizing the dynamic range of an analysis will be illustrated for the separation of acetic, propionic and butyric acids. Indirect detection is used for the detection of these analytes, but elements of the optimizing strategy can be used for direct detection as well. The strategy involves selection of the indirect chromophore–electrolyte and optimizing its concentration and detection wavelength for the analyte concentration range of interest. Dynamic concentration range for the separation is extended by matching the mobility of the electrolyte to an analyte of interest. Mobility tuning was accomplished through complexation of the electrolyte with cyclodextrin. The concentration of cyclodextrin is adjusted to where the effective mobility of the electrolyte–cyclodextrin complex mat-

ches the analyte of interest. Usually this would be an analyte of intermediate mobility.

#### Chromophore–electrolyte selection

An electrolyte of optimum mobility will not normally be found. While it might seem easy to find electrolytes of any desirable mobility, we have not found this to be the case. Therefore, an electrolyte is selected that has a mobility faster than the middle of the analyte range. The electrolyte should have a large molar absorptivity in the wavelength range of the detector. It should be stable in basic solutions and it must complex with  $\beta$ -cyclodextrin. The indirect chromophore–electrolyte selected for this separation is 2,6-naphthalenedicarboxylic acid (Fig. 1). At a pH of 9 the dianion of this acid has a mobility slightly greater than acetate and the electroosmotic flow is fast enough to achieve short analysis times.

**Case 1: Analytes present at similar concentration greater than about 1 mg/l.** In this case the electrolyte should be as concentrated as possible to minimize concentration overload. Column current sets an upper limit on electrolyte concentration; it should not be so high that column heating is a problem. With our system an electrolyte concentration of 7 mM is optimum, but this could be different for systems that have different means for column thermostating or different column dimensions and voltages. The next step is to select a wavelength so that the background absorbance is about 0.1 AU, in this case 283 nm. Under these conditions the dynamic range for the analysis is about 1 to 400 mg/l when the analytes are in equal concen-

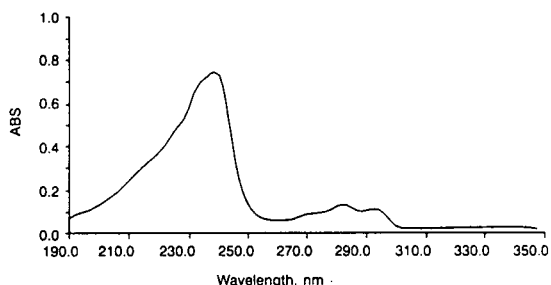


Fig. 1. Spectrum of 2,6-naphthalenedicarboxylate aqueous solution pH 9;  $A_{240} = 62\,000$ ,  $A_{283} = 11\,000$ .

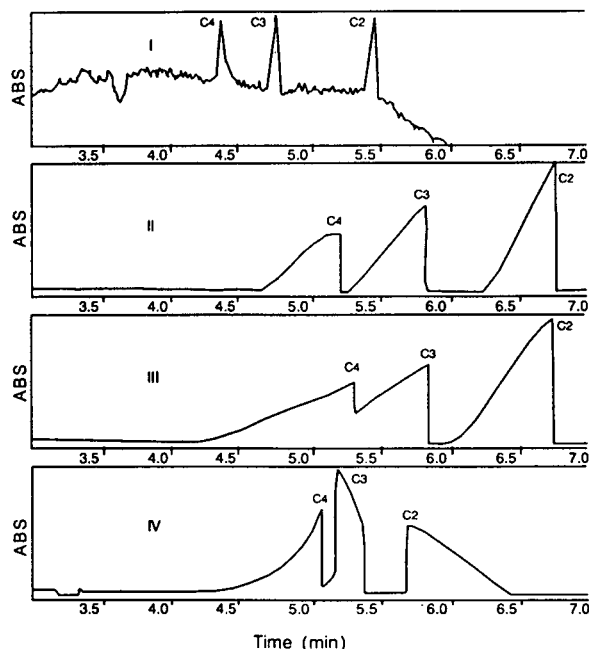


Fig. 2. Electropherograms of butyric (C4), propionic (C3) and acetic (C2) acids. Electrolyte, 7 mM 2,6-naphthalenedicarboxylate, pH 9; 283 nm. (I) 1 mg/l each acid; (II) 400 mg/l each acid; (III) 1000 mg/l each acid; (IV) 1000 mg/l each acid with 5 mM  $\beta$ -cyclodextrin.

trations (see Fig. 2). The sample is diluted so the analytes fall in this range. This range will depend on the mobility of the electrolyte. Ideally the mobility should fall in the middle of the range of analytes, but in this case it is somewhat greater than acetate as shown by the fronting peaks.  $\beta$ -cyclodextrin will complex many aromatic molecules, including 2,6-naphthalenedicarboxylate [18]. Even a small tendency to complex with the relatively large  $\beta$ -cyclodextrin molecule will lower the apparent mobility of the electrolyte. By changing the concentration of  $\beta$ -cyclodextrin the electrolyte mobility can be tuned to match any of the analytes. With no cyclodextrin, the analytes front because the electrolyte mobility is greater than the analyte mobility (Fig. 3). As the cyclodextrin concentration is increased, the peaks become symmetrical and then tail as the effective mobility of the electrolyte becomes equal to and then less than the mobility of the analytes. By tuning the mobility to match propionic acid, the upper end of the dynamic range for the separation can be increased to over 1000

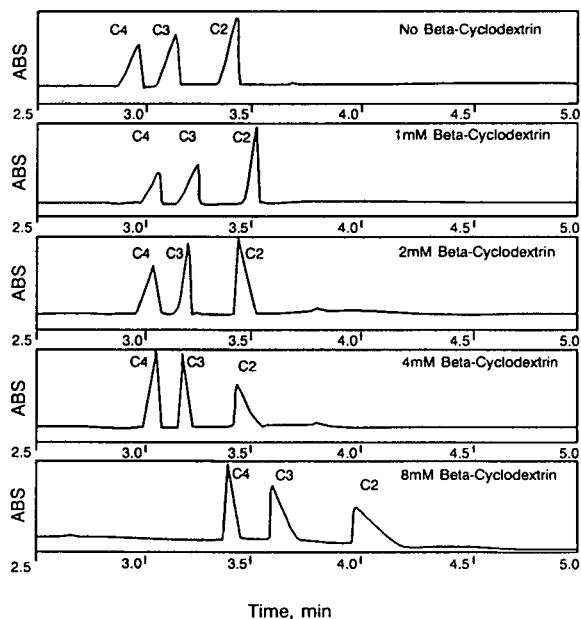


Fig. 3. Electropherograms of 10 mg/l butyric (C4), propionic (C3) and acetic (C2) acids. Electrolyte, 1 mM 2,6-naphthalenedicarboxylate, pH 9 with  $\beta$ -cyclodextrin added.

mg/l (Fig. 2). The dynamic range is 1000 under these conditions, an improvement of ten-fold over previous work [8].

It should be noted that the mobility match of the electrolyte for this separation is exceptionally good without tuning with  $\beta$ -cyclodextrin. In cases where the inherent mobility of the electrolyte is more poorly matched the improvement is even greater.

*Case 2: Analytes at similar concentration less than 1 mg/l.* For this case the detection limit must be optimized at the expense of the upper concentration limit. The detector wavelength is changed to 240 nm where the molar absorptivity of the chromophore–electrolyte is largest and the concentration is lowered to 1 mM to keep the background absorbance to about 0.1 AU. Under these conditions the detection limit for these acids is 0.025 mg/l, but the upper limit for analysis is now only 50 mg/l (Fig. 4). Tuning the electrolyte mobility to match propionate also improves the upper separation limit in this case (Fig. 4).

These examples illustrate how the dynamic range for an analysis can be adjusted up and

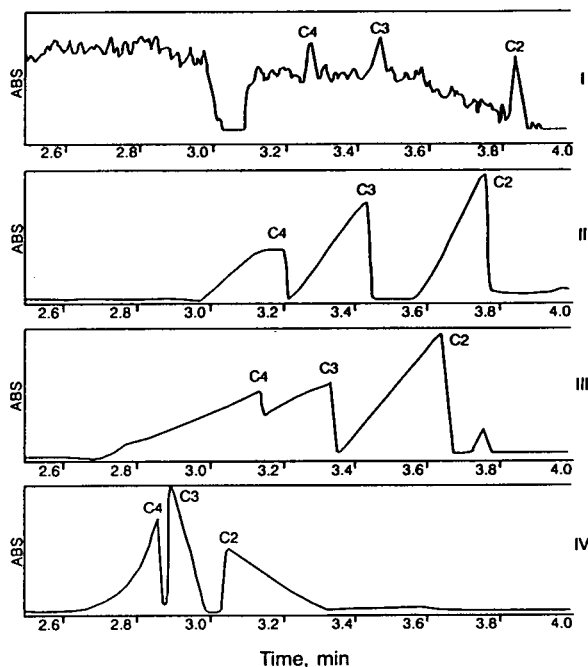


Fig. 4. Electropherograms of butyric (C4), propionic (C3) and acetic (C2) acids. Electrolyte, 1 mM 2,6-naphthalenedicarboxylate, pH 9; 240 nm. (I) 0.025 mg/l each acid; (II) 50 mg/l each acid; (III) 100 mg/l each acid; (IV) 100 mg/l each acid with 3 mM  $\beta$ -cyclodextrin.

down to accommodate samples with different concentrations. The overall range is impressive, 0.025 to 1000 mg/l. This range is competitive with other means of determining ions and aliphatic acids.

*Case 3: Analytes present at widely different concentration (trace component analysis).* This is the most difficult case for analysis by CZE. For this illustration it will be assumed that the major component peak will be severely concentration overloaded to detect the trace component. By electrolyte selection, mobility tuning and flow reversal it may be possible to arrange for the trace component to be on the sharp side of the overloaded component. In this case it is best to mobility tune the electrolyte to the trace component for maximum sensitivity [16]. The improvement in sensitivity can be significant. For example, the relative molar responses, normalized for migration time, for acetate, propionate, and butyrate are 1.00:0.77:0.57 with the 2,6-naphthalenedicarboxylate electrolyte. Significant

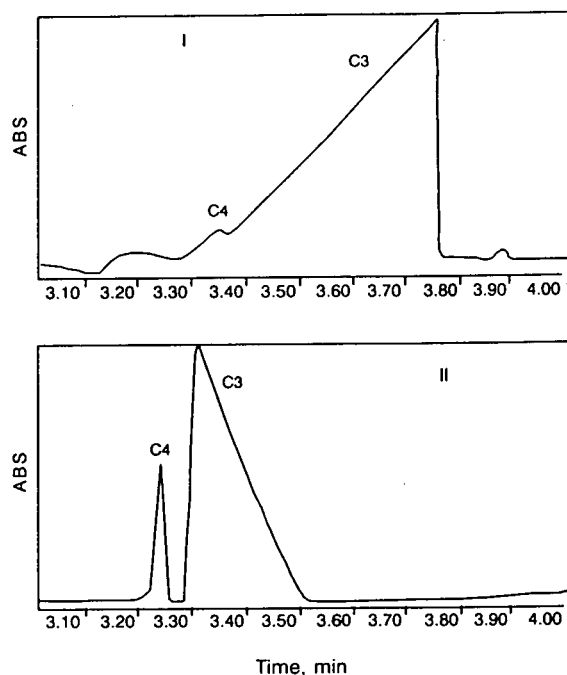


Fig. 5. Electropherograms of 10 mg/l butyric (C4) and 100 mg/l propionic (C3) acid. Electrolyte, 1 mM 2,6-naphthalenedicarboxylate, pH 9; 240 nm. (I) No  $\beta$ -cyclodextrin added; (II) with 4.5 mM  $\beta$ -cyclodextrin.

sensitivity can be gained when mobilities match. If the trace component falls in the tail or front of the major component peak, tuning the electrolyte to match the mobility of the major component may narrow this peak and expose the trace component (Fig. 5).

#### CONCLUSION

The optimization strategy described can be extended to other cases and mobility tuning can be applied to some analyses where direct detection is used. Electrolyte mobility tuning with

cyclodextrin should be generally applicable to aromatic acid electrolytes. Other electrolytes, for example borates and phosphates, might be tuned by other complexation reactions. While the nature of the complexation reaction will vary depending on the electrolyte, the principle of continuously reducing the mobility of an electrolyte through complexation should be generally applicable. Mobility tuning will result in improved dynamic range and enable CZE to be applied to more analytical problems.

#### REFERENCES

- 1 K.D. Altria and C.F. Simpson, *Chromatographia*, 24 (1987) 527.
- 2 S. Hjertén, K. Elenbring, F. Kilar, J. Liao, A.J.C. Chen, C.J. Siebert and M. Zhu, *J. Chromatogr.*, 470 (1989) 299.
- 3 X. Huang, J.A. Luckey, M.J. Gordon and R.N. Zare, *Anal. Chem.*, 61 (1989) 766.
- 4 B.F. Kenny, *J. Chromatogr.*, 546 (1991) 423.
- 5 T. Wang and R.A. Hartwick, *J. Chromatogr.*, 589 (1992) 307.
- 6 P. Jandik, W.R. Jones, A. Weston and P.R. Brown, *LC·GC*, 9 (1991) 3.
- 7 M.W.F. Nielsen, *J. Chromatogr.*, 588 (1991) 321.
- 8 G.W. Tindall and R.L. Perry, *J. Chromatogr.*, 633 (1993) 227.
- 9 F. Foret, S. Fanali and L. Ossicini, *J. Chromatogr.*, 470 (1989) 299.
- 10 H. Small and T.E. Miller, *Anal. Chem.*, 54 (1982) 462.
- 11 M.W.F. Nielsen, *J. Chromatogr.*, 588 (1991) 321.
- 12 V. Šustáček, F. Foret and P. Boček, *J. Chromatogr.*, 545 (1991) 239.
- 13 M.T. Ackermans, F.M. Everaerts and J.L. Beckers, *J. Chromatogr.*, 549 (1991) 345.
- 14 P. Jandik and W.R. Jones, *J. Chromatogr.*, 546 (1991) 431.
- 15 T. Wang and R.A. Hartwick, *J. Chromatogr.*, 607 (1992) 119.
- 16 H. Poppe, *Anal. Chem.*, 65 (1992) 1908.
- 17 F.E.P. Mikkers, F.M. Everaerts and Th.P.E.M. Verheggen, *J. Chromatogr.*, 169 (1979) 1.
- 18 W.L. Hinze, *Sep. Purif. Methods*, 10 (1981) 159.

## Short Communication

---

# Determination of proline by reversed-phase high-performance liquid chromatography with automated pre-column *o*-phthaldialdehyde derivatization

Guoyao Wu

*Department of Animal Science and Faculty of Nutrition, Texas A&M University, College Station, 77843-2471 TX (USA)*

(First received December 8th, 1992; revised manuscript received March 12th, 1993)

---

### ABSTRACT

A simple and sensitive fluorometric HPLC method was developed for the analysis of proline in biological samples. The HPLC apparatus consisted of an autosampler, a binary solvent delivery system, a 3- $\mu\text{m}$  reversed-phase  $\text{C}_{18}$  column (150  $\times$  4.6 mm I.D.) guarded by a 40- $\mu\text{m}$  reversed-phase  $\text{C}_{18}$  column (50  $\times$  4.6 mm I.D.), a fluorescence detector, and a computer workstation. Proline was oxidized to 4-amino-1-butanol in the presence of chloramine-T and  $\text{NaBH}_4$  in a 60°C water bath, which took 11 min. 4-Amino-1-butanol was automatically derivatized with *o*-phthaldialdehyde in the presence of 2-mercaptoethanol. The proline derivative was separated on a 25-min gradient program, employing solvent A (0.1 M sodium acetate–0.5% tetrahydrofuran–9% methanol; pH 7.2) and solvent B (methanol). Fluorescence was monitored with excitation at 340 nm and emission at 450 nm. The conversion of proline to 4-amino-1-butanol was quantitative, reproducible, and linear with proline concentrations ranging from 25 to 500  $\mu\text{M}$  commonly present in biological samples. The described method can be readily used for quantifying proline in biomedical research.

---

### INTRODUCTION

A number of sensitive methods have been developed for analysis of amino acids including proline, using high-performance liquid chromatography (HPLC) during the last 10 years. These include the pre-column derivatization of amino acids with 4-chloro-7-nitrobenzofurazan (NBD-Cl) [1], 9-fluorenyl methylchloroformate (FMOC) [2,3], and phenylisothiocyanate (PITC) [4]. The NBD-Cl method not only requires the heating of both the reactor and the reaction coil at 65°C but also gives relatively low detection sensitivity for proline derivative and considerable

side reactions [1]. The FMOC method calls for (1) the absolute pre-column removal of the excess FMOC, which is highly fluorescent itself, either by multiple extractions with pentane [2] or by reaction with another added chemical [3], (2) additional heating facilities to maintain the analytical column at 45°C [3], and (3) the need of highly qualified detectors with liquid filters due to the fluorescent property of the FMOC derivatives [2,3]. On the other hand, the PITC method is associated with multiple steps of pre-column sample preparations, including lyophilization and evaporation of reacting solutions, amino acid derivatization, and purification of

amino acid-derivatives by ion-exchange chromatography for biological samples. In addition, this method requires a long running time of 105 min (including 25 min for column regeneration) for separation of proline in physiological samples [4].

The analysis of primary amino acids by reversed-phase HPLC using the pre-column derivatization with *o*-phthalaldehyde (OPA) has been widely performed in many laboratories [5–8]. This is largely owing to the many advantages offered by the OPA method. These include (1) the rapid derivatization of amino acids with OPA and the efficient separation of amino acid derivatives at room temperature, (2) high sensitivity of detection (pmol range), (3) easy automation on the HPLC apparatus, and (4) few, if any, interfering side reactions. However, there is a significant problem with this OPA method in that proline does not react directly with OPA [5–8]. Attempts to overcome this shortcoming have involved the post-column [9,10] and pre-column [1,11] oxidation of the imino acid ring of proline, using chlorinated oxidizing agents.

It is noteworthy that Cooper *et al.* [12] introduced a simple procedure for the oxidation of the imino acid ring of proline using chloramine-T in the presence of borohydride, which probably yielded 4-amino-1-butanol. The study of Cooper *et al.* [12], however, involved only serine and imino acid standards. It is not known if there are any interfering reactions between the derivatizing agents (chloramine-T and  $\text{NaBH}_4$ ) and the amino acids or other compounds found in physiological samples. As a result, the general usefulness of the Cooper *et al.*'s oxidation method for proline analysis in biomedical research remains to be determined. The objective of this study was therefore to investigate the potential use of the Cooper *et al.*'s method [12] in quantifying proline in biological samples.

## MATERIALS AND METHODS

### Chemicals

All L-amino acids, sodium borate, lithium hydroxide, chloramine-T, dimethyl sulfoxide, sodium borohydride, benzoic acid, sodium acetate, *o*-phthalaldehyde, tetrahydrofuran, 2-

mercaptoethanol, and Brij-35 were purchased from Sigma (St. Louis, MO, USA). 4-Amino-1-butanol was obtained from Aldrich (Milwaukee, WI, USA). HPLC-grade methanol and HPLC-grade water were purchased from Fisher Scientific (Houston, TX, USA) and were used throughout the study.

### Plasma sample

Jugular vein blood (5 ml) was withdrawn from 28-day-old pigs into heparinized tubes and immediately centrifuged at 1000 g for 10 min. The plasma (supernatant) was then collected. An aliquot of 1 ml of plasma was deproteinized with 1 ml of 1.5 M  $\text{HClO}_4$ . The supernatant was neutralized with 0.5 ml of 2 M  $\text{K}_2\text{CO}_3$  and used for the analysis of free proline.

### Milk sample

An aliquot of 10 ml of milk was manually collected from sows on day 28 of lactation. The milk was immediately centrifuged at 1000 g for 10 min to remove fat and suspended cells including lymphocytes and macrophages. Defatted milk (1 ml) was deproteinized with 1 ml of 1.5 M  $\text{HClO}_4$ . The supernatant was neutralized with 0.5 ml of 2 M  $\text{K}_2\text{CO}_3$  and used for the analysis of free proline. The precipitated milk protein was washed 3 times with 10 ml of deionized water, air-dried, and then suspended in 5 ml of 6 M HCl for hydrolysis at 110°C for 24 h under nitrogen. The hydrolysates were evaporated by freeze-drying, and the residues were dissolved in 10 ml of HPLC-grade water for the analysis of protein-bound proline.

### Skeletal muscle

Gastrocnemius muscles were isolated from 3-month old rats. Muscle (1 g) was homogenized in 1 ml of 1.5 M  $\text{HClO}_4$ , and the homogenates were centrifuged at 1000 g for 10 min. The supernatant was neutralized with 0.5 ml of 2 M  $\text{K}_2\text{CO}_3$ , and used for the analysis of free proline.

### Incubated enterocytes

Enterocytes (absorptive cells in the small intestine) were prepared from 29-day old pigs as described by Watford *et al.* [13]. Cells (10 mg protein) were incubated at 37°C for 30 min in 2

ml of oxygenated (95% O<sub>2</sub>/5% CO<sub>2</sub>) Krebs–Henseleit bicarbonate buffer (pH 7.4) containing 5 mM L-glutamine. The incubation was terminated by addition of 0.2 ml of 1.5 M HClO<sub>4</sub>. The acidified medium was neutralized with 0.1 ml of 2 M K<sub>2</sub>CO<sub>3</sub>, and the supernatant was used for proline analysis.

#### Recovery of proline from plasma, milk, protein hydrolysates, muscle extracts, and enterocyte extracts

The recovery rates of proline from plasma, milk, protein hydrolysates, muscle extracts, and enterocyte extracts were checked by adding 60 μl of 0.5 mM proline or water to 0.2 ml of plasma, milk, protein hydrolysates, muscle extracts, or enterocyte extracts. The processing of the samples for proline analysis was performed as described above.

#### Conversion of proline to 4-amino-1-butanol

The optimal conditions reported by Cooper *et*

*al.* [12] for converting proline to probably 4-amino-1-butanol were confirmed and employed in this study. Briefly, 200 μl of 0–500 μM proline standard (amino acid standard mixture or samples) were added to 200 μl of 13.3 mM chloramine-T preheated at 60°C for 2 min in a water bath. Following 1 min incubation at 60°C, 200 μl of 333 mM NaBH<sub>4</sub> was added to the solution and the mixture was further incubated at 60°C for 10 min. After cooling at room temperature, 0.1 ml of the reaction mixture (or 0.5 ml for enterocyte samples) was directly used for proline analysis without any extraction or purification.

#### OPA reagent

OPA reagent was prepared by dissolving 50 mg OPA in 1.25 ml methanol, followed by addition of 11.2 ml of 0.04 M sodium borate (pH 9.5), 50 μl 2-mercaptoethanol, and 0.4 ml Brij-35 [1]. Although the prepared OPA reagent is usually stable for more than 24 h, it is routinely

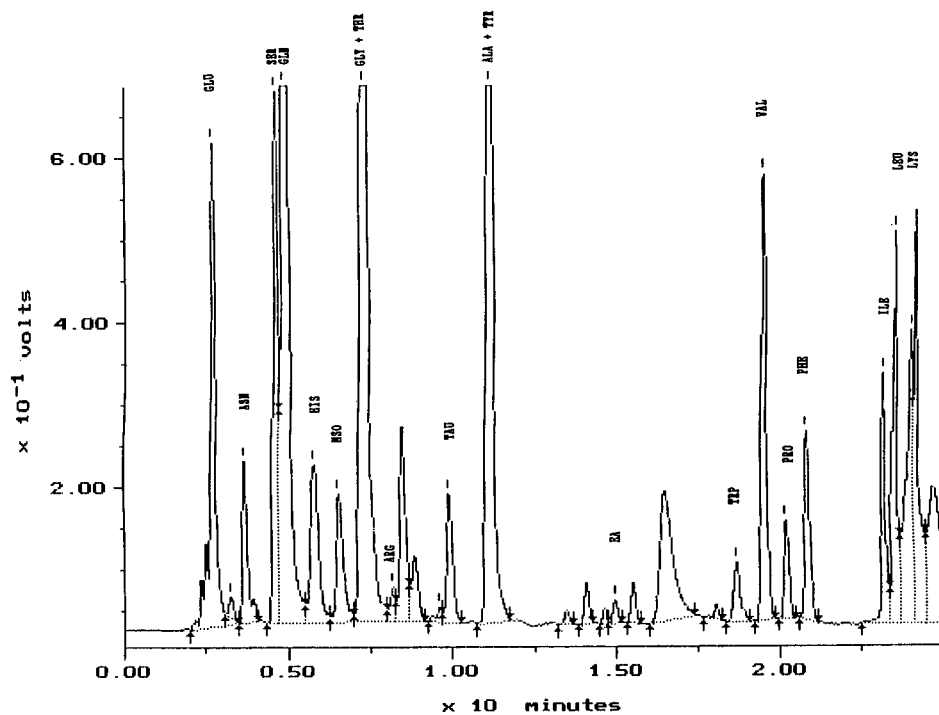


Fig. 1. Elution profiles of OPA derivatives of plasma free amino acids. An aliquot (0.2 ml) of deproteinized pig plasma was used for the conversion of proline to 4-amino-1-butanol in the presence of chloramine-T and NaBH<sub>4</sub>. A portion (0.1 ml) of the reaction mixture was used for HPLC analysis as described in the text. Methionine was oxidized by chloramine-T and NaBH<sub>4</sub> to form methionine sulfoxide. Non-standard abbreviations used: MSO = methionine sulfoxide; TAU = taurine; EA = ethanolamine.





reagent into the HPLC column without a delay mixing time. Fluorescence was monitored with excitation at 340 nm and emission at 450 nm. Amino acids and proline-derived 4-amino-1-butanol were identified with the aid of authentic standards. Peak integrations were performed by a Waters Model 810 Baseline Workstation.

## RESULTS AND DISCUSSION

4-Amino-1-butanol was previously proposed to be the oxidation product of proline in the presence of chloramine-T and  $\text{NaBH}_4$  [12]. This suggestion was supported by the following lines of evidence from the present study. First, proline standard treated with chloramine-T and  $\text{NaBH}_4$  yielded a peak which was co-eluted with authentic 4-amino-1-butanol standard (data not shown). There were no side reactions or interfering peaks on the resulting HPLC chromatograms. Second, there was no peak for 4-amino-1-butanol on HPLC chromatograms, when a mixture of all

amino acid standards but proline were treated with chloramine-T and  $\text{NaBH}_4$ . This indicates that amino acids other than proline were not converted to 4-amino-1-butanol under the conditions used. Third, when a mixture of all amino acid standards containing proline (without 4-amino-1-butanol) were treated with chloramine-T and  $\text{NaBH}_4$ , there was a peak with the same retention time as 4-amino-1-butanol, which was satisfactorily separated from all other amino acid derivatives (data not shown).

The linearity of the oxidation of proline to 4-amino-1-butanol with proline concentrations from 25 to 500  $\mu\text{M}$  was obtained ( $r = 0.996$ ,  $n = 7$ ,  $P < 0.01$ ). The conversion of proline to 4-amino-1-butanol was quantitative, reproducible, and linear with proline concentrations ranging from 25 to 500  $\mu\text{M}$  which are commonly present in biological samples. The standard errors were less than 3% of the means at each of the proline concentrations used. This indicates the good reproducibility of both the proline

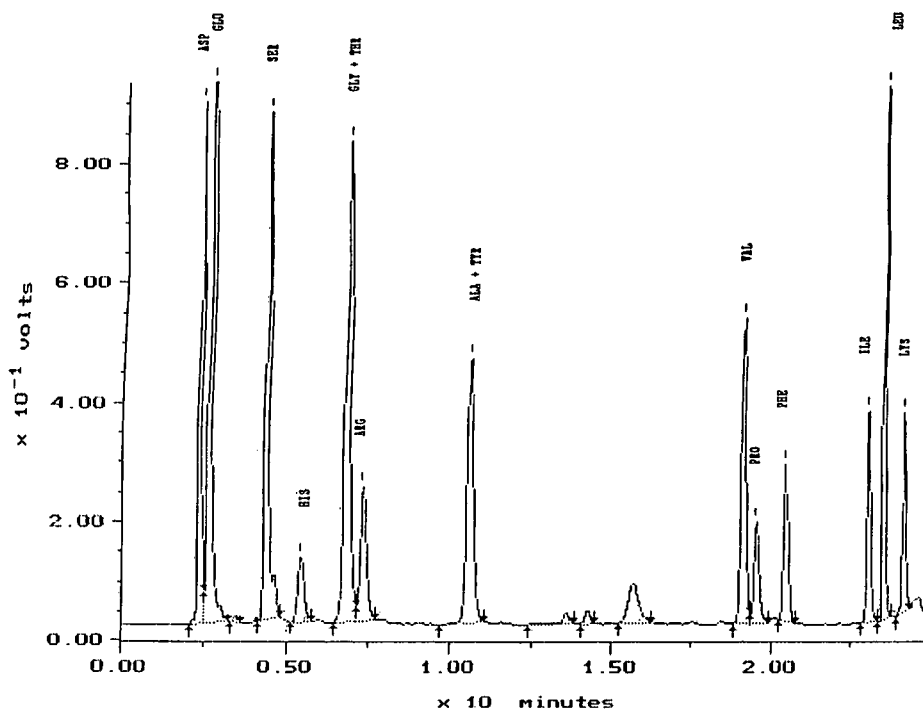


Fig. 3. Elution profiles of OPA derivatives of milk protein-bound amino acids. An aliquot (0.2 ml) of milk protein hydrolysates was used for the conversion of proline to 4-amino-1-butanol in the presence of chloramine-T and  $\text{NaBH}_4$ . A portion (0.1 ml) of the reaction mixture was used for HPLC analysis as described in the text.

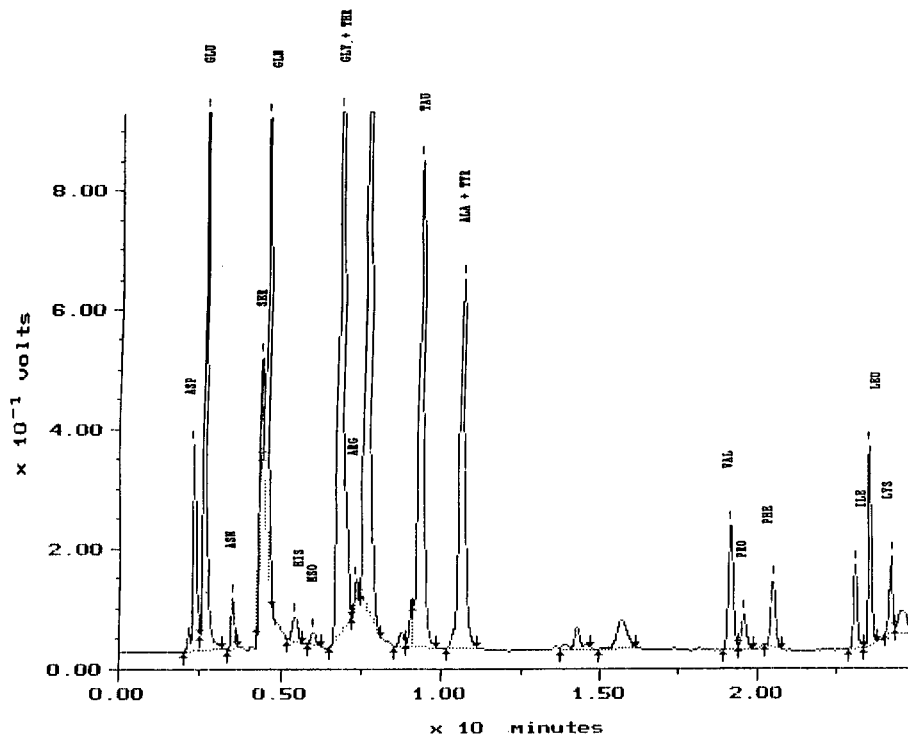


Fig. 4. Elution profiles of OPA derivatives of gastrocnemius muscle free amino acids. An aliquot (0.2 ml) of muscle extracts was used for the conversion of proline to 4-amino-1-butanol in the presence of chloramine-T and  $\text{NaBH}_4$ . A portion (0.1 ml) of the reaction mixture was used for HPLC analysis as described in the text. Non-standard abbreviations used: MSO = methionine sulfoxide; TAU = taurine.

derivatization procedure and the HPLC analysis. The detection limit for the proline derivative, 4-amino-1-butanol, was 2.5 pmol, when using the Waters 420-AC Fluorescence Detector at a gain setting of 8 (maximum setting of up to 128). This high detection sensitivity is sufficient enough for the analysis of proline in various physiological samples.

The fluorometric HPLC method as described above was satisfactorily applied to the analysis of proline in biological samples, including plasma (Fig. 1), milk (Fig. 2), milk protein (Fig. 3), skeletal muscle (Fig. 4), and enterocyte extracts (Fig. 5). The satisfactory resolution of proline-derived 4-amino-1-butanol from other amino acid derivatives were achieved, using a 25-min gradient program (including the time for column regeneration). It is evident from Figs. 1–5 that proline was readily detected in all the samples used, even though they were diluted by 50 times (or 10 times for enterocyte extracts) before use

for HPLC analysis (see the Materials and methods section). It is noteworthy that there were minimal interfering peaks on the HPLC chromatograms for all the samples studied (Figs. 1–5), demonstrating the absence of side reactions in the oxidation of proline to 4-amino-1-butanol. These results indicate that the pre-column oxidation of proline to 4-amino-1-butanol with chloramine-T and  $\text{NaBH}_4$  [12] is suitable for the analysis of proline in biological samples including incubated cells. This sensitive HPLC method for proline analysis is useful for quantifying proline concentrations in both cellular fluids and tissue proteins and for studying its metabolism in animal cells. For example, the low concentration of proline in the extracts of the pig enterocytes incubated with 5 mM glutamine, relative to glutamate and aspartate (Fig. 5), suggests that proline is not a major product of glutamine metabolism in these cells. The present simple method was also readily

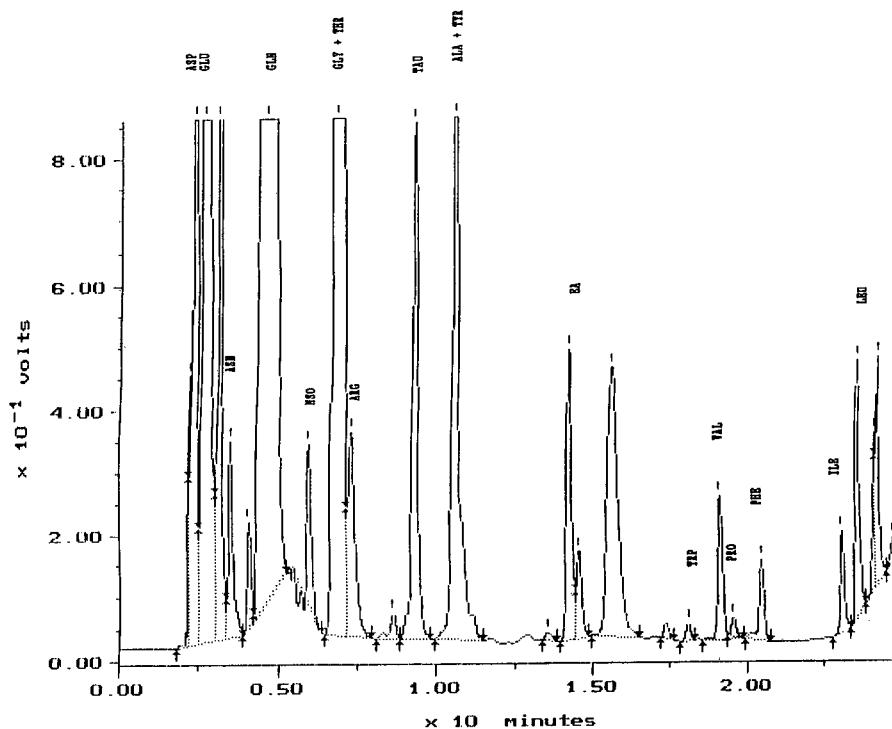


Fig. 5. Elution profiles of OPA derivatives of free amino acids in pig enterocyte extracts. An aliquot (0.2 ml) of enterocyte extracts was used for the conversion of proline to 4-amino-1-butanol in the presence of chloramine-T and  $\text{NaBH}_4$ . A portion (0.5 ml) of the reaction mixture was used for HPLC analysis as described in the text. Non-standard abbreviations used: MSO = methionine sulfoxide; TAU = taurine; EA = ethanolamine.

employed to determine free proline in rat livers and kidneys (data not shown).

The recovery rates (means  $\pm$  S.D.,  $n = 6$ ) of proline from plasma, milk, protein hydrolysates, skeletal muscle extracts, and enterocyte extracts were  $90.6 \pm 2.1$ ,  $85.3 \pm 2.6$ ,  $96.3 \pm 2.7$ ,  $88.7 \pm 2.4$ , and  $97.8 \pm 3.1\%$ , respectively. The coefficients of variation ranged from 2.3% for the plasma to 3.1% for the enterocyte extracts. This further demonstrates the good reliability of the present method for proline analysis in biological samples.

The present procedure for proline analysis in the biological samples offers some advantages. First, there is no need for any pre-column purification of amino acid derivatives in contrast to the PITC method [4], or for the removal of excess reagents prior to HPLC analysis as absolutely required by the FMOC method [2,3]. Second, both rapid derivatization of 4-amino-

1-butanol with the OPA reagent and efficient separation of 4-amino-1-butanol from other amino acid derivatives are achieved at room temperature. This facilitates an easy automation procedure on the HPLC apparatus and does not require additional facilities on the HPLC apparatus to maintain the column or the reactor and the reaction coil at high temperatures as rigidly needed in the FMOC ( $45^\circ\text{C}$ ) [3] and NBD-Cl ( $65^\circ\text{C}$ ) [1] methods, respectively.

In conclusion, proline was quantitatively oxidized to 4-amino-1-butanol in the presence of chloramine-T and  $\text{NaBH}_4$  in a  $60^\circ\text{C}$  water bath, which took 11 min. 4-Amino-1-butanol was automatically derivatized with OPA and satisfactorily separated from other amino acid derivatives on a 25-min gradient program, using reversed-phase HPLC. This fluorescent method is sensitive and reliable, and can be readily used for quantifying proline in biological samples.

## ACKNOWLEDGEMENTS

The author wishes to thank Dr. Darrell A. Knabe for the provision of the pig's plasma, milk and small intestine and for many helpful comments. The secretarial and technical assistance of Mrs. D. Tunnell and Mrs. W. Yan is gratefully acknowledged. This research was supported by a competitive grant (No. 92-37206-8004) from the United States Department of Agriculture.

## REFERENCES

- 1 A. Carisano, *J. Chromatogr.*, 318 (1985) 132.
- 2 S. Einarsson, B. Josefsson and S. Lagerkvist, *J. Chromatogr.*, 282 (1983) 609.
- 3 B. Gustavsson and I. Betner, *J. Chromatogr.*, 507 (1990) 67.
- 4 L.E. Lavi, J.S. Holcenberg and D. Cole, *J. Chromatogr.*, 377 (1986) 155.
- 5 B.N. Jones and J.P. Gilligan, *J. Chromatogr.*, 266 (1983) 471.
- 6 H.W. Jarrett, K.D. Cooksy, B. Ellis and J.M. Anderson, *Anal. Biochem.*, 153 (1986) 189.
- 7 G. Wu and J.R. Thompson, *Biochem. J.*, 265 (1990) 593.
- 8 S. Palmero, M. de Marchis, M. Prati and E. Fugassa, *Anal. Biochem.*, 202 (1992) 152.
- 9 D.G. Drescher and K.S. Lee, *Anal. Biochem.*, 84 (1978) 559.
- 10 P. Bohlen and M. Mellet, *Anal. Biochem.*, 94 (1979) 313.
- 11 K. Yaegaki, J. Tonzetich and A.S.K. Ng, *J. Chromatogr.*, 356 (1986) 163.
- 12 J.D.H. Cooper, M.T. Lewis and D.C. Turnell, *J. Chromatogr.*, 285 (1984) 484.
- 13 M. Watford, P. Lund and H.A. Krebs, *Biochem. J.*, 178 (1979) 589.

## Short Communication

---

# New labelling agent, 2-[2-(isocyanate)ethyl]-3-methyl-1,4-naphthoquinone, for high-performance liquid chromatography of hydroxysteroids with electrochemical detection

Masaharu Nakajima, Hiroyuki Wakabayashi, Susumu Yamato and Kenji Shimada\*

*Department of Analytical Chemistry, Niigata College of Pharmacy, 13-2 Kamishin'ei-cho 5-chome, Niigata 950-21 (Japan)*

(First received December 1st, 1992; revised manuscript received March 31st, 1993)

---

### ABSTRACT

2-[2-(Isocyanate)ethyl]-3-methyl-1,4-naphthoquinone has been synthesized and developed as a highly sensitive labelling agent for hydroxysteroids in HPLC with electrochemical oxidation after post-column reduction with platinum catalyst. Optimum reaction conditions were examined with cholesterol. The reagent reacted with hydroxysteroids in acetone to give the corresponding carbamic acid esters. The detection limit (signal-to-noise ratio = 3) of cholesterol was 17 fmol as the injected amount. The reagent is suitable for labelling of a relatively unhindered hydroxy group in a hydroxysteroid.

---

### INTRODUCTION

Various UV or fluorescence derivatization reagents, *e.g.* 3,5-dinitrobenzoyl chloride [1], 1-anthroyl nitrile [2], 7-methoxycoumarin-3- and -4-carbonyl azides [3], pyrene-1-carbonyl nitrile [4], 3,4-dihydro-6,7-dimethoxy-4-methyl-3-oxoquinoxaline-2-carbonyl acid [5], 2-(carboxyphenyl)-5,6-dimethylbenzimidazole [6] and 3-(2-phthalimidyl)benzoyl azide [7] have been reported for the determination of aliphatic alcohols and hydroxysteroids by high-performance liquid

chromatography (HPLC). In contrast, only a few reagents for electrochemical detection (ED) have been developed for the derivatization of alcohols [8]. In the previous studies, 2-[2-(azidocarbonyl)ethyl]-3-methyl-1,4-naphthoquinone (AMQ) used as an ED labelling reagent for hydroxy group was reported [9]. However, the procedure for its derivatization requires a long time (30 min) with cholesterol [10]. Therefore we have studied AMQ analogues to improve the reagent reactivity and developed 2-[2-(isocyanate)ethyl]-3-methyl-1,4-naphthoquinone (IMQ) with isocyanate as a reacting group. This paper describes the preparation of IMQ and the optimum conditions for ED pre-column labelling of hydroxysteroids with IMQ in HPLC.

---

\* Corresponding author.

## EXPERIMENTAL

## Chemicals

Steroids were purchased from Sigma (St. Louis, MO, USA). Other chemicals were obtained from Tokyo Kasei (Tokyo, Japan). Organic solvents were distilled and dried prior to use in the usual manner. All other chemicals and solvents employed were of analytical-reagent grade.

Stock solutions (2.5  $\mu\text{mol/ml}$ ) of hydroxy-steroids were prepared by dissolving each in benzene and diluting to appropriate concentrations prior to use.

## Apparatus and chromatographic conditions

The HPLC system used in this work was a Hitachi L-6200 pump (Hitachi, Tokyo, Japan) equipped with a TOA ICA 3060 amperometric detector (Toa Electronics, Tokyo, Japan) with glassy carbon working electrode and a Ag/AgCl reference electrode (applied potential +0.7 V) and with a Shimadzu CR-6A integrator (Shimadzu, Kyoto, Japan). An Inertsil C<sub>8</sub> column (15 cm  $\times$  4.0 mm I.D., particle size 5  $\mu\text{m}$ ; GL Sciences, Tokyo, Japan) was used at ambient temperature. Methanol–water (95:5) containing 0.05 M sodium perchlorate was used as the mobile phase at a flow-rate of 1.0 ml/min. The effluent from the column was directly passed through the platinum catalyst column (10  $\times$  4.6 mm I.D. in stainless-steel column) [9,11]. This column was packed with platinum catalyst (5% on alumina, 10  $\mu\text{m}$ , provided by Toa Electronics) by tapping, and purged with water at a flow-rate of 10 ml/min for 5 min.

Mass spectra were measured with a Hitachi M-1000 LC API mass spectrometer. Proton (<sup>1</sup>H) nuclear magnetic resonance spectra were recorded on a JEOL JNM-PMX60SI NMR spectrometer with tetramethylsilane (TMS) as an internal standard, and for the infrared spectra a Perkin-Elmer FT-IR 1720 was used.

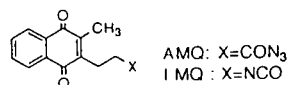


Fig. 1. Structures of labelling reagents.

## Synthesis of IMQ

AMQ (500 mg), previously synthesized by the authors [9] (see Fig. 1), was dissolved in 10 ml of benzene. The solution was heated at 100°C for 1 h and then cooled. The reaction mixture was evaporated to dryness *in vacuo*, and the residue was dissolved in ethyl acetate and purified by column chromatography on silica gel with ethyl acetate–hexane (1:10). IMQ (400 mg, 89%): m.p. 70–71°C; <sup>1</sup>H NMR (C<sup>2</sup>HCl<sub>3</sub>)  $\delta$  2.2 (3H, s), 2.9 (2H, t, 7 Hz), 3.5 (2H, t, 7 Hz), 7.5–8.2 (4H, m); IR (CHCl<sub>3</sub>) cm<sup>-1</sup> 1598, 1621, 1662, 2276; MS *m/z* 274 (M<sup>+</sup> + CH<sub>3</sub>OH + 1), 242 (M<sup>+</sup> + 1), 199 (M<sup>+</sup> – NCO).

## Chemical analysis of IMQ cholesterol derivative

IMQ (90 mg, 0.37 mmol) and cholesterol (100 mg, 0.25 mmol) were dissolved in 4 ml of acetone. The solution was placed in a test tube (10 ml), heated at 100°C for 30 min and then cooled to room temperature. The reaction mixture was then evaporated to dryness *in vacuo*, and the residue was dissolved in 2 ml of ethyl acetate and chromatographed on a silica gel C-200 (Wako, Osaka, Japan) with hexane–ethyl acetate (9:1). The main fraction was evaporated to dryness under reduced pressure, and the residue was recrystallized from hexane–ethyl acetate to give IMQ cholesterol derivative as yellow needles (134 mg, 82%): m.p. 167–169°C; <sup>1</sup>H NMR (C<sup>2</sup>HCl<sub>3</sub>)  $\delta$  0.7 (3H, s), 0.89 (3H, d), 0.95 (6H, d), 1.53 (3H, s), 0.7–2.4 (29H, m), 2.2 (3H, s), 2.8–3.1 (2H, m), 3.2–3.6 (2H, m), 4.6 (1H, m), 5.3 (1H, m), 7.5–8.2 (4H, m); IR (CHCl<sub>3</sub>) cm<sup>-1</sup> 1509, 1598, 1660, 1712, 2950, 3019, 3457. MS *m/z* 628 (M<sup>+</sup> + 1), 369.

## Derivatization procedure for HPLC analysis

A 5- $\mu\text{l}$  aliquot of a test solution of hydroxy-steroids in benzene (2.5  $\mu\text{mol/ml}$  each) was placed in a test tube (10 ml), and then 200  $\mu\text{l}$  of 0.1% IMQ in acetone were added. The mixture was heated at 100°C for 15 min. (The solvents were almost distilled off.) After cooling, 1 ml of methanol was added to the mixture, and 10  $\mu\text{l}$  of the reaction mixture were injected into the chromatograph.

## RESULTS AND DISCUSSION

IMQ was readily prepared from AMQ. This chemical structure was confirmed by the mass,  $^1\text{H}$  NMR and IR spectral data. IMQ was stable for more than a year below  $0^\circ\text{C}$ . The acetone solution of the reagent was stable for at least a week in a refrigerator.

To investigate the reactivity of IMQ with hydroxysteroids, we have used cholesterol (CE) as a model compound. The derivatization yield was estimated by comparing the peak height with that of the authentic sample. In this study, acetone was found to be suitable for labelling with respect to reactivity in contrast to other solvents, ethyl acetate, dichloromethane, acetonitrile and benzene. The derivatization reaction with CE proceeded at increasing reaction temperature. Constant peak height was attained at a concentration of 0.1% IMQ in the reaction solution at  $100^\circ\text{C}$  for 15 min; the reaction yield was 97%. However, at  $120^\circ\text{C}$ , the peak height decreased with heating time (Fig. 2). Fig. 3 shows a typical chromatogram of cholesterol and cholestanol derivatized with IMQ. The detection limit ( $S/N = 3$ ) of CE was 17 fmol as the injected

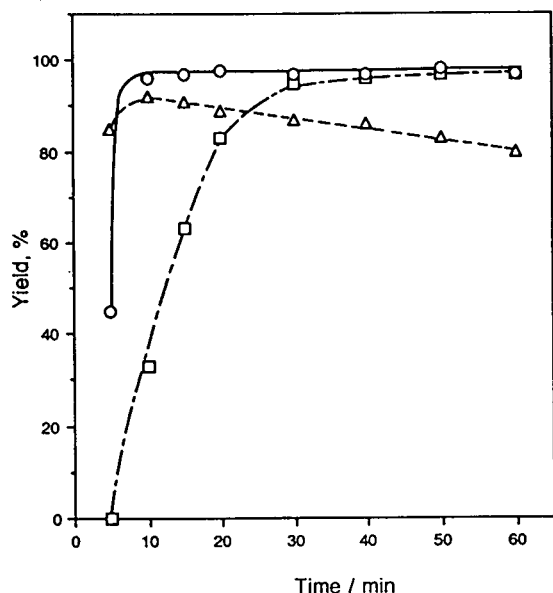


Fig. 2. Effects of reaction time and temperature on IMQ derivatization of cholesterol. □ =  $80^\circ\text{C}$ ; ○ =  $100^\circ\text{C}$ ; △ =  $120^\circ\text{C}$ .

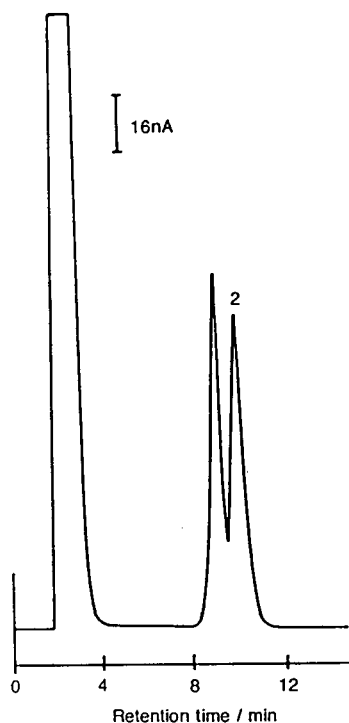


Fig. 3. Chromatogram of IMQ derivatives of cholesterol and cholestanol. A  $5\text{-}\mu\text{l}$  portion of benzene solution ( $2.5\ \mu\text{mol/ml}$  each) was treated with IMQ, and  $10\ \mu\text{l}$  ( $125\ \text{pmol}$  each) of the reaction mixture were injected into HPLC as described in the Experimental section. Peaks: 1 = cholesterol; 2 = cholestanol. Mobile phase: 95% methanol (containing  $0.05\ \text{M}$  sodium perchlorate).

amount, with dilution to appropriate concentration of stock solution prior to the derivatization procedure.

The reactivity of IMQ with various hydroxysteroids was investigated under the same conditions. The reaction yields and retention times of the compounds examined under these conditions are shown in Table I. Derivatization of the hydroxy group of C-3 and C-17 proceeded with ease, providing the carbamic esters in 70–97% yield. On the other hand, less reactivity was observed for the 11- and phenolic hydroxy groups. This difference in the reactivity of hydroxysteroids can probably be ascribed to steric hindrance due to the steroid moiety and acidity.

The new reagent has excellent characteristics concerning reactivity and sensitivity for the derivatization of hydroxysteroids, and is more stable than AMQ. Therefore, IMQ should be

TABLE I  
RETENTION TIMES AND REACTION YIELDS FOR THE IMQ DERIVATIVES OF HYDROXYSTERIODS

Compound	Position of hydroxyl group <sup>a</sup>	Reaction yield (%) <sup>b</sup>	Retention time (min) <sup>c</sup>
5-Cholesten-3 $\beta$ -ol (cholesterol)	3 $\beta$ (e)	97 $\pm$ 2	8.8 (95)
5 $\alpha$ -Cholestan-3 $\beta$ -ol (cholestanol)	3 $\beta$ (e)	90 $\pm$ 3	9.6 (95)
5 $\alpha$ -Androstan-3 $\alpha$ -ol-17-one (androsterone)	3 $\alpha$ (a)	78 $\pm$ 2	25.2 (70)
4-Androsten-17 $\beta$ -ol-3-one (testosterone)	17 $\beta$ (qe)	81 $\pm$ 3	17.0 (70)
4-Androsten-17 $\alpha$ -ol-3-one (17 $\alpha$ -epitestosterone)	17 $\alpha$ (qa)	70 $\pm$ 3	15.2 (70)
4-Pregnene-11 $\alpha$ -ol-3,20-dione (11 $\alpha$ -hydroxyprogesterone)	11 $\alpha$ (e)	42 $\pm$ 3	25.7 (60)
4-Androstene-11 $\beta$ -ol-3,17-dione	11 $\beta$ (a)	0	–
3-Hydroxy-1,3,5 (10)-estratrien-17-one (estrone)	3 (phen)	10 $\pm$ 2	12.2 (70)

<sup>a</sup> a = axial, e = equatorial, qe = quasiequatorial, qa = quasial, phen = phenolic.

<sup>b</sup> Mean  $\pm$  S.D. ( $n = 4$ ).

<sup>c</sup> Mobile phase, aqueous methanol (% v/v).

useful as an ED derivatization reagent in HPLC of a micro amount of hydroxysteriods. We have observed a linear relationship between the peak heights of IMQ-cholesterol and IMQ-cholestanol and reaction amounts up to 10 ng, and a coefficient of correlation ( $r$ ) of 0.998 and 0.981, respectively [10]. These results suggest that the use of this reagent is enough to determine cholesterol and cholestanol in serum. Application to the determination of cholesterol and cholestanol in biological fluids is the subject of a future communication.

#### REFERENCES

- J.F. Lawrence and R.W. Frei, *Chemical Derivatization in Liquid Chromatography*, Elsevier, Amsterdam, 1976, p. 151.
- J. Goto, N. Goto, F. Shamsa, M. Saito, S. Komatsu, K. Suzuki and T. Nambara, *Anal. Chim. Acta*, 147 (1983) 397.
- A. Takadate, M. Irikura, T. Suehiro, H. Fujino and S. Goya, *Chem. Pharm. Bull.*, 33 (1985) 1164.
- J. Goto, S. Komatsu, M. Inada and T. Nambara, *Anal. Sci.*, 2 (1986) 585.
- M. Yamaguchi, T. Iwata, M. Nakamura and Y. Ohkura, *Anal. Chim. Acta*, 193 (1987) 209.
- M. Katayama, Y. Masuda and H. Taniguchi, *J. Chromatogr.*, 585 (1991) 219.
- Y. Tsuruta, Y. Date and K. Kohashi, *Anal. Sci.*, 7 (1991) 411.
- K. Shimada, S. Orii, M. Tanaka and T. Nambara, *J. Chromatogr.*, 352 (1986) 329.
- M. Nakajima, H. Wakabayashi, S. Yamato and K. Shimada, *Anal. Sci.*, 7, Supplement. 173 (1991).
- M. Nakajima, H. Wakabayashi, S. Yamato and K. Shimada, unpublished data.
- H. Wakabayashi, M. Nakajima, S. Yamato and K. Shimada, *J. Chromatogr.*, 573 (1992) 154.



## Short Communication

# Analytical studies of *dl*-stylophine in *Chelidonium majus* L. using high-performance liquid chromatography

Jean-Pierre Rey\*, Joël Levesque and Jean-Louis Pousset

Laboratoire de Pharmacognosie, Faculté de Médecine et de Pharmacie, 34 Rue du Jardin des Plantes, B.P. 199, 86005 Poitiers Cedex (France)

(First received February 5th, 1993; revised manuscript received April 6th, 1993)

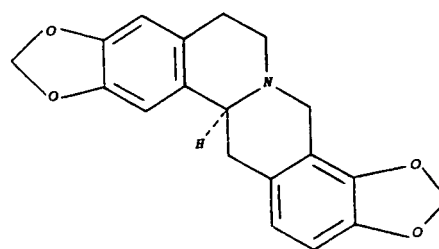
### ABSTRACT

A low-pressure liquid chromatographic method using silica gel 60 with hexane–chloroform–ethyl acetate proportions varying from 80:20:0 to 20:20:8 (v/v/v) as eluent is described for the isolation of *dl*-stylophine from the flowered aerial parts of *Chelidonium majus* L. An isocratic high-performance liquid chromatographic (HPLC) method using a Superspher Si 60 column with chloroform–methanol (90:10, v/v) containing 0.1% trifluoroacetic acid as mobile phase and UV detection at 292.5 nm that allows the determination of *dl*-stylophine in greater celandine is described. The total alkaloid fraction is 0.34% for the flowered aerial parts and 2.17% for the underground parts and the amount of *dl*-stylophine is 61.3 and 4.9% of the total alkaloid fraction, respectively.

### INTRODUCTION

Further to our studies of the application of high-performance liquid chromatography (HPLC) to the analysis of medicinal plants with sedative and spasmolytic properties, we have examined the components of *Chelidonium majus* L. There have been many investigations into the alkaloidal constituents of this plant [1–8], and almost twenty isoquinoline alkaloids have been isolated. It appears that greater celandine is variable in its alkaloid content and that many differences exist between different parts of the plant. The major alkaloids proved to be chelidonine, chelerythrine, sanguinarine and *dl*-

stylophine [2–4]. The minor alkaloids are mainly protopine, berberine, coptisine, chelidamine and chelamidine [3].



DL-STYLOPINE

Numerous studies on the benzo[*c*]phenanthridine group of *C. majus* L. have been undertaken using thin-layer chromatography (TLC) [9–15], isotachophoretic analysis [16] and HPLC

\* Corresponding author.

[14,17–19], but no work has been reported on the determination of *dl*-stylopine in greater celandine using HPLC. In this paper, we describe a simple method for the isolation of this alkaloid and a normal-phase HPLC method for the determination of *dl*-stylopine which can be used as a specific tracer in *C. majus* L.

## EXPERIMENTAL

### Chemicals

Chloroform and methanol were of HPLC quality from Rathburn (Walkerburn, UK). All other solvents were of analytical-reagent grade from Labosi (Paris, France).

### High-performance liquid chromatography

A Varian Model 5000 chromatograph was used, equipped with a Rheodyne Model 7125 injector and a Merck L 3000 photodiode-array detector under computer control (Merck HPLC Manager). Analyses were conducted at 20°C.

Analytical HPLC was carried out on a normal-phase Superspher Si 60 column (125 × 4 mm I.D., particle size 4 μm) (Merck) used with a LiChrospher Si 60 precolumn (4 × 4 mm I.D., particle size 5 μm) (Merck). The mobile phase was chloroform–methanol (90:10, v/v) containing 0.1% trifluoroacetic acid (TFA) at a flow-rate of 1 ml/min. The injection volume was 10 μl and UV detection at 292.5 nm was applied.

### Alkaloid extraction

A 500-g amount of flowered aerial parts of *Chelidonium majus* L. (harvested in Maine et Loire, France, May 1992), dried at room temperature and finely powdered, was moistened with dilute ammonia solution and kept for 2 h before Soxhlet extraction with chloroform (5 l). The organic solution was evaporated under reduced pressure at 40°C to a final volume of about 100 ml, and then extracted with 5 × 50 ml of 0.25 M sulphuric acid. The acidic layers were mixed and filtered. After alkalization with ammonia (pH 10), they were extracted with 4 × 50 ml of chloroform. The organic layers were washed with 70 ml of distilled water, filtered and evaporated under reduced pressure, affording a res-

idue (1.68 g) corresponding to the total alkaloid fraction (0.34% dry material).

An alkaloid extraction was also applied to the underground parts of the same plant material harvested at the same date. The extraction procedure was the same as above (total alkaloid fraction = 2.17% dry material).

### Isolation of *dl*-stylopine

*dl*-Stylopine was isolated using low-pressure liquid chromatography preparative separation (Fig. 1). <sup>1</sup>H NMR spectrometry (Bruker AC 200 P NMR spectrometer), mass spectrometry (MS) (Nermag R 1010 C mass spectrometer), melting point determination and UV spectrophotometric analysis confirmed the identification of the isolated pure compound as *dl*-stylopine: m.p. 220–221°C [2,4,20]; <sup>1</sup>H NMR spectra identical with the literature [5]; electron

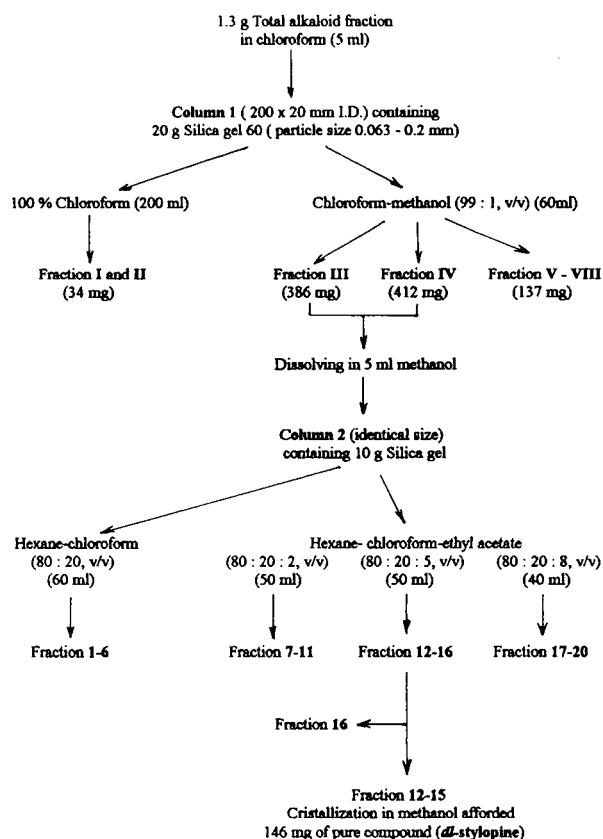


Fig. 1. Low-pressure liquid chromatography preparative separation of *dl*-stylopine.

impact MS,  $m/z$  323 ( $M^+$ ), 148 (100), 91 (75) [2]; UV  $\lambda_{\max}$  [chloroform–methanol–TFA (90:10:0.1, v/v/v)] 246 and 292.5 nm ( $\log(\epsilon)$  2.4 and 3.9) [3].

## RESULTS AND DISCUSSION

In contrast to the separation of the alkaloids of *Chelidonium majus* L. using reversed-phase HPLC [18,19] or ion-pair chromatography [17,18], and in comparison with the separation of chelidonine, chelerythrine and sanguinarine using a LiChrosorb Si 60 column with toluene–methanol (96:4, v/v) [17], we made use of normal-phase HPLC on Superspher Si 60 with chloroform–methanol (90:10, v/v) containing 0.1% TFA, which resulted in a considerable improvement in the chromatographic profile. TFA was chosen because of its low absorbance in the UV region. Moreover, it increases the column efficiency and improves the column resolution in both the reversed-phase [21] and normal-phase modes.

For quantitative analysis, the calibration graph shows a linear correlation from 0.1 to 2 mg/ml between the amounts of *dl*-stylophine injected and the intensity of the absorption at 292.5 nm [correlation coefficient ( $r^2$ ) = 0.9983]. Five determinations were carried out on each sample of greater celandine, in order to test the precision of the method. The determination of *dl*-stylophine was attempted on the total alkaloid fraction of

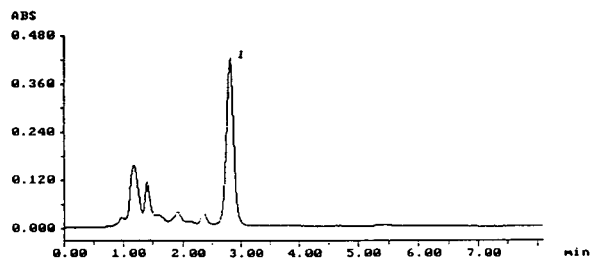


Fig. 2. HPLC of a total alkaloid fraction of flowered aerial parts of *Chelidonium majus* L. Peak: 1 = *dl*-stylophine. Conditions: column, Superspher Si 60 (125 × 4 mm I.D.; particle size 4  $\mu$ m); precolumn, LiChrospher Si 60 (4 × 4 mm I.D.; particle size 5  $\mu$ m); mobile phase, chloroform–methanol (90:10, v/v) containing 0.1% TFA; flow-rate, 1 ml/min; UV detection at 292.5 nm.

flowered aerial parts (Fig. 2) and underground parts of *Chelidonium majus* L.

The results obtained (*dl*-stylophine = 61.3% of the total alkaloid fraction whose extraction efficiency is 0.34% dry material) for the flowered aerial parts harvested in May, in comparison with those observed for the underground parts of the same plants harvested at the same date (*dl*-stylophine = 4.9% of the total alkaloid fraction whose extraction efficiency is 2.17% dry material), show the importance of seasonal changes in alkaloid contents in greater celandine [12]. Moreover, this is correlated with the high percentage of *dl*-stylophine in the siliques [2,4] and with the variation in the qualitative and quantitative composition of alkaloids from *Chelidonium majus* L. during its growth [22].

Nevertheless, we must consider that the alkaloid extraction described does not permit the extraction of quaternary compounds. In fact, a tetrahydroprotoberberine alkaloid such as *dl*-stylophine should be oxidized to form coptisine under these conditions. Thus this possibility cannot be excluded.

In conclusion, the proposed method allows the isocratic separation of *dl*-stylophine in greater celandine and can be used in its routine determination in drugs and in medicinal plant extracts containing other Papaveraceae species [23].

## ACKNOWLEDGEMENT

Thanks are due to Association Nationale de la Recherche Technique (ANRT, Paris) for providing financial support.

## REFERENCES

- 1 J. Slavik and L. Slavikova, *Collect. Czech. Chem. Commun.*, 20 (1954) 21.
- 2 J. Slavik, *Collect. Czech. Chem. Commun.*, 20 (1955) 198.
- 3 J. Slavik, L. Slavikova and J. Brabenec, *Collect. Czech. Chem. Commun.*, 30 (1965) 3697.
- 4 R. Lavenir and R.R. Paris, *Ann. Pharm. Fr.*, 23 (1965) 307.
- 5 M. Shamma, *The Isoquinoline Alkaloids: Chemistry and Pharmacology (Organic Chemistry: a Series of Monographs, Vol. 25)*, Academic Press, New York, 1972, p. 315.

- 6 J. Slavik and L. Slavikova, *Collect. Czech. Chem. Commun.*, 42 (1977) 2686.
- 7 F. Santavy, *Alkaloids (N.Y.)*, 17 (1979) 385.
- 8 G. Kadan, T. Gozler and M. Shamma, *J. Nat. Prod.*, 53 (1990) 531.
- 9 W. Debska and R. Walkowiak, *Farm. Pol.*, 29 (1973) 695.
- 10 C. Scholtz, R. Haensel and C. Hille, *Pharm. Ztg.*, 121 (1976) 1571.
- 11 W.E. Freytag, *Planta Med.*, 40 (1980) 278.
- 12 D. Kustrak, J. Petricic, Z. Kalodera and L. Holik, *Acta Pharm. Jugosl.*, 32 (1982) 225.
- 13 W. Maciejewicz, *Acta Polon. Pharm.*, 40 (1983) 219.
- 14 T. Dzido, L. Jusiak and E. Soczewinski, *Chem. Anal. (Warsaw)*, 31 (1986) 135.
- 15 M. Tamas, E. Chindris, L. Roman and M. Tuia, *Cluj. Med.*, 60 (1987) 256.
- 16 D. Walterova, V. Preininger and V. Simanek, *Planta Med.*, 50 (1984) 149.
- 17 W.E. Freytag, *Dtsch. Apoth. Ztg.*, 126 (1986) 1113.
- 18 C. Bugatti, M.L. Colombo and F. Tome, *J. Chromatogr.*, 393 (1987) 312.
- 19 T. Dzido, *J. Chromatogr.*, 439 (1988) 257.
- 20 A.R. Battersby, R.J. Francis, M. Hirst, E.A. Ruveda and J. Staunton, *J. Chem. Soc., Perkin Trans. 1*, 11 (1975) 1140.
- 21 J.P. Rey, J. Levesque, J.L. Pousset and F. Roblot, *J. Chromatogr.*, 587 (1991) 314.
- 22 A.A. Butalov, G.N. Buzuk, M.Ya. Lovkova and N.S. Sabirova, *Khim. Farm. Zh.*, 24 (1990) 50.
- 23 J.P. Rey, J. Levesque, J.L. Pousset and F. Roblot, *J. Chromatogr.*, 596 (1992) 276.

## Short Communication

---

# Reversed-phase high-performance liquid chromatographic determination of sulphide in an aqueous matrix using 2-iodo-1-methylpyridinium chloride as a precolumn ultraviolet derivatization reagent

Edward Bald\* and Stanisław Sypniewski

*Department of Chemical Technology and Environmental Protection, University of Łódź, 91-416 Łódź (Poland)*

(First received September 30th, 1992; revised manuscript received March 5th, 1993)

---

### ABSTRACT

A high-performance liquid chromatographic method was developed for the determination of sulphide in water. The procedure involves precolumn derivatization of sulphide with 2-iodo-1-methylpyridinium chloride to form 1-methyl-2-thiopyridone, followed by reversed-phase HPLC separation and UV detection. A linear calibration graph was obtained over the range 0.04–50  $\mu\text{g}$  of  $\text{S}^{2-}$  in 10 ml of final analytical solution and the relative standard deviations were 0.2% at the 1  $\mu\text{g}/\text{ml}$  and 3.2% at the 10  $\mu\text{g}/\text{l}$  sulphide levels. The proposed method is tolerant towards thiols and many common cations and anions.

---

### INTRODUCTION

Sulphide is formed throughout nature and industry. In nature it is often produced by the bacterial action on sulphur compounds present in organic wastes and by reduction of sulphate. The main industrial sources of sulphide are kraft pulp mills, petroleum refineries, the gasification of coal, meat processing plants and sewage treatment plants. This sulphide is readily converted into hydrogen sulphide which causes odour, corrosion and toxicity problems. The toxicity of

the sulphide ion is caused by its great ability to coordinate with many metals involved in human metabolism. For these reasons, the determination of sulphide assumes considerable importance and many methods have been developed.

Most of the methods published up to 1976 have been described in several books (*e.g.*, refs. 1 and 2). More recent methods for the determination of sulphide at trace levels are instrumental, including the use of spectrophotometry [3–8], inductively coupled plasma atomic emission spectrometry [9], polarography [10,11], potentiometry with ion-selective electrodes [12–14], cathodic stripping voltametry [15,16], spectrofluorimetry [17–19] and flow-injection analysis

---

\* Corresponding author.

with various detection procedures [20–24]. Chromatographic methods have also been reported, including gas chromatography [25–27], ion chromatography [28–34] and reversed-phase HPLC [35].

Sulphide is difficult to determine by ion chromatography, as explained by Haddad and Heckenberg [35]. They demonstrated that sulphide exists in solution as neutral hydrogen sulphide if the solution is not alkaline. Even if the mobile phase is a solution of sodium hydroxide, sulphide exists mainly as  $\text{HS}^-$  and is weakly retained on anion-exchange columns. Detections of sulphide also causes problems. Conductimetric detection excludes suppressed ion chromatography and the sensitivity attainable is relatively poor. Potentiometric detection with a silver sulphide ion-selective electrode [32] and amperometric detection using gold [30] and mercury-coated platinum [31] or silver [29] electrodes are very good methods in terms of low detection limits, but there can be problems with non-linearity of calibration at low concentrations. Further, sulphide can be adsorbed on the ion-exchange columns used and oxidized prior to and during the chromatographic analysis.

This paper describes a reversed-phase HPLC method for the determination of sulphide in an aqueous matrix after its reaction with 2-iodo-1-methylpyridinium chloride to form 1-methyl-2-thiopyridone. This procedure converts sulphide into a stable product and permits UV detection.

## EXPERIMENTAL

### Chromatographic apparatus

The HPLC apparatus consisted of a Hewlett-Packard Model 1050 isocratic pump, a Hewlett-Packard Model 1050 variable-wavelength detector and a Model 4100 line recorder (Laboratorní Přístroje, Prague, Czech Republic). The samples were injected using a Rheodyne Model 7125 injection valve fitted with a 20- $\mu\text{l}$  loop. The column used was 5- $\mu\text{m}$  ODS-2 (125  $\times$  4.0 mm I.D.), operated at a flow-rate of 0.7 ml/min. UV spectra were recorded on a Carl Zeiss Jena UV-Vis spectrophotometer (1-cm cells).

### Chemicals and reagents

Chemicals of analytical-reagent grade were used as received. Other chemicals were purified by distillation or recrystallization.

*2-Iodo-1-methylpyridinium chloride.* The reagent was prepared by quaternization of 2-chloropyridine with methyl iodide and subsequent halogen exchange. A mixture of 2-chloropyridine (15.0 g, 132 mmol) and methyl iodide (20.0 g, 140 mmol) were heated (oil-bath, 75°C) overnight. A yellow precipitate appeared gradually. The cooled mixture was filtered and washed with diethyl ether. Triple recrystallization from ethanol gave 24.21 g (72%) of white needles, which could be resolved into pure 2-iodo-1-methylpyridinium chloride (m.p. 208–209°C).

For sulphide derivatization prior to HPLC, a 0.01 M aqueous solution of 2-iodo-1-methylpyridinium chloride was used.

*1-Methyl-2-thiopyridone.* The compound was prepared as described previously [5].

*Buffer solutions.* Borate and phosphate buffers of concentration 0.1 M were used throughout.

*Standard sulphide solution.* A sulphide solution (ca. 0.04 M in 0.04 M sodium hydroxide) was prepared from freshly washed large crystals of  $\text{Na}_2\text{S} \cdot 9\text{H}_2\text{O}$  after absorption of the water with filter-paper. The solution was standardized by the *o*-hydroxymercuribenzoate method. Working standard solutions of sulphide in the range 0.1–10  $\mu\text{g/ml}$  were prepared just before measurement by appropriate dilution with water.

*Mobile phase and sample preparation.* The mobile phase was methanol–0.005 M aqueous  $\text{KH}_2\text{PO}_4$  (pH 4.7) (20:80, v/v) at ambient temperature. The solvents and the solutions of samples were filtered through a 0.45- $\mu\text{m}$  membrane filter and degassed before use.

### Sample derivatization

In a 10-ml calibrated flask were placed 1 ml of working reagent solution and an aliquot of sample, then 3 ml of buffer solution (pH 8) were added. The flask was stoppered, mixed by inversion and put aside for 30 min. The mixture was then diluted to the mark with water and a 20- $\mu\text{l}$

aliquot was injected into the liquid chromatographic system. The derivatization procedure was applied to working standard solutions of sulphide to obtain a calibration graph.

#### Assay procedure

An aliquot of the sample solution was subjected to the derivatization procedure and 20  $\mu\text{l}$  of the final analytical solution were injected into the liquid chromatograph in triplicate. Unknown samples were run concurrently with standard solutions. The peak height was measured and the amount of sulphide in each of the samples was then calculated by interpolation on the calibration graph.

#### Chromatography

Chromatographic separations were carried out under isocratic conditions on an ODS-2 reversed-phase column. For routine determination of sulphide, a mobile phase consisting of methanol–0.005 M  $\text{KH}_2\text{PO}_4$  (pH 4.7) (20:80, v/v) at a flow-rate of 0.7 ml/min and a detector wavelength of 340 nm were found to be appropriate, allowing an adequate separation of the sulphide adduct from excess of the derivatization reagent and the other possible reaction mixture components, e.g., thiol adducts.

#### RESULTS AND DISCUSSION

The reaction of 2-iodo-1-methylpyridinium chloride with sulphide was first carried out on a preparative scale and the isolated reaction product, 1-methyl-2-thiopyridone, was found to be in agreement with assigned structure. Details of this experiment have been described in a previous paper [5] devoted to a spectrophotometric method for determining sulphide. The same paper presented details of the reactions on an analytical scale for derivatization purposes.

Experiments were carried out to determine the minimum reaction time required to produce the maximum peak height for a given sulphide concentration, and it was found that for 40 ng of sulphide in a 10-ml reaction vessel the maximum peak height was obtained after 30 min. There-

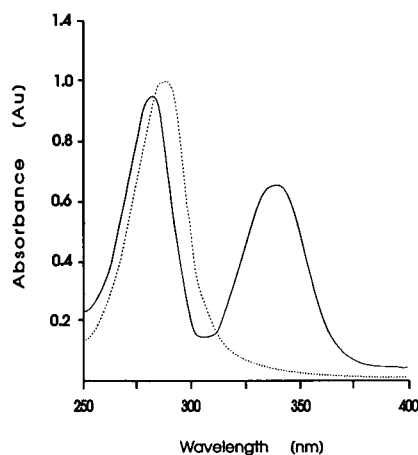


Fig. 1. Absorption spectra of 1.6  $\mu\text{g}$  of sulphide (solid line) and a blank solution (broken line) treated according to the proposed derivatization procedure. Cells with an optical path length of 1 cm were used.

fore, this time was applied in all subsequent determinations.

Fig. 1 shows the absorption spectra of a sulphide sample and a blank solution, treated according to the procedure described under Experimental. These spectra show that the reaction product, 1-methyl-2-thiopyridone, had two absorbance maxima at 272 and 340 nm with molar absorptivities of  $9.5 \cdot 10^3$  and  $7.4 \cdot 10^3$   $\text{l mol}^{-1} \text{cm}^{-1}$ , respectively. It was therefore possible to monitor the reaction product at both points by selecting the appropriate wavelength according to the sample matrix composition.

Fig. 2 shows a chromatogram obtained for 38 ng of sulphide in final volumes of 10 and 1 ml with detection at 340 nm. 1-Methyl-2-thiopyridone was eluted as a well resolved, slightly tailed peak at a retention time of 4.2 min. Injection of an authentic sample of 1-methyl-2-thiopyridone gave the same peak.

When a detection wavelength of 272 nm was used, the height of the analyte peak increased in accordance with the molar absorptivity (Fig. 1). Excess of reagent was eluted in the form of broad peak at a retention time of about 8 min; at 340 nm the peak could not be seen.

#### Analytical parameters

A linear calibration graph was obtained over the range 0.04–50  $\mu\text{g}$  of  $\text{S}^{2-}$  (4  $\mu\text{g}/\text{l}$ –5  $\mu\text{g}/\text{ml}$ )

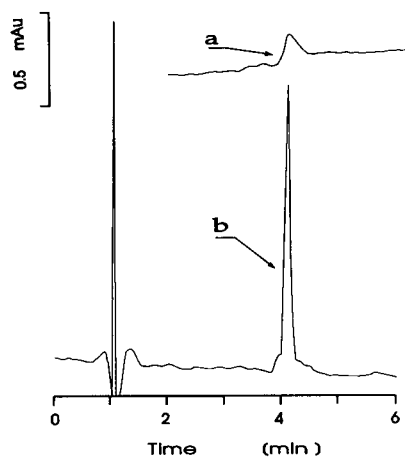


Fig. 2. Chromatogram of 38 ng of sulphide in standard solution derivatized to form 1-methyl-2-thiopyridone, (a) in 10 and (b) in 1 ml of final analytical solution. Conditions: column, 5- $\mu$ m ODS-2 (125  $\times$  4 mm I.D.); mobile phase, methanol–0.005 M  $\text{KH}_2\text{PO}_4$  (pH 4.7) (20:80, v/v) at a flow-rate of 0.7 ml/min; injection volume, 20  $\mu$ l; detection, 340 nm.

with relative standard deviations of 0.2% at the 1  $\mu$ g/ml and 3.2% at the 10  $\mu$ g/l sulphide level (Table I). The detection limit, determined as the concentration of sulphide in the final analytical solution (using a 20- $\mu$ l injection) giving a signal equal to three times the baseline noise, was 2  $\mu$ g/l. The average recovery obtained for a 100  $\mu$ g/l standard solution of sulphide was 97%. Once formed, 1-methyl-2-thiopyridone, was stable for several weeks in the final analytical solution.

TABLE I

DETERMINATION OF SULPHIDE AS 1-METHYL-2-THIOPYRIDONE

Detection wavelength, 340 nm.

Taken ( $\mu$ g in 10 ml)	Found <sup>a</sup> ( $\mu$ g)	Error (%)	S.D. ( $\mu$ g)	R.S.D. (%)
0.058	0.055	-4.4	0.005	8.6
0.116	0.112	-3.4	0.003	2.8
0.232	0.226	-2.7	0.003	1.3
0.580	0.597	2.96	0.012	2.0
1.16	1.149	-1.0	0.013	1.1
5.8	5.787	-1.3	0.016	0.3
11.6	11.617	1.7	0.015	0.2

<sup>a</sup> Mean result,  $n = 5$ . Regression equation:  $y = 2.79x - 0.006$ , where  $y$  = peak height (mAu) and  $x$  = amount taken ( $\mu$ g/10 ml). Correlation coefficient was 0.9997.

### Effect of foreign species

Interference studies were conducted for a wide range of species. Common inorganic anions including chloride, iodide, nitrate, carbonate, sulphite, thiocyanate, acetate and phosphate at a 0.1 M concentration ( $5 \cdot 10^5$ -fold excess over sulphide in the final analytical solution) showed no interference. Thiosulphate at the same concentration as sulphide at the 1  $\mu$ g/ml level gave a 10% positive interference, probably because of partial desulphurization of the thiosulphate ion with formation of 1-methyl-2-thiopyridone. The exact mechanism of this interference will be elucidated by some additional experiments that are outside the scope of this paper. Thiols (*e.g.*, glutathione) react with the reagent to form ionic thio ethers, which are easily resolved from 1-methyl-2-thiopyridone owing to their much shorter retention times under reversed-phase conditions. Interference by thiols was the chief drawback to the spectrophotometric method described previously [5].

### CONCLUSIONS

2-Iodo-1-ethylpyridinium chloride appears to be a useful HPLC derivatization reagent, having good reactivity and selectivity towards sulphide under mild reaction conditions. The compound is cheap, soluble in the water, stable and, as a crystalline substance, very easy to handle. 1-Methyl-2-thiopyridone, the derivatization reaction product, is also crystalline and can be used instead of sulphide for calibration graph preparation. Ultraviolet detection provides a reliable, sensitive and simple method for the determination of sulphide in an aqueous matrix. This means of detection is free from the defects in the amperometric [29,30,31] and potentiometric [32] methods mentioned in the Introduction.

The analytical parameters of this method are similar to those of the reversed-phase HPLC modification of the methylene blue method of Haddad and Heckenberg [35]; the precision (R.S.D.) at the 10  $\mu$ g/l level were 3.2% (this work) and 3.7% [35], and the corresponding detection limits were 2 and 0.8  $\mu$ g/l. The methylene blue method is more sensitive, but it has been reported that, in some real situations,



preliminary dilution of samples is required [36]. It is known that the rate of colour formation in the methylene blue method is highly dependent on both the temperature and the total volume. The separation of methylene blue is column dependent and cannot be reproduced on other C<sub>18</sub> columns reported in the original paper [35].

The present method is tolerant to large excesses of thiols and most common cations and anions; only thiosulphate give a positive interference. If excess of thiosulphate is suspected, sulphide must be separated by one of the reported methods [37,38].

In the methylene blue HPLC method iodide interferes strongly by inhibiting colour formation, whereas in the present method it does not. The high selectivity of the method is the main advantage over the spectrophotometric approach. For all these reasons, the HPLC method based on reaction with 2-iodo-1-methylpyridinium chloride is recommended for determining sulphide in a long series of samples. In environmental analysis the derivatization stage can be performed outside the laboratory in order to convert sulphide into stable product as rapidly as possible.

Further applications of 2-halopyridinium salts as derivatization reagents are currently being explored.

#### REFERENCES

- J.H. Karchmer, in A.W. Hanley and F.W. Chech (Editors), *The Analytical Chemistry of Sulphur and Its Compounds*, Part I, Wiley-Interscience, New York, 1970, Ch. 5.
- W.J. Williams, *Handbook of Anion Determination*, Butterworth, London, 1979, Ch. 5.
- S.R. Bahat, J.H. Eckert, R. Gibson and J.M. Goyer, *Anal. Chim. Acta*, 108 (1979) 293.
- C.F. Wood and I.L. Marr, *Analyst*, 113 (1988) 1635.
- E. Bald and W. Ciesielski, *Chem. Anal. (Warsaw)*, 33 (1988) 925.
- N. Balasubramanian and B.S. Kumar, *Analyst*, 115 (1990) 859.
- T. Koh, Y. Miura, N. Yamamura and T. Takaki, *Analyst*, 115 (1990) 1133.
- J. Anwar, N. Ajum and M. Faroogi, *J. Chem. Soc. Pak.*, 12 (1990) 107.
- K. Lewin, J.N. Walsh and D.L. Miles, *J. Anal. At. Spectrom.*, 2 (1987) 249.
- G. Luter, A.E. Giblin and R. Varsolona, *Limnol. Oceanogr.*, 30 (1975) 727.
- L.K. Leung and D.E. Bartek, *Anal. Chim. Acta*, 131 (1981) 167.
- M. Glaister, G.J. Moody and J.D.R. Thomas, *Analyst*, 110 (1985) 113.
- H. Clyster, F. Adams and F. Verbeek, *Anal. Chim. Acta*, 83 (1976) 27.
- Y. Asano and S. Ito, *Denki Kagaku Oyobi Kogyo Butsuri Kagaku*, 58 (1990) 1125; *C.A.*, 114 (1991) 108575c.
- K. Shimizu and R. Osteryoung, *Anal. Chem.*, 53 (1981) 584.
- S. Jaya, T.P. Rao and G.P. Rao, *Analyst*, 111 (1986) 717.
- A. Punta, F.J. Barragan, M. Ternero and A. Guiraum, *Analyst*, 115 (1990) 1499.
- Y. Arikawa and H. Kawai, *Bunseki Kagaku*, 35 (1986) 720; *C.A.*, 105 (1986) 145216w.
- S. Bottrell, D. Banks, D. Bird and R. Raiswell, *Environ. Technol.*, 12 (1991) 393.
- X. Qian, Y. Guo, M. Yamada, E. Kobayashi and S. Suzuki, *Talanta*, 36 (1989) 505.
- O.F. Kamsan, *Anal. Chim. Acta*, 211 (1988) 299.
- N. Korsakowa, T. Kukina, T. Sushchevskaya and G. Varshal, *Geokhimiya*, (1991) 45.
- M. Yagoob, M. Anwar, H. Masood and M. Masoom, *Anal. Lett.*, 24 (1991) 581.
- J. Lima and L. Rocha, *Int. J. Environ. Anal. Chem.*, 38 (1990) 127.
- F. Caron and J.R. Cramer, *Anal. Chem.*, 61 (1989) 114.
- L. Goodwin, D. Fracom, A. Urso and F. Dieken, *Anal. Chem.*, 60 (1988) 216.
- J. May and T. Francis, *Lab. Pract.*, 40 (1991) 65.
- R.J. Williams, *Anal. Chem.*, 55 (1983) 851.
- K. Han and W.F. Koch, *Anal. Chem.*, 59 (1987) 1016.
- A.M. Bond, I.D. Heritage and G.G. Wallace, *Anal. Chem.*, (1982) 582.
- W.F. Koch, *J. Res. Natl. Bur. Stand.*, 88 (1983) 157.
- W.-N. Wang, Y.-J. Chen and M.-T. Wu, *Analyst*, 108 (1984) 281.
- R.E. Pulson and H.M. Berger, *J. Chromatogr. Sci.*, 25 (1987) 409.
- O.N. Obrezkow, V.I. Shlyamin, O.A. Spigin and Y.A. Zololov, *Mendeleev Commun.*, (1991) 38.
- P.R. Haddad and A.L. Heckenberg, *J. Chromatogr.*, 447 (1988) 415.
- K. Grasshoff and K. Chan, *Anal. Chim. Acta*, 53 (1971) 442.
- Standard Methods for the Examination of Water and Wastewater*, American Public Health Association, Washington, DC, 14th ed., 1976, Section 428.9, p. 499.
- L. Bark and A. Rixon, *Analyst*, 95 (1970) 786.

## Short Communication

---

# Capability of a carbon support to improve the gas chromatographic performance of a liquid crystal phase in a packed column for some volatile oil constituents

T.J. Betts

*School of Pharmacy, Curtin University of Technology, GPO Box U1987, Perth, Western Australia 6001 (Australia)*

(First received March 1st, 1993; revised manuscript received April 2nd, 1993)

---

### ABSTRACT

“Graphpac” was investigated to see if carbon was a better gas chromatographic support than silica for columns of 3% of the liquid crystal bismethoxybenzylidenebutyloluidine or (MBT)<sub>2</sub>. Six volatile oil component solutes exhibited the same elution sequence as from silica, but with lower relative retention times with respect to linalol—about 50% for some aromatics, reflecting the much lower polarity of the carbon-supported packing indicated by cuminal/caryophyllene ratio. Caryophyllene had greatly increased relative retention, and this was further raised if a low-loading of 0.3% (MBT)<sub>2</sub> was used on “Graphpac”, indicating even lower polarity. This column was not reliable below 200°C, but an initial period at 203°C, followed by rapid heating to 230°C, gave reasonable results for some significant constituents of teatree oil. Nevertheless, 3% (MBT)<sub>2</sub> on “Graphpac” was preferable for assaying this and sweet fennel oil by providing a more reliable melted liquid crystal stationary phase, with low temperature versatility.

---

### INTRODUCTION

We have previously [1–3] used packed columns of liquid crystal phases for the gas chromatographic study of constituents of volatile oils. Some authors claim that the normal silica support we have used is not the optimum for liquid crystal performance. In 1984 Rayss and Waksmundzki [4] studied the influence of graphite support for the liquid crystal *p*-butyl-*p*-hexanoylazobenzene (PHPB). The logarithm of retention volumes for *n*-octanol against the reciprocal of temperature showed breaks in the plot indicating the two transition temperatures (solid to nematic liquid crystal; liquid crystal to normal isotropic liquid) of PHPB only if at least

3% of it was present. However, the lower loading of 1.3% still revealed the “influence of the graphite support”, in contrast to silica support where at least 7.7% PHPB was needed to show the transitions. Without such amounts of PHPB “the occurrence of a solid/nematic phase transition becomes impossible (due to) the influence of the silica gel surface on the liquid crystal layer directly adjacent” to it. They concluded that “in the surface film of PHPB on graphite, about ten times more molecules are present than on silica (in) a polymolecular film” so that carbon, as graphite, was a more ‘empathetic’ support for their liquid crystal than silica.

Economic low loadings of expensive liquid

crystals should thus be possible, and recently Nazarova *et al.* [5] studied a presumed monolayer of the liquid crystal bis(hexyloxybenzylidene)phenylenediamine [(HB)<sub>2</sub>PD] on carbon. Polyaromatic isomers were better resolved than with a 5% loading on normal support "Chromaton", although the latter did indicate the transitions. In contrast, the 0.33% (HB)<sub>2</sub>PD on graphitized carbon they used gave only straight line plots like a normal liquid of log retention volume against temperature reciprocal, indicating that "no phase transition . . . takes place". This was because they considered (HB)<sub>2</sub>PD was "in a (continuous) structured state similar to the mesomorphic" liquid crystal at temperatures above and below its transition points. Rayss and Waksmundzki [4] had agreed in observing practically a straight line plot with 0.5% PHPB on graphite. Their explanation was that "at the solid surface a film of PHPB molecules may be formed oriented differently than in the layer more distant" when thicker loadings were present.

It was therefore of interest to see if a carbon support would improve the performance of a liquid crystal that we previously used on silica [1,3], bismethoxybenzylidenebitoluidine (MBT)<sub>2</sub>, for the gas chromatography of volatile oil constituents, applied in both normal (3%) and very low (0.3%) loadings. It is a dianil aromatic diether, like (HB)<sub>2</sub>PD, but with four aromatic rings instead of three.

## EXPERIMENTAL

### Apparatus

A Pye GCD gas chromatograph was used fitted with a flame ionisation detector. This had no temperature programming facility, but altering the temperature-setting dials caused rapid heating at about 40°C min<sup>-1</sup>. Cooling from high temperature was allowed without opening the oven to minimise disturbance of the liquid crystal phase. The oven temperatures were observed with a Technoterm 7300 probe. Chromatographs were plotted with a Hewlett-Packard 3390A integrator/recorder.

The glass columns (1.5 m × 2 mm I.D.) were packed with 3% or 0.3% (w/w) (MBT)<sub>2</sub> from

T.C.I. (Tokyo, Japan) [1] on uncoated "Graphpac-GC" 80–100 mesh (Alltech) claimed to have a surface area of 10–13 m<sup>2</sup> g<sup>-1</sup>. The weighed amounts of liquid crystal and support were dispersed in dichloromethane and taken to dryness in a rotary evaporator.

### Materials and methods

Sources of most solutes [1–3] and oils [1,6] have been given before. Fenchone was from Aldrich. Injections were 0.1 μl oil, or trace residues of solutes from an "emptied" microsyringe. Nitrogen was the mobile phase flowing at 15 ml min<sup>-1</sup> at the outlet of the 3% (MBT)<sub>2</sub> column, but twice as fast from the low-loaded column. Holdup times were deducted from observed retention times, obtained by extrapolating to methane the retention times of *n*-heptane and *n*-hexane plotted on semi-logarithmic graph paper.

## RESULTS AND DISCUSSION

Average results are given in Table I where some significant solutes are numbered at the left. The present values are related to those previously obtained on silica supports.

The 3% (MBT)<sub>2</sub> on Graphpac column showed the same sequence for four aromatic solutes (Table I, solutes 2, 3, 4 and 5) as on silica [1,3], namely estragole (quickest)–safrole–cuminal–thymol (slowest). However, the 0.3% on Graphpac phase showed thymol ahead of cuminal, almost level with safrole. Typically for liquid crystals [3], safrole was always quicker than anethole. In the present work, anethole (the *trans*-isomer) was constantly slower than thymol (solutes 6 and 5), indicating that the Graphpac columns always differed from the "conventional" sequence, even when first used. Once again, there was a distinction between unmelted (heated from cold) behaviour of 3% loading at 160°C and the supercooled response at the same temperature after heating above the 180°C melting point of (MBT)<sub>2</sub>. On the unmelted phase, thymol was only just ahead of anethole, and never well behind it as on silica support [1]. There was no anethole-thymol sequence "shift"

TABLE I

AVERAGE RELATIVE RETENTION TIMES (LINALOL = 1.00) ON GRAPHAC AND SILICA SUPPORTS (ITALIC RESULTS ON SILICA) COATED WITH (MBT)<sub>2</sub>3% (MBT)<sub>2</sub> loading used except where indicated otherwise. Values in italics obtained previously [1–3].

Solute	230°C		203°C		200°C	181°C	175°C	160°C		160°C		
	3%	3%	0.3%	0.3%				3%	<i>supercooled</i>	<i>unmelted</i>		
<b>6</b> Anethole	2.77	<i>4.81</i>	2.62	2.8–3.1	3.07	<i>5.87</i>	3.19	<i>7.06</i>	3.41	<i>7.88</i>	2.65	<i>3.72<sup>b</sup></i>
Caryophyllene	2.68	<i>2.00<sup>b</sup></i>	<i>3.68<sup>b</sup></i>	<i>4.04<sup>b</sup></i>	2.75	<i>2.22<sup>b</sup></i>	2.81	<i>2.41<sup>b</sup></i>	<i>2.98<sup>b</sup></i>	<i>2.33<sup>b</sup></i>	<i>3.00<sup>b</sup></i>	<i>2.80<sup>b</sup></i>
<b>5</b> Thymol	2.35	<i>3.96</i>	<i>1.86<sup>b</sup></i>	<i>2.00<sup>b</sup></i>	2.59	<i>4.90</i>	2.75	<i>5.19</i>	3.00	<i>5.88</i>	2.62	4.53
<b>4</b> Cuminal	2.26	<i>3.71</i>	2.08	2.1–2.4	2.34	<i>4.38</i>	2.30	<i>4.62</i>	2.36	<i>4.82</i>	2.06	3.35
<b>3</b> Safrole	2.11	<i>3.55</i>	1.85	1.97	2.17	<i>4.10</i>	2.15	<i>4.24</i>	2.12	<i>4.46</i>	1.79	2.93
Geraniol	1.77		1.70	1.90			1.97	<i>3.29</i>				
<b>2</b> Estragole	1.58	<i>2.38</i>	1.44	1.42	1.59	<i>2.58</i>	1.57	<i>2.75</i>	1.57	<i>2.80</i>	1.35	1.79
<b>1</b> $\alpha$ -Terpineol	1.53	<i>1.96</i>	1.44	<i>1.47<sup>b</sup></i>	1.52	<i>2.20</i>	1.51	<i>2.34</i>	1.51	<i>2.39</i>	<i>1.43<sup>b</sup></i>	<i>1.94<sup>b</sup></i>
4-Terpineol	1.35		1.25	1.25			1.33					
Fenchone	0.87		0.72	0.67			0.75					
Limonene	0.62		0.62	0.58			0.54		<i>0.49</i>			<i>0.39<sup>b</sup></i>
Cineole (1,8-)	0.59		0.51	0.50			0.50		<i>0.43</i>			<i>0.43</i>
$\alpha$ -Pinene	0.36		0.34	0.32			0.30					
<i>c</i> ratio <sup>a</sup> and polarity of column	<i>0.63</i>	<i>1.39</i>	<i>0.42</i>	<i>0.43</i>	<i>0.64</i>	<i>1.48</i>	<i>0.61</i>	<i>1.44</i>	<i>0.59</i>	<i>1.55</i>	<i>0.51</i>	<i>0.90</i>
	<i>Low</i>	<i>High</i>	<i>Very low</i>	<i>Very low</i>	<i>Low</i>	<i>High</i>	<i>Low</i>	<i>High</i>	<i>Low</i>	<i>Very high</i>	<i>Low</i>	<i>Intermediate</i>

<sup>a</sup> *c* ratio is  $3 \times (\text{cuminal value}) / 4 \times (\text{caryophyllene value})$  [8].<sup>b</sup> Value out of sequence in table.

on melting the liquid crystal; although the terpineol-estragole one was still evident (Table I),  $\alpha$ -terpineol being ahead unless the (MBT)<sub>2</sub> was not melted, or the low loaded (0.3%) Graphpac was used (solutes 1 and 2).

There was no sign of “naive” column behaviour with the 3% (MBT)<sub>2</sub> on Graphpac, even when new, which would have been shown by anethole emerging ahead of cuminal (solutes 6 and 4) and safrole ahead of  $\alpha$ -terpineol (solutes 3 and 1) [1]. After melting the liquid crystal (results at 181°C and above, and supercooled to 160°C) the sequence of six original test solutes (1–6 in Table I) was the same as on silica support [1]. However, relative retention values were usually lower, about 50% of the values on silica for the three chemically distinct aromatics 3, 4 and 5, although over 60% for  $\alpha$ -terpineol (solute 1). This and aromatics 2, 3 and 4, exhibited almost constant values. Although (MBT)<sub>2</sub> is a tetraaromatic molecule, the carbon support does not promote its relative retention

of different aromatic substances. Surprisingly, this packing did increase the relative retention of the sesquiterpene caryophyllene (Table I) and it may be useful for chromatographing this type of hydrocarbon, especially at 0.3% loading. Other solutes with long relative retention times (5 and 6) gave the usual decline in values with increasing temperature [7] whilst those with short times showed the usual increase on the (MBT)<sub>2</sub> on Graphpac.

The low-loaded (0.3% (MBT)<sub>2</sub>) on Graphpac could not be used below 200°C, at which temperature some aromatics gave variable results—larger amounts injected producing shorter retention times, unlike conventional phases. Most values were lower than with the 3% loading on Graphpac, but caryophyllene relative retention times increased considerably (well after anethole) so indicating a considerable reduction in polarity [8] with the low loading. Reduced values for thymol were distinctive here, bringing this polar solute close to safrole. Nevertheless,

by using an initial isothermal period at 203°C, followed by rapid heating to about 230°C, quite good volatile oil assays resulted, although early monoterpene hydrocarbons were not resolved. A teatree oil previously evaluated on a silica column of 3% (MBT)<sub>2</sub> gave values (Fig. 1a) a little lower than those before [1] of 41.1% 4-terpineol and 3.8%  $\alpha$ -terpineol. These two monoterpenols probably provide the desired antiseptic character of this oil, and are better resolved and more reliably assayed on the 3% (MBT)<sub>2</sub> on Graphpac which can be heated up in stages from initial lower temperatures (unmelted) like 110°C (Fig. 1b) to give the terpineol separation at 130°C. It also gives some resolution of the earlier terpinenes. Fig. 1c shows that a sample of sweet fennel oil recently assayed [6] on four different capillaries (including a liquid crystal polysiloxane) gave results close to their averages of 6.3% fenchone, 4.1%

estragole, 66.4% *trans*-anethole and 0.8% feniculin.

On silica, the 3% melted liquid crystal allowed caryophyllene to pass through as quickly as  $\alpha$ -terpineol, indicating a high polarity packing [8] in relation to cuminal (Table I). The same loading on Graphpac saw caryophyllene emerging after, or with, thymol; the packing now being of low polarity. The low-load of 0.3% (MBT)<sub>2</sub> on Graphpac rates as "very low" polarity, 0.4, although not as low as the about 0.3 *c* ratio of methylpolysiloxane. With its high operational temperature (above 200°C) this should make it useful for sesquiterpene hydrocarbons like the later peaks from tea tree oil. Increasing the load to 3% (melted) on Graphpac raises the *c* ratio to 0.6—still low polarity. Intermediate polarities are given by values between 0.8 and 1.2, and this is exhibited by unmelted 3% (MBT)<sub>2</sub> on silica. On this support with melted liquid crystal, the *c*

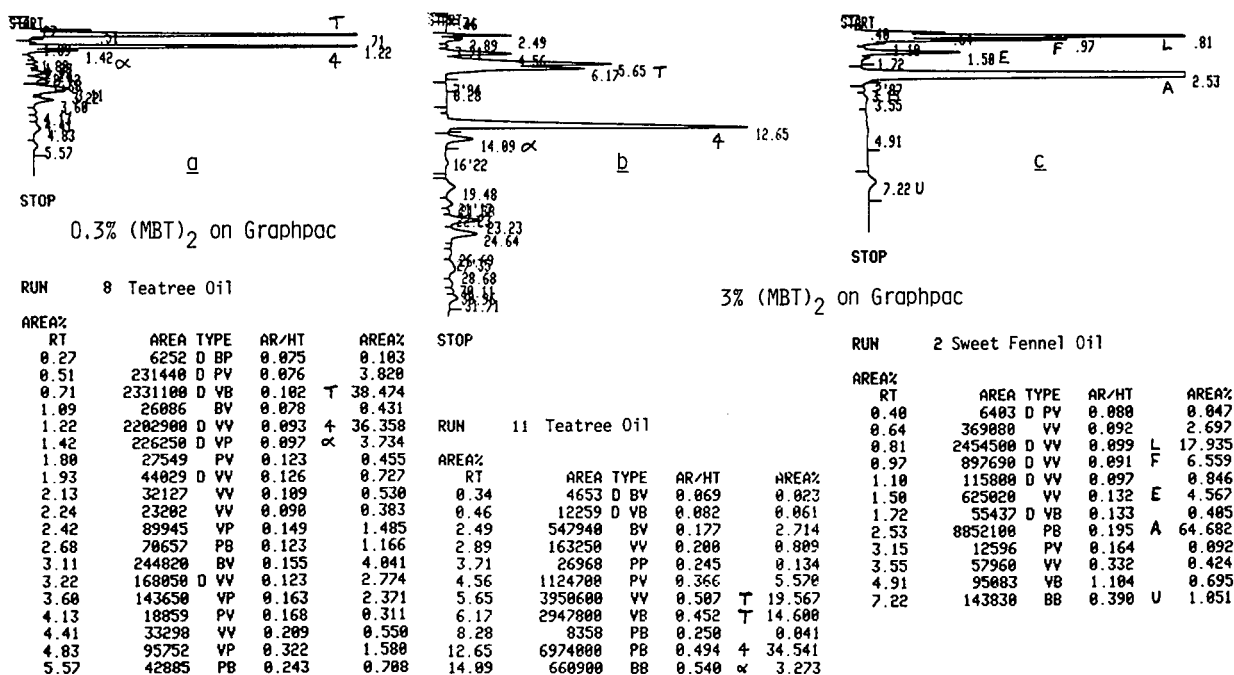


Fig. 1. Chromatograms of oils on packed columns of liquid crystal phase on Graphpac carbon. (a) Teatree oil on 0.3% (MBT)<sub>2</sub> at 203°C for 1.5 min, then rapidly heated to 232°C.  $\alpha$  =  $\alpha$ -Terpineol; 4 = 4-terpineol; T =  $\alpha$ - and  $\gamma$ -terpinenes, plus other monoterpenes. (b) Teatree oil on 3% (MBT)<sub>2</sub> at 110°C for 3.8 min, then heated to 131°C till 16.2 min, then to 145°C at 21.1 min, then to 160°C at 27.3 min. All unmelted conditions. Incomplete printout shown. Abbreviations as for (a). (c) Sweet fennel oil on 3% (MBT)<sub>2</sub> at 203°C for 2.9 min, then rapidly heated to 230°C. A = *trans*-Anethole; E = estragole; F = fenchone; L = limonene plus other monoterpenes; U = feniculin. Printout peak types: B = peak starts/ends on baseline; D = distorted peak; P = penetration of baseline (reset); V = valley between peaks. RT = Retention time in min. AR/HT = peak width at half height.

ratios rise to a high polarity 1.4, or even over 1.5 under supercooled conditions, a value like Carbowax 20M. This range of apparent polarities agrees with the concept of a molecular-orienting effect by the carbon support on the liquid crystal molecules, changing in relation to their concentration. Carbon here gives packed columns of quite different polarities to silica.

The low-loaded melted Graphpac column gave very similar results to the unmelted 3% (MBT)<sub>2</sub> on Graphpac for  $\alpha$ -terpineol, cuminal and anethole (solutes **1**, **4**, **6**) and close resemblance for estragole and safrole. This may be due to adsorbing uncoated carbon support dominating the (MBT)<sub>2</sub> present. So to reliably see the liquid crystal effect on solutes, it is best to use 3% loading and ensure that it is melted. Graphpac support gave packed columns with closer analysis results than silica for the sweet fennel and mace oils previously assayed on capillaries [6], and the 3% liquid crystal packing was more versatile than the low load. Capillaries provide better resolution of the trace constituents of oils, and so

many more peaks. However, well-chosen packed columns should yield good results for the main constituents, which may be all that is needed.

#### ACKNOWLEDGEMENT

Thanks to Mr. B. MacKinnon for preparing the columns used.

#### REFERENCES

- 1 T.J. Betts, C.M. Moir and A.I. Tassone, *J. Chromatogr.*, 547 (1991) 335.
- 2 T.J. Betts, *J. Chromatogr.*, 587 (1991) 343.
- 3 T.J. Betts, *J. Chromatogr.*, 588 (1991) 231.
- 4 J. Rayss and A. Waksmundzki, *J. Chromatogr.*, 292 (1984) 207.
- 5 V.I. Nazarova, K.D. Shcherbakova and O.A. Shcherbakova, *J. Chromatogr.*, 600 (1992) 59.
- 6 T.J. Betts, *J. Chromatogr.*, 626 (1992) 294.
- 7 P.N. Breckler and T.J. Betts, *J. Chromatogr.*, 53 (1970) 163.
- 8 T.J. Betts, *J. Chromatogr.*, 628 (1993) 138.

## Short Communication

---

# Unusual deuterium isotope effect on the retention of formamides in gas–liquid chromatography

Jaroslav Mráz\*

*National Institute of Public Health, Šrobárova 48, 100 42 Prague 10 (Czech Republic)*

Parmjit Jheeta and Andreas Gescher

*Pharmaceutical Sciences Institute, Aston University, Birmingham B4 7ET (UK)*

Michael D. Threadgill

*School of Pharmacy and Pharmacology, University of Bath, Claverton Down, Bath BA2 7AY (UK)*

(First received October 6th, 1992; revised manuscript received March 26th, 1993)

---

### ABSTRACT

The deuterium isotope effect on gas chromatographic retention of a series of N,N-dimethylformamide, N-methylformamide and formamide isotopomers was studied on methyl and phenyl methyl polysiloxane and polyethylene glycol stationary phases. The deuterium isotope effect was substantially affected by the position of deuterium in the molecule. Whereas methyl-deuterated  $(C^2H_3)_2NCHO$  and  $C^2H_3NHCHO$  eluted, as expected, earlier than their non-labelled analogues, elution of formyl-deuterated  $(CH_3)_2NC^2HO$ ,  $CH_3NHC^2HO$  and  $NH_2C^2HO$  was always delayed. The presence of chemically inequivalent deuterium atoms in  $(C^2H_3)_2NC^2HO$  and  $C^2H_3NHC^2HO$  resulted in final deuterium isotope effects to which the contributions of the individual groups were additive. The elution order of the individual isotopomers was not affected by the polarity of the stationary phase. Interpretation of the deuterium isotope effect observed is provided by the theory of vapour pressure isotope effects.

---

### INTRODUCTION

Changes in the chromatographic retention of molecules with different isotopic composition have often been noted. Perhaps most reports deal with the effect of replacing  $^1H$  by  $^2H$  (deuterium) (for review, see ref. 1). The great majority of reported gas chromatographic (GC)

separations result in earlier elution of heavier  $^2H$ -labelled compounds, which is referred to as the inverse isotope effect [1]. Accordingly, in a series of isotopomers differing by a number of deuterium atoms within some structural unit, *e.g.* in an alkyl group [2,3] or on an aromatic ring [4], the compounds are eluted in the order of decreasing number of deuterium atoms. The normal isotope effect, *i.e.* later elution of heavier species, is observed mainly in absorption GC (GSC), for example on alkali-etched glass capillary columns [5,6]. Examples of normal isotope

---

\* Corresponding author.

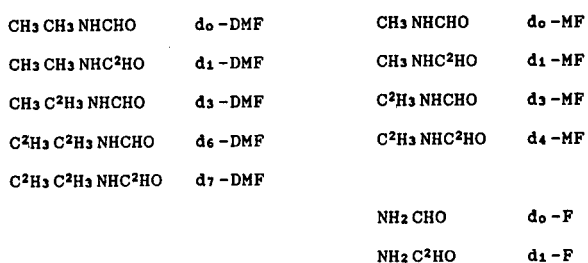


Fig. 1. Structures of DMF, MF and F isotopomers.

effects in partition GC (GLC) are very scarce [3,5].

In this paper we report on an unusual observation, namely that the deuterium isotope effect on GC retention may be substantially affected by the position of deuterium atoms in the molecule. The observation is discussed in terms of the theory of vapour pressure isotope effects.

## EXPERIMENTAL

### Chemicals

Unlabelled N,N-dimethylformamide ( $\text{d}_0\text{-DMF}$ ), N-methylformamide ( $\text{d}_0\text{-MF}$ ) and formamide ( $\text{d}_0\text{-F}$ ) were bought from Aldrich (Gillingham, UK),  $\text{d}_7\text{-DMF}$  was bought from Sigma (Poole, UK). Compounds  $\text{d}_6\text{-DMF}$ ,  $\text{d}_3\text{-DMF}$  and  $\text{d}_3\text{-MF}$  were prepared from  $\text{d}_6\text{-dimethylamine hydrochloride}$  (Sigma),  $\text{d}_3\text{-dimethylamine hydrochloride}$  (a gift from Dr. R.P. Hanzlik, University of Kansas) and  $\text{d}_3\text{-methylamine hydrochloride}$  (Sigma), respectively, and ethyl formate [7]. By analogy,  $\text{d}_1\text{-DMF}$ ,  $\text{d}_1\text{-MF}$

and  $\text{d}_1\text{-F}$  were prepared from the respective amine hydrochlorides and  $\text{d}_1\text{-methyl formate}$  (Aldrich). Compound  $\text{d}_4\text{-MF}$  was prepared from  $\text{d}_3\text{-methylamine hydrochloride}$  and  $\text{d}_1\text{-methyl formate}$ . N,N-Dimethylacetamide (DMA) was bought from Aldrich; propyl-N-methylcarbamate was prepared as described previously [8]. For structures of DMF, MF and F isotopomers see Fig. 1.

### GC analysis

Retention times were measured on an HP-5890 A gas chromatograph with 3394 A integrator. The fused-silica capillary columns used were HP-20M (polyethylene glycol 20M), 25 m  $\times$  0.32 mm I.D., 0.3  $\mu\text{m}$  film thickness, and HP-50+ (cross-linked 50% phenyl methyl silicone gum), 15 m  $\times$  0.53 mm I.D., 1.0  $\mu\text{m}$  film thickness, both from Hewlett-Packard, and DB-1 (cross-linked 100% methyl silicone gum), 15 m  $\times$  0.53 mm I.D., 3.0  $\mu\text{m}$  film thickness, from J & W Scientific. The injector was in a split mode with a 1:30 splitting ratio, and the nitrogen-selective detector was used. Helium was employed as carrier gas. Experimental conditions of the measurements and informative values of dead and retention times are shown in Table I.

A typical sample was a solution of a single isotopomer (1 mM) and an internal standard (1 mM) in acetone (1  $\mu\text{l}$ ). The internal standards were DMA for DMF, propyl-N-methylcarbamate (on HP-20M) or DMA (on HP-50+ and DB-1) for MF, and MF for F.

TABLE I

EXPERIMENTAL CONDITIONS OF GAS CHROMATOGRAPHIC MEASUREMENTS

	HP-20M				HP-50+				DB-1			
	Temp. (°C)	Flow-rate (ml/min)	$t_M$ (min)	$t_R^a$ (min)	Temp. (°C)	Flow-rate (ml/min)	$t_M$ (min)	$t_R^a$ (min)	Temp. (°C)	Flow-rate (ml/min)	$t_M$ (min)	$t_R^a$ (min)
DMF	90	0.9	1.9	7.3	75	2.1	1.4	5.1	75	2.3	1.2	4.8
MF	130	0.7	2.0	7.7	75	2.1	1.4	5.0	75	2.3	1.2	4.3
F	130	0.7	2.0	12.1	75	2.1	1.4	3.5	Not measured <sup>b</sup>			

<sup>a</sup>  $t_R$  of the non-deuterated isotopomer.

<sup>b</sup> Not measured because of the strong tailing and dose dependence of the retention time.



### Calculations

In this study, the deuterium isotope effect on chromatographic retention is expressed using relative retention,  $r_{12}$ , between a deuterated compound and its non-deuterated analogue:  $r_{12} = t'_R(\text{deuterated})/t'_R(\text{non-deuterated})$ . Here  $t'_R = t_R - t_M$ , where  $t_R$  is retention time,  $t'_R$  is corrected retention time and  $t_M$  is dead time. In the most straightforward way,  $r_{12}$  can be measured upon injection of both compounds together. This could not be applied here since in some cases peaks of isotopomers could not be resolved sufficiently. Thus, separate injection of each compound was necessary. The absolute values of retention time, however, may be affected by the drift or fluctuations in experimental conditions during measurement. On the other hand, accuracy of the retention parameters determined should be very high. Therefore, a retention of each isotopomer (i) including the non-deuterated compound was related to the retention of an internal standard (I.S.), which was added for this purpose to the sample. Auxiliary relative retentions  $r_{12\text{aux}}$  were calculated as  $r_{12\text{aux}} = t'_R(i)/t'_R(\text{I.S.})$  and, finally, the  $r_{12}$  value for each deuteromer was obtained:

$$r_{12} = r_{12\text{aux}}(\text{deuterated})/r_{12\text{aux}}(\text{non-deuterated}).$$

### RESULTS AND DISCUSSION

The deuterium isotope effect on the GC retention of a series of deuteromers of DMF, MF and F was studied on three fused-silica capillary columns of different polarity. As an index of the deuterium isotope effect, values of the relative retention  $r_{12}$  of a pair of deuterated/non-deuterated isotopomers were measured. The results (Table II) are consistent for DMF, MF and F, and can be summarized as follows.

(a) The presence of deuterium in the methyl position of formamides results in lower retention.

(b) The presence of deuterium in the formyl position of formamides results in higher retention. The formyl-related deuterium isotope effect is more pronounced than the methyl-related deuterium isotope effect: the corresponding val-

TABLE II

DEUTERIUM ISOTOPE EFFECT ON THE RETENTION OF N,N-DIMETHYLFORMAMIDE, N-METHYLFORMAMIDE, AND FORMAMIDE ISOTOPOMERS

Compound	$r_{12}^a$		
	HP-20M	HP-50+	DB-1
d <sub>0</sub> -DMF	1.000	1.000	1.000
d <sub>1</sub> -DMF	1.023	1.013	1.009
d <sub>3</sub> -DMF	0.998	0.989	0.990
d <sub>6</sub> -DMF	0.995	0.979	0.982
d <sub>7</sub> -DMF	1.017	0.991	0.989
d <sub>0</sub> -MF	1.000	1.000	1.000
d <sub>1</sub> -MF	1.017	1.014	1.010
d <sub>3</sub> -MF	0.982	0.977	0.980
d <sub>4</sub> -MF	1.000	–	–
d <sub>0</sub> -F	1.000	1.000	– <sup>b</sup>
d <sub>1</sub> -F	1.019	1.024	– <sup>b</sup>

<sup>a</sup> The values are mean of at least eight measurements; S.D. was less than 0.001 in most cases.

<sup>b</sup> Not measured because of the strong tailing and dose dependence of retention time.

ues of an index  $(r_{12} - 1)/N_D$  (where  $N_D$  is number of deuterium atoms in the molecule) were 0.009 to 0.024 and  $-0.001$  to  $-0.008$ , respectively. The separation of MF isotopomers is shown in Fig. 2.

(c) The presence of chemically inequivalent deuterium atoms results in the final deuterium isotope effect, to which the contributions of individual deuterium atoms are additive. Thus,  $r_{12}$  of d<sub>7</sub>-DMF or d<sub>4</sub>-MF is consistent with that

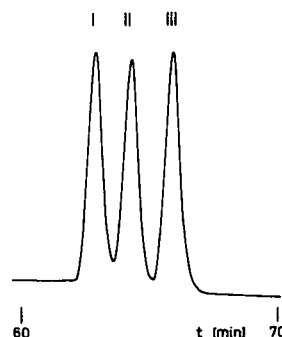


Fig. 2. Resolution of C<sup>2</sup>H<sub>3</sub>NHCHO (I), CH<sub>3</sub>NHCHO (II) and CH<sub>3</sub>NHC<sup>2</sup>H<sub>3</sub>O (III) on fused-silica capillary column HP-20M 25 m × 0.32 mm I.D., 0.3 μm film thickness; column temperature 70°C; carrier gas helium, 1.0 ml/min.

estimated from the individual  $r_{12}$  values of partially deuterated analogues  $d_6$ -DMF and  $d_1$ -DMF, or  $d_3$ -MF and  $d_1$ -MF, respectively.

(d) The observations described under (a) to (c) are similar on strongly polar (HP-20M), slightly polar (HP-50+), and low polar (DB-1) columns.

Numerous reports on GC of isotopomers are consistent in that the deuterium isotope effect related to deuterium in methyl or methylene groups is regularly the inverse effect [1,9,10]. This has been interpreted to be a consequence of shorter C– $^2$ H internuclear distances as compared with C–H bonds, resulting in lower molar volumes and thus weaker dispersion forces. The effect on dispersion forces is thus responsible for the inverse deuterium isotope effect related to C $^2$ H $_3$  groups in DMF and MF (even when the contribution of these forces to overall interaction does not have to be prevailing). Dispersion forces seem to predominate in the interaction of formamides with non-polar stationary phases such as DB-1, as judged from the elution in the order of F, MF and DMF, *i.e.* with increasing molar volume. In contrast, these compounds are eluted in the opposite order where polar interactions (dipole–dipole, dipole–induced dipole, etc.) prevail, as in the case of elution from polar HP-20M column. The increasing role of polar interactions in the order of DMF to F is consistent with the order of boiling points: DMF, 153°C; MF, 185°C; F, 195°C.

Unlike methyl-deuterated compounds, the normal DIE as observed with formyl-deuterated formamides seems to be surprising and difficult to account for by simple considerations. The key to understanding this phenomenon is provided by the theory of isotope effects, especially vapour pressure isotope effects, supported by numerous experimental data (for review, see ref. 11). All available reports show that deuterium at saturated carbon displays inverse vapour pressure isotope effect, whereas substitution in groups that form hydrogen bonds and associate often results in normal vapour pressure isotope effect. There is an intrinsic relationship between isotope effect and molecular motion; normal isotope effects correlate with blue and inverse isotope effects with red frequency shifts.

Good examples to study the vapour pressure

isotope effect related to deuterium in different groups of the same compound are methylacetylenes and alkylamines [12–14]. Here, deuterium in the methyl group results in an inverse vapour pressure isotope effect, whereas CH $_3$ CC $^2$ H, CH $_3$ N $^2$ H $_2$  and (CH $_3$ ) $_2$ N $^2$ H exhibit a normal vapour pressure isotope effect. The above effects were interpreted with the aid of Bigeleisen theory [15]. In a most simplified way, the vapour pressure isotope effect is calculated using the equation  $\ln P'/P = A/T^2 - B/T$ , where  $P'$  and  $P$  are the vapour pressures of the heavier and lighter isotopomers, respectively,  $A$  (lattice term) and  $B$  (zero-point energy term) represent external and internal frequency modes, respectively, and  $T$  is temperature. In this model, replacement of H by  $^2$ H in the methyl group affects only the  $A$  term, which is always positive so that inverse vapour pressure isotope effects occur. On the other hand, the location of deuterium in methynic or amino groups affects both  $A$  and  $B$  terms, the latter being responsible for the normal vapour pressure isotope effect observed. Analysis of the shape of an experimental plot of  $\ln P'/P$  vs.  $T$  for CH $_3$ CC $^2$ H, CH $_3$ N $^2$ H $_2$  and (CH $_3$ ) $_2$ N $^2$ H revealed temperature-dependency of  $B$ , which is indicative of molecular association in condensed phases [12–14]. This view was further reinforced by finding that the vapour pressure isotope effect as measured for CH $_3$ N $^2$ H $_2$  or (CH $_3$ ) $_2$ N $^2$ H in solution with hexane changed from a normal to inverse effect at high dilution [13,14], in which the association was negligible.

The data on formamides presented here are obviously in good agreement with those on methylacetylenes and amines. Thus, the normal isotope effect related to GC retention of formyl-deuterated formamides is likely to reflect stronger interaction of those compounds, via the formyl group (compared with their non-labelled counterparts), with each other as well as with other molecules such as GC stationary phases. Owing to the polar nature of those interactions one can expect that the magnitude of the deuterium isotope effect on GC retention of formyl-deuterated formamides will increase with polarity of the stationary phase. This was in fact the case, except for F (Table II). Another similarity was observed between the sets of

methylacetylene, methyl- and dimethylamine and formamide isotopomers, namely that the presence of chemically inequivalent deuterium atoms resulted in a final deuterium isotope effect to which contributions of individual deuterium atoms were additive.

In conclusion, the deuterium isotope effect on GC retention of formamides reported here, despite its unusual character, complies well with the general theory of isotope effects.

#### ACKNOWLEDGEMENTS

We wish to thank the European Science Foundation Fellowships in Toxicology for support to J.M. to spend a research sabbatical year at Aston University. We also thank Dr. R.P. Hanzlik (University of Kansas) for the kind gift of  $d_3$ -dimethylamine hydrochloride.

#### REFERENCES

- 1 M. Matucha, W. Jockisch, P. Verner and G. Anders, *J. Chromatogr.*, 588 (1991) 251.
- 2 M. Mohnke and J. Heybey, *J. Chromatogr.*, 471 (1989) 37.
- 3 A. Liberti and L. Zoccolillo, *J. Chromatogr.*, 49 (1970) 18.
- 4 J. Bermejo, C.G. Bianco and M.D. Guillén, *J. Chromatogr.*, 351 (1986) 425.
- 5 G.P. Cartoni, A. Liberti and A. Pela, *Anal. Chem.*, 39 (1967) 1618.
- 6 F. Bruner, G.P. Cartoni and A. Liberti, *Anal. Chem.*, 38 (1966) 298.
- 7 M.D. Threadgill and E.N. Gate, *J. Labelled Compd. Radiopharm.*, 20 (1983) 447.
- 8 J. Mráz, P. Jheeta, A. Gescher, R. Hyland, K. Thummel and M.D. Threadgill, *Chem. Res. Toxicol.*, 6 (1993) 197.
- 9 R. Kaliszan, *Quantitative Structure–Chromatographic Retention Relationships*, Wiley, New York, 1987.
- 10 V.P. Chizhkov and L.A. Sinitsina, *J. Chromatogr.*, 104 (1975) 327.
- 11 G. Jancso and W.A. Van Hook, *Chem. Rev.*, 74 (1974) 689.
- 12 W.A. Van Hook, *J. Chem. Phys.*, 46 (1967) 1907.
- 13 H. Wolff and A. Höpfner, *Ber. Bunsenges. Phys. Chem.*, 69 (1965) 710.
- 14 H. Wolff and R. Würtz, *J. Chem. Phys.*, 74 (1970) 1600.
- 15 J. Bigeleisen, *J. Chem. Phys.*, 34 (1961) 1485.

## Short Communication

---

# Quantitative determination of dehydroabietic acid methyl ester in disproportionated rosin

Maria João Brites, Ana Guerreiro, Bárbara Gigante\* and M.J. Marcelo-Curto

*Instituto Nacional de Engenharia e Tecnologia Industrial, Departamento de Tecnologia de Indústrias Químicas, Estrada das Palmeiras, 2745 Queluz (Portugal)*

(First received January 28th, 1993; revised manuscript received April 5th, 1993)

---

### ABSTRACT

A simple, rapid and accurate capillary gas chromatographic (GC) method for the quantitative determination of dehydroabietic acid in commercially disproportionated rosins was developed and tested. Dehydroabietic acid was converted into its methyl ester derivative and quantified by GC with flame ionization detection using a DB-1 column with methyl stearate as the internal standard. The method can also be applied to the quantitation of dehydroabietic acid in rosin or in other rosin derivatives.

---

### INTRODUCTION

Dehydroabietic acid is the main component of disproportionated rosin, an important rosin derivative used industrially in paper sizing, in various coating compositions and synthetic resins and especially as an emulsifying agent in the manufacture of styrene-butadiene rubber. There are several commercial-grade disproportionated rosins available on the market containing between 30 and 65% dehydroabietic acid. Variations in disproportionation processes cause considerable variation in dehydroabietic acid content as a result of incomplete disproportionation of the conjugated diene acids, such as abietic, neoabietic and palustic acids. This reduces the overall stability to oxidation and the usefulness

of the end product, hence the need for a method of quantitation of dehydroabietic acid.

Since the first application of gas chromatography to rosin acid analysis in 1959 [1], a number of publications have appeared describing the GLC separation and characteristics of rosin acids, evaluated first for packed columns with a variety of stationary phases [2–5] and later for capillary columns [6–10]. Zinkel and Han [11] reviewed the state of the art for both packed and capillary columns applied to rosin acids analyses.

Most of the literature methods [1–11] were developed for the determination of rosin acid composition in the matrix by normalizing total peak areas to 100%. Although this approach is adequate for many purposes, it is not fully quantitative in that detector responses for individual rosin acids can vary by nearly 10%.

The need to find a simple, rapid, accurate and reproducible procedure for quantitative analyses of dehydroabietic acid in rosins and modified

---

\* Corresponding author.

rosins from different industrial sources led us to the development of the present method using a capillary column with methyl stearate as the internal standard.

## EXPERIMENTAL

### *Reagents and chemicals*

Methanol, diethyl ether, methyl *tert.*-butyl ether and potassium hydroxide (Merck) were analytical-grade reagents. Diazomethane was generated from *N*-methyl-*N*-nitroso-*p*-toluenesulphonamide (Sigma) by a standard procedure [6–10].

### *Reference standards and standard solutions*

Stearic acid (Sigma) and dehydroabiatic acid (Helix-Biotech) were analytical-grade reagents; samples of rosin and disproportionated rosin were gifts from various companies.

An internal standard stock solution of methyl stearate in *tert.*-methyl butyl ether at a concentration of  $1.0 \text{ mg ml}^{-1}$  was used. The reference stock solution was prepared by accurately weighing about 50 mg of methyl dehydroabietate and dissolving with *tert.*-methyl butyl ether in a 50-ml volumetric flask. The reference solution for analysis of disproportionated rosin was prepared by measuring 2.0 ml of the reference stock solution and 3 ml of internal standard stock solution into a 10-ml volumetric flask and diluting to volume with *tert.*-methyl butyl ether.

To prepare standard solutions for the calibration graph, appropriate volumes were measured out of the reference solution, mixed with internal standard (3 ml) and diluted to 10 ml with *tert.*-methyl butyl ether. The calibration was carried out over a concentration range of 0.05–0.5  $\text{mg ml}^{-1}$  for dehydroabiatic acid as its methyl ester.

### *Apparatus*

A Carlo Erba HRGC 5160 gas chromatograph equipped with a Spectra-Physics computer integrator Model SP 4270, flame ionization detector and a  $15 \text{ m} \times 0.25 \text{ mm}$  I.D. fused-silica column coated with a methyl silicone film (DB-1, J&W, Folsom, CA, USA) with a thickness of  $0.10 \mu\text{m}$  was used for analyses. A  $1\text{-}\mu\text{l}$  aliquot of the 10-ml methyl *tert.*-butyl ether solutions was used

for the determination of methyl dehydroabietate content by capillary GC.

The split injection port of the instrument was adjusted to a split ratio of 1:100. Helium was used as the carrier gas at a flow-rate of 2 ml/min (68 cm/s) through the column with an inlet pressure of 65 (70) kPa. The column temperature was maintained at 195°C. The detector and injector port temperatures were set at 300°C and 275°C, respectively. Methyl dehydroabietate was quantified by comparing the peak areas of the detector response to injections of samples with known amounts of a standard of methyl dehydroabietate.

### *Esterification of standards and samples*

About 50 mg of the sample dissolved in a mixture of diethyl ether and methanol (9:1) were esterified with excess diazomethane [11]. The esterification was complete when bubbles were no longer visible and the yellow colour of the solution was stable. Excess diazomethane was removed in a well ventilated fume cupboard under a nitrogen flow. After evaporation of the solvent, the sample was dried under vacuum, accurately weighed and stored at 4°C until GC analysis.

### *Sample for analysis*

The sample solution was prepared by accurately weighing about 50 mg of the esterified sample and diluting with methyl *tert.*-butyl ether in a 50-ml volumetric flask. The injection solution was prepared by accurately measuring 2 ml of the sample solution, mixing with 3 ml of internal standard stock solution and diluting with methyl *tert.*-butyl ether in a 10-ml volumetric flask.

## RESULTS AND DISCUSSION

A capillary GC method that does not require time-consuming purification steps prior to analysis has been developed for the rapid and accurate determination of dehydroabiatic acid as its methyl ester in commercially disproportionated rosins. Derivatization to the methyl ester, carried out in diethyl ether–methanol (9:1) [11], was chosen since it leads to clean, fast and

complete reactions, no sample purification being required; consequently, losses involved in the procedure are minimized.

In spite of the many industrial uses of disproportionated rosin, which is superior to rosin for many applications, the only two relevant publications are those describing reversed-phase partition chromatography of disproportionated rosin [12] or a colorimetric method comparing the colour intensity of the violet solution with permanganate solutions of different concentrations [13].

An internal standard method was employed, with methyl stearate as the internal standard. Upon application of the analytical procedure to commercially disproportionated rosins, the separation of the critical pair of peaks 2 and 3 (Fig. 1) was achieved through adjustment of temperature and flow-rate at the expense of a slightly increased analysis time (*ca.* 9.5 min).

A bonded methyl silicone, DB-1 capillary fused-silica column having 15 m length, 0.25 mm internal diameter and a film thickness 0.10  $\mu\text{m}$ , was used. This column was previously tested for resin acids analysis [11] and proved to have good resolution and short analysis time.

The linearity of the detector response to

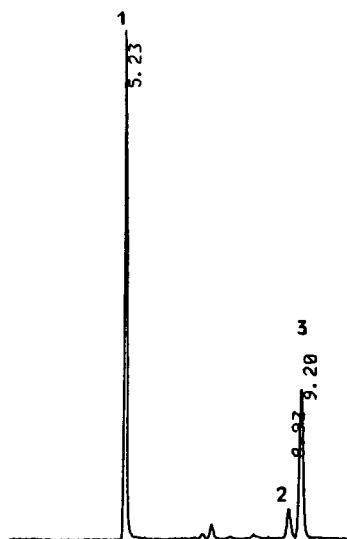


Fig. 1. Chromatogram of a sample of commercially disproportionated rosin. Peak 1 is methyl stearate (internal standard, 0.3  $\text{mg ml}^{-1}$ ) and peak 3 is methyl dehydroabietate (0.20  $\text{mg ml}^{-1}$ ). Values at peaks are retention times in min.

variations in concentration was determined by constructing a calibration graph of peak area *versus* concentration over the range of 0.05–0.5  $\text{mg ml}^{-1}$  methyl dehydroabietate. For each concentration, replicate determinations ( $n = 5$ ) with five injections were made and the average values of peak area were plotted. The slope, the intercept and the correlation coefficient were, respectively, 0.3731,  $-0.0304$  and 0.9991 ( $n = 5$ ) for peak area measurements and were obtained by linear regression analysis.

The repeatability and reproducibility of the method were tested with replicate ( $n = 5$ ) analysis of samples ( $n = 5$ ) corresponding to the average weight of samples with an average concentration of dehydroabietic acid. The results show a 0.82–1.73% R.S.D. between the analysis and the low value of the overall R.S.D. between the analysis and the low value of the overall R.S.D. (1.31%).

The precision of the method was determined using two methyl dehydroabietate standard solutions with concentrations 1.662  $\mu\text{g ml}^{-1}$  and 2.216  $\mu\text{g ml}^{-1}$ , each injected five times. The method is accurate for the above concentrations with a 99% confidence level (Table I).

For commercial disproportionated rosin, the results were in agreement with state levels. This method can be applied to the quantitation of minor amounts of dehydroabietic acid in gum rosin, provided a high enough mass of sample is used to work within the calibration graph limits.

The method is simple, specific, exact and reproducible and therefore can be applied to various commercial modified rosins.

TABLE I  
CALIBRATION DATA FOR ANALYSIS

St. conc. = standard concentration;  $\bar{x}$  = arithmetic mean;  $\sigma_x$  = standard deviation;  $t$  = Student's constant;  $n$  = number of measurements.

St. conc., $X$ ( $\mu\text{g ml}^{-1}$ )	$\bar{x}$	$\sigma_x$	$(X - \bar{x})$	$t\sigma_x/\sqrt{n}$
1.662	1.636	0.022	0.026	0.045
2.216	2.106	0.215	0.110	0.443

## REFERENCES

- 1 J.A. Hudy, *Anal. Chem.*, 31 (1959) 1754.
- 2 F.H.M. Nestler and D.F. Zinkel, *Anal. Chem.*, 35 (1963) 1747.
- 3 N. Mason Joye, Jr., A.T. Rouveaux and R.V. Lawrence, *J. Am. Oil Chem. Soc.*, 51 (1974) 195.
- 4 F.H.M. Nestler and D.F. Zinkel, *Anal. Chem.*, 39 (1967) 1118.
- 5 D.F. Zinkel and C.C. Engler, *J. Chromatogr.*, 136 (1977) 245.
- 6 B. Holmbom, E. Avela and S. Pekkala, *J. Am. Oil Chem. Soc.*, 51 (1974) 397.
- 7 D.O. Foster and D.F. Zinkel, *J. Chromatogr.*, 248 (1982) 89.
- 8 J.S. Han and D.F. Zinkel, *Naval Stores Rev.*, 101 (1991) 13.
- 9 J.C. Hansson and M.V. Kulkani, *Anal. Chem.*, 44 (1972) 1586.
- 10 M. Mayr, E. Lorbeer and K. Kratzl, *J. Am. Oil Chem. Soc.*, 59 (1982) 52.
- 11 D.F. Zinkel and J.S. Han, *Naval Stores Rev.*, 96 (1986) 14.
- 12 V.M. Loeblich and R.V. Lawrence, *J. Am. Chem. Soc.*, 33 (1956) 320.
- 13 W. Sanderman and R. Casten, *Holzforschung*, 25 (1971) 40.

## Book Review

---

*A practical guide to HPLC detection*, edited by D. Parriott, Academic Press, San Diego, New York, Boston, London, 1993, X + 293 pp. price US\$ 59.95, ISBN 0-12-545680-8.

Detection is clearly an important part of chromatography. While new monographs on HPLC detection are published once in a while, this book has more of a practical flavor to it than most of its competitors. The editor has assembled a nice collection of authors who are either instrument manufacturers or serious users in the industrial laboratory. It is noteworthy that the chapters do not show particular biases or commercial overtones that reflect the authors' backgrounds.

After a brief introductory chapter, refractive index detectors are presented. There is a good collection of basic properties of chromatographic solvents, such as temperature and pressure dependences. Typical working curves for compounds are shown to provide the readers with a good feel for non-linearities that can be expected. Even artifacts due to column temperature changes and degassing of solvents are illustrated. The information is very useful to the user because the subtle features of the detectors are all exposed. Normally, one would have to rely on experience or trial-and-error to obtain similar insights.

The next two chapters deal with the workhorses of HPLC —absorbance detection at a single wavelength or by diode-array detectors. There is some duplication in the discussion of monochromators and flow cells. Quite useful is a collection of traces of actual detector noise under various operating conditions, such as wavelength and time constant. I would have liked to see a bit more discussion on how noise is affected by light intensity and by the electronics associated with each instrument. Some discussion on microcolumn detectors would also be appropriate. For array detection, there is a good introduction

to the utilization of the multiwavelength information in assessing peak purity and to enhance chromatographic resolution. Missing is a comparison with the scanning multiwavelength approach (oscillating mirror), which is a serious alternative.

Chapter 5 presents fluorescence detection. Many instrumental features such as phototube response, filter characteristics, grating efficiencies and spectra of light source are included. This provides the users with the nuts and bolts of experimental design without having to search through several catalogs from manufacturers of optical components. The section on chemiluminescence seems a bit out of place, since the topic is also discussed in Chapter 8. It would have made more sense if the instrumental modifications to the fluorescence detector were described in the context of chemiluminescence detection. Since fluorescence applications depend so heavily on chemical derivatization, it would be useful to include a more extensive list of examples. This does not need to duplicate the information already included in Chapter 8. Rather, one can learn more by seeing actual chromatograms. This can become a serious issue in view of incomplete reaction, chemical noise, and residual fluorescence from the reagent.

The next chapter deals with electrochemical detection. The coverage is broad but the discussion on each method is brief. There are plenty of references to follow up on. To be consistent with the earlier chapters, it would have been better to include also evaluation of noise sources and some drawings of the instrumentation. The topic of mass spectrometry as an LC detection technique could take a whole monograph to present comprehensively. The chapter here does a



reasonable job in summarizing the various approaches. This is probably all the LC practitioner is expected to know. After all, any real attempts in applying LC–MS should involve the collaboration of a serious mass spectrometrists.

The book concludes with chapters on post-column derivatization and “other modes” of detection. These are good introductions to the topics. Some discussion on the problems of pre-column derivatization would also be helpful in terms of how it affects separation and interferences. The 300 references of other detection modes is a very useful collection for the routine user of LC.

Overall, this is a nice addition to the LC literature. It has succeeded in reaching the user of LC as a practical guide as opposed to a review monograph. One can argue about the balance of topics and depth here and there. But, having authored a monograph on LC detectors myself, I can appreciate how difficult it is to cover everything that may be of interest. The present monograph will prove to be an asset to every LC laboratory.

*Ames, IA (USA)*

**E.S. Yeung**

## PUBLICATION SCHEDULE FOR THE 1993 SUBSCRIPTION

*Journal of Chromatography and Journal of Chromatography, Biomedical Applications*

MONTH	1992	J	F	M	A	M	J	J	
Journal of Chromatography	Vols. 623-627	628/1 628/2 629/1 629/2	630/1 + 2 631/1 + 2 632/1 + 2 633/1 + 2	634/1 634/2	635/1 635/2 636/1 636/2	637/1 637/2 638/1 638/2	639/1 639/2 640/1 + 2	641/1 641/2 642/1 + 2 643/1 + 2 644/1	The publication schedule for further issues will be published later.
Cumulative Indexes, Vols. 601-650									
Bibliography Section				649/1			649/2		
Biomedical Applications		612/1	612/2	613/1	613/2 614/1	614/2 615/1	615/2 616/1	616/2 617/1	

### INFORMATION FOR AUTHORS

(Detailed *Instructions to Authors* were published in Vol. 609, pp. 437-443. A free reprint can be obtained by application to the publisher, Elsevier Science Publishers B.V., P.O. Box 330, 1000 AH Amsterdam, Netherlands.)

**Types of Contributions.** The following types of papers are published in the *Journal of Chromatography* and the section on *Biomedical Applications*: Regular research papers (Full-length papers), Review articles, Short Communications and Discussions. Short Communications are usually descriptions of short investigations, or they can report minor technical improvements of previously published procedures; they reflect the same quality of research as Full-length papers, but should preferably not exceed five printed pages. Discussions (one or two pages) should explain, amplify, correct or otherwise comment substantively upon an article recently published in the journal. For Review articles, see inside front cover under Submission of Papers.

**Submission.** Every paper must be accompanied by a letter from the senior author, stating that he/she is submitting the paper for publication in the *Journal of Chromatography*.

**Manuscripts.** Manuscripts should be typed in **double spacing** on consecutively numbered pages of uniform size. The manuscript should be preceded by a sheet of manuscript paper carrying the title of the paper and the name and full postal address of the person to whom the proofs are to be sent. As a rule, papers should be divided into sections, headed by a caption (e.g., Abstract, Introduction, Experimental, Results, Discussion, etc.) All illustrations, photographs, tables, etc., should be on separate sheets.

**Abstract.** All articles should have an abstract of 50-100 words which clearly and briefly indicates what is new, different and significant. No references should be given.

**Introduction.** Every paper must have a concise introduction mentioning what has been done before on the topic described, and stating clearly what is new in the paper now submitted.

**Illustrations.** The figures should be submitted in a form suitable for reproduction, drawn in Indian ink on drawing or tracing paper. Each illustration should have a legend, all the legends being typed (with double spacing) together on a *separate sheet*. If structures are given in the text, the original drawings should be supplied. Coloured illustrations are reproduced at the author's expense, the cost being determined by the number of pages and by the number of colours needed. The written permission of the author and publisher must be obtained for the use of any figure already published. Its source must be indicated in the legend.

**References.** References should be numbered in the order in which they are cited in the text, and listed in numerical sequence on a separate sheet at the end of the article. Please check a recent issue for the layout of the reference list. Abbreviations for the titles of journals should follow the system used by *Chemical Abstracts*. Articles not yet published should be given as "in press" (journal should be specified), "submitted for publication" (journal should be specified), "in preparation" or "personal communication".

**Dispatch. Before sending the manuscript to the Editor please check that the envelope contains four copies of the paper complete with references, legends and figures. One of the sets of figures must be the originals suitable for direct reproduction. Please also ensure that permission to publish has been obtained from your institute.**

**Proofs.** One set of proofs will be sent to the author to be carefully checked for printer's errors. Corrections must be restricted to instances in which the proof is at variance with the manuscript. "Extra corrections" will be inserted at the author's expense.

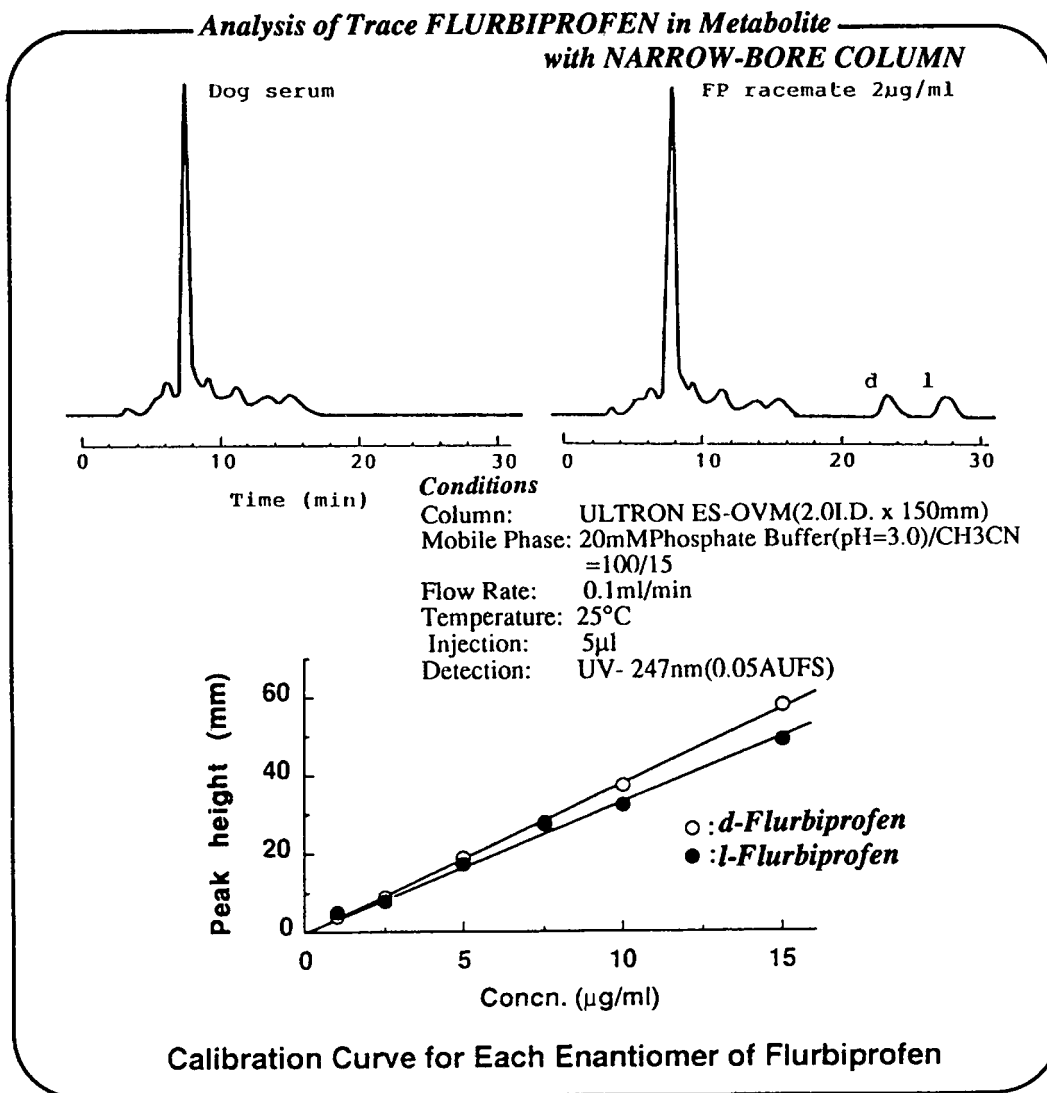
**Reprints.** Fifty reprints will be supplied free of charge. Additional reprints can be ordered by the authors. An order form containing price quotations will be sent to the authors together with the proofs of their article.

**Advertisements.** The Editors of the journal accept no responsibility for the contents of the advertisements. Advertisement rates are available on request. Advertising orders and enquiries can be sent to the Advertising Manager, Elsevier Science Publishers B.V., Advertising Department, P.O. Box 211, 1000 AE Amsterdam, Netherlands; courier shipments to: Van de Sande Bakhuyzenstraat 4, 1061 AG Amsterdam, Netherlands; Tel. (+31-20) 515 3220/515 3222, Telefax (+31-20) 6833 041, Telex 16479 els vi nl. *UK:* T.G. Scott & Son Ltd., Tim Blake, Portland House, 21 Narborough Road, Cosby, Leics. LE9 5TA, UK; Tel. (+44-533) 753 333, Telefax (+44-533) 750 522. *USA and Canada:* Weston Media Associates, Daniel S. Lipner, P.O. Box 1110, Greens Farms, CT 06436-1110, USA; Tel. (+1-203) 261 2500, Telefax (+1-203) 261 0101.

# Ovomucoid Bonded Column for Direct Chiral Separation

## ULTRON ES-OVM

Narrow-Bore Column ( 2.0 I.D. x 150 mm ) for Trace Analyses  
Analytical Column ( 4.6 I.D. , 6.0 I.D. x 150 mm ) for Regular Analyses  
Semi-Preparative Column ( 20.0 I.D. x 250 mm ) for Preparative Separation



## SHINWA CHEMICAL INDUSTRIES, LTD.

50 Kagekatsu-cho, Fushimi-ku, Kyoto 612, JAPAN  
Phone:+81-75-621-2360 Fax:+81-75-602-2660

In the United States and Europe, please contact:

### Rockland Technologies, Inc.

538 First State Boulevard, Newport, DE 19804, U.S.A.

Phone: 302-633-5880 Fax: 302-633-5893

This product is licenced by Eisai Co., Ltd.